THE UNIVERSITY
of EDINBURGH

The expression of the fibrillin gene family in the development, differentiation and maintenance of mesenchyme cell types

Margaret Rose Davis

Doctor of Philosophy

College of Medicine and Veterinary Medicine

University of Edinburgh

2015

Declaration

The thesis presented is the work of the author except when clearly stated otherwise by reference and/or acknowledgement. Any work performed in collaboration or conducted by others is explicitly acknowledged. The work has not been submitted for any other degree or professional qualification.

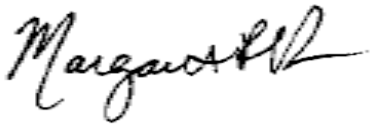

Margaret R. Davis Date: 5 May 2015

Abstract

Connective tissue initially arises from embryonic mesenchymal stem cells (MSC) that originate from the mesoderm during embryogenesis and are capable of differentiating into connective tissue lineages such as adipocytes, osteoblasts, chondrocytes and fibroblasts. Connective tissue is composed of cells held together by the extracellular matrix (ECM). The fibrillins and latent transforming growth factor binding proteins form a superfamily of ECM proteins characterised by the presence of a unique domain, the 8-cysteine transforming growth factor beta binding domain (TGFß). The fibrillin proteins (fibrillin-1, fibrillin-2 and fibrillin-3 in most vertebrates, encoded by the *FBN1, FBN2* and *FBN3* genes respectively), are major components of the 10nM microfibrils found in ECM of many tissue types, for example mesenchyme-derived connective tissues. Fibrillin-1 and fibrillin-2 are also thought to be required for stabilization and storage of latent TGFβ complexes. Mutations in *FBN1* cause Marfan syndrome, a connective tissue disorder characterised by abnormalities in the microfibrils resulting in musculoskeletal, ocular, cardiovascular and other complications. *FBN2* mutations lead to congenital contractural arachnodactyly, which has a musculoskeletal phenotype similar to Marfan syndrome. There are currently no known diseases associated with *FBN3* mutations.

In this project, the expression of fibrillins was investigated using human cell lines during early development, mesenchymal stem cell differentiation and in further differentiated mesenchymal cell lines, for example in osteocytes (osteosarcomas), chondrocytes and fibroblast lineage. Immunocytochemistry was used to examine protein expression, real-time PCR and expression microarrays to determine mRNA synthesis and RNAi suppression of gene expression to determine possible functions of fibrillins and associated ECM proteins. In addition, a genome wide bioinformatics evaluation was performed of transcription start sites for the fibrillin gene family utilising the information obtained from the FANTOM5 consortium.

The three fibrillin genes showed differing expression patterns in cell lines depending on the stage of development/differentiation. During embryogenesis, expression of *FBN3, FBN2* and *FBN1* increased sequentially in that order. Expression of *FBN3* followed the same pattern as expression of known pluripotency markers, while expression of *FBN2*

correlated with expression of markers for later stages of mesoderm differentiation. *FBN1* expression was associated with mesenchymal markers, and this was supported by a study of mesenchymal stem cells differentiation to the adipose lineage. Fibrillin-1 microfibrils and RNA expression were present early in primary adult human MSC differentiating to adipocytes, suggesting that a fibrillin matrix is required for initial MSC attachment. As differentiation proceeded, fibrillin -1 expression decreased, with rapid degradation of the microfibrils. Fibrillin-2 expression increased following differentiation and fibrillin-3 was not expressed. These results suggest that fibrillin-1 plays an important structural and regulatory role in the early stages of connective tissue development but is not required to maintain the differentiated state.

Many genes showed the same expression pattern as *FBN1*. To better understand the importance of fibrillin-1 and its interaction with these coexpressing genes, fibrillin-1 was knocked down using siRNA in fibroblast, chondrocyte and osteosarcoma cell lines. There were little to no effects identified in chondrocyte and osteosarcoma cell lines, and only a few genes were altered following the reduction of fibrillin-1 mRNA in fibroblasts, suggesting that fibrillin-1 is not a central regulator but an endpoint. This was surprising given its potential role in controlling bioavailability of TGFβ, a key regulator of mesenchymal cells.

In addition, the evolution of the fibrillin gene family was studied and it was found that the gene structure, amino acid sequence and genomic positions of each gene are widely conserved across vertebrates, suggesting an important role in vertebrate body structure. However, the differences in gene structure and sequence between the three fibrillin genes suggest divergent function. Fibrillin-1 mutations with the most severe phenotypes are located in regions that are highly conserved. This study shows that there is a clear developmental and evolutionary distinction between the three fibrillins. Fibrillin-3 was associated with pluripotency and its presence in differentiating foetal liver and brain may suggest that there are residual pluripotent cells in these developing tissues. Fibrillin-2 appeared to be a marker for the mesodermal stage and its role in adult cells is currently not clear. Fibrillin-1 was present in cells already predetermined to go to mesenchymal lineages, but it was minimal in the advanced stages of differentiation suggesting that it

may be a marker for relatively plastic mesenchymal cells prior to commitment to a specific lineage.

These results will assist in the understanding of disorders resulting from fibrillin gene mutations and have identified coexpressed proteins, potential modifiers that could be the targets of gene therapy and candidates for similar connective tissue

Publications and Presentations

PEER REVIEWED PUBLICATIONS

Davis MR, Andersson R, Severin J, de Hoon M, Bertin N, Baillie JK, Kawaji H, Sandelin A, Forrest AR, Summers KM; FANTOM Consortium. (2014) Transcriptional profiling of the human fibrillin/LTBP gene family, key regulators of mesenchymal cell functions. Molecular Genetics and Metabolism. 112(1): 73-83. (Chapter 6)

Gawthorne, J., Tan, N., Bailey, U., **Davis, M.R.,** Wong, W.L., Nadiu, R., Fox, K., Jennings, M., & Schulz, B.L. (2014) Selection against glycosylation sites in potential target proteins of the general HMWC N-glycosyltransferase in *Haemophilus influenzae.* Biochemical and Biophysical Research Communication 445(3): 633-38.

Davis, M.R., & Summers, K.M. (2012) Structure and function of the mammalian fibrillin gene family: implications for human connective tissue disease. Molecular Genetics and Metabolism. 107(4): 635-47.

Arner, E., Daub, C. O., Vitting-Seerup, K., Andersson, R., Lilje, B., Drablos, F., Lennartsson, A., Ronnerblad, M., Hrydziuszko, O., Vitezic, M., Freeman, T. C., Alhendi, A. M., Arner, P., Axton, R., Baillie, J. K., Beckhouse, A., Bodega, B., Briggs, J., Brombacher, F., **Davis, M.R**, et al. (2015) Gene regulation. Transcribed enhancers lead waves of coordinated transcription in transitioning mammalian cells. Science, 347, 1010-4.

Manuscripts in preparation

Davis, M.R., Duffy, C., DeSousa, P., MacRae, V.,, the FANTOM5 consortium *et al.,* Summers, K.M. (2015) Fibrillin-1 and body shape: role in adipose differentiation.

Davis, M.R., MacRae, V., the FANTOM5 consortium, *et al.,* Summers, K.M. (2015) Early and late changes in gene expression during mineralisation of SAOS-2, a human osteosarcoma cell line model for bone formation.

Davis, M.R., MacRae, V., the FANTOM5 consortium, *et al.,* Summers, K. M. (2015) Fibrillin expression in differentiating human embryonic stem cells.

Acknowledgements

I would like to express a tremendous thank you to my primary PhD supervisor, Professor Kim Summers, without whom this thesis would not have been possible. Kim was an excellent role model throughout this entire process through leading by example, providing consistent support, encouragement and understanding. In addition, her leadership skills and genuine interest in my future scientific career were highly appreciated. I am truly grateful for her influence.

I would like to thank my secondary supervisor, Dr. Vicky MacRae, and the remainder of the thesis committee, Professor Tom Freeman and Dr. David Collie for their guidance and support at each stage of the project.

I would also like to express my gratitude to Ailsa Carlisle, Dr. Mark Barnett, Dr. Clare Pridans and all the remaining members of the Summers, Hume and Freeman lab groups, for their scientific knowledge and input. I am forever grateful for the excellent advice both in and out of the laboratory.

Furthermore, I would like to thank my parents Dwight and Elizabeth Davis, and sisters, Dr. Liz Salerno, Dr. Holly Davis and Laura Davis for their loving support and for always being at the other end of the phone! Their words of encouragement and support helped me to remain clear-headed and confident over the last four years. As well as my gorgeous nephew Pete Salerno and future nieces Baby A (Alyssa Beth) and Baby B (Sophia Rita) for keeping the smile on my face! And finally, I owe thanks to Louise Welch, Rachel Moodie, Annemarie Wannamaker, SaraJane Vogt and Jessica Hakamaa, for their friendship and encouragement both at home and abroad.

Table of Contents

Table of Figures

Chapter 1. Introduction

Chapter 2. General Methods

Chapter 3. The fibrillin gene family in early and later differentiation

Chapter 4. Fibrillin expression in human connective tissue cell types

Chapter 5. Investigating the functional role of fibrillin-1 in cell lines

Chapter 6. Identification and expression of promoters of the fibrillin gene family

Chapter 7. Evolutionary conservation of the fibrillin gene family

Table of Tables

Chapter 1. Introduction

Chapter 2. General Methods

Chapter 3. The fibrillin gene family in early and later differentiation

Chapter 4. Fibrillin expression in human connective tissue cell types

Chapter 5. Investigating the functional role of fibrillin-1 in cell lines

Chapter 6. Identification and expression of promoters of the fibrillin gene family

Chapter 7. Evolutionary conservation of the fibrillin gene family

List of Abbreviations

ADMSC	Adipose derived mesenchymal stem cell
Bp	Base Pair
bFGF	Recombinant human fibroblast growth factor- basic
BLAT	BLAST (Basic Local Alignment Search Tool) - like alignment tool
CAGE	Cap analysis gene expression
CCA	Congenital contractural arachnodactyly
DMEM	Dulbecco's modified eagle medium
ECM	Extracellular matrix
ETOH	Ethanol
FANTOM5	Functional Annotation of the Mammalian Genome
FBN1, FBN2, FBN3	Fibrillin-1, Fibrillin-2, Fibrillin-3
FBS	Fetal Bovine Serum
GDS	Genomic data sharing
GEO dataset	Gene Expression Ominbus repository
GO terms	Gene ontology terms
GSE	Genomic Spatial Event
hES	Human embryonic stem cells
hESMP	Mesenchyme progenitors derived from hES cells
HI	Heat Inactivated
ICC	Immunocytochemistry
KD	Knock down
MFS	Marfans Syndrome
MIM	Mendelian Inheritance in Man
mRNA	Messenger ribonucleic acid
MSC	Mesenchymal stem cell
OMIM	Online Mendelian Inheritance in Man
PBS	Phosphate buffer saline

RNA	Ribonucleic acid
RNAi	Ribonucleic acid interference
siRNA	Small interfering ribonucleic acid
TF	Transcription factor
Ts	Transition mutation
TSS	Transcription start site
Tv	Transversion mutation

Chapter 1. Introduction

Connective tissue forms the support for the organs and tissues of the animal body. Adipose, cartilage and bone are all forms of connective tissue. Connective tissue is comprised of specific cells that arise from the mesoderm in early development and a dynamic extracellular matrix (ECM). The ECM is composed of many fibrous and non-fibrous constituents including proteins of the fibrillin family, key components of 10nM microfibrils within the ECM (Sakai *et al.*, 1986, Zhang *et al.*, 1994, Corson *et al*., 2004). Mutations in the genes encoding fibrillin-1 and fibrillin-2 have been implicated in a variety of phenotypes, affecting multiple connective tissues within the body **(Sections 1.3.4 and 1.3.5)**, indicating their importance within the ECM. The role of the third fibrillin, fibrillin-3 has yet to be completely understood. This thesis presents a detailed study of expression of the fibrillin gene family and defines co-regulated genes in cells of mesenchyme origin, the basis of connective tissue. The overall aim is to better understand the role that the fibrillin gene family plays in the ECM of connective tissues.

1.1 Mesenchymal Connective Tissue

Connective tissue supports various structures in the body of vertebrates by providing strength, elasticity and cushioning. It arises from embryonic mesenchymal stem cells (MSCs) (Choo and Lim, 2011), which originate in the mesoderm layer during embryogenesis and are capable of differentiating into multiple connective tissue cell types (Caplan, 1991). During mammalian development the mesoderm layer becomes segmented, sequentially producing the paraxial, intermediate and lateral plate mesoderm (Gilbert, 2000). Progenitor connective tissue cells (produced from the various mesoderm layers) can be further differentiated into specialised cell types of multiple lineage pathways leading to, for example, adipocytes, chondrocytes, myocytes, osteoblasts and fibroblasts ***(*summarized in *Figure 1.1)*** (Bruder *et al*., 1994, Prockop, 1997, Pittenger *et al*., 1999). Cells of these lineages are also involved in connective tissue repair and are the major cellular component in scarring and fibrosis (Olivieri *et al*., 2010, Ferrari *et al.*, 1998).

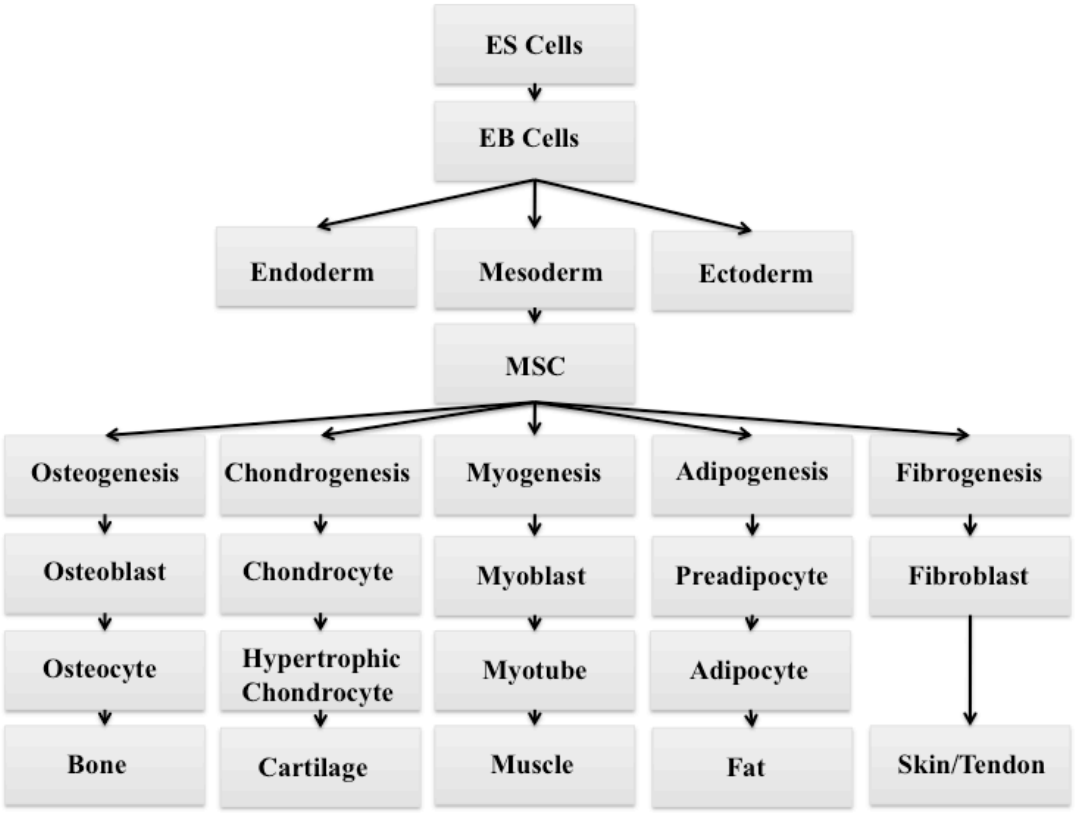

Figure 1.1. A schematic diagram of ES (embryonic stem) cells differentiating to connective tissue. This figure demonstrates the potential of ES cells to differentiate to EB (embryoid bodies) and continue to form three layers, including the mesoderm. The mesoderm layer gives rise to mesenchymal stem cells (MSC) and which then differentiate into multiple lineages. Image adapted from (Bodas and Vij, 2010).

The mesenchyme derived stem cells continue to form various connective tissues within the body, for example bone, cartilage, adipose (fat) and fibroblasts ***(Figure 1.1)***. This thesis will examine the role of the fibrillin gene family in early differentiation, adipogenesis, fibroblasts, bone and cartilage model systems. The mechanism of maturation of these tissue types is described below.

1.1.1 Dermal fibroblast formation

Fibroblasts are the most undifferentiated and primitive cells created from MSCs. ***Figure 1.1*** depicts the cells' ability to differentiate to skin and tendons (Driskell *et al*., 2013), though fibroblasts are also capable of differentiating into adipocytes (Tontonoz *et al*., 1994) and smooth muscle cells (Karamariti *et al.,* 2013). They are dispersed in multiple

connective tissue types, for example myocardium (Camelliti *et al.,* 2005, Ieda *et al.,* 2009, Goldsmith *et al.,* 2004) and cartilage (Alberts, 2002b). Fibroblasts are responsible for ECM secretion during connective tissue formation for wound repair and are the most widely spread connective tissue cell type (Driskell *et al.,* 2013). Their primary function is to maintain the structural integrity of connective tissues (Ross and Greenlee, 1966) and synthesise collagen (Goldberg and Green, 1964). The studies reported in this thesis used neonatal dermal fibroblasts.

The dermis is located between the epidermis and the subcutaneous tissue of the skin and consists of two distinct layers, the papillary and reticular layers (Driskell *et al.,* 2013, Janson *et al.,* 2012, Janson *et al.,* 2013). The papillary layer has a thinner ECM and a dense cell population while the reticular layer has a dense ECM and lower cell density (Driskell *et al.,* 2013). These layers act together to provide a matrix of diverse constituents. The layers have distinct cell morphology in that reticular fibroblasts in culture are square and stretched in appearance while papillary fibroblasts in culture are lean, spindle shaped cells. The precise role of the layers remains unknown, though recent microarray analysis demonstrated significant differential expression of 116 genes (Janson *et al.,* 2012). For example *CNN1* (calponin 1)(OMIM:600806), *CALD1* (caldesmon 1) (OMIM: 114213), *GALNT10* (N-Acetylgalactosaminyltransferase 10 (OMIM: 608043) and *NEXN* (nexilin)(OMIM: 613121) were upregulated in the reticular layer while *DCN* (decorin)(OMIM: 125255) was upregulated in the papillary layer. In addition, the authors proposed *MGP* (matrix gamma carboxyglutamate protein) to be a candidate genetic marker for the reticular layer, though the precise role is unknown. The ECM components of dermal fibroblasts will be discussed further in **Section 1.2**.

1.1.2 Adipose formation

As shown in ***Figure 1.1***, MSCs are also capable of differentiating into adipocytes that mature to form adipose connective tissue or fat (Rosen and MacDougald, 2006). Adipose tissue stores energy, provides cushioning for the skeletal and organ systems within the body, provides thermal insulation (Li *et al.,* 2014), and maintains communication with the endocrine system through a nutrient gradient regulating hormone levels such as

insulin and cortisol (Galic *et al.,* 2009, Greenwood *et al.,* 1966) and communication with the thyroid gland (Santini *et al.,* 2014). There are three types of fat found within the human body: white adipose tissue (WAT), brown adipose tissue (BAT) and beige adipose (Giralt and Villarroya, 2013, Xue *et al.,* 2007, Wu *et al.,* 2012). WAT is widely localised throughout the body, and has a major role in lipogenesis and the glucose-lipid equilibrium and inhibition of lipolysis (Vazquez-Vela *et al.,* 2008). BAT and beige fat are heavily involved in thermogenesis (reviewed in (Harms and Seale, 2013). One distinguishing genetic marker for BAT and beige adipose is the upregulation of UCP1 (uncoupling protein 1) (Wu *et al.,* 2012, Okamatsu-Ogura *et al.,* 2014, Matthias *et al.,* 2000). They also have more abundant mitochondria (Shabalina *et al.,* 2013).

The process of adipogenesis will be discussed in greater detail in **Chapter 3**. Briefly, mature adipocytes are formed from MSCs, by progression to preadipocytes, early adipocytes and ultimately mature adipocytes. There are several key factors involved in lineage determination, including IGF1 (insulin-like growth factor 1)(OMIM: 147440)(Kloting *et al.,* 2008), CSF1 (macrophage colony-stimulating factor)(OMIM: 120420)(Tanny *et al.,* 2007, Umezawa *et al.,* 1991), glucocorticoids (Chapman *et al.,* 1985, Zubiria *et al.,* 2014), and fatty acids (Das, 2006, Bochicchio *et al.,* 2014).

The precursors for adipocyte formation (preadipocytes) are derived from MSCs that exhibit high expression of key adipose transcription factor markers, *CEBP* (CCAAT enhancer binding protein) (OMIM: 116897) and *PPARG* (peroxisome proliferator activated receptor-gamma)(OMIM: 601487). WAT and BAT adipose express high levels of *PPARG* (Nedergaard *et al.,* 2005, Barak *et al.,* 1999). Similar to osteo- and chondrogenesis, adipose differentiation is driven by changes in the extracellular matrix (ECM), mainly an upregulation of collagen IV (Pierleoni *et al.*, 1998), leading to thicker collagen based fibres within the basal membrane. In addition, proliferation ceases and lipid vacuoles form within the intracellular space (Gross and Silver, 2014). Lipid vacuoles are the major storage units for lipids in adipose tissue (Hahm *et al.,* 2014, Mannik *et al.,* 2014). The precise morphological changes and role of matrix genes will be discussed in detail in **Chapter 3**.

1.1.3 Cartilage

Cartilage is a highly elastic connective tissue mainly found between bones, providing cushioning and flexibility within the body. There are three major types of cartilage found within mammals, hyaline, elastic and fibro-cartilage. Hyaline cartilage is located in joints and the lining of bones, for example costal cartilage, and contains 60-85% water (Padalkar *et al.,* 2013, Palukuru *et al.,* 2014). Elastic cartilage is localised to auditory tubes and the larynx and is similar to hyaline cartilage, though it contains elastic bundles within the matrix, causing a more rigid and supportive structure. In addition, hyaline cartilage can be differentiated to elastic cartilage to aid in tissue regeneration (Mizuno *et al.,* 2014). Fibro-cartilage is primarily located within the intervertebral disks, and sites joining tendons or ligaments to bones (Sunshine, 1999). The three types of cartilage are generated in a similar fashion, though the ECM composition is distinct (Zambrano *et al.,* 1982)**(Discussed in Section 1.2)**. Chondrogenesis is a process in which undifferentiated MSCs differentiate to a chondrocyte lineage, proliferate, then either mature to hypertrophic chondrocytes (terminal differentiation) producing cartilage or undergo chondrocyte apoptosis (intermediate chondrocytes) leading into endochondral ossification **(Discussed in Section 1.1.5)** (Goldring *et al.,* 2006).

Proliferating chondrocytes begin to create a collagen matrix (mainly collagen II, collagen IX and collagen XI), which is also rich in proteoglycans including aggrecan (Goldring *et al.,* 2006). Aggrecan consists of three globular domains. It is secreted by chondrocytes during development and binds to hyaluronan (a viscous ground substance of the ECM) providing a gel that supports cartilage load-bearing properties (Kiani *et al.,* 2002). In addition an upregulation of *SOX9* (Sry-Box 9) is a highly characteristic marker of chondrogenesis (OMIM: 608160). *Sox-9* has been shown to directly regulate *Col2a1* (Collagen 2, alpha type 1), a key component in chondrogenesis (Bell *et al.,* 1997), in mice. It is regulated by FGFs (fibroblast growth factors) (Murakami *et al.,* 2000) and essential in the prevention of hypertrophic chondrocyte formation (Huang *et al.,* 2001, Chikuda *et al.,* 2004, Goldring *et al.,* 2006). As upregulation of key chondrocytic markers occurs, the chondrocytes begin to condense, the actin fibres of the cytoskeleton change and cellular adhesion increases (Benjamin and Ralphs, 1998, Daniels and Solursh, 1991).

As the chondrocytes differentiate, they become hypertrophic (enlarged) and express high levels of *ALPL* (alkaline phosphatase)(Richany *et al.,* 1959). Expression of *SOX9* is decreased and both *RUNX2* and *RUNX3* (Michigami, 2014) are upregulated, leading to either further cartilage production (elastic or fibro-cartilage) or endochondral ossification (hyaline cartilage)(Goldring *et al.,* 2006). Hypertrophic chondrocytes and intermediate chondrocytes produce varying ECM components throughout the process **(Discussed in Section 1.1.5 and 1.2)**.

1.1.4 Bone

Bone is a dynamic connective tissue, undergoing continuous repair and remodelling throughout the organism's life span. There are three distinct lineages that arise from the mesoderm to produce bone tissue (Gilbert, 2000). Somites (located within the paraxial mesoderm) form the axial skeleton (Resende *et al.,* 2014, Christ and Wilting, 1992, Verbout, 1985), the lateral plate mesoderm creates the limb skeleton (Onimaru *et al.,* 2011, Johnson and Tabin, 1997, Chevallier *et al.,* 1977, Christ *et al.,* 1977) and the paraxial mesoderm layer interacts with the cranial neural crest (within the ectoderm) giving rise to craniofacial bones (Yoshida *et al.,* 2008, Evans and Noden, 2006). Typical bone formation begins with the clustering of undifferentiated MSC cells that undergo osteogenesis to produce osteoblasts, ultimately forming osteocytes ***(Figure 1.1).*** There are several transcription factors essential for the conversion of MSCs to osteoblasts, for example RUNX2 (runt-related transcription factor 2), OSX (osterix, also known as transcription factor SP7), IHH (Indian hedgehog), β-catenin, and ATF4 (activating transcription factor 4). RUNX2 is considered the master regulator of osteoblast differentiation and is required for terminal differentiation (Thomas *et al.,* 2004, Stein *et al.,* 2004) and IHH is a key regulator of osteogenesis (OMIM[1]: 600726)(Yoshida *et al.,* 2004). ATF4 is involved in regulating osteocyte terminal differentiation (Yang *et al.,* 2004).

[1] OMIM: Online Mendelian Inheritance in Man (www.ncbi.nlm.nih.gov/OMIM)

A calcifying matrix is essential in the production of bone, and expression of specific genes, for example, *ENPP1* (ectonucleotide pyrophosphatase /phosphodieserase 1) (Thomas *et al.,* 2004), and *PHOSPHO1* (a bone specific phosphotase)(Macrae *et al.,* 2010, Houston *et al.,* 2004), are essential in maintaining a homeostatic mineralised ECM. OSX (OMIM: 606633) has been shown to be required for mineralisation of the matrix with *Osx* null mice showing no mineralisation during endochondral ossification (Nakashima et al., 2002). Furthermore, *OSX* mutation in humans has been associated with osteogenesis imperfecta type XII (MIM: 613849), a disease associated with decreased bone mineral density and high incidence of fractures.

Bone homeostasis, essential for repair and maintenance, involves an ongoing process of synthesis of bone by osteoblasts and bone degradation by osteoclasts, phagocytic cells of monocyte lineage. β-catenin activity becomes obvious in later bone development and couples with the Wnt signalling pathway to regulate osteoclast /osteoblast turn over (Kramer *et al.,* 2010, Kokubu *et al.,* 2004, Glass *et al.,* 2005, Bodine and Komm, 2006). In addition, members of the TGFß (transforming growth factor beta) **(discussed in Section 1.3.1)** and BMP (bone morphogenetic protein) families have regulatory functions in bone development (Chen *et al.,* 2012). For example *Tgfb1* depleted mice had decrease bone growth and mineralisation (Geiser *et al.,* 2005) and the loss of *Bmp2* and *Bmp4* severely disrupted osteogenesis (Bandyopadhyay *et al.,* 2006). *BMP2* is also a regulator of *OCN* (osteocalcin), a leading gene in bone mineralisation (Huang *et al.,* 2010).

There are two types of bone tissue, depending on the characteristics of the osteoid matrix: woven bone and lamellar bone, that are developed during intermembranous or endochondral ossification, respectively. Ossification refers to the process of bone formation. Intramembranous ossification is a process that synthesises bone directly from connective tissue sheets (Dallas and Bonewald, 2010). The formation of lamellar bone and endochondral ossification will be discussed in **Section 1.1.5**.

1.1.5 Endochondral Ossification

As previously introduced **(Section 1.1.4)**, there are two major mechanisms involved in early bone formation: intramembranous ossification and endochondral ossification. Intramembranous ossification leads to the formation of cranial, jaw, and clavicle bone in the absence of cartilage tissue, ultimately forming flat bones in a developing organism **(Section 1.1.4)**. Endochondral ossification is the mechanism that creates and sustains long bone formation in the body, via a process of cartilage turn over and osteoblast mediated mineralisation (Goldring *et al.,* 2006, Mackie *et al.,* 2008).

Endochondral ossification (reviewed in (Mackie *et al.,* 2008) is initiated by chondrocyte driven production of hyaline cartilage. The hyaline cartilage (composed of condensed hypertrophic chondrocytes, producing a primary ossification centre) is encased in a perichondrium, a membrane that is then invaded by blood vessels transforming it into vascularised periosteum ***(Figure 1.2A)***. The newly formed vascularised periosteum recruits osteoblasts that then begin to secrete osteoid, forming a collar around the hyaline cartilage diaphysis (shaft) to maintain structure during mineralisation. Cartilage within the centre of the diaphysis (primary ossification site) begins to calcify and cavitates. This occurs due to chondrocyte apoptosis resulting from a lack of nutrients surrounding the chondrocytes and leading to the deterioration of the cartilage matrix ***(Figure 1.2B)***. Osteoblasts then invade the internal cavity (primary ossification site), laying down a mineralised matrix forming trabecular bone and the medullary cavity (storage unit for bone marrow). In addition, blood vessels invade the primary ossification site, and promote bone marrow formation. This requires vasculature formation as well as the presence of osteoblasts and osteoclasts. Osteoblasts secrete osteoid around the remaining hyaline cartilage to promote mineralisation and bone growth, and osteoclasts break down the calcified cartilage matrix during life ***(Figure 1.2C)***. Secondary ossification sites appear at both ends of the newly formed bone (epiphyses), and the above process is repeated ***(Figure 1.2B-Figure 1.2D)***. There is continuous bone turnover throughout the organism's lifespan. The bone collar is defined as compact bone later in life.

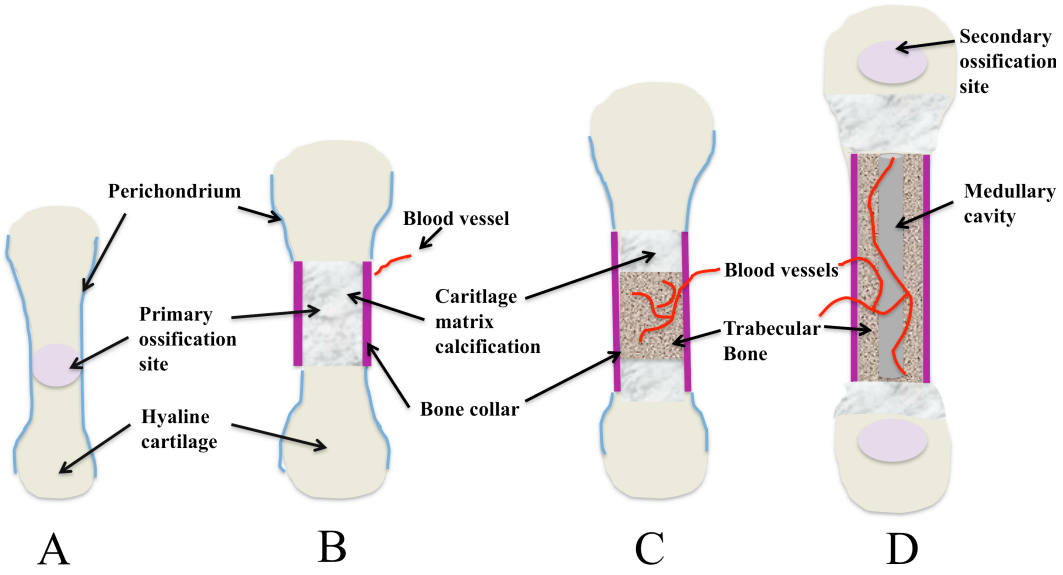

Figure 1.2. Endochondral ossification, producing long bones. (A) Hyaline cartilage becomes encased in a perichondrium casing (blue lines) and a primary ossification centre is formed (light purple). (B) Osteoid secretion promotes the growth of the bone collar (dark purple lines). The primary ossification site begins to calcify and produces pores (cavities) causing the deterioration of the hyaline cartilage matrix (noted by white mesh-work within the hyaline cartilage). (C) Osteoblasts and blood vessels invade the primary ossification centre promoting calcification and bone marrow production, respectively. The calcification leads to the formation of trabecular bone (dark grey stripped in the image), and the deterioration of the hyaline cartilage matrix continues on both the distal and proximal ends of the trabecular bone. (D) The medullary cavity is formed and bone marrow production begins. In addition, secondary ossification centres form at the distal and proximal ends of the newly created long bone, and steps (A-C) are repeated.

1.2 Extracellular Matrix

The ECM is a key characteristic of multi-cellular organisms and is composed of a meshwork of elastic and collagenous fibres, embedded in a hydrophilic ground substance consisting primarily of proteoglycans and glycoproteins (Alberts, 2002a). The basal lamina consists of two major compartments, an ECM space comprised of threadlike fibres and pores as well as a basement membrane consisting of sheet-like scaffolding that creates a platform for cells and boundaries between tissue compartments (Eshghi, 2008). In addition to providing a structural frame to various mesenchyme-derived tissues, the ECM mediates interactions between a range of growth factors and surface receptors (Alberts, 2002a). As mentioned above, there are differences in the ECM of connective tissue types. The differences are indicated by several factors, for example fibre organisation and components (**discussed in the following sections of Chapter 1**). The

major components of the ECM include, but are not limited to, collagens, laminins, fibronectin, elastin (reviewed in (Halper and Kjaer, 2014, Frantz *et al.,* 2010), the fibrillin family (Sakai *et al.,* 1986, Zhang *et al.,* 1994, Corson *et al.,* 2004, Keene *et al.,* 1991) and proteoglycans (such as decorin (Melo and Brandan, 1993) and biglycan (Mercado *et al.,* 2006)) embedded in a viscous ground substance hyaluronan (Toole, 2000)(***Figure 1.3)***. Hyaluronan (HA) is the ground substance of the ECM and is a viscous fluid that surrounds the ECM fibres (Laurent *et al.,* 1996) ***(Figure 1.3)***. HA is a polymer of the disaccharide glucuronic acid alternating with N-acetyl glucosamine and is a member of the GAG (glycosaminoglycan) polysaccharide family (Heatley and Scott, 1988). Unlike the majority of the GAG family, HA contains no sulphate groups, but like other GAG family members, it is a massive carbohydrate polymer of 10^4-10^5 kDa, and is synthesised in the inner side of the plasma membrane (Sedwick *et al.,* 1979, Kakehi *et al.,* 2003). Originally HA was thought to be responsible mainly for maintenance and structural integrity of the ECM, though it recently has been shown to be important in formation of embryonic heart (Toole, 2000) and cerebellum (Baier *et al.,* 2007).

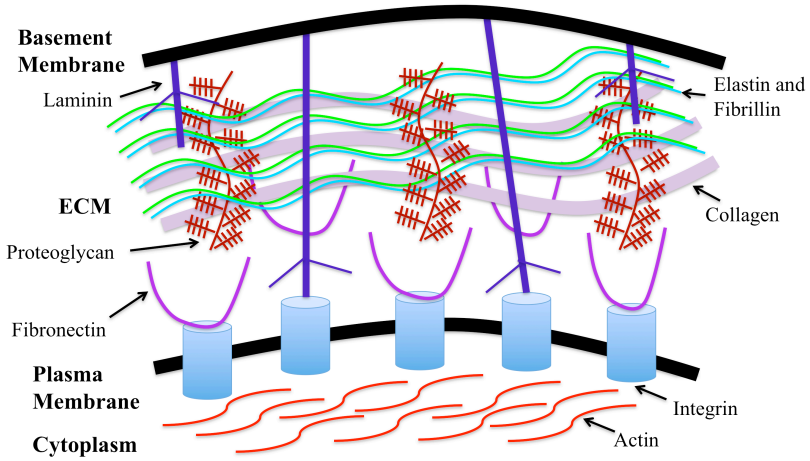

Figure 1.3. A schematic diagram of the ECM. This image depicts the various components of the ECM discussed in detail throughout Section 1.2. Legend from Top to Bottom: The black thick line represents the basement membrane (basal lamina). Laminin (dark blue trimers) extends downward into the ECM. Elastin (light blue) and fibrillin (bright green) 10 nM microfibres extend across the matrix. Collagen fibres (thick light purple lines) are stretched across the ECM in an organised fashion, and proteoglycans (maroon "tree" like structures) are vertically aligned between the basement and plasma membranes. Fibronectin (purple fibres) are either within in the ECM or bound to integrins (blue cylinders) that are embedded in the plasma membrane. The cytoplasm contains an actin (red fibres) network. Hyaluronan (not pictured) is present within the ECM, surrounding the described ECM components.

1.2.1 Collagen

Specific collagens provide tensile strength, maintain connective tissue organisation and make up one of the most abundant fibre types in the ECM. Initially, fibroblasts **(see Section 1.1.1)** were thought to be responsible for the secretion and synthesis of collagen fibres (Goldberg and Green, 1964), but epithelial cells have now been shown to have the capability to synthesise collagen (Hayashi *et al.,* 1988). There are currently 28 identified forms of collagen, though 80-90% of the collagen in the mammalian body consists of collagen I, II and III (Lodish *et al.*, 2000).

The structures of fibrous collagen proteins are similar. A description of collagen I, the main collagen constituent in bone, is given here. Collagen I consists of three coiled subunits, two alpha 1 chains and one alpha 2 chain. Each subunit has 1050 amino acids, containing repeating sequences of Gly-Pro-X (X=any amino acid) allowing these three subunits to combine to form a distinct three-stranded left-handed helical conformation, then binding of the strands continues to form a right handed triple helical structure (Ramachandran and Kartha, 1954, Ramachandran and Kartha, 1955, Rich and Crick, 1955, Bhattacharjee and Bansal, 2005, Shoulders and Raines, 2009)***(Figure 1.4)***. *COL1A1* and *COL1A2* mRNA is translated into procollagens, which are glycosylated, and hydroxylated in the endoplasmic reticulum (Yamauchi and Sricholpech, 2012, Jurgensen *et al.,* 2011). After posttranslational modification is complete, the triple helical monomers are assembled in the ECM and the propeptide sequence is removed, allowing the triple helical structure to polymerize with other collagen fibres (Stephens, 2012)(***Figure 1.4)***. The collagen fibres are then cross-linked side-by-side to form packed bundles (Fortunati *et al.,* 2014, van den Bogaerdt *et al.,* 2009) ***(Figure 1.3)***. The initial triple-helical structure and the packing into fibres assists in providing strength to bone in the body (Fortunati *et al.,* 2014).

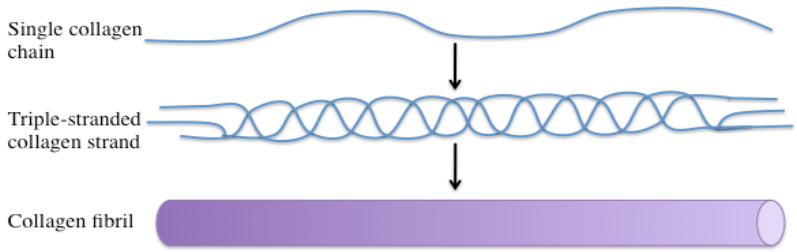

Figure 1.4. A schematic of collagen formation. A single polypeptide collagen chain is synthesised in ER. The chain self assembles following posttranslational modifications, to form a three stranded helical collagen strand within the ER. The propeptides are secreted into the ECM and cleaved to from the triple helical structure and the collagen is self assembled into collagen fibrils. The collagen fibrils are bound (Section 1.2.1), and the collagen fibres are incorporated into the ECM as shown in *Figure 1.3*.

There are many other collagen-packing techniques that have been recognised in connective tissues. As previously mentioned in **Section 1.1.3**, cartilage tissue is mainly comprised of collagen II and collagen IX. Collagen II fibres are smaller in diameter than collagen I fibres, and are randomly dispersed throughout the ECM in a proteoglycan rich and hyaluronan based viscous ECM (Li *et al.,* 2006). It is this compressible structure that allows for shock absorption in vertebrate joints. Collagen IX is a non-fibrous short chain collagen protein that contains two alpha subunits, and assists in cross-linking collagen molecules (McCormick *et al.,* 1987, Mayne *et al.,* 1985). For example, in cartilage collagen IX anchors (through crosslinking) collagen II fibres to the proteoglycans (Diab *et al.,* 1996, Eyre *et al.,* 2004). The role of collagen II in cartilage is highlighted by the phenotypes associated with mutations within the collagen II gene (*COL2A1*) which give rise to multiple connective tissue diseases (OMIM: 120140) including osteoarthritis with mild chondrodysplasia (MIM: 604864). Similarly, the regulatory role of collagen IX in cartilage maintenance is also evident from the phenotype of *Col9a1* null mice, which develop chronic joint disease (Fassler *et al.,* 1994).

In addition to bone and cartilage, collagen is a major component of skin and adipose connective tissue. Collagen IV is synthesised in the ER producing procollagen strands (Abreu-Velez and Howard, 2012). However, once the strands emerge from the ER, the C-terminus propeptide is not removed. The amino acid sequence does not contain the glycine residue every three bases (Abreu-Velez and Howard, 2012), allowing this

collagen to align in a head to tail fashion within the basement membrane along with laminin **(Discussed in Section 1.2.3)** (Vega *et al.,* 1995). This arrangement allows the tissue to be more pliable and form collagen-based sheets, and along with epithelial cells, give rise to the structure of the epidermis.

Although collagen IV is the leading collagen fibre produced by dermal fibroblasts, foetal bovine fibroblast studies indicated the importance of a collagen VI matrix in the development of the ECM in skin (Kielty *et al.,* 1993). Collagen VI can be found in most connective tissues of the body although it was characterised in bovine skin samples (Kielty *et al.,* 1992, Sato *et al.,* 1979). mRNA for different collagen VI alpha chains are also abundant in adipose and smooth muscle cells (http://biogps.org) and protein expression has been characterised in the synovial lining of human and bovine joints (Waggett *et al.,* 1993). Collagen VI is the highest expressing collagen in adipose tissue and levels of both protein and mRNA are elevated in obese patients (Pasarica *et al.,* 2009). Collagen VI forms triple-helical trimer structures, which are then disulfide bonded in pairs forming anti-parallel dimers (Engel *et al.,* 1985). Two of these dimers are crosslinked to form a secreted tetramer that is assembled in a head to tail, beaded fashion (Engel *et al.,* 1985, Keene *et al.,* 1991). Collagen VI may be involved in adipose tissue inflammation (Pasarica *et al.,* 2009).

1.2.2 Elastin

Elastin, encoded by *ELN* (OMIM: 130160) is an important fibrous structure of the ECM. It is a component of the elastic fibres and is anchored to the ECM by microfibrillar components, such as fibrillin **(See Section 1.3)** ***(Figure 1.3)***. Microfibrils are abundant within the ECM of elastic tissues (Kielty *et al.,* 1991). The tropoelastin protein is a 72kDa soluble polypeptide which consists mainly of glycine, proline and other hydrophobic amino acid residues that are translated to produce monomers, that then self assemble into fibres due to the hydrophobic domains (Cirulis *et al.,* 2008). The monomers are crosslinked to one another through lysine residues by multiple members of the lysyl oxidase family, forming desmosine crosslinks (Kagan and Sullivan, 1982,

Noblesse *et al.,* 2004). Elastin polymers make up the majority of the elastic fibres. Non-elastin components include proteins such as the fibrillins **(Discussed in Section 1.3)** ***(Figure 1.3)***. A key feature of elastin fibres is their elastic and recoil capabilities. As the elastin monomers assemble, they create left-handed helices (similar to collagen) (**Section 1.2.1)** that contain no intramolecular hydrogen bonds (Bochicchio and Tamburro, 2002, Rauscher *et al.,* 2006). This along with multiple glycine rich domains provides flexibility to the protein and thus to the elastic fibres (Jensen *et al.,* 2000). Elastin aligns to fibrillin-1 or fibrillin-2 microfibrils (Michie *et al.,* 2000, Zhang *et al.,* 1994) and is thought to be stabilised by desmosine crosslinks (Akagawa and Suyama, 2000, Ma *et al.,* 2003, Bernstein *et al.,* 1994). The elastin based fibres are cross-linked to fibrillin microfibrils to form the elastic matrix of the ECM, which has been widely observed in both foetal and adult bovine fibroblasts for many years (Jones *et al.,* 1980, Ross and Bornstein, 1969, Kewley *et al.,* 1978). The fibrillin proteins will be discussed in detail in **Section 1.3**.

1.2.3 Laminin

Laminins are a key structural component of the basement membrane and are secreted into the ECM of connective tissues to assist in the maintenance of elasticity and cell adhesion (Yurchenco *et al.,* 2004) ***(Figure 1.3)***. The basement membrane is comprised of both an internal basal lamina and external reticular lamina layer, both with distinct protein composition. To date, a total of 16 heterotrimeric laminin proteins, consisting of an alpha, beta and gamma subunit, have been identified (Aumailley *et al.,* 2005). The proteins are assembled intracellularly starting with the beta and gamma subunits followed by the addition of the alpha subunit (Hamill *et al.,* 2009). The heterotrimeric protein is then secreted into the ECM where they interact with the integrins of the plasma membrane. Integrins are heterodimeric receptors that link the intracellular cytoskeleton to the ECM ***(Figure 1.3)***, and are responsible for the majority of communication between the intra and extracellular regions of the cell through interactions with laminins (Kikkawa *et al.,* 2000, Delwel *et al.,* 1994, Nishiuchi *et al.,* 2006) and fibronectin **(Discussed in Section 1.2.4)** (Engel *et al.,* 1981). Laminins can also be connected with the basement membrane, forming a link between the cell and its surrounding environment ***(Figure 1.3)***.

1.2.4 Fibronectin

Fibronectin (encoded by *FN1*) (OMIM: 135600) is a 440kDa glycoprotein that is important in the maintenance of the ECM and cellular adhesion. Mature fibronectin consists of two homologous monomers linked by a disulfide bond (Singh *et al.,* 2010). Alternate splicing of the *FN1* mRNA leads to different isoforms (Ffrench-Constant and Hynes, 1989, Barnes *et al.,* 1995, Gutman and Kornblihtt, 1987). Fibronectin exists as a plasma soluble form (localised mainly to blood plasma) (Ylatupa *et al.,* 1995, Zardi *et al.,* 1979, Chauhan *et al.,* 2008) and an insoluble cellular form (To and Midwood, 2011), mainly secreted by fibroblast cells (Grinnell and Feld, 1979), that can be present on cell surfaces (Xu *et al.,* 2009) and within the basement membrane **(Section 1.2.3)**, throughout connective tissues (Mao and Schwarzbauer, 2005)(http://biogps.org). Insoluble fibonectin is organised as an elongated, branched fibril network tightly controlled for fast up or down regulation (Sevilla *et al.,* 2010) ***(Figure 1.3)***. In addition to ECM development it is involved in cytoskeleton organisation via interactions with the cell membrane (Baneyx *et al.,* 2002, Welch *et al.,* 1990). The fibronectin fibre network is assembled at the cell surface after secretion. Soluble compact fibronectin dimers are within the extracellular space can then bind to membrane bound integrins (Yonezawa *et al.,* 1996). The dimers of fibronectin cluster and stretch or lengthen across the cell surface. Fibronectin contains one RGD (Arg-Gly-Asp) ligand-binding site demonstrating integrin mediated binding capability. It is also capable of direct binding with membrane bound integrin alpha 9 beta 1 and alpha 4 beta 1 (Liao *et al.,* 2002). Integrin binding supports cell adhesion (Ruoslahti, 1996, Shiokawa *et al.,* 1999) and integrin- RGD binding is essential in embryonic development (Takahashi *et al.,* 2007). Fibronectin contains heparan sulphate binding sites (Mostafavi-Pour *et al.,* 2001) and dermatopontin binding sites (involved in wound repair) (Kato *et al.,* 2014) as well as binding sites for many other molecules. Fibronectin protein expression was shown to be essential within multiple organ systems when *Fn1* null mice were found to be embryonic lethal (Howerton *et al.,* 2008). Fibronectin has been implicated as a lead protein in wound repair **(discussed in Chapter 4)**, through interactions with the acidic ECM protein dermatopontin (Okamoto and Fujiwara, 2006, Kato *et al.,* 2014). Fibronectin, in mesenchymal cell types, is also

required for 10 nm microfibril deposition (Sabatier *et al.,* 2009, Kinsey *et al.,* 2008), anchors the collagen matrix to the plasma membrane (Erat *et al.,* 2013) and assists in the organisation of the collagen fibres (Sevilla *et al.,* 2013, Li *et al.,* 2003).

1.2.5 Cytoskeletal actin

The ECM interacts with the interior of the cell through cytoskeleton proteins, particularly cytoskeletal actin. Actin is a major cytoskeletal protein forming approximately 7nM actin filaments, known as microfilaments (reviewed by (Dominguez and Holmes, 2011)), found within the cytoskeleton ***(Figure 1.3)***. Microfilaments are highly ordered structures that can be synthesised to form either actin bundles (Splettstoesser *et al.,* 2011) or a three dimensional network (Narita *et al.,* 2011, Tang *et al.,* 2001). These structures provide mechanical support (Chanet and Martin, 2014), form adherens junctions (Peglion *et al.,* 2014, de Rooij, 2014), and determine cell shape (Mogilner and Rubinstein, 2010) and cellular movement (Mitchison and Cramer, 1996, Kozuka *et al.,* 2007). Actin monomers are globular proteins (G-actin) and consist of approximately 375 amino acids (Vandekerckhove and Weber, 1979). Three G-actin monomers, containing multiple G-actin binding sites, then arrange in a head to tail configuration-forming F-actin (filamentous actin)(Holmes *et al.,* 1990). The head to tail arrangement creates polarity on the ends of the F-actin, one end with a positive charge and the other with a negative charge (Cooper, 2000). Filamentous actin bundles are synthesised by two different mechanisms depending on the proteins bound to the monomers (Cooper, 2000). For example, in microvilli of the intestines, bundling protein, fimbrin, binds actin monomers in a tight parallel fashion (Mukherjee and Williams, 1967). In the creation of contractural bundles, alpha actinin binds the G-actin loosely in a parallel fashion (Rimm *et al.,* 1995), improving interactions with contractile protein, myosin (Burnette *et al.,* 2014). Three-dimensional networks are formed by crosslinking F-actin by filamin proteins that form a V shaped conformation (Holmes *et al.,* 1990). This allows the network to create adherens junctions and interact with plasma membrane integrins that directly interact with the ECM (Hirata *et al.,* 2014), including fibrillins ***(Figure 1.3)***.

1.3 Fibrillins

Although collagens, laminins and fibronectin are the main protein components of the ECM **(see Section 1.2)** the glycoprotein family consisting of fibrillins (fibrillin-1, fibrillin-2 and fibrillin-3 in most mammals) are major proteins in the structure and function of 10nm elastin associated microfibrils within the ECM (Sakai *et al.,* 1986) (Zhang *et al.,* 1994, Corson *et al.,* 2004) ***(Figure 1.3)***. In addition to a structural role in the microfibrils, fibrillin is thought to aid in the sequestering of TGFβs through interactions with latent TGFβ- binding proteins, LTBP1, LTBP3 and LTBP4 (Isogai *et al.,* 2003, Massam-Wu *et al.,* 2010, Nistala *et al.,* 2010b, Zilberberg *et al.,* 2012).

Fibrillins are glycoproteins of approximately 350kD that are located throughout the ECM. They are associated with the majority of connective tissue types (Sakai *et al.,* 1986, Keene *et al.,* 1991). Fibrillin-1 was first isolated from human fibroblast cultures and identified as the leading component of 10nm microfibrils in the ECM, through immunogold electron microscopy using a monoclonal antibody (Sakai *et al.,* 1986). The *FBN1* gene is ubiquitously expressed in mesenchymal cell types (Summers *et al.,* 2010). Fibrilllin-1 is first synthesised as a proprotein and processing occurs outside the cell by members of the furin family (Wallis *et al.,* 2003, Milewicz *et al.,* 1995). The *FBN2* gene was identified through its homology with *FBN1* and fibrillin-2 protein was shown to be a microfibril component through immunohistochemistry and localisation techniques in a human osteosarcoma cell line, MG-63, and human foetal tissue sections (Lee *et al.,* 1991, Zhang *et al.,* 1994). It is particularly prevalent in elastin rich matrices (Zhang *et al.,* 1994, Lin *et al.,* 2002). As discussed below, *FBN2* mRNA is found in fewer tissues and developmental stages than *FBN1*, although both are expressed at high levels in bone, osteoblasts and chondrocytes (Summers *et al.,* 2010). While the localization and expression of fibrillin-1 and fibrillin-2 have been well characterised, expression of fibrillin-3 is primarily in foetal tissues, particularly the brain, and was reported to be absent from the Muridae family (Corson *et al.,* 2004), where only a degenerate *Fbn3* gene could be detected.

1.3.1 Fibrillin makes 10nm microfibrils

Fibrillin-based microfibrils can form one, two and three-dimensional structures. For example, the linear fibres (lamina cribrosam) of the ciliary zonule, which anchor the eye lens, are composed primarily of fibrillin-1, without elastin (Hernandez, 1992, Wess *et al.,* 1997, Wess *et al.,* 1998, Hanssen *et al.,* 1998). Intercalating between the smooth muscle of the aortic tunica media, they form a two-dimensional network while in skin fibrillin microfibrils form a three dimensional meshwork of microfibrils complexed with elastin to form elastic fibres (Ramirez *et al.,* 2004, Kielty and Shuttleworth, 1997).

The exact mechanism for the assembly of these structures is not well understood. Fibrillin monomers link in a head to tail manner resulting in a beaded appearance (Kielty *et al.,* 2002, Reinhardt *et al.,* 1996), which has been hypothesised to mediate the ability of the proteins to form multi-dimensional interactions (Sakai *et al.,* 1986, Arnaout, 2004, Lin *et al.,* 2002, Kielty and Shuttleworth, 1993a, Mariencheck *et al.,* 1995). In vascular smooth muscle formation, fibrillin is known to provide a structured framework for tropoelastin deposition that then cross link to form elastic microfibrils **(See Section 1.2.2)**. Elastin interacts with fibrillin-1 near the third TB (TGFß-binding protein-like) domain **(Section 1.3.2)**. The cross linking of elastin to fibrillin microfibrils may be an important aspect of elastic fibre assembly (Rock *et al.,* 2004). However, in *Fbn1* null mice which lack fibrillin-1 protein, the vascular smooth muscle cells (VSMC) produced viable cross linked elastic fibres, although there was abnormal medial ECM formation (Carta *et al.,* 2006). This suggested that fibrillin-1 is not necessary for tropoelastin cross linking in elastin fibre formation.

Fibrillin-2 appears in microfibrils in the early stages of embryogenesis (in contrast to fibrillin-1, which was first detected later in development), and is primarily restricted to bone and cartilage matrices in adult tissues (Zhang *et al.,* 1994, Nistala *et al.,* 2010b, Mariencheck *et al.,* 1995). It is not understood how fibrillin-3 contributes to microfibril structure, but the similarity of its protein structure to fibrillin-1 and fibrillin-2 suggests that the same interactions are possible **(Section 1.3.2)**. *FBN3* mRNA is mainly present in embryonic and foetal tissues, where its expression is low (Corson *et al.,* 2004).

Continuing research will be required to better understand the unique mechanism of multi-dimensional microfibril formation and the role of the three fibrillins at different developmental stages.

1.3.2 Fibrillin and LTBP structure

The primary protein structure of members of the fibrillin family is shown in ***Figure 1.5***. Fibrillins contain 47 epidermal growth factor-like (EGF) domains of which 43 are calcium binding EGF type (cbEGF domains) ***(*shown in *Figure 1.5)***. EGF domains are found in a range of proteins, including BMP1 (bone morphogenetic protein) (NM_001199), TGFα (transforming growth factor alpha, NM_ 001099691) and NOTCH 1 (a member of the type 1 transmembrane protein family, NM_017617). The cbEGF domains (along with calcium) have important structural significance in the production of beaded fibrillin microfibres (Kielty and Shuttleworth, 1993b, Reinhardt *et al.,* 1997). Unique to fibrillins and the closely related latent transforming growth factor beta binding proteins (LTBPs) are the 8 cysteine domains (TB domains) of which seven are found in fibrillins (Dyer *et al.,* 1995) while three are present in each LTBP protein (Robertson *et al.,* 2010). LTBP proteins are smaller than fibrillins but their overall structure is similar (Robertson *et al.,* 2010, Davis *et al.,* 2014). A degenerate form of the 8 cysteine domain (containing only 6 cysteines) is also found in two members of the follistatin family, FST and FSTL3, which do not share any other functional domains (Wilson *et al.,* 2009).

The structural elements of the fibrillin proteins vary slightly in that fibrillin-1 contains a proline-rich internal domain, while in fibrillin-2 this domain is composed of a glycine-rich region. Fibrillin 3 contains an internal domain rich in both glycine and proline ***(Figure 1.5)***.

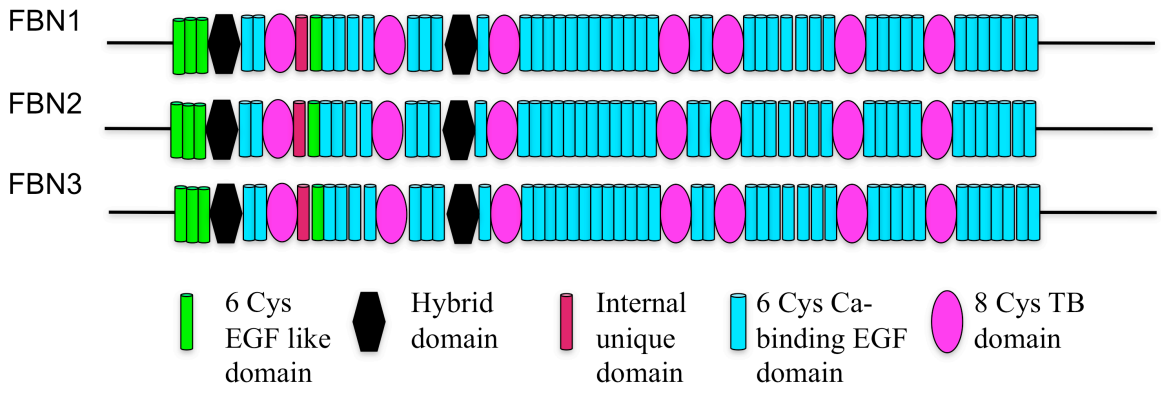

Figure 1.5. The structural components of the fibrillin and LTBP protein family. (Redrawn from (Charbonneau *et al.,* 2004, Handford *et al.,* 2000, Isogai *et al*., 2003).

Fibrillin-1, fibrillin-2 and fibrillin-3 also contain heparan sulfate binding motifs (Cain *et al.,* 2008, Cain *et al.,* 2012, Sabatier *et al.,* 2014, Ritty *et al.,* 2003). Heparan sulfate proteoglycans are glycoproteins, which interact with multiple ligands, mediate matrix cell migration and wound repair, aid in protecting against proteolysis, can act as receptors for proteases and their inhibitors as well as aiding in cell-ECM attachment through integrin binding. Their roles and functions are extensively reviewed in (Sarrazin *et al.,* 2011). Fibrillin -1 has over six well-documented heparan sulphate binding sites, and recently more have been identified in the C and N terminus regions of the protein (Cain *et al.,* 2008). The heparan sulphate binding sites in the N terminus and C terminus of fibrillin-1 mediate different regulatory pathways. For example, heparan binds to the C-terminal heparan-binding site of fibrillin-1, inhibiting interactions with tropoelastin, therefore causing disruption in elastin deposition (Cain *et al.,* 2008). The N terminus binding sites are crucial in fibrillin-1 polymerisation during fibre assembly (Cain *et al.,* 2008). Fibrillin-2 has several high affinity heparan binding sites in both the N and C terminus, and fibrillin-3 has binding regions within the C terminus (Sabatier *et al.,* 2014). It is predicted that the heparan sulfate interactions with the fibrillin family are important in microfibril formation and structure.

1.3.3 Fibrillin in the sequestering of TGFß

LTBPs together with fibrillin-1 and fibrillin-2 are involved in the inactivation of TGFβ, an important regulator of connective tissue function (Flaumenhaft *et al.,* 1993, Nakajima *et al.,* 1997). The proposed mechanism is shown in ***Figure 1.6***. There are three genes encoding TGFβ molecules (*TGFB1*, *TGFB2* and *TGFB3*). All three are initially synthesised as larger precursor molecules, which are then cleaved to form two peptides. The N-terminal end forms the latency associated peptide (LAP) while the remainder contains the active TGFβ molecule, which forms a homodimer, which is complexed with the LAP in the cytoplasm to form the small latency complex, or SLC. The SLC binds to an LTBP molecule (LTBP1, LTBP3 or LTBP4) through disulphide bonds to the second 8-cysteine domain, forming the large latency complex (LLC). The LLC is then secreted into the ECM where it maintains TGFβ in an inactive state ***(Figure 1.6A)***. Release of the TGFβ homodimer from the LLC allows it to bind to its receptors (TGFBR1 and TGFBR2) on the cell surface and initiate a response, primarily through SMAD signalling, which contributes to the regulation of cell division and the epithelial mesenchyme transition (EMT) (**Chapter 3**)(Annes *et al.,* 2003, Derynck *et al.,* 1985, Dubois *et al.,* 1995, Saharinen *et al.,* 1996) ***(Figure 1.6B)***. TGFβ can be activated (released) through RGD-mediated integrin binding in the LAP (Yang *et al.,* 2007), conformational changes within the SLC (Annes *et al.,* 2004, Wipff and Hinz, 2008), and/or the SLC interacting through the actin cytoskeleton (Annes *et al.,* 2004, Munger *et al.,* 1999, Yoshinaga *et al.,* 2008, Shi *et al.,* 2011). Fibrillin-1 and fibrillin-2 are thought to aid in the inactivation of TGFβ in the ECM through interactions with LTBPs (Isogai *et al.,* 2003)(***Figure 1.6A).*** The role of fibrillin-3 in modulating levels of active TGFβ has not been clarified. The current understanding of fibrillin, LTBP and TGFβ interaction is depicted in ***Figure 1.6***.

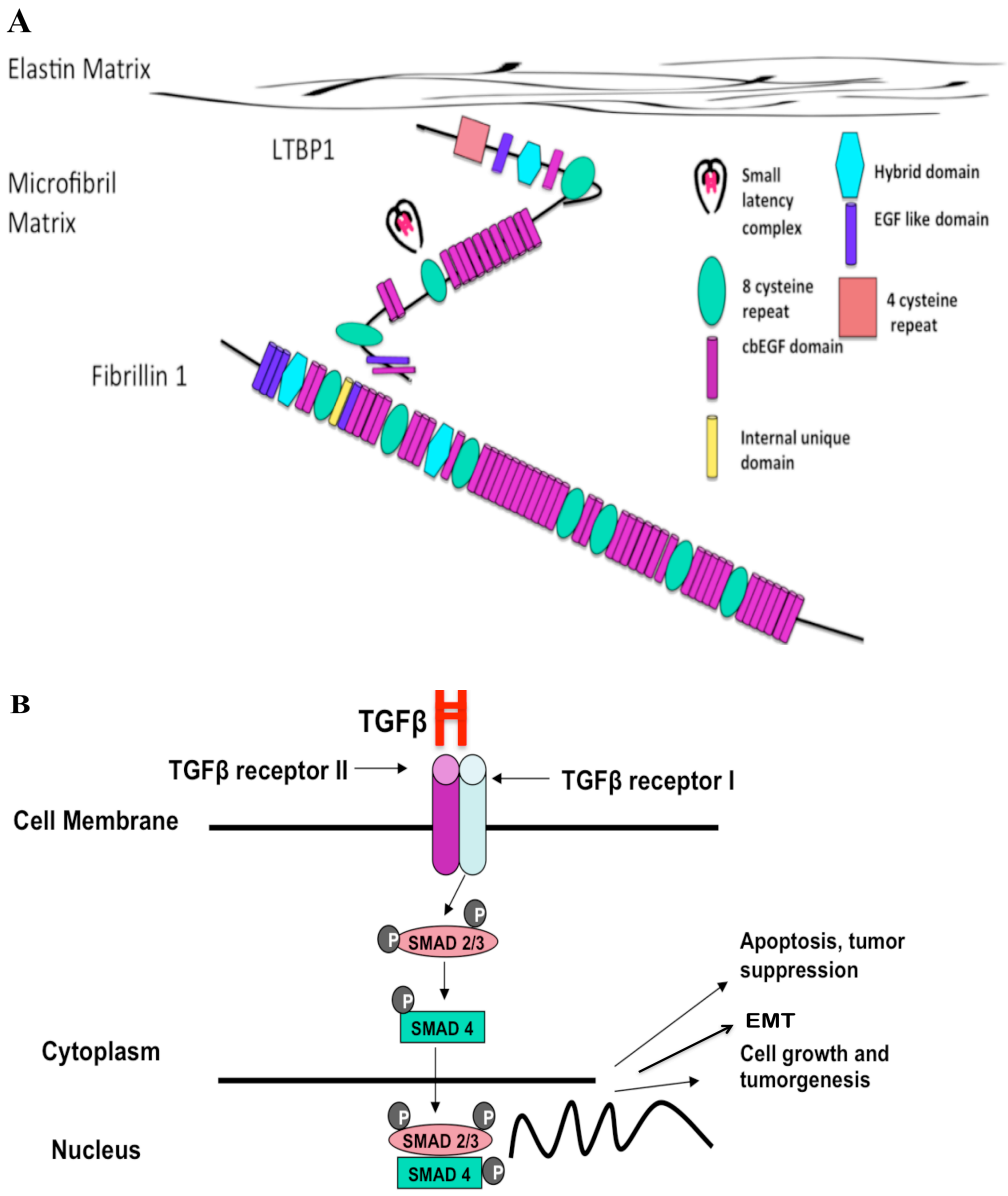

Figure 1.6. LTBP and Fibrillin 1 interactions leading to the sequestering of TGFß. (A) Interactions between fibrillin and LTBP controlling the bioavailability of TFGß. Both the mature TGFβ homodimer and the LAP are contained within the SLC that then forms a disulfide bond to the second TB domain of LTBP1 forming the LLC. The LLC is released from the cell and binds to the N terminus of fibrillin-1 thereby sequestering TGFβ in an inactive form. (B) TGFß activation and SMAD signalling. Active TGFβ is released (See Section 1.3.3) and binds with TGFβ receptors. This stimulates a phosphorylation cascade involving SMAD signalling. SMAD 2/SMAD3 are phosphorylated, leading to the phosphorylation of SMAD 4. SMAD2/3 and SMAD4 cross the nuclear membrane and act as transcription factors to signal further cellular process such as cell growth and apoptosis. TGFβ can also signal via a non-canonical ERK pathway (not shown)(Discussed in Chapter 5). The image was adapted from (Hyytiainen *et al.*, 2004).

The LLC is anchored to the ECM by an interaction between the C-terminus of LTBP-1 and the N terminus region of fibrillin-1 (Isogai *et al.,* 2003) ***(Figure 1.6A)***. LTBP-1 has been shown to co-localize with fibrillin-1 and fibrillin-2 during microfibril assembly (Massam-Wu *et al.,* 2010). LTBP-4 binds with the N terminus of fibrillin-1 with high affinity while LTBP-3 does not bind with the same region, suggesting alternative binding sites throughout fibrillin-1 (Isog*ai et al.,* 2003). LTBP2 appears to compete with LTBP1 for binding with fibrillin-1 microfibrils, therefore LTBP2 maybe an indirect negative regulator for TGFβ storage (Isogai *et al.,* 2003, Hirani *et al.,* 2007). Although the fibrillins do not bind TGFβ or the SLC directly, these interactions with the LTBPs indicate a contribution of the fibrillins to the regulation of TGFβ (Massam-Wu *et al.,* 2010). Since TGFβ is a major factor in the differentiation of epithelial cell types to mesenchymal cell types (epithelial-mesenchyme transition, EMT) (Zavadil and Bottinger, 2005)**(Described in Chapter 3)** and in maintaining ECM formation (Miettinen *et al.,* 1994), the interactions with LTBPs and hence TGFβ suggest fibrillin proteins may play an important regulatory role in the process of differentiation.

The TGFβs are members of a large gene and protein superfamily, which also includes the BMP proteins, myostatin, the activin/inhibin subfamily, and other structurally related members. TGFβs and BMPs (but not myostatin) are widely sequestered throughout the bone matrix, through interactions with LTBPs and fibrillins (Nistala *et al.,* 2010b, Ramirez and Sakai, 2009, Arteaga-Solis *et al.,* 2001, Sengle *et al.,* 2010, Sengle *et al.,* 2008), as discussed above. In addition, TGFBR2 has a key role in endochondral ossification, and studies in mouse models have shown that depletion of *Tgfbr2* led to incomplete and defective long bone formation (Sueyoshi *et al.,* 2012). Sueyoshi *et al.,* (2012) showed that the downregulation of *Tgfbr2* had a direct effect on chondrogenesis in endochondral ossification, therefore showing that TGFβ signalling is important in chondrogenesis. TGFβ also plays a role in regulating fibroblast activity (Clark *et al.,* 1997), with stimulation of a wound repair matrix following treatment with TGFβ. Furthermore, TGFβ signalling has a role in adipose homeostasis. As previously described, TGFβ binds to its receptors initiating a SMAD phosphorylation cascade ***(Figure 1.6B)***. In *Smad3* knockout mice, it was shown that blocking TGFβ signalling

protected the mice from weight gain, a common phenotype in *Smad3* depleted mice (Yadav *et al.,* 2011), thereby implicating TGFβ in inducing adipose formation.

It is thus thought that fibrillins have both a structural role in forming the 10nm microfibrils and a regulatory role in the sequestration of TGFβ, which is made more obvious in connective tissue disorders arising from mutations in the *FBN1* and *FBN2* genes, for example Marfan syndrome. These will be discussed in the following sections.

1.3.4 Phenotypes associated with Fibrillin-1 Mutations

As shown above, fibrillins are an integral component of the ECM, and therefore mutations in the genes encoding them are likely to cause disruption of the connective tissue. Over 2,000 *FBN1* mutations have been identified and the majority are associated with the autosomal dominant connective tissue disorder, Marfan syndrome (MFS, OMIM 154700)(Collod-Beroud *et al.,* 2003). The prevalence of MFS is about1 in 5,000 affected individuals worldwide (Genetics Home Reference Database, http://ghr.nlm.nih.gov/condition /marfan-syndrome). MFS causes multiple signs and symptoms primarily affecting the ocular, skeletal and cardiovascular systems (Dietz *et al.,* 1991, Loeys *et al.,* 2010, McInerney-Leo *et al.,* 2014). Marfan syndrome is currently diagnosed using the revised Ghent criteria (reviewed by (Summers *et al.,* 2012)). The MFS phenotype includes chest wall abnormalities, ectopia lentis, aortic aneurysm and dissection, overgrowth of long bones and depleted adipose tissue. These manifestations of *FBN1* mutations are consistent with the structural role of fibrillin-1 in the ECM. In addition, studies of mouse models and cultured skin fibroblasts from patients have shown that the level of active TGFβ is higher in patients and mutant mice than in controls (Neptune *et al.,* 2003, Nataatmadja *et al.,* 2006, Matt *et al.,* 2009)***(Table 1.2)***. In *Fbn1* null mice, TGFß and BMP levels are also very high in osteoblasts (Nistala *et al.,* 2010b). These results suggest that the control of TGFß activity is an important physiological function of fibrillin-1 in at least the cardiovascular and skeletal systems.

The phenotype of *FBN1* mutations in humans varies from a severe neonatal form of MFS, which is lethal in the first few years of life to relatively mild familial ectopia lentis or familial scoliosis (Loeys *et al.,* 2010, McInerney-Leo *et al.,* 2014, Faivre *et al.,* 2007).

Some families with autosomal dominant familial aortic aneurysm segregate *FBN1* mutations, which are also associated with a number of other dominant conditions **(Table 1.1)**.

Disorder/Syndrome/Phenotype	**OMIM number**
Marfan Syndrome	154700
Ectopia lentis	129600
MASS syndrome	604308
Sphrintzen-Goldberg craniosynostosis	182212
Stiff skin syndrome	184900
Weill-Marchesani syndrome	608328
Acromicric dysplasia	102370
Geleophysic dysplasia	614185
Ascending aortic aneurysm and dissection	(Francke *et al.,* 1995)
Lipodystrophy	(Graul-Neumann *et al.,* 2010)

Table 1.1. Phenotypes associated with mutations in *FBN1*. Data derived from Online Mendelian Inheritance in Man (OMIM, http://www.ncbi.nlm.nih.gov.ezproxy.is.ed.ac.uk/omim/) except where a reference is given.

Most of the mutations in *FBN1* are missense, usually adding or removing a cysteine residue or involving one of the amino acids of the calcium-binding pocket. The neonatal MFS mutations (responsible for the severe disease) appear within the confines of exon 24 (encoding the fifth TB domain, ***Figure 1.5***) to exon 32 (Faivre *et al.,* 2009).

Knockout and transgenic mice have been created for fibrillin-1 and fibrillin-2. The phenotypes of the mouse models are summarised in ***Table 1.2.*** The mouse models do not always replicate the human phenotype. For example, mutation or inactivation of mouse *Fbn1* may not show a heterozygous phenotype, nor the phenotypic variability common in human families. However the phenotypes are consistent with connective tissue abnormalities similar to those seen in human disease, such as MFS and fibrillin-2 associated disorders **(Chapter 1, Section 1.3.5)*(Table 1.2)***.

Gene	Mutation	Phenotype	Reference
Fbn1$^{tm1.2Lysa}$	Inversion, Insertion- targeted mutation	MFS model	Charbonneau *et al.,* 2010
Fbn1$^{tm2.1Iysa}$	Insertion/Deletion/Targeted	MFS Model	Charbonneau *et al.,* 2010
Fbn1$^{tm3.2Lysa}$	Insertion/Deletion/Targeted	MFS model	Sengle et al., 2010
Fbn1^{tm1Hcd}	Single mutation	MFS model, including respiratory defects	Judge *et al.,* 2004
Fbn1$^{tm2.1Hcd}$	Insertion	Early MFS model (embryonic lethal)	Gerber et al., 2013
Fbn1$^{tm3.1Hcd}$	Insertion	Skin defects	Gerber et al., 2013
Fbn1^{tm1Lper}	Insertion, deletion	MFS model	Lima *et al.,* 2010
Fbn1^{tm1Rmz}	Deletion	MFS model, including respiratory defects	Pereira *et al.,* 1997
Fbn1^{tm2Rmz}	Insertion	Cardiovascular, respiratory, skeletal and muscular defects, mortality	Pereira *et al.,* 1999
Fbn1^{tm3Rmz}	Insertion and intragentic deletion	Cardiovascular and skeletal defects	Carta *et al.,* 2006
Fbn1^{tsk}	Spontaneous partial duplication	MFS, scleroderma, Stiff skin syndrome, tight skin	Blake et al., 2014
Fbn2^{fp-2J}	Spontaneous allele deletion	Arachnodactyly	Blake et al., 2014
Fbn2^{fp}	Spontaneous allele deletion	Fused phalanges	Blake et al., 2014
Fbn2^{mz}	Allele deletion, chemically induced	CCA	Miller *et al.,* 2010
Fbn2^{fp-4J}	Spontaneous allele deletion	CCA	Blake et al., 2014
Fbn2^{fp-3J}	Allele deletion, chemically induced	CCA	Munroe *et al.,* 2000
Fbn2^{tm1Rmz}	Targeted mutation	CCA	Arteaga-Solis *et al.,* 2001

Table 1.2. A list of *Fbn1* and *Fbn2* knockout and transgenic mouse models.

There is currently no cure for MFS. However, some drug therapies have been shown to be effective in reducing the risk of aortic dissection/aneurysm and osteopenia (a mild decrease in bone mineral density). Due to the progressive nature of aortic dissection and aneurysm leading to premature death in patients with severe MFS, one of the first therapeutic treatments offered was the use of beta-blockers, propanolol (Shores *et al.,*

1994) and atenolol (Vaidyanathan, 2008, Yetman *et al.,* 2005). These drugs belong to the class of beta-adrenergic blocking agents that prevent the binding of the hormone adrenaline to its receptors on the cell surface, thereby lowering heart rate and blood pressure. The reduced blood pressure and heart rate were thought to lower the stress applied to the aorta and other cardiovascular components. Early studies of the use of beta-blockers in MFS patients showed that it slows the rate of dissection and aneurysm, though beta-blockers do not have regenerative properties (Ose and McKusick, 1977, Shores *et al.,* 1994). Angiotensin-converting enzyme (ACE) inhibitors have also been used to slow aortic dilatation in patients with intolerance to beta blockers (Yetman *et al.,* 2005). They act to inhibit the conversion of angiotensin I to angiotension II, which is catalyzed by ACE. The reduction of angiotensin in the system leads to vasodilatation and therefore a decrease in blood pressure and stress on the cardiovascular system (van Vark *et al.,* 2012). For example, ACE inhibitor enalapril was shown to reduce aortic stiffness and progression of dissection (Yetman *et al.,* 2005). More recently, treatment with losartan, an angiotensin II receptor 1 blocker, was found to lower TGFß activity, improve aortic wall recovery and prevent aortic dissection in a mouse model (Nistala *et al.,* 2010a, Habashi *et al.,* 2006, Groenink *et al.,* 2013, Trindade, 2013, Pees *et al.,* 2013), and was more effective than treatment with enalapril (Habashi *et al.,* 2011). Losartan is currently undergoing clinical trials to assess its therapeutic effectiveness on the cardiovascular and other affected systems in patients with MFS (Sandor et al., 2014) (Lacro et al., 2014) (Yacoub and Radford, 2014) (Groenink et al., 2013).

As previously mentioned, overgrowth of long bones occurs in Marfan syndrome associated with the development of osteopenia, resulting from over active osteoclasts. Alendronate (Fosamax), a bisphosphonate drug used in the treatment of osteoporosis, was effective in treating bone loss through restricting osteoclast activity, in mouse models (Nistala *et al.,* 2010a).

Mutations in some of the closely related LTBP loci are associated with phenotypes similar to aspects of MFS. For example, mutations in *LTBP2* cause ocular problems (OMIM 602091) including glaucoma (MIM: 613086) and ectopia lentis (MIM: 251750).

Mutations in other genes involved in TGFß signalling also show some similarities with *FBN1* mutations. For example, mutations of the TGFß receptor genes (*TGFBR1* and *TGFBR2*) can give rise to Loeys Dietz syndrome, which manifests Marfan-like symptoms including arachnodactyly (spider fingers), pectus deformities and aortic dissection and dilation (OMIM: 610380, 609192, 610168, 608967). Advances in treatment of Loeys Dietz syndrome include use of dexamethasone, which facilitates proper microfibril processing in human fibroblast cultures showing abnormal matrix assembly (Barnett *et al.,* 2011).

There are currently no known therapeutic agents available for treating other signs and symptoms of MFS, including ectopia lentis, adipose depletion and cartilage and bone deformities, though some problems, such as pectus deformities and lens dislocation can be corrected with surgery.

1.3.5 Phenotypes associated with Fibrillin-2 Mutations

FBN2 mutations have been associated with congenital contractural arachnodactyly, CCA (OMIM 121050) (Putnam *et al.,* 1995). CCA mimics many of the musculoskeletal defects of MFS, presenting with long limbs, contractures, spider fingers (arachnodactyly) and scoliosis. CCA affects less than 1 in 10,000 individuals (http://ghr.nlm.nih.gov/condition /marfan-syndrome), making it less prevalent than MFS. According to Universal Mutation Database (http://www.umd.be), there are 113 recorded *FBN2* mutations resulting in CCA (Frederic *et al.,* 2009). These *FBN2* mutations reside primarily between exon 24 and exon 33, a cbEGF domain rich region of fibrillin-2, while only two are recorded near the N terminus, in exons 8 and 9. The majority present as missense and deletion mutations, thought to prevent proper calcium binding and protein folding through impeding disulfide bond formation (Frederic *et al.,* 2009). Interestingly, the fibrillin-2 mutations are found in the region corresponding to the region of mutations observed in fibrillin-1 in severe neonatal MFS (Frederic *et al.,* 2009). It has been proposed that this region (exon 24-32 in *FBN1* and *FBN2*), which displays 71.2% homology (Mega Align, Clustal W alignment) (see **Chapter 7**), is critical to the function

of the proteins. Based on the differing severity of the phenotypes in neonatal MFS and CCA, fibrillin-1 has a more universal role than fibrillin-2. A detailed analysis of this region in both fibrillin-1 and fibrillin-2 will be presented in **Chapter 7**. Though CCA rarely shows the severe cardiovascular effects seen in MFS patients, some CCA mutations result in early lethality due to cardiovascular defects (Gupta *et al.,* 2004).

1.3.6 Phenotypes associated with Fibrillin 3 Mutations

There is no specific condition known to be caused by *FBN3* mutation, although genetic variation at the *FBN3* locus was recently linked to polycystic ovary syndrome (PCOS). Polymorphism of microsatellite D19S884, located in intron 55 of *FBN3,* was associated with an increase in susceptibility to PCOS (Urbanek *et al.,* 2007). However another study failed to replicate the PCOS association (Prodoehl *et al.,* 2009). Since fibrillin-3 is degenerate in mice, it has not been possible to create null mice to explore its function further.

1.4 Analysis of fibrillin gene expression

Expression of a eukaryotic gene begins with the transcription of an RNA copy of the gene's DNA. Transcription is initiated through promoter site recognition by the RNA polymerase enzyme guided by transcription factors that bind to specific DNA motifs in the promoter region. The RNA polymerase then transcribes an RNA copy of the DNA sequence. In eukaryotes, the nascent RNA must then be processed, including tagging of the 5' end with a modified guanine (the 5' cap), cleavage and removal of introns (splicing) and enzymatic addition of a string of A nucleotides at the 3' end (polyadenylation). The mature mRNA then exits the nucleus into the cytoplasm where it binds to the ribosomal subunits to initiate protein synthesis. In the case of ECM proteins like the fibrillins, the ribosome is targeted to the endoplasmic reticulum and extensive posttranslational processing occurs before and after secretion into the ECM. The final manifestation of gene expression requires that each of the stages from initiation of transcription to the final activation of the protein is permissive, and regulation can occur at any stage.

1.4.1 Expression of the fibrillin gene family extracted from publically available database, BioGPS

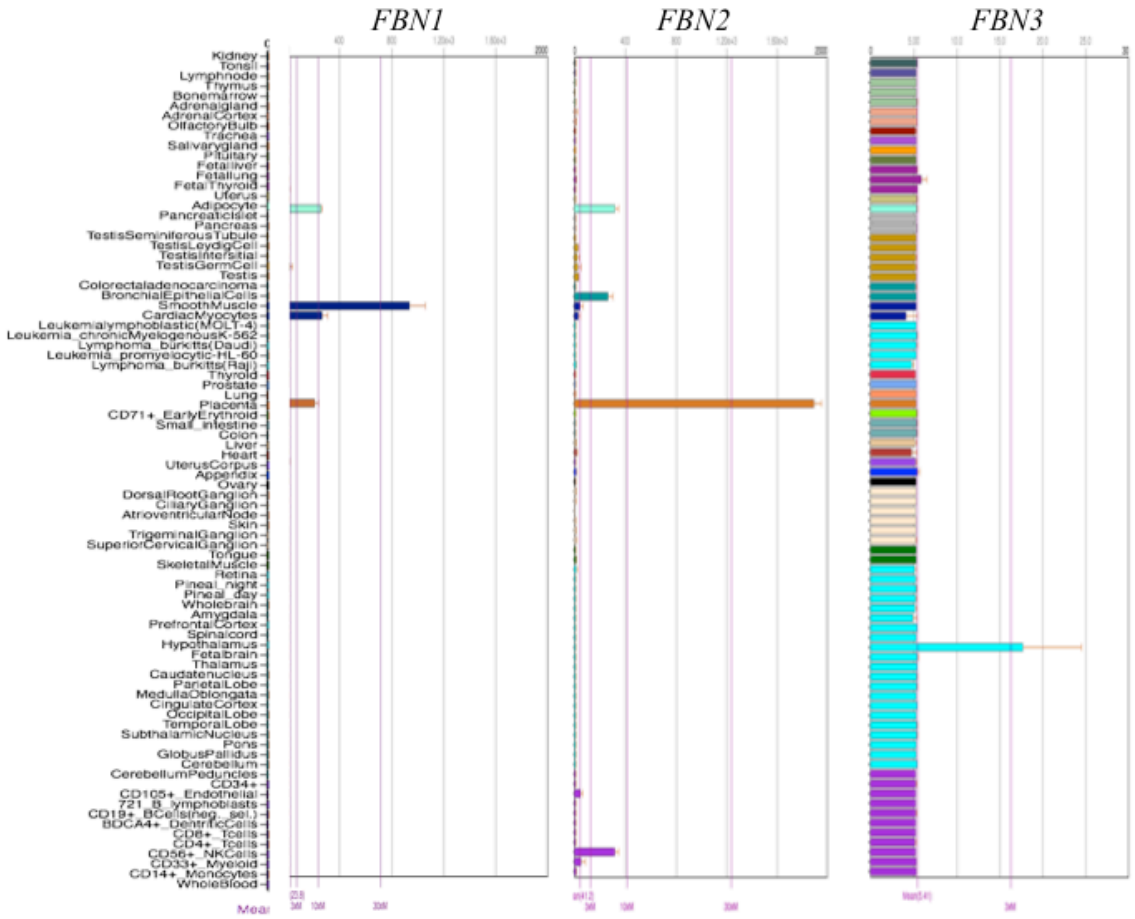

Figure 1.7. The mRNA expression of the fibrillin gene family. mRNA expression of fibrillin-1 (probeset: 202765_s_at), fibrillin-2 (probeset: 203184_at) and fibrillin-3 (probeset: gnflh00776_at). Images captured from http://biogps.org. Y- axis shows the cells and tissues sampled. The X-axis shows the relative expression intensity using Affymetrix U133A human gene expression microarray.

The publicly available database BioGPS (http://biogps.org), shows gene expression of the fibrillin family in humans (GeneAtlas U133A data set) ***(Figure 1.7).*** Consistent with their role in connective tissue, fibrillins are expressed primarily in cell types and tissues of mesenchymal origin. *FBN1* and *FBN2* were highly expressed in adipocytes, smooth muscle cells, cardiac myocytes, and placenta ***(Figure 1.7)***. Furthermore, *FBN2* showed mRNA expression in bronchial endothelial cells and CD33+ myeloid cells ***(Figure 1.7)***. In humans the expression of *FBN3* appears restricted to embryonic/foetal cell types (Corson *et al.,* 2004), with some recent data sets showing expression in meiosis phase II oocytes (Kocabas *et al.,* 2006). Furthermore, *FBN3* mRNA showed high expression in

foetal brain and lower expression in foetal lung (Corson *et al.,* 2004) ***(Figure 1.7)***. This initial survey of gene expression in the fibrillin family demonstrates the broad mesenchyme specificity of *FBN1*, the more restricted expression in *FBN2* and the limited expression of *FBN3* in early development.

1.4.2 Analysis of co-expressed genes

Genes with similar expression patterns are likely to be co-regulated and interact (Allocco *et al.,* 2004). BioLayout *Express* ^{3D} is a network visualisation tool that employs an unstructured approach to cluster genes based gene expression patterns across the sample set, which has been used extensively to develop lists of co-expressed (and potentially co-regulated) genes (Hume *et al.,* 2010, Freeman *et al.,* 2007, Theocharidis *et al.,* 2009, http://biolayout.org).

Gene clustering analysis has been performed on various cell lines and tissue samples in mice using published data from Affymetrix microarrays (Summers *et al.,* 2010, Chang *et al.,* 2008, Lattin *et al.,* 2008). Summers *et al.,* (2010) used BioLayout *Express* ^{3D} to analyze microarray data available from GEO (Gene expression omnibus) DataSets downloaded from www.ncbi.nlm.gov/gds, the first widescale expression study focusing on genes co-expressing with the fibrillin gene family. The BioLayout *Express* ^{3D} clustering results yielded a mesenchyme specific cluster of 205 co-expressed unique genes, containing two *Fbn1* probes (1425896_a_at and 1460208_at) in the centre of the cluster ***(Figure 1.8A and1.8B).*** This cluster was referred to as the *Fbn1* cluster in (Summers *et al.,* 2010), therefore that terminology will be maintained throughout this section. The *Fbn1* cluster contained 205 genes at r≥0.90 ***(Figure 1.8)*** and 31 of these genes were present in a cluster with *Fbn1* at a higher stringency of r≥0.95. Genes in the *Fbn1* cluster showed elevated expression in cell lines of mesenchymal origin including osteoblasts, both embryonic and adult fibroblasts and myoblasts ***(Figure 1.8)***. Expression of *Fbn1* was very low in hematopoietic samples and moderate in endothelial cell types and ES cells ***(Figure 1.8)***.

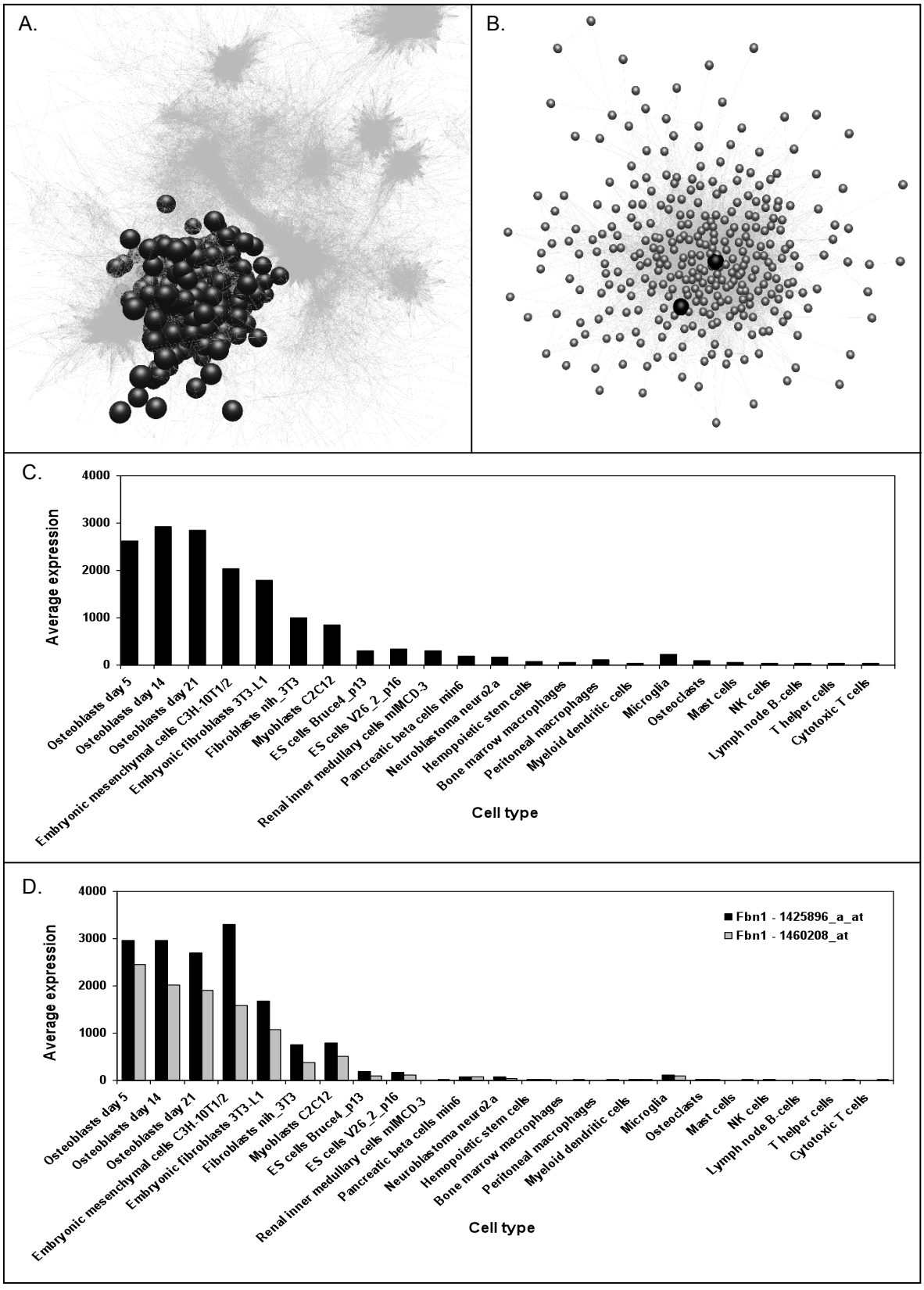
A.
B.
C.
Average expression
4000
3000
2000
1000
0
Osteoblasts day 5
Osteoblasts day 14
Osteoblasts day 21
Embryonic mesenchymal cells C3H-10T1/2
Embryonic fibroblasts 3T3-L1
Fibroblasts nih_3T3
Myoblasts C2C12
ES cells Bruce4_p13
ES cells V26.2_p16
Renal inner medullary cells mIMCD-3
Pancreatic beta cells min6
Neuroblastoma neuro2a
Hemopoietic stem cells
Bone marrow macrophages
Peritoneal macrophages
Myeloid dendritic cells
Microglia
Osteoclasts
Mast cells
NK cells
Lymph node B-cells
T helper cells
Cytotoxic T cells
Cell type
D.
Average expression
4000
3000
2000
1000
0
Fbn1 - 1425896_a_at
Fbn1 - 1460208_at
Osteoblasts day 5
Osteoblasts day 14
Osteoblasts day 21
Embryonic mesenchymal cells C3H-10T1/2
Embryonic fibroblasts 3T3-L1
Fibroblasts nih_3T3
Myoblasts C2C12
ES cells Bruce4_p13
ES cells V26.2_p16
Renal inner medullary cells mIMCD-3
Pancreatic beta cells min6
Neuroblastoma neuro2a
Hemopoietic stem cells
Bone marrow macrophages
Peritoneal macrophages
Myeloid dendritic cells
Microglia
Osteoclasts
Mast cells
NK cells
Lymph node B-cells
T helper cells
Cytotoxic T cells
Cell type

Figure 1.8 The *Fbn1* cluster. (a) A 3D image of the *Fbn1* cluster (nodes in the cluster shown by black spheres, edges by grey lines). Other clusters shown by edges only. (b) A 2D image of the *Fbn1* cluster with the two *Fbn1* probes shown as black spheres. (c) Normalised mean expression of genes of the *Fbn1* cluster across all cell types. The means of two experiments are shown. (d) Expression of the two *Fbn1* probes, 1460208_at (black) and 1425896_a_at (grey). The means of two experiments performed in triplicate are shown for each probe. Raw data available for download at GEO DataSets (accession number GSE10246). The above figure was used with permission from Nature Publishing Group (Summers *et al.*, 2010).

GO (Gene Ontology) terminology was used to determine the localisation and functions of proteins encoded by genes within the cluster (at r≥0.90) and showed that a total of 33.9% were localised to the ECM, 26.0% localised to cellular membranes and 11.3% of genes were located in the cytoskeleton. In addition, 25% of the gene products were found to be involved in cell proliferation and 10.0% involved in ECM function. Classic mesenchyme related genes included in the *Fbn1* cluster were *Acta2* (smooth muscle actin, alpha 2), *Bgn* (biglycan), a total of 12 collagen genes including *Col1a1* (collagen type I alpha 1), *Col1a2* (collagen type I alpha 2), *Col3a1* (collagen type 3 alpha 1), *Fn1* (fibronectin 1), *Lama4* (Laminin alpha 4), *Lox* (Lysyl oxidase), *Sparc* (osteonectin), *Sox9, Tgfb2* (transforming growth factor beta 2), *Tgfb3* (transforming growth factor beta 3) and *TgfbIiI* (transforming growth factor beta 1 induced 1).

Clustering which included different data sets showed that this mesenchymal cluster of co-expressed genes including *Fbn1* is relatively robust (Hume *et al.,* 2010, Mabbott *et al.,* 2011). For example, the original datasets that generated the fibrillin-1 cluster did not contain cell types from chondrocyte lineages, therefore further analysis was used which included timecourse samples of primary chondrocytes derived from embryonic foot pads in mice (James *et al.,* 2005)(Summers *et al.,* 2010). The clustering analysis revealed a cluster containing *Fbn1* and many other genes that were in the original *Fbn1* cluster, demonstrated high levels of expression across the whole time course. Since the studies presented were specified to cell lines, the researchers performed further BioLayout *Express* ^{3D} analysis on mouse tissues using publicly available microarray data (Su *et al.,* 2004, Summers *et al.,* 2010). The analysis produced a 119 gene cluster including classic ECM genes *Fbn1*, *Fbn2*, *Eln* (elastin), *Fbln2* (fibulin 2) and eight collagen genes (for

example *Col2a1, Col16a1*, *Col4a1*, *Col4a2* and *Col5a1*) at r≥0.75 (Summers *et al.,* 2010).

Overall the study by Summers *et al.,* (2010) was able to demonstrate a core set of genes that usually co-expressed with *Fbn1* as well as indicating possible regulators of fibrillin-1 in mesenchymal cell lines and tissues. Though fibrillin-2 did not cluster with fibrillin-1 in all the analyses, the expression data showed high expression of *FBN2* in osteoblasts and C3H10T1/2 (differentiating to chondrocyte cells (James *et al.,* 2005)), indicating that *Fbn2* may be a more bone/cartilage specific gene. However, because mice lack a functional *Fbn3* transcript, its function and possible gene co-regulators remained undefined. Therefore, this thesis will present a wide-scale microarray analysis across several human mesenchyme cell lines, as well as early development of human ES cells to analyze expression of the entire fibrillin gene family.

1.4.3 Functional Annotation of the Mammalian Genome, FANTOM

Throughout my postgraduate studies, I had the privilege of being involved in the FANTOM5 consortium, which is a worldwide transcriptome based project sponsored by the RIKEN Centre for Life Science Technologies in Yokohama, Japan. The consortium has generated five major phases of experiments (FANTOM1-5) from sequenced-based gene mapping and annotation to determining specific promoter expression (http://fantom.gsc.riken.jp). The data produced by the FANTOM5 projects identified transcription start site (TSS) regions and novel alternate promoter usage and provided detailed promoter expression levels for both the human and mouse cells and tissues (Forrest *et al.,* 2014). Through privileged access to the data from the project (prior to publication), extensive information was obtained on expression and regulation of the fibrillin gene family (Davis *et al.,* 2014), which will be presented in **Chapter 6.**

The FANTOM project originated with the identification of over 20,000 full-length mouse cDNAs (Kawai *et al.,* 2001). The cDNA libraries were clustered based on 3'end sequence similarity and the clusters were fully sequenced using revolutionary technology, which involved inserting biotin onto the cap structure of eukaryotic mRNA (Carninci *et al.,* 1996). The sequences were then mapped to both the human and mouse genome,

contributing to annotation of existing gene families as well as identifying novel genes (Kawai *et al.,* 2001). The FANTOM2 project expanded on the existing knowledge of FANTOM1 producing an extensive transcriptome of mice and generating a database including information on alternate splicing, regulatory elements of UTR regions. FANTOM2 identified non-protein coding RNAs as well as antisense RNA (Okazaki *et al.,* 2002). FANTOM 1 and 2 developed a large-scale cDNA library for mouse. FANTOM3 was a genome-wide analysis of promoter usage, using cap analysis of gene expression (CAGE) technology (Carninci *et al.,* 2005, Shiraki *et al.,* 2003, Kodzius *et al.,* 2006). CAGE technology is a high-throughput method for identification of the 5'ends of mRNAs, thus identifying transcription start sites (TSS) and the promoter sequence that precedes them (Maeda *et al.,* 2008).

FANTOM3 showed that most promoters are located in regions rich in cytosine and guanine bases (CpG islands) and initiate transcription over a broad sequence of bases. This contrasts with the precise initiation on a single base of TATA box promoters, the minority of promoters in the mammalian genome (Carninci *et al.,* 2005, Carninci *et al.,* 2006). Since the number of times a sequence is detected by CAGE is proportional to the number of mRNA molecules with that sequence, the data from FANTOM3 and subsequent projects also provides quantitative information of expression of the gene from a specific promoter. The FANTOM4 project combined CAGE and next generation sequencing (deepCAGE) to evaluate promoter usage and regulation in a single cell line undergoing a transition in state following activation and showed the regulatory network associated with this transition (Suzuki *et al.,* 2009).

FANTOM5 applied deepCAGE technology to analyze over 900 human and mouse tissues, primary cells and cell lines (Forrest *et al.,* 2014). The development of a novel browser, ZENBU, allowed for extensive, user-friendly visualization of the CAGE data (Severin *et al.,* 2014). FANTOM5 data was used to analyse the fibrillin gene family to determine alternate promoter usage and transcript specific expression patterns within the family **(Chapter 6)** (Davis *et al.,* 2014)).

1.5 Aims and objectives of the project

This introduction has provided a survey of available literature, outlined the origin of connective tissues and described mature and developing mesenchyme tissue types. Furthermore, I have introduced many components of the ECM with an emphasis on the fibrillin family. The work described in this thesis is a detailed expression analysis of the fibrillin gene family and provides evidence for the role of the fibrillin gene family in cells of mesenchyme origin. It leads to a better understanding of the role of the gene family in connective tissues. Furthermore, the work assesses the hypothesis that fibrillin-1 is a critical regulator of differentiation of mesenchymal cells (Summers *et al.,* 2010). The specific aims of the work presented in this thesis were: (1) To analyze the expression of the three fibrillin genes at different stages of differentiation and development using *in vitro* cell models, (2) to identify genes that are co-expressed with members of the fibrillin gene family, (3) to analyze use of alternate TSS in different tissue and cell types and (4) to explore the evolution of the promoter regions and critical protein coding sequences of the fibrillin gene family.

This thesis shows that there is a clear developmental distinction between the three fibrillins, and the results presented will assist in the understanding of disorders resulting from fibrillin gene mutations and identified co-expressed genes, potential modifiers that could be the targets of gene therapy.

Chapter 2. General Methods

Determining expression of the fibrillin genes and identifying genes that are co-expressed across mesenchyme cell types was important in understanding the relevance and interactions of the genes and gene products in connective tissue cell types. In this study connective tissue cell types were represented by cultured human cell lines and expression of both mRNA and protein was monitored through a number of approaches, which are outlined in this chapter. Detailed materials and methods will also appear in the respective chapters.

2.1 Primary cells and cell lines

There are three types of human cell culture models presented in this thesis: primary cell cultures, transformed cell lines and cancerous cell lines. Primary cells are extracted from tissues and closely mimic the physiological state of cells *in vivo*. They are adapted to a cell culture environment and can be maintained for a finite number of generations. Transformed cell lines are populations of extracted cells that have been manipulated to become immortal in the laboratory, so that they can undergo cell division indefinitely. The final cell types used in this thesis were cancer cell lines. Cancer cell lines derive from tumours. They have escaped normal growth controls and are therefore immortal.

While primary cells are considered the best material for *in vitro* studies (Forrest *et al.,* 2014), this study aimed to determine the expression patterns of the fibrillin genes in humans and there were ethical and accessibility issues associated with generating primary cells for all the relevant tissues. Primary cells were used when available, supplemented by cell lines, selected to reflect some of the cell types affected in Marfan syndrome **(Chapter 1 Section 1.3.4)**. The use of transformed cell types lead to limitations of the work presented in this thesis **(Chapter 3, 4 and 5)**, and if more time were available, primary cell types would have been examined. The following subsections will describe the cell types used in this thesis.

2.1.1 Osteosarcoma cell lines

In this study two human osteosarcoma cell lines, SAOS2 and MG63 (Pautke *et al.,* 2004), were used to analyse the role of fibrillins in bone cells. Osteosarcomas are derived from osteoblast progenitors, which have undergone a cancerous transformation (Mutsaers and Walkley, 2014). MG63 was isolated in 1977 from an osteosarcoma of a 14 year old Caucasian male (Billiau *et al.,* 1977) and SAOS2 was established in 1973 from an osteosarcoma removed from an 11 year old female patient (Fogh *et al.,* 1977). The utility of MG63 and SAOS2 as model systems for normal bone formation has been debated. Though varying cellular morphology and proliferation have been observed (Boskey and Roy, 2008), both cell lines demonstrate physiological levels of multiple osteoblastic markers including osteocalcin (OC), bone sialoprotein (BSP) and decorin (DCN) (Pautke *et al.,* 2004). SAOS2 cells are capable of mineralisation in a calcifying environment, while MG63, a less mature cell line, does not mineralise (Houston *et al.,* 2004). In addition to these differences in ECM mineralisation, the cell lines demonstrate varying levels of *FBN1* and *FBN2* mRNA (Davis *et al.,* 2014), thereby making these cell lines interesting in the study of fibrillin expression. Professor Colin Farquharson (The Roslin Institute, University of Edinburgh), kindly supplied cryopreserved SAOS2 and MG63 cell lines.

2.1.2 Chondrocyte cell lines

In addition to osteoblast formation, mesenchymal stem cells can differentiate into chondrocytes, producing cartilage **(Chapter 1 Section 1.1.3)**. Human chondrocyte cell lines, C20A4 and TC28A2 were immortalised through transfection with the virus SV40 (Small *et al.,* 1982, Chaney *et al.,* 1986, Arbiser *et al.,* 1991) and were chosen based on cartilage specific gene expression, including collagens type II, IX and XI (Goldring *et al.,* 1994). The line C20A4 was established from costal cartilage of a 5 year old male while TC28A2 was derived from the costal cartilage of a 15 year old female. Both patients had undergone surgery for pectus excavatum. The line C28I2 is a subclone from TC28A2 (Goldring *et al.,* 1994). Permission to use the chondrocyte cell lines was granted by Dr. Mary Goldring (Goldring *et al.,* 1994) and cryopreserved vials of the cells were supplied by Professor Colin Farquharson.

2.1.3 Fibroblast cell line

Fibroblasts are common connective tissue cells that give rise to a collagen and microfibril extracellular matrix **(Chapter 1, Section 1.2)**, and have been used as a model system for studying fibrillin formation and function (Brenn *et al.,* 1996, Sabatier *et al.,* 2009, Wallis *et al.,* 2001, Kielty and Shuttleworth, 1994, Samuel *et al.,* 2003). Primary human neonatal fibroblast cells, NHDF, were derived from juvenile foreskin cells, and kindly supplied by Dr. Finn Grey (The Roslin Institute, University of Edinburgh).

2.1.4 Human embryonic kidney cell line

Human embryonic kidney cell line, HEK293, was derived from human embryonic kidney cells transformed with adenovirus type 5 DNA (Graham *et al.,* 1977, Graham and van der Eb, 1973, Graham *et al.,* 1974). HEK293 cells have been used to study the gene and protein expression levels of fibrillin-1 and fibrillin-2 (Guo *et al.,* 2013, Kirschner *et al.,* 2011, Wang *et al.,* 2012), though it has been shown that expression levels in this cell line are low compared with those of the mesenchymal cell types such as MG63 (Summers *et al.,* 2009). The origin of this cell line remains undefined. Though the cells have been classically described as epithelial-derived, Shaw *et al.,* (2002) found that the cell line had more in common with neurological cells. This cell line was included in the analysis because of its relatively low expression of *FBN1*. The studies could also further clarify the origin of the cell line.

2.1.5 Hemopoietic cell line

Human leukaemia cell line, THP-1, was derived from the blood of a one year old boy diagnosed with acute monocytic leukaemia (Tsuchiya *et al.,* 1980). The monocytic nature of the cell line has been verified by the identification of monocytic marker α-naphthyl butyrate esterase, and lysozyme production (Tsuchiya *et al.,* 1980). A detailed study of THP-1 cells during activation revealed no measurable expression of fibrillin-1 or fibrillin-3, but very low expression of fibrillin-2 (Suzuki *et al.,* 2009). This is a mesoderm derived hemopoietic cell line that grows in suspension rather than in adherent culture, so there is no ECM. Therefore, THP-1 was used as a negative control.

2.1.6 Human embryonic stem cells

Human embryonic stem cells (ES) give rise to the mesoderm layer, which then continues to form connective tissue **(Chapter 1, Section 1.1)(Chapter 3)**. Since fibrillin-3 is expressed in tissues of foetal origin and in early embryogenesis **(Chapter 1, Section 1.4.1)** an expression study of the fibrillin gene family from ES cells differentiating to mesoderm was performed. RNA from H1 and RH1 (human ESC cell lines) were kindly supplied by Professor Lesley Forrester and Dr. Paul DeSousa (Scottish Centre for Regenerative Medicine, The University of Edinburgh), respectively. The methods will be discussed **Chapter 3**.

2.1.7 Mesenchymal stem cells

As previously described **(Chapter 1 Section 1.1)**, the mesoderm gives rise to mesenchymal stem cells, which continue to form various connective tissue cell types within the body. Fibrillin-1 mutations have been associated with lipodystrophy (depletion of adipose tissue) (Graul-Neumann *et al.,* 2010, Goldblatt *et al.,* 2011, Takenouchi *et al.,* 2013) (**Chapter 1 Section 1.3.4**). There is currently very little known about the role that fibrillin plays in adipogenesis. Therefore, both primary human adipose derived mesenchyme stem cells (ADMSC) and a human embryonic stem cell derived mesenchymal stem cell line (hESMP) were differentiated towards the adipose lineage. This was to investigate the gene and protein expression of the fibrillin family at various timepoints throughout adipogenesis.

2.1.1.7 Adipose derived MSCs

Cryopreserved human ADMSC cells were kindly supplied by Dr. Paul De Sousa, Centre for Regenerative Medicine, The University of Edinburgh. The cells were originally obtained from the Edinburgh Adipose Tissue Bank, Queens Medical Research Institute (QMRI), The University of Edinburgh (West *et al.,* 2014). Research was approved by South East Scotland Research Ethics Committee 03 (Reference: 1-0/S1103/45). These cells and the differentiation protocol are discussed further in **Chapter 3**.

2.1.1.8 hESMP cell line

hESMP cells were obtained from Cellartis AB (Cellectis Bioresearch, Paris, France) and the Materials Transfer Agreement (MTA) was signed by Professor Kim Summers on April 25, 2012 in Edinburgh, Scotland, UK **(See Chapter 3)**.

2.2 Standard Cell Culture

Cell culture conditions for the ten different cell types examined in this thesis are defined in ***Table 2.1***. All cells were incubated in a humidified incubator at 37°C and 5% CO_2, and treated with Pen Strep (100ug/ml streptomycin and 100U/ml penicillin)(Gibco, Paisley, UK), unless otherwise stated. NHDF, ADMSC and hESMP cells required the cell culture vessels to be coated with 0.1% gelatin (Sigma-Aldrich, Poole, Dorset, UK) to assist with adherence. Cells were all passaged using trypsin (TrypLE ^{TM} Express, Gibco). Additional cell culture treatments for differentiation and knockdown experiments are highlighted in **Chapter 3 and 5**, respectively.

Cell Type	Name	Media requirements	Media Supplements	RNA extraction method
Osteosarcoma cell line	SAOS2	McCoy5A (modified)	10% HI-FBS	RNABee
Osteosarcoma cell line	MG63	McCoy5A (modified)	10% HI-FBS	RNABee
Chondrocyte cell line	C20A4	DMEM	10% non-HI FBS	RNABee
Chondrocyte cell line	TC28A2	DMEM	10% non-HI FBS	RNABee
Chondrocyte cell line	C28I2	DMEM	10% non-HI FBS	RNABee
Neonatal fibroblast cells	NHDF	DMEM	10% HI-FBS	RNAEasy Kit
Embryonic kidney cell line	HEK293	DMEM	10% non-HI FBS	RNABee
Monocyte cell line	THP1	RPMI-1640	10% HI-FBS 1x GlutaMAX	RNABee
Primary adipose derived mesenchyme stem cell	ADMSC	DMEM	10% HI-FBS 1xGlutaMAX 1ug/ul bFGF	RNABee
Embryonic stem cell derived mesenchyme cell line	hESMP	DMEM	10% HI-FBS 1xGlutaMAX 1ug/ul bFGF	RNABee

Table 2.1. A table of cell culture requirements. GlutaMAX 100x (Gibco), HI-FBS (heat-inactivated foetal bovine serum, GE Healthcare, Little Chalfont, UK), non-HI-FBS (Sigma-Aldrich), DMEM (Sigma-Aldrich), modified McCoy's5A (+25mM HEPES, Gibco), RPMI-1640 (Sigma-Aldrich), and bFGF (PeproTech, RockyHills, NJ, USA).

2.3 Analysis of Gene Expression

2.3.1 RNA purification

Total RNA extractions were performed using one of two methods throughout this thesis ***(Table 2.1)***. The first method used RNABee (Amsbio, Abingdon, UK) as per manufacturer's instructions. Briefly, cells were lysed in RNABee, which is a mixture of guanidine isothiocyanate (a protein denaturant) and phenol. Upon addition of chloroform two phases were formed with the RNA in the aqueous phase and DNA and protein in the

organic phase. RNA was precipitated with isopropanol and washed with ethanol before being dissolved in 30-50µl of H_2O and stored at -80°C. The second method employed in total RNA extraction was the Qiagen RNeasy Mini kit (Qiagen, Crawley, UK), as per manufacturer's instructions. After removal of culture medium, cells were lysed and transferred into an RNeasy spin column, which bound the RNA. The column was washed and RNA was eluted off the membrane with 30µl of RNase-free H_2O and stored at -80°C. All RNA samples are listed in Appendix A.

DNA was removed from all RNA samples using DNase Treatment and Removal (Ambico, Invitrogen), as per manufacturer's instructions. This process uses recombinant DNase1 to digest any co-purified DNA in the sample. RNA samples dissolved in H_2O were thawed prior to treatment. Following treatment, DNase1 was inactivated and samples were stored at -80°C mixed with 2vol of 100% absolute ethanol and 0.1vol of 3M sodium acetate (ethanol precipitation solution). The samples were stored at -80°C until RNA validation.

2.3.2 cDNA synthesis

The following protocol for cDNA synthesis was adapted from (Barnett *et al.,* 1998). A range of 1ug/ul to 100ng/ul of RNA was added to cDNA synthesis reactions. 3.3µM random primers (Invitrogen), 1xPCR buffer (Invitrogen), 3µM $MgCl_2$ (Invitrogen), 500µM combined deoxynucleotide triphosphates (dNTPs) (Promega, Southampton, UK) and 1µM/µl of RNase inhibitor (Promega) was added to the RNA and the mixture was incubated at 42°C for 5 minutes. 2 µl of MMLV (Moloney murine leukaemia virus) reverse transcriptase (Invitrogen) was then added and cDNA synthesis occurred at 60°C for 60 minutes, then 95°C for 5 minutes (Bioer GenePro PCR Machine, Alpha Laboratories, Eastleigh, UK). Samples were stored at 4°C. Concentration was determined using a spectrophotometer, ND-1000 (Nano-drop, Lab-Tech, East Sussex, UK).

2.3.3 Primer design and validation

The Universal Probe Library System - Assay Design Centre (http://www.roch-applied-science.com) was used in designing the real time PCR primers ***(Table 2.2)***. The primers were designed to flank an intron to ensure that amplification of genomic DNA (gDNA)

was prevented, with annealing temperatures of 60°C. *FBN1*primers, UQ200 and UQ201, were previously designed and validated in (Summers *et al.,* 2009). Primers were synthesised by Invitrogen. The primers for human housekeeping gene, *GAPDH* (Hs_GAPDH_2_SG), were purchased from Qiagen (Hilden, Germany).

Gene Target	Primer	Primer Sequence 5'-3'
FBN1	FWD	GCTCCCAAACCCTGCAATTT
	RVS	GGCAGTTGTGTTGCTTGGTTG
FBN2	FWD	TGTGCTGAAGGGTTACACGA
	RVS	TCACAGATTCCTGGCTTGGT
FBN3	FWD	ACCTGGACGAATGCACCTC
	RVS	CTGAGCTGACCAGGGTGAAG
ACTA2	FWD	AGCCAAGCACTGTCAGGAAT
	RVS	TTGTCACACACCAAGGCAGT
BGN	FWD	CCCAGACCTCAAGCTCCTC
	RVS	TGGGACAGAAGTCGTTGACA
COL1A1	FWD	GCCTGGTCAGAGAGGAGAGA
	RVS	CTCCAGAGGGACCTTGTTTG
COL1A2	FWD	AACACGTCTGGCTAGGAGAAAC
	RVS	TTTCCTTGGAAGTCACTCCTTC
LTBP1	FWD	GCCCTAATGGTGAGTGTTTGA
	RVS	AGATCACAGGGGGATCAGG
LTBP2	FWD	TGCCCTAGTGGAAAAGGCTA
	RVS	TCACACACTCATCCGCATCT
LTBP3	FWD	CACCTGAGGACACAGAGGAAG
	RVS	GAGATCAGCTCGGGGTAGG
LTBP4	FWD	CGTCAGGCCACCTACACAG
	RVS	CAGGGCCTCGAAGTCATCT

Table 2.2. List of primers used throughout this thesis. Both forward and reverse primers are presented in 5'-3' orientation.

All primers were initially validated using a standard PCR reaction consisting of the following reagents: 10µM each of forward and reverse primer, 10mM combined dNTPs, 50mM $MgCl_2$, 10X PCR buffer (Invitrogen), 5U/µl *Taq* polymerase (Invitrogen), 1µl of 1 µg/µl cDNA, and DNase / RNase free water to a final volume of 25µl. PCR cycling conditions were as follows: 94°C for 10 minutes then 35 cycles of 30 seconds denaturation at 94°C, 30 seconds annealing at 60°C and 45 seconds extension at 72°C,

followed by one cycle of 10 minutes at 72°C. Samples were run on 1% agarose (Invitrogen) gels in TAE buffer, and primer product was measured against GeneRuler™ 1KB Plus Ladder (Thermo Scientific, Leicestershire, UK). All amplicons were prepared for sequencing by Ailsa Carlisle (The Roslin Institute, The University of Edinburgh) and sequenced by Edinburgh Genomics (University of Edinburgh) to ensure that the correct sequence was amplified. All primers produced amplicons of the predicted size and all gave the correct sequence.

2.3.4 qPCR

2.3.4.1 qPCR Conditions

qPCR was carried out using standard protocols described for SYBR Green 1 Master Mix (Roche, West Sussex, UK). 96 well plates were used (Light Cycler 480 multiwell plate 96, white, Roche). 10µl reactions consisted of 2.5µl of cDNA (1µg/µl) and 7.5µl of SYBR Green 1 Master Mix (5µl of SYBR Green 1, 0.5µl each of 10µM forward and 10µM reverse primers and 1.5µl of H_20). The reaction was run on a LightCycler 480 machine (Roche) using the SYBR Green 1 96-II run template, with the following modifications: the annealing time was altered to 15 seconds at 60°C and the single extension time to 30 seconds. All qPCR analysis was carried out with the LightCycler480 software (Roche) provided with the system, using Advanced Quantification which involved ΔCT calculations using previously established primer standard curves (**Section 2.3.4.2**).

2.3.4.2 Primer validation and optimisation

Serial dilutions of cDNA were used to assess the efficiency of quantitative amplification for each set of primers. RNA was extracted from cultures of NHDF and MG63 cells after seven days of culture and cDNA produced as detailed in **Section 2.3.2**. The cDNA was diluted 1:10, 1:100, 1:1000 and 1:10,000. qPCR was carried out as outlined in **Section 2.3.4.1**. Analysis of standard curve output was completed using Absolute Quantification / 2nd Derivative Maximum, using LightCycler480 software (Roche). The optimal slope for the primers was -3.3 though a range of -3.1 to -3.45 was considered acceptable, and with

an efficiency of 2 (efficiency = $10^{-1/slope}$). Furthermore, the error of the slope and efficiency was acceptable at <0.2.

2.3.5 Microarray analysis

The RNA in ethanol precipitation solution **(Section 2.3.1)** was removed from -80°C and centrifuged at 12,000g for 20 minutes. The RNA pellet was resuspended in 30-50µl of RNase-free water. The total RNA concentration was determined using a Nano-drop spectrophotometer **(Section 2.3.2)**. RNA quality was routinely assessed through the A_{260}/A_{280} ratio. For microarray analysis, RNA quality was assessed using Agilent R6K Screen Tape System (Agilent, Waldbronn, Germany) as per manufacturer's instruction. Agilent 2200 TapeStation software was used to calculate the RNA integrity number (RIN^E) values for each RNA sample. RIN^E values ranged from 1 to 10 and values over 7 were considered to show appropriate quality RNA for microarray analysis.

Analysis of RNA using the Affymetrix U219 human microarray platform was performed by Edinburgh Genomics, University of Edinburgh. 96 RNA samples with RIN^E values > 7 were analysed (**Appendix A**). The RNA samples were labelled using the 3' IVT Express Kit (P/N 901229, Affymetrix, High Wycombe, UK). The extended protocol can be located at http://www.affymetrix.com. The samples were hybridised to the Affymetrix Human U219 96 well plate in the GeneTitan ® machine (Affymetrix standard hybridisation, wash and stain protocols).

2.3.5.1 Normalisation of microarray data

A total of 96 .CEL files (samples listed in **Chapter 9, Appendix A**) supplied by Edinburgh Genomics after microarray analysis were loaded into the Affymetrix Expression Console (Affymetrix) and the HG_U219 library file of probe annotations was downloaded. Normalization was performed using 3' Expression Arrays-RMA (Robust Multi-Array average) procedure. The quality control metrics were examined. The analysis rendered a tabular report that assessed the 96 samples across a range of intensity, signal and housekeeping probes. Suitable samples for further analysis are defined as "within bounds" and those that fail one or more of the QC checks are classified as

"outside bounds". A total of 95 samples were found to be within bounds, while Sample M0080 was outside bounds (**Chapter 9, Appendix A**). This sample contained human ES cells at Day 0. The sample failed at both Housekeeping_AFFX-HSAC07/X00351_5 and Housekeeping_AFFX-HUMANGAPDH/M33197_5, though the sample passed for all other housekeeping probes. Though M0080 was designated as outside bounds, the sample was used in further analysis because it did not appear to be a consistent outlier according to further QC, including Principle Component Analysis (PCA) **(*Figure 2.1*)**, and the signal box plot visualisation ***(Figure 2.2).***

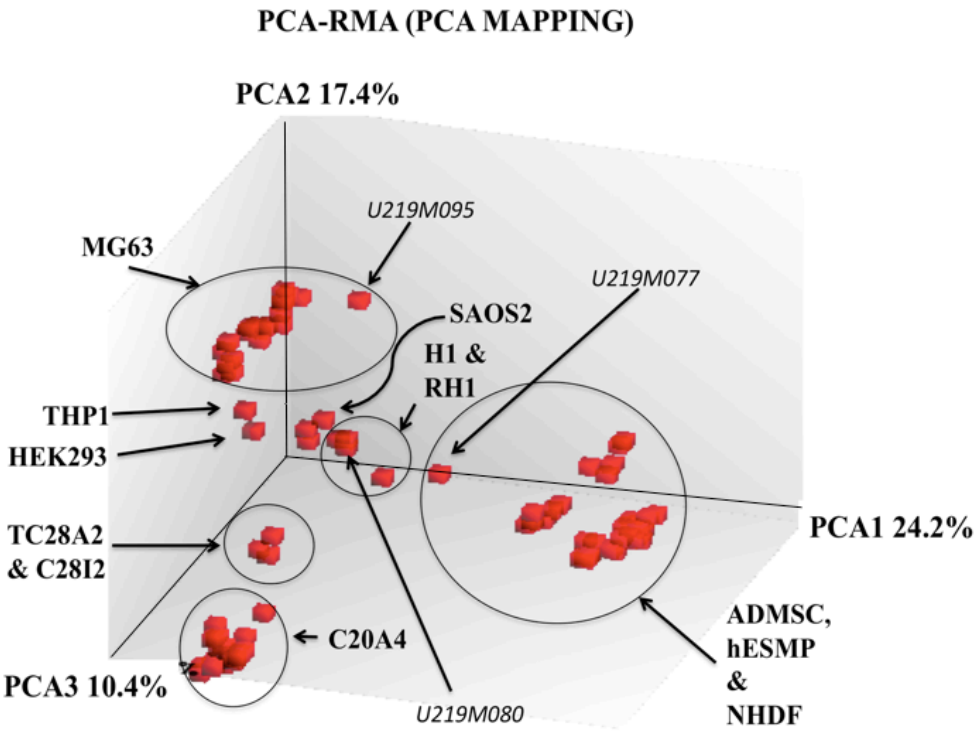

Figure 2.1. A three-way PCA plot of RNA samples analysed with the Affymetrix U219 human microarray. The figure displays the 96 RNA samples and their PCA clustering based on signal intensity expression using three components depicted as PCA1, PCA2 and PCA3. The image was rendered from the Affymetrix Expression Console (www.affymetrix.com). See Section 2.3.5.1.

The PCA-RMA mapping was obtained from the Affymetrix Expression console, and showed that 52.2% of the cases (96 RNA samples) fell into the PCA variable confines (PCA1, PCA2 and PCA3) ***(Figure 2.1)***. The analysis showed similar cell types clustering together yielding only two expression outliers ***(Figure 2.1)***. The MG63 cell type RNA samples clustered together, with sample U219M0095 somewhat distant from the other replicates. This sample was treated with mineralizing reagents **(Chapter 4)**, therefore the

sample was cultured under different conditions, reflected in the PCA analysis. In addition, samples of early mesenchyme origin ADMSC and hESMP samples clustered along with NHDF (neonatal fibroblast cells). This was indicative of the primitive differentiation of the fibroblast cell type. There appeared to be a single outlier in this cluster, U219M0077, representing the hESMP Day 3 control sample, similar to results presented in the signal box plot tool ***(Figure 2.2).***

The signal box plot tool displays a box plot visualization of the ratio of individual probe intensity against the median probe intensity, across the entire microarray ***(Figure 2.2)***. Sample U219M0077 appeared to have lower signal intensities (similar to U219M0008), though the samples passed all the quality control and was defined as "within bounds" by the Affymetrix Expression Console. Therefore, all samples were included in the analysis.

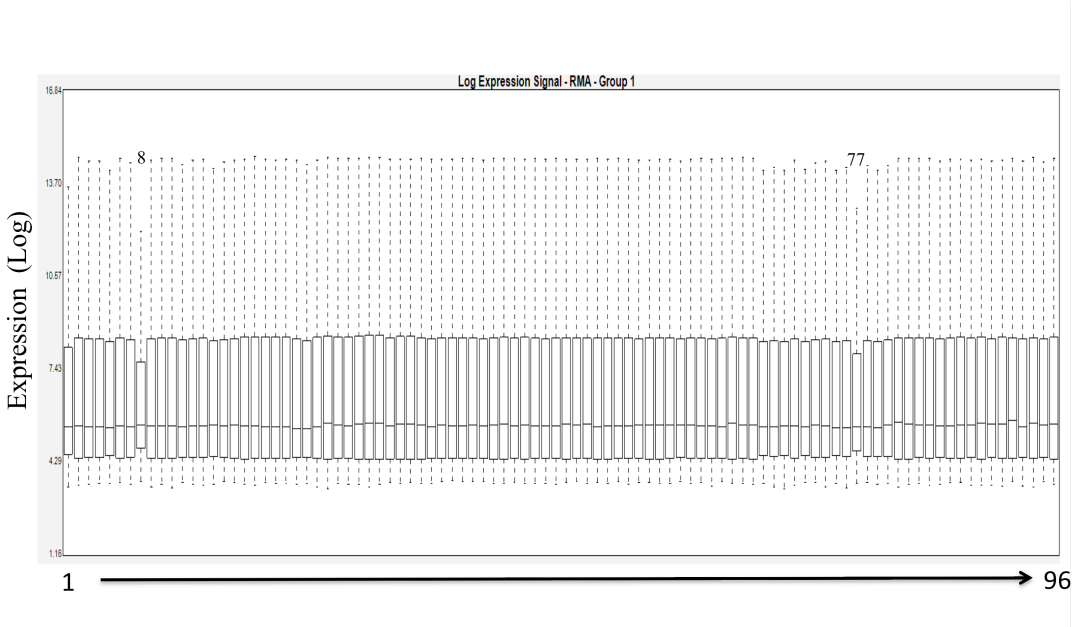

Figure 2.2. Logarithmic expression box plot of microarray intensities across the 96 samples (Appendix A). The only obvious variations are within sample M0008 and M0077 (Appendix A), though the samples passed the quality control (QC) analysis of the Affymetrix Expression Console (http://www.affymetrix.com).

2.3.6 BioLayout *Express* ^{3D}

The normalised results were annotated using the Affymetrix annotation file in the Affymetrix Expression Console. The annotated normalised results were imported into Microsoft Excel and further filtered using Microsoft Excel (filtration parameters

described in **Chapter 3, 4 and 5**, respectively). The normalised results were exported from the Expression Console as log2, and all probe intensity values were unlogged prior to analysis. The filtered spreadsheets were saved as tab delimited files (.expression) and imported into BioLayout *Express* 3D (**Chapter 9, Appendix B**)(All files are accessible via the compact disc in rear cover of this thesis). The layout was created at p values of ≥0.80-0.95 (p values for each analysis are provided in **Chapters 3, 4 and 5**) using Fast Multiple Multilevel Method (FMMM) graph layout format. The analysis was clustered at a Markov Cluster Algorithm (MCL) inflation value of ≥ 1.7 (see **Chapters 3, 4, and 5**). The clustering analysis shows a network of nodes (vertices) statically connected by edges (links). All clustering images presented in this thesis were obtained from the "snapshot" function within BioLayout *Express* ^{3D} and formatted in Microsoft Power Point.

2.3.7 DAVID analysis, evaluation of GO terms

Database for Annotation, Visualisation and Integrated Discovery (DAVID) analysis (Huang da et al., 2009a) was used to explore the functions of genes in the clusters identified by BioLayout *Express*^{3D}. Cluster gene lists were individually placed into the upload tool bar of DAVID 6.7 functional annotation tool (http://www.david.abcc.ncifcrf.gov/) (Huang da *et al.,* 2009b, Huang da *et al.,* 2009a). OFFICIAL_GENE_SYMBOL was selected from the drop down menu as the identifier for the gene list. The background selected was "*Homo sapiens"* and the minimum cluster of genes and terms was set at the default of 2. P-values were calculated using adopted Fisher Exact methodology, accounting for enrichment values of genes associated with the categorized GO term. The P-value threshold was set to the default of $p \leq 0.1$. Terms for each cluster were collected and analysed under the following categories: Biological Pathways, Cellular Components, and Disease.

2.4 Protein Analysis

2.4.1 Determining a fixative for immunocytochemistry (ICC)

To study fibrillin-1 protein, 4% paraformaldehyde (PFA) was inappropriate for cell fixation as it destroys the epitope detected by the anti-fibrillin-1 antibody (personal communication, Professor Kim Summers). A range of alternate fixative agents were

tested including, 100% CH_3OH (methanol), 100% $(CH_3)_2CO$ (acetone) and 95% CH_3CH_2OH (ethanol/EtOH) / 5% CH_3COOH (acetic acid). MG63 cells were cultured in standard tissue culture 12 well plates (NUNC, Thermo-Scientific, Leicestershire, UK) on EtOH treated glass slides (Provided by Dr. Mark Barnett) for 14 days. Cells were fixed with l ml of 100% methanol, 100% acetone or 95% EtOH/5% acetic acid, and placed at -20ºC for 15 minutes. Cells were washed three times with phosphate buffered saline (PBS) for 5 minutes. It was determined that acetone was inappropriate as it began to break down the culture vessel structure after 10 minutes. Therefore, 95% EtOH / 5% acetic acid and 100% methanol were compared for fibrillin-1 fluorescent staining ***(Figure 2.3)*****(Section 2.4.2**).

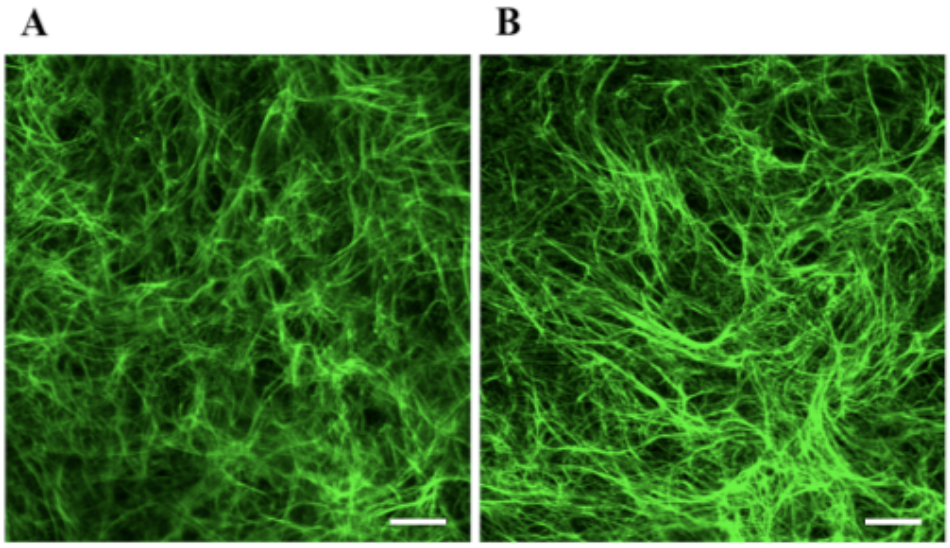

Figure 2.3. Testing fixative agents for cell cultures. The image depicts fibrillin-1 immunofluorescent staining (Section 2.4.2) of Day 14 MG63 cells in culture. A) MG63 cells fixed with 100% methanol (20x)B) MG63 cells fixed with 95% ETOH / 5% acetic acid (20x). The fibrillin-1 fibres are shown in green. The cells were mounted with ProLong Gold (Invitrogen). The cells were visualised using a Zeiss confocal microscope. The microscope bars (white) represent 50µm.

It was determined that 95% ETOH / 5% acetic acid provided better defined fibres in imaging results then when compared to 100% methanol ***(Figure 2.3)***, and this was subsequently used for all fluorescent immunocytochemistry (ICC) experiments.

2.4.2 General Staining Method for Fluorescent ICC

PBS washed live cells, in 8 well chamber slides (Lab-Tek® Chamber Slides™ 8 well glass slides, Rochester, NY, USA), were fixed with ice cold 95% ETOH/ 5% acetic acid (**Section 2.4.1**) and placed at -20°C for 10 minutes, washed 3x for 5 minutes with PBS and blocked with 1% BSA (bovine serum albumin)(Sigma-Aldrich) in PBS for 1.5 hours at room temperature. Primary antibody ***(Table 2.3)*** was added following blocking, and the slides were placed at 4°C, overnight in a humidified chamber. The corresponding secondary antibody ***(Table 2.3)*** was added following 3x 5 minute PBS washes, and the slides were incubated at room temperature for 1 hour.

Protein	Primary Antibody (Supplier) (Dilution Used)	Secondary Antibody (Supplier) (Dilution Used)
FBN1 (Fibrillin-1)	Anti-fibrillin-1 Mouse monoclonal IgG1 (Abcam3090) (1:100)	AlexaFluor488® Goat anti-mouse IgG (Invitrogen) (1:1,000)
FBN2 (Fibrillin-2)	Anti-fibrillin-2, clone 48 Mouse monoclonal (Millipore, Temecula, CA,USA) (1:50)	AlexaFluor488® Goat-anti-mouse IgG (Invitrogen) (1:1,000)
ACTA2 (Smooth muscle actin 2)	Anti-ACTA2 Rat monoclonal IgG (Abcam15684) (1:100)	Texas Red Goat anti-Rat IgG (Invitrogen) (1:1,000)
BGN (Biglycan)	Anti-biglycan rabbit polyclonal (Abcam49701) (1:100)	Alexa Fluor568 Goat anti-Rabbit IgG (Invitrogen) (1:1,000)
COL1 (Collagen type 1)	Anti-collagen I goat polyclonal (Abcam19811) (1:100)	Alexa Fluor633 Donkey-anti-Goat IgG (Invitrogen) (1:1,000)

Table 2.3. ICC antibodies. All primary antibody dilutions were chosen based on serial antibody testing from 1:50-1:500. All secondary antibodies were tested in serial dilutions 1:1000-1:10,000 with their respective primary antibody and without a primary antibody to record background readings. In addition, antibodies were tested against the following isotype controls: Mouse IgG1 purified isotype control (Invitrogen), Rat IgM kappa monoclonal [RTK2118] isotype control (Abcam, Cambridge, UK)(Data not shown). Isotype controls were not done for BGN or COL1 antibodies, though the secondary antibody testing and additional appropriate controls were negative (Data not shown). All antibody testing was performed on MG63 cells, and completed as outlined in Section 2.4.2.

The cells were then washed with PBS, and mounted with ProGold + DAPI (Invitrogen). Samples were viewed using Zeiss LSM 710 confocal microscope and analysed with ZEN software at standard settings (Zeiss, Cambridge, United Kingdom).

Chapter 3. The fibrillin gene family in early and later differentiation.

3.1 Introduction

The three fibrillin proteins are very similar in structure (**Chapter 1, *Figure 1.4*),** but they are present at different stages in development (reviewed by (Davis and Summers, 2012)). The study in this chapter investigated the expression of mRNA from each of the three genes during two developmental processes, the early differentiation of embryonic stem cells towards the mesoderm lineage and the differentiation of mesenchymal stem cells to adipocytes.

3.1.1 Embryonic stem cell differentiation

Human embryonic stem cells (hESC) are pluripotent cells that can differentiate into all the cell types in the body. hESCs can be cultured to produce embryoid bodies, which then further differentiate into ectoderm, mesoderm or endoderm specific lineages, which can produce the cell types present in the adult human (**Chapter 1, Section 1.1**). The study of hESCs has allowed for the examination of both gene expression and protein synthesis during human embryonic development and differentiation.

This chapter will explore the role of the fibrillin gene family through this very early stage of development and differentiation. The first analysis was performed on mRNA from hESC cell line H1. H1 stem cells were originally derived in 1998 from a cleavage staged human embryo donated from an *in vitro* fertilisation (IVF) clinic (Thomson *et al.,* 1998). Thomson *et al*. (1998) allowed the embryo to develop to blastocyst stage and isolated the inner cell mass to create the H1 line. H1 hESCs have a stable XY karyotype, high levels of telomerase activity demonstrating a highly proliferative life span and positive staining for several markers of undifferentiated human ESC cells, for example SSEA-3/4 (stage specific embryonic antigens -3 and -4), TRA-1-60, TRA-1-80 (human pluripotent stem cell antigens) and ALPL (alkaline phosphatase) (Thomson *et al.,* 1998). A second hESC line, RH1, was used for some analyses. This line originated from a Day 6 post-insemination human blastocyst, cultured in an animal-product free culture system and ES

cell validation is described in Fletcher *et al.,* (2006). These cells were used to determine the role of members of the fibrillin gene family in early development.

3.1.2 From mesoderm to mesenchyme

The three embryonic germ layers that develop during embryogenesis are the ectoderm, endoderm and mesoderm ***(Figure 3.1).*** Mesenchymal stem cells are derived from the mesoderm layer through a relatively unknown mechanism, though specific characteristics are beginning to be understood. The process begins with pluripotent cells that have epithelial characteristics within a blastocyst (Lamouille *et al.,* 2014). These epithelial-like cells have upregulated laminin and cytokeratin, form tight adherens junctions through E-cadherin (OMIM: 192090)(Schafer *et al.,* 2014, von Gise and Pu, 2012), and have a well-structured basement membrane ***(Figure 3.1A)***.

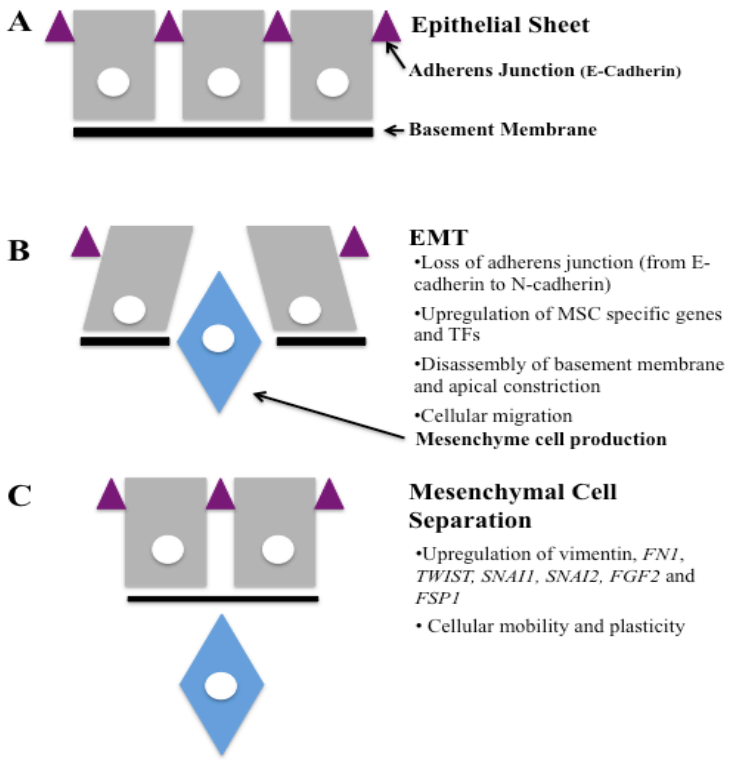

Figure 3.1. The epithelial- mesenchyme transition (EMT). The process is described in the Section 3.1.2. Adapted from (von Gise and Pu, 2012).

The EMT is described as the loss of epithelial traits accompanied by the gaining of mesenchymal traits such as upregulation of vimentin and myosin, and cellular motility

(Hay, 2005). During EMT the basement membrane is disassembled, a downregulation of the adherens junctions occurs, there is a loss of cellular polarity and cells become migratory (von Gise and Pu, 2012) ***(Figure 3.1B)***. Evseenko *et al.,* (2010) performed a large-scale genetic study of the early stages of mesoderm differentiation, demonstrating an upregulation of several key early genes and transcription factors. For example, they confirmed the importance of upregulation of *FGF2* (human fibroblast growth factor 2) (Ciruna and Rossant, 2001, Tsutsumi *et al.,* 2001) and additional genes, *SNAI1* (snail family zinc finger1)(OMIM: 604238), *SNAI2* (snail family zinc finger 2)(OMIM: 602150), *TWIST1* (twist family BHLH transcription factor 1)(Martin and Cano, 2010), *EOMES* (eomesodermin)(OMIM: 604615)(Russ *et al.,* 2000), *MESP1* (mesoderm posterior 1) (OMIM: 608689)(Saga *et al.,* 1996), and *MESP2* (mesoderm posterior 2)(OMIM: 605195)(Evseenko *et al.,* 2010). Further studies have also shown that during the EMT, levels of *FSP1* (fibroblast specific protein 1) (Strutz *et al.,* 1995) and *FN1* **(Chapter 1, Section 1.2.4)**(Park and Schwarzbauer, 2013) are increased, contributing to the MSC characteristics of the cells ***(Figure 3.1C)***. Once the MSC population is formed, differentiation can continue as described in **Chapter 1, Section 1.1,** and specifically for adipocyte formation below.

3.1.3 Adipose differentiation

As previously discussed (**Chapter 1, Section 1.1**), mesenchymal stem cells can be differentiated into multiple connective tissue lineages including adipocytes **(Chapter 1, Section 1.1.2)**. Adipocytes are cells that store fat in the adipose tissue, both brown (BAT) and white (WAT). BAT is mainly associated with early development (Gilsanz *et al.,* 2012), while WAT is maintained well into and throughout adulthood (Peirce *et al.,* 2014). Adipose tissue develops through a cascade of events leading to production of preadipocytes, which then terminally differentiate to mature adipocytes (**Chapter 1, Figure 1.1**). The major transcription factors responsible for turning on the cascade of adipose specific genes include master adipose regulator gene, *PPARG* (Tontonoz *et al.,* 1994) and *CEBP* **Chapter 1, Section 1.1.2)**(Miller *et al.,* 1996). As reviewed by Mariman and Wang (2010), there are over 65 proteins shown to be components of adipocyte ECM, including fibrillin-1, fibronectin, collagen type I alpha 2, osteonectin and

transforming growth factor binding protein 1. These proteins are involved in not only the maintenance of the ECM in adult adipose tissue, but also in early and late differentiation (Mariman and Wang *et al.,* 2010). It is currently understood that there are two phases of ECM reorganisation during adipogenesis, (1) during preadipocyte formation where the fibrillar (i.e. collagen VI) matrix is highly expressed and important in providing a scaffold for the lipid monolayer leading to, (2) ECM reorganisation to increase storage space facilitating adult adipose energy-storing properties **(Chapter 1, Section 1.1.2)**(Mariman and Wang, 2010, Catalan *et al.,* 2012). In addition, the ECM in adult adipose tissue is under constant overturn to accommodate storage space (Mariman *et al.,* 2010). Though fibrillin-1 is secreted by adult rat adipocytes (Lim *et al.,* 2008), the function of fibrillin-1 in adipogenesis has yet to be understood. There has been increasing interest in the development and function of adipose tissue, as the incidence of obesity in the population increases (Wang and Beydoun, 2007). Understanding the role of fibrillins in the formation of adipocytes has the potential to contribute more widely to understanding and treatment of obesity.

3.1.4 Adipose depletion in MFS and CCA

Though interest in adipose tissue is mostly associated with the obesity epidemic, adipose tissue depletion is a common phenotype of Marfan syndrome and CCA patients (Summers *et al.,* 2005, Kumta *et al.,* 1976). In addition, lipodystrophy, a disorder causing severe adipose depletion, has been recently identified in patients with mutations in the carboxyl terminus of fibrillin-1 (Takenouchi *et al.,* 2013, Horn and Robinson, 2011, Goldblatt *et al.,* 2011, Graul-Neumann *et al.,* 2010). These four patients shared similar phenotypes, such as progeroid (prematurely aged) appearance, arachnodactyly, retrognathia (abnormal maxilla or mandible) and eye proptosis (bulging eyes). They varied in the extent of phenotypic characteristics of Marfan syndrome, including severe myopia (severe nearsightedness), cardiovascular complications and ectopia lentis (dislocating lens) (Takenouchi *et al.,* 2013). The presence of lipodystrophy in patients with similar *FBN1* exon 64 mutations suggests an important role of fibrillin-1 in the development and differentiation of adipose tissue. This chapter studies the role of the fibrillin gene family in primary adipose derived mesenchymal stem cells (ADMSC) and a

human embryonic stem cell derived mesenchymal stem cell line (hESMP) differentiating to the adipose lineage.

The ADMSC cells were extracted from a female liposuction patient in accordance with the ethical clearance outlined in (West *et al.,* 2014), and were supplied by Dr Paul De Sousa **(Chapter 2, Section 2.1.1.7)**. In brief, the extracted adipose tissue was digested and centrifuged to pellet the stromal vascular fraction (SVF). The mesenchyme derived cells were selected from the SVF based on adherence to tissue culture vessels and flow cytometry for mesenchyme specific markers (West *et al.,* 2014) such as CD105, CD73 and CD90 (Lin, 2012). Furthermore, to be classified as mesenchyme, the cells were shown to be capable of differentiating to osteogenic, adipogenic and chondrogenic lineages (Lin, 2012). The hESMP mesenchymal stem cells were commercially produced from hESC cell lines by CellartisAB (Cellectis Bioresearch) **(Chapter 2, Section 2.1.1.8)**. The hESMP cells have upregulated expression of CD166, CD105, CD13 and CD10 (www.cellectis-bioresearch.com), common mesenchyme specific markers (Halfon *et al.,* 2010, Rahman *et al.,* 2013, Mariotti *et al.,* 2008).

3.1.5 Aims of the chapter

The overall aim of this study was to understand the role of the fibrillins in early development and mesenchymal differentiation. Protein and mRNA levels were examined in ADMSC and hESMP cells differentiating to the adipose lineage and undifferentiated RH1 hESCs and H1 hESCs differentiating to mesoderm. Genes that co-express with fibrillin genes in these models of differentiation and development were used to confirm the likely function of the fibrillins through association. The study will show that each fibrillin has a distinct pattern of expression and distinct co-expression partners.

3.2 Materials and Methods

3.2.1 Human H1 embryonic stem cell samples

Formation of embryoid bodies from the H1 stem cells (WiCell Inc. Madison, Wisconsin, USA) was carried out in the laboratory of Professor Lesley Forrester, Scottish Centre for Regenerative Medicine, University of Edinburgh, as shown in ***Figure 3.2***. Embryoid body formation was initiated through the hanging drop method (Huang *et al.,* 2013). At

day 3, the embryoid bodies were disaggregated and cultured with hematopoietic cytokines to progress to the mesoderm lineage. RNA from Day 0, Day 3 and Day 5 of culture was kindly supplied by Professor Forrester.

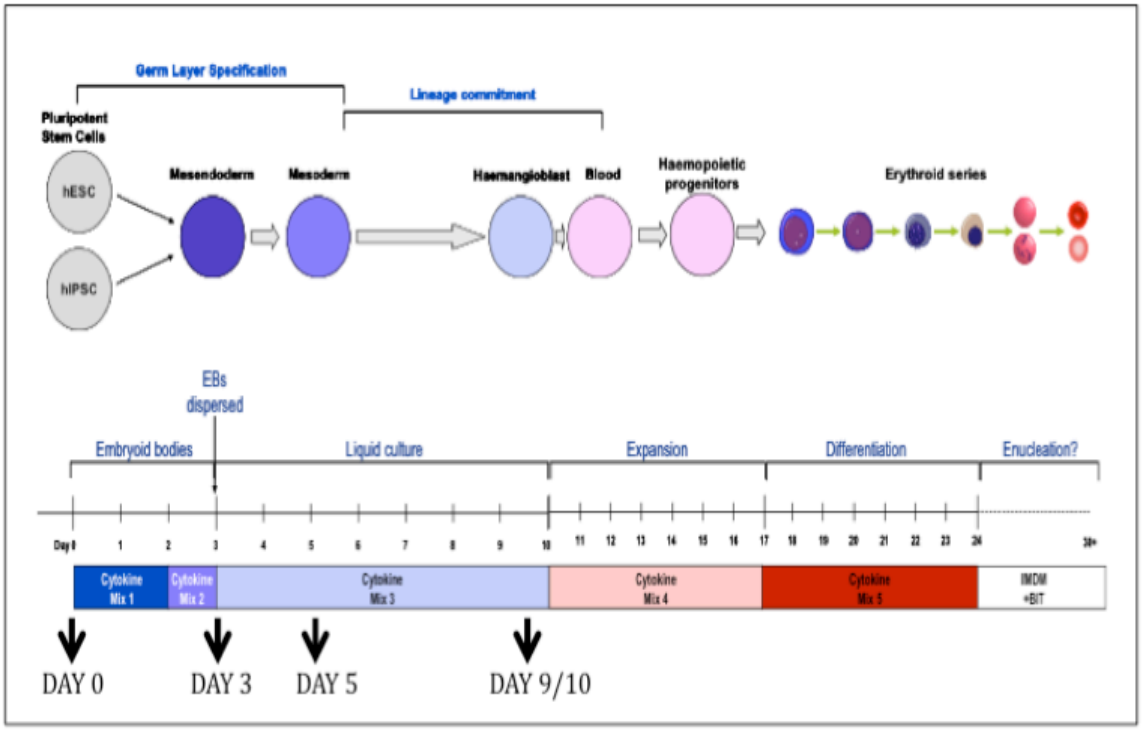

Figure 3.2. H1 differentiation protocol. Diagram supplied by Professor L. Forester, Scottish Centre for Regenerative Medicine, University of Edinburgh.

Dr. Paul DeSousa (Scottish Centre for Regenerative Medicine, University of Edinburgh) provided a cell pellet from Day 2 and Day 5 cultures of human embryonic stem cell line, RH1 (Fletcher *et al.,* 2006). The cells had been grown in media designed to suppress differentiation (Personal communication, Dr. Paul DeSousa). Day 2 RH1 RNA was extracted using the RNABee method described in **Chapter 2, Section 2.3.1**. Day 5 cell culture samples (in 8 well chamber slides (NUNC)) were fixed by Cairnan Duffy (Scottish Centre for Regenerative Medicine, The University of Edinburgh) with 95% ethanol and 5% acetic acid (ice cold) for 20 minutes and washed three times with PBS. The samples were stored at 4˚C in PBS until used for ICC studies.

3.2.2 Adipose differentiation

StemPro® Adipogenesis Differentiation Medium (Gibco) consisted of prewarmed (37ºC) StemPro® Adipogenesis Differentiation Basal Medium (90mL), thawed StemPro® Adipogenesis Supplement (10mL) and 50µl of 1xGlutaMAX. This adipose differentiation medium will be referred to as adipose media throughout the remainder of the thesis. The adipose media was filtered through a 100mL 75mm filter unit (Thermo Scientific, Leicestershire, UK). ADMSC and hESMP cells were cultured, separately, as follows: 20,000 cells/ well were placed into 8 well chamber slides (NUNC), and 250,000 cells were placed in T25 cell culture flasks (NUNC). Both the 8 well chamber slides and T25 cell culture vessels had been coated in 0.1% Gelatin. The cells were grown in standard ADMSC/hESMP media (**Chapter 2, Section 2.2, Table 2.1**) for 24 hours at 37ºC in 5% CO_2 to achieve 75-80% confluency. 100µl (NUNC 8 well chamber slides) and 2mL (T25 flasks) of adipose media was added to the differentiating ADMSC's and hESMP cultures, and the same volume of normal ADMSC/hESMP media was added to the undifferentiating samples. Samples for ICC fluorescent staining (8 well chamber slides) were fixed with 95% Ethanol and 5% acetic acid (20 minutes at -20ºC) at the following time points (days after induction of adipogenesis) Day 0, Day 1, Day 3, Day 7 and Day 14. Cells in T25 flasks were lifted at Day 1, Day 2 and Day 18 with 1mL of RNABee for RNA extraction (**Chapter 2, Section 2.3.1**).

3.2.3 Oil Red O staining

Oil Red O stock solution was prepared with 0.7g Oil Red O (Sigma-Aldrich) and 200ml of isopropanol, stirred over night and filtered through a 0.2µm filter unit. Solution was stored at room temperature. Oil Red O working solution was prepared with 6 parts Oil Red O stock solution and 4 parts dH_2O, mixed and incubated at room temperature for 20 minutes, then filtered through a 0.2µm Millex syringe filter unit (Millipore, Cork, Ireland).

ADMSC (Passage 4-6) and hESMP (passage 2-6) cells were plated at 50,000 cells per well in a 1% gelatin coated 6 well plate and cultured in DMEM (**Chapter 2, *Table 2.1*)** at 37ºC in 5% CO_2 for 24 hours to achieve 75-80% confluency. The media was replaced

with 1ml of adipose media or normal ADMSC/hESMP culture media (**Chapter 2, *Table 2.1***) for the undifferentiating samples and the media was changed every 48 hours. Samples were fixed at Day 1, Day 3, Day 6, Day 8 and Day 18 post induction of adipogenesis for both differentiating and nondifferentiating ADMSC and hESMP cell types. Cells were fixed with 10% neutral buffered formalin solution (Sigma-Aldrich for 5 minutes, then replaced with fresh 10% formalin and incubated at room temperature for 1 hour. The 10% formalin fixative was removed and the wells were briefly washed with 60% isopropanol, and allowed to air dry completely at room temperature. 200µl Oil Red O working solution was added to each well for 10 minutes at room temperature, then removed and wells were immediately washed with dH_2O four times for 10 minutes. Wells were imaged using Axio Lab.A1 microscope (Zeiss).

3.2.4 Analysis of samples

All ICC techniques were carried out as described in **Section 2.4.2 of Chapter 2.** Initial mRNA expression levels were quantified using qPCR techniques described in **Section 2.3.1 of Chapter 2**.

Gene expression levels in RNA samples were determined using the U219 human microarray platform (as described in **Chapter 2, Section 2.3.5)** for the following samples: ADMSC at Day 1, Day 2 and Day18 for both adipose differentiating and control samples, hESMP at Day 1, Day 2 and Day 18 for both differentiating and control samples, H1 samples at Day 0, Day 3 and Day 5 for CD34+ differentiation and RNA from Day 2 RH1 cells **(Chapter 9, Appendix B)**. The results were normalised as described in **Chapter 2, Section 2.3.5.1**. Probes were removed from the data set that did not show a difference of at least two fold across samples, removing 26.6% (13,171) of the low dynamic range probes. The remaining 36,214 probeset intensity results were loaded into BioLayout *Express* ^{3D}. The clustering analysis was run at $r \geq 0.95$ at an MCL inflation value of 1.7, producing 1,147 clusters.

Cluster gene lists for large Cluster003, Cluster006 and Cluster008 were individually placed into the upload tool bar of DAVID 6.7 functional annotation tool (www.david.abcc.ncifcrf.gov/) **(Chapter 2, Section 2.3.7).**

3.3 Results

3.3.1 Fibrillin gene family expression in the H1 timecourse

Initial qPCR analysis performed on differentiating H1 cells at Day 0, Day 3 and Day 5 time points demonstrated distinctive fibrillin gene expression ***(Figure 3.3).*** *FBN1* expression was highest at Day 5, *FBN2* showed increased expression at Day 3 which remained steady at Day 5 ***(Figure 3.3)***. Though *FBN3* mRNA showed the lowest overall expression (maximum about half that of *FBN2* and one quarter that of *FBN1*), the highest expression was found at Day 0, with steadily declining values and lowest expression at Day 5 ***(Figure 3.3)***.

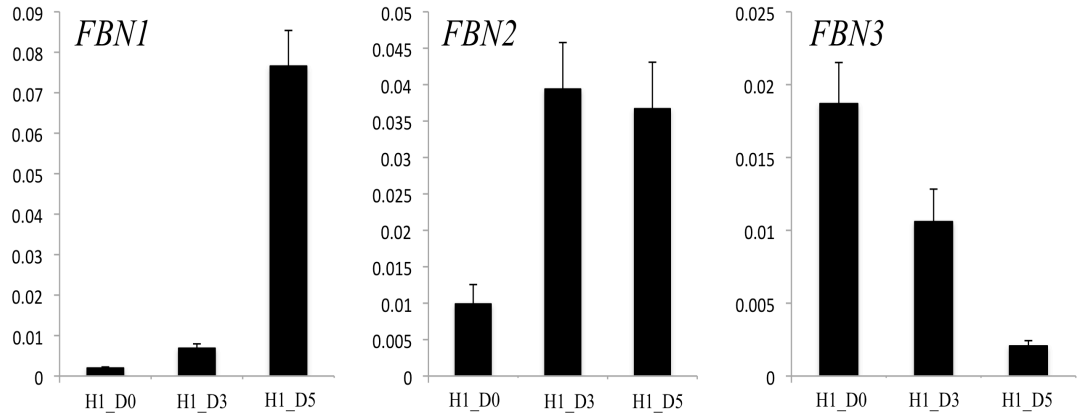

Figure 3.3. qPCR results for the H1 timecourse. Expression of *FBN1*, *FBN2* and *FBN3* at Day 0 (H1_D0), Day 3 (H1_D3) and Day 5 (H1_D5). Expression levels were normalised using the housekeeping gene *GAPDH* and mean standard error is displayed (technical replicates=3). Y-axis: target/housekeeping gene ratio. The x-axis depicts the samples.

qPCR results for *FBN1, FBN2* and *FBN3* mRNA in undifferentiated RH1 hESC at Day 2 of culture showed variation among the three genes. *FBN2* had the highest expression, followed by *FBN1* and *FBN3* ***(Figure 3.4)***. Fibrillin-1 and fibrillin-2 protein staining patterns were different at Day 5 of RH1 cell culture ***(Figure 3.4)***. There were visibly high levels of fibrillin-2 expressed intracellularly, while only very low levels of fibrillin-1 fibres could be detected ***(Figure 3.4)***.

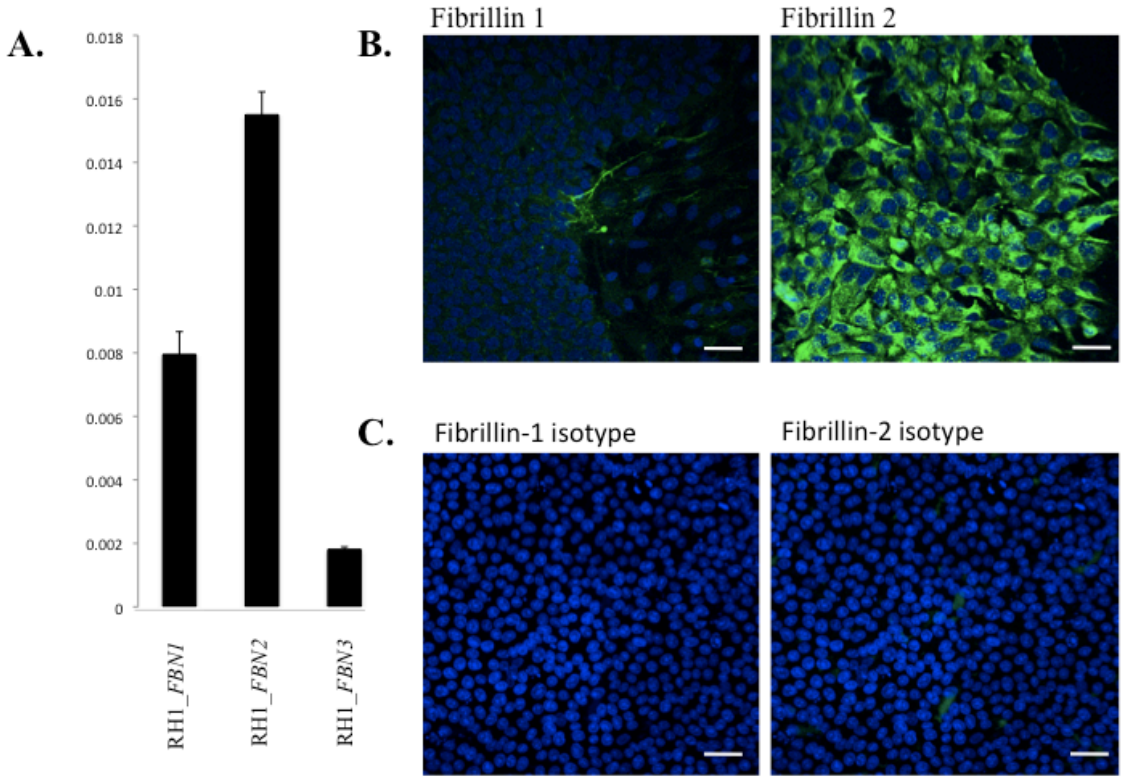

Figure 3.4. Fibrillin gene and protein expression in undifferentiated human RH1 embryonic stem cells. (A) Expression patterns of *FBN1*, *FBN2* and *FBN3* mRNA at Day 2 of culture. Expression levels were normalised using the housekeeping gene GAPDH and mean standard error is displayed (technical replicates=3). Y axis = target/housekeeping gene ratio. (B) ICC of fibrillin-1 and fibrillin -2 in undifferentiated RH1 cells at Day 5 of culture. The green fluorescence shows the distribution of fibrillin-1 (left panel) and fibrillin-2 (right panel). (C) Fibrillin-1 and fibrillin-2 isotype controls (Chapter 2, Section 2.4.2) The nuclei (blue) were counterstained with DAPI. Magnification 20X. The scale bars (white) show 50µm, n=2.

3.3.2 Validation of adipogenesis in the hESMP and ADMSC adipose differentiation time courses

Oil Red O staining was used to validate adipose differentiation (**Section 3.2.3**). The undifferentiated ADMSCs showed slight red staining at day 8 and day 18 ***(Figure 3.5)***. The ADMSC differentiated cells developed stainable lipid droplets by day 3, which was maintained with increased number and size of droplets by Day 18 ***(Figure 3.5)***. Cell line hESMP treated with the adipose medium showed different results ***(Figure 3.6)***. The nondifferentiated cells showed no Oil Red O staining or lipid droplet formation, while the hESMP cells being driven towards the adipose lineage showed a small amount of lipid accumulation ***(Figure 3.6)***. The lipid droplet formation was comparable to that of

ADMSC undifferentiated samples at Day 3 ***(Figure 3.5 and Figure 3.6)***. Hence, over this time period, very little adipogenesis had occurred in this cell line.

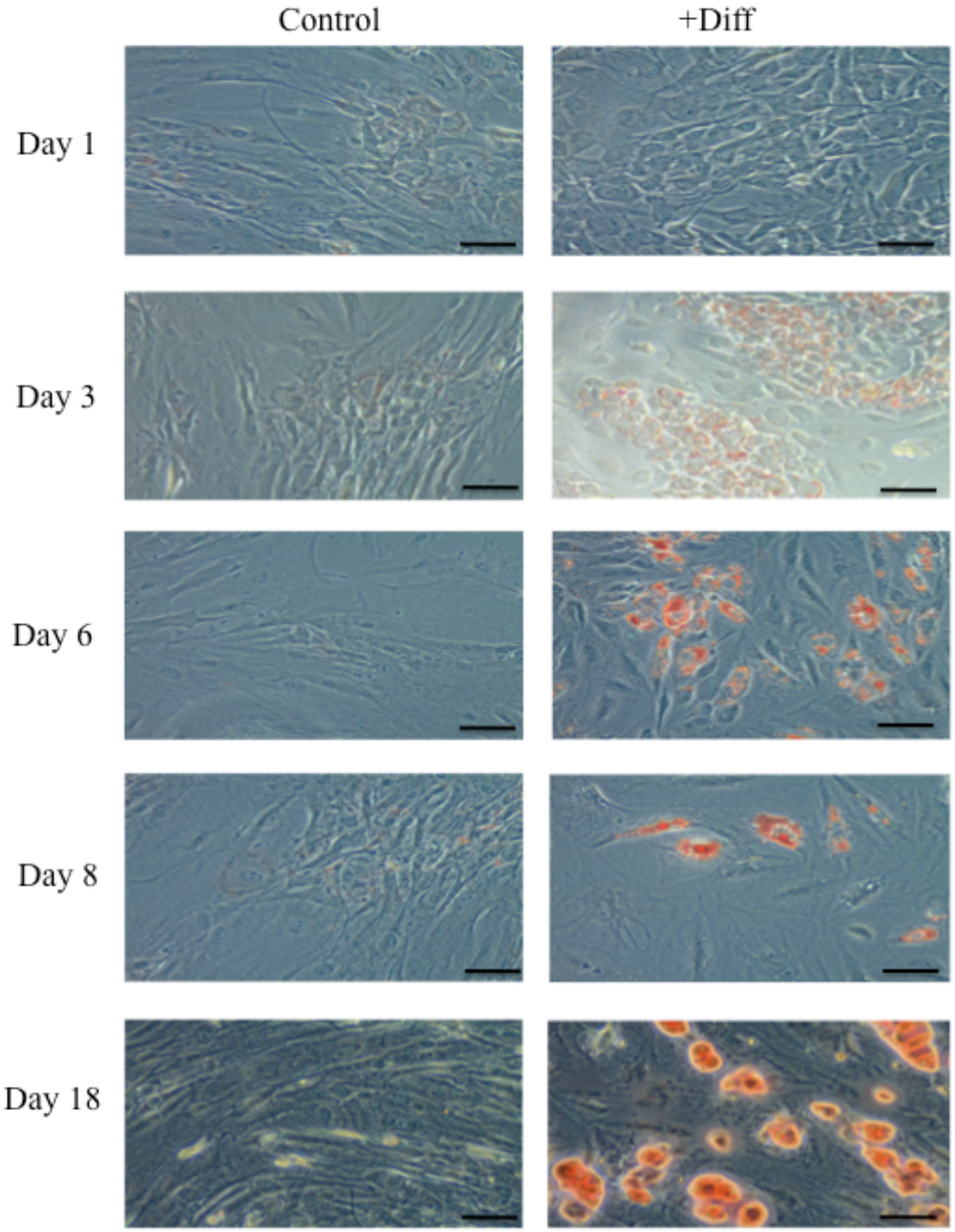

Figure 3.5. Lipid droplet formation in the ADMSC timecourse. ADMSC control cells (left panel) and ADMSC cells differentiating to adipose (right panel) stained with Oil Red O at Day 1, Day 3, Day 6, Day 8 and Day 18. The red color shows Oil Red O binding with lipid droplets forming within the cells. The images were taken using a Zeiss AX10 microscope at magnification of 20x. The scale bars show 50µm, n=2.

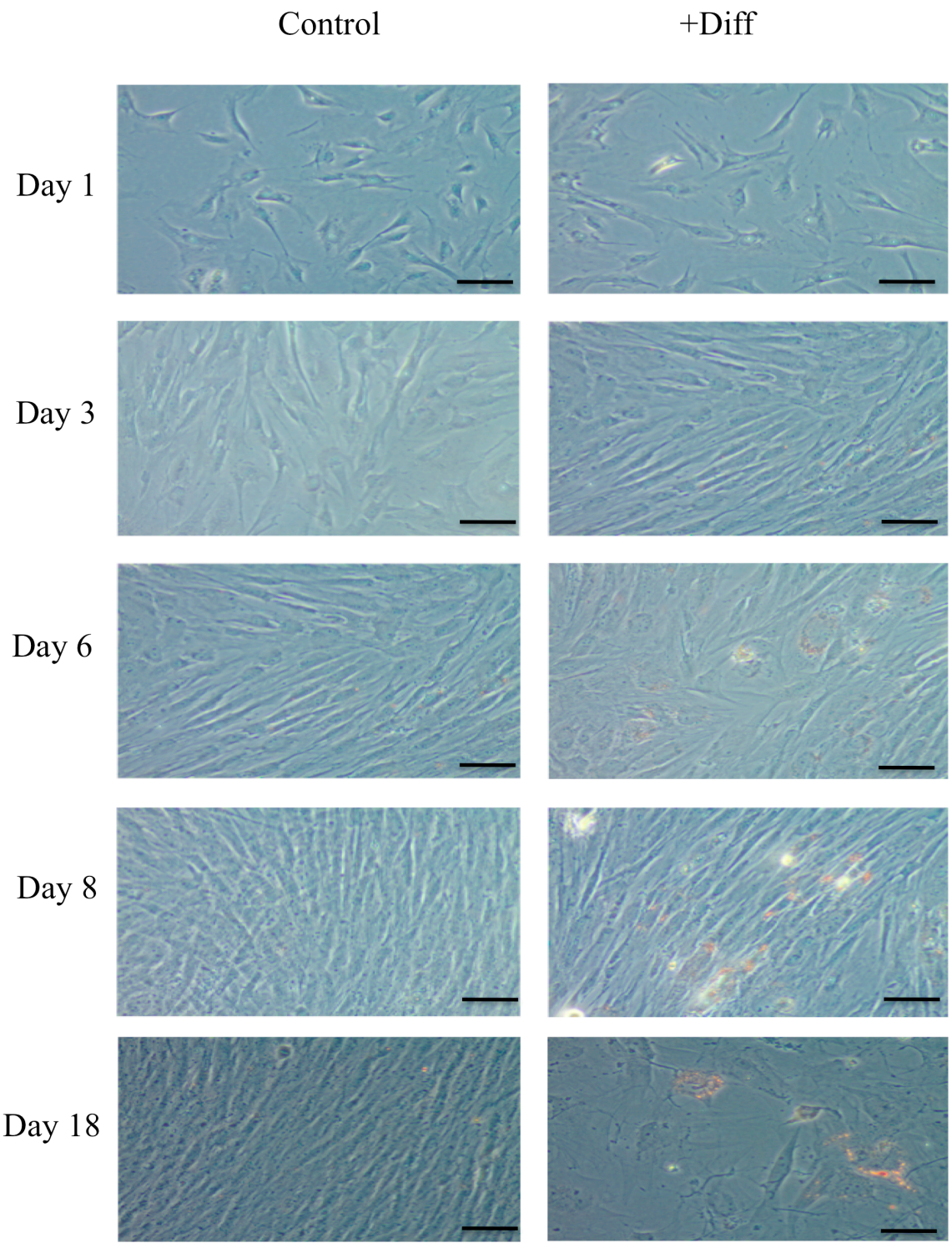

Figure 3.6. Lipid droplet formation in the hESMP timecourse. hESMP control cells (left panel) and hESMP cells differentiating to adipose (right panel) stained with Oil Red O staining at Day 1, Day 3, Day 6, Day 8 and Day 18. The red color shows Oil Red O binding with lipid droplets forming within the cells. The images were taken using a Zeiss AX10 microscope at magnification of 20x. The scale bars show 50µm, n=2.

3.3.3 Identifying Fibrillin-1 protein expression patterns during adipose differentiation.

The presence of fibrillin-1 proteins was assessed across the adipose differentiation time course using ICC (**Chapter 2, Section 2.4.2**).

Fibrillin-1 fluorescent ICC of ADMSC and hESMP was performed at the following times after induction of adipogenesis: Day 0, Day 1, Day 3, Day 7 and Day 14 ***(Figure 3.7)***. ADMSC cells undergoing adipose differentiation showed an extensive network of fibrillin-1 fibrils at Day 1, decreasing at Day 3, with very little fibrillin-1 staining after the completion of differentiation ***(Figure 3.7)***. These results differed from the undifferentiated cells where staining of the fibrillin-1 matrix increased over the time course. The hESMP differentiating culture demonstrated a vast fibrillin-1 matrix at Day 1 that was maintained through to Day 14 ***(Figure 3.7)***. Quality images of hESMP controls for Day 3, 7 and 14 were unable to be processed. Further replicates would be required to determine fibrillin-1 fibre formation in hESMP cells. The lack of lipid droplet formation in hESMP and the resemblance of fibrillin-1 protein staining to that of the untreated ADSMC suggest that the hESMP cells were not being pushed towards the adipose lineage. The cells were further assessed using microarray analysis to better determine the lineage progression of the hESMP cells.

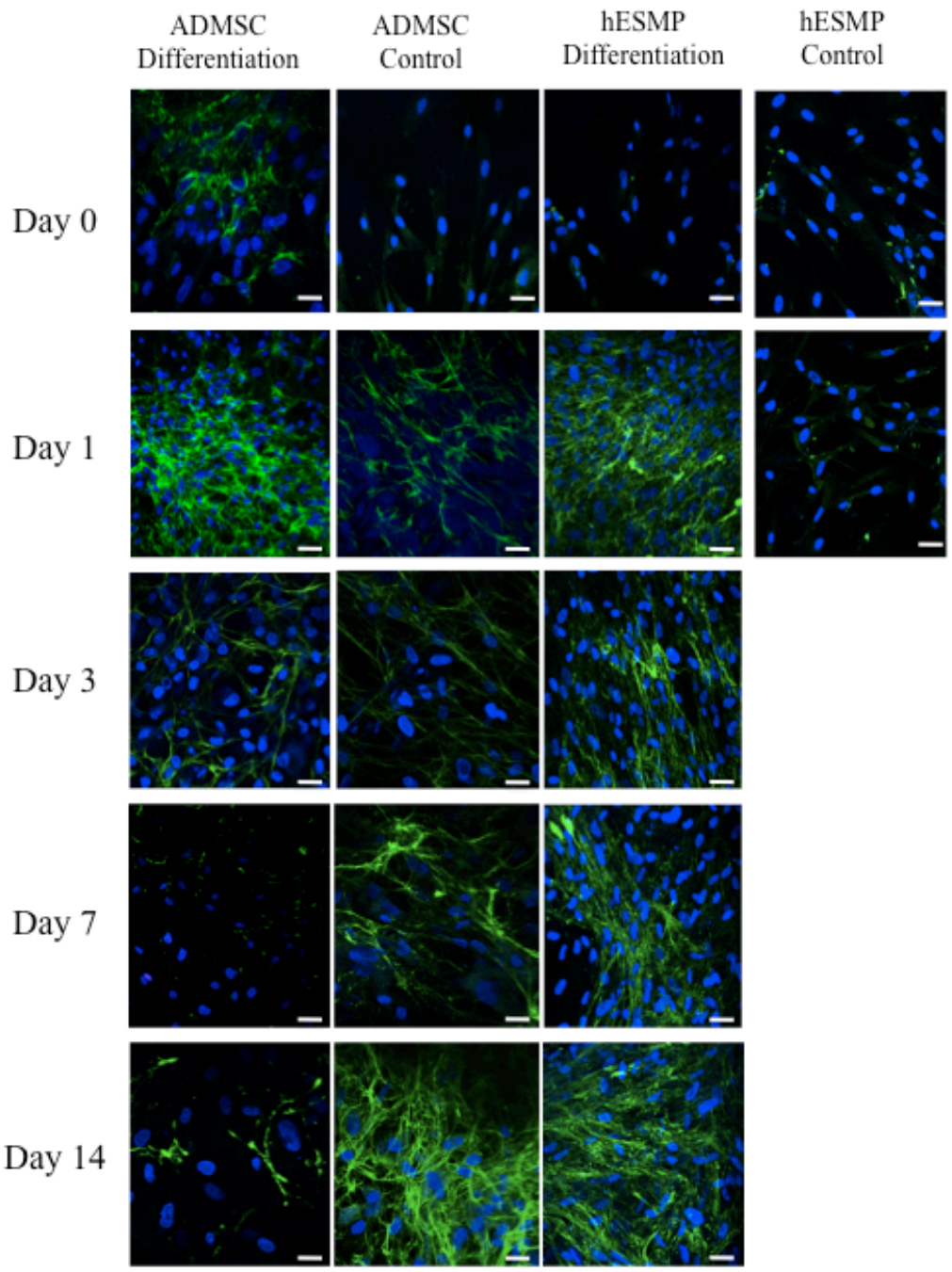

Figure 3.7. Fibrillin-1 immunofluorescence staining of the ADMSC and hESMP undergoing adipose differentiation. ADMSC control shows untreated ADMSC cells across the timecourse, ADMSC and hESMP differentiation shows ADMSC and hESMP cells progressing to the adipose lineage. hESMP controls for Day 3, 7 and 14 are unavailable (n=1). Fibrillin-1 is shown by green fluorescence (Chapter 2, Section 2.4.2). The nuclei are shown in blue (ProLong gold + DAPI (Invitrogen)). Images show results representative of n=3 replications. Magnification at 40x and the scale bars represent 20µm.

3.4 Gene clustering using BioLayout *Express* ^{3D}

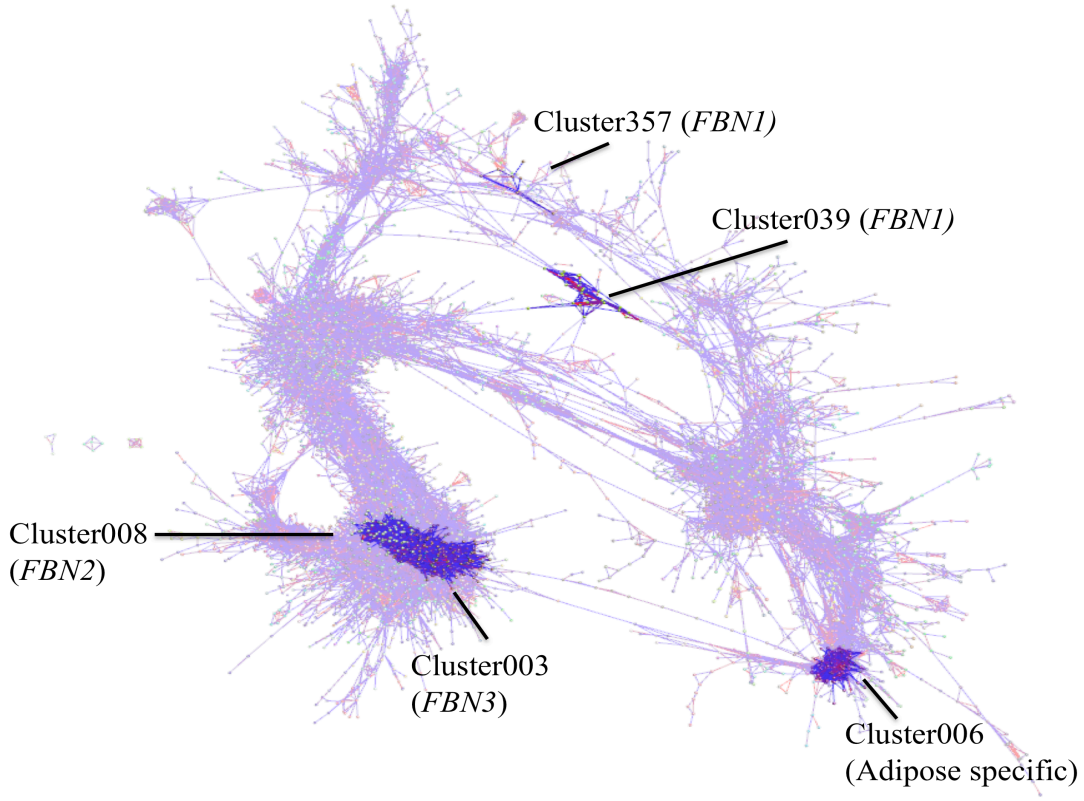

Figure 3.8. Network visualization and clustering of the transcriptomes of the H1, ADMSC and hESMP cells undergoing differentiation. The image depicts the network diagram produced by BioLayout *Express* ^{3D} using data from the Affymetrix U219 gene expression microarray platform. Spheres (nodes) represent individual probesets and the lines between them (edges) show correlations in expression pattern of r ≥ 0.95. The nodes were clustered using an MCL inflation value 1.7 (Chapter 2, Section 2.3.6). The background of the image displays the whole network and clusters discussed in the text are highlighted. Cluster357 and Cluster 039 contained *FBN1* probes, Cluster003 had *FBN3* probes, Cluster008 had *FBN2* probes and Cluster006 was specific to adipose lineage.

Probeset intensity values obtained using the human U219 microarray platform were used to determine clusters of genes that were co-expressed across the early and adipose differentiation timecourses using the tool BioLayout *Express* ^{3D}, which groups genes based on similarity of expression pattern across a sample set. This showed a large network of clusters containing a total of 21,098 nodes and 673,702 edges ***(Figure 3.8)***. Visual inspection of the clusters revealed probes for fibrillin genes in 5 clusters ***(Figure 3.8)***. Cluster 357 contained three probes for fibrillin-1 (FBN1: 11720507, FBN1: 11720509_a_at and FBN1: 11758093_s_at) and Cluster 039 contained a single fibrillin-1 probe (FBN1: 11754368_a_at) ***(Table 3.1)***.

Gene	Probset ID	Chromosome position	Region covered	Cluster
FBN1	11720509_a_at	15:48700505-48938046	Whole transcript (237,541bps)	357
	1175368_a_at	15:48702269-48758055	Exon 39 through the 3'UTR region (55,786bps)	039
	11720507_at	15:48700505-48938046	Whole transcript (237,541bps)	357
	1758093_s_at	5:48700504-48700908	Downstream of exon 65 within the 3'UTR (404bps)	357

Table 3.1. Fibrillin-1 probe identification on Human U219 Affymetrix microarray.

Cluster 008 contained a single probe for fibrillin-2 (FBN2: 11763384_at, NM_01999) and Cluster003 had the probe for fibrillin-3 (FBN3: 11732438_a_at, NM_032447). Clusters008 and 003 were specific to embryonic expression and were located close to each other in the network graph, while the clusters containing *FBN1* probesets showed expression in the mesenchymal stem cells (ADMSC / hESMP) as well as in the differentiated state for both mesenchymal cells and embryonic stem cells. In addition, Cluster006 consisted of multiple adipocyte markers expressed at high level towards the end of the ADSMC differentiation time course. The content of the clusters is described in detail in the following sections.

3.4.1 FBN1 is co-expressed with ECM related genes in both Cluster039 and Cluster357

FBN1 probesets were found in two gene clusters (Cluster039 and Cluster357). The mean expression patterns of all genes in the clusters are illustrated in ***Figure 3.9***. In the early development time course, *FBN1* showed highest levels of expression at Day 5 of hESC development/differentiation ***(Figure 3.9)***. The only discrepancy between the two clusters in the hESC samples was the level of expression in RH1 cells (undifferentiated) ***(Figure 3.9)***. The earlier qPCR analysis validated the microarray information, showing the same expression patterns ***(Figure 3.3)***. The majority of the genes associated with the *FBN1* clusters were of mesenchyme origin and active in the extracellular matrix, and highly expressed in ADMSC and hESMP cell types.

Cluster 039 contained a total of 34 nodes, corresponding to 11 unique genes, including one probeset for *FBN1* (FBN1: 11754368_a_at), joined by 163 edges. The genes in the

cluster mainly encoded components of the extracellular matrix and extracellular interacting proteins ***(Table 3.2).*** The mean expression of the genes remained unchanged regardless of differentiation stage ***(Figure 3.9)***. Cluster 357 consisted of 8 nodes, representing a total of 5 genes ***(Table 3.2)***, and 12 edges. The mean and individual probe expression patterns of all 8 nodes remained consistent in Cluster357 ***(Figure 3.9)***. There was a slight decrease in expression at Day 18 of adipose differentiation that was not found at Day 18 of the undifferentiated sample.

Cluster039		
Gene symbol	**Gene name**	**OMIM**
CAV1	Caveolin 1	601047
COL1A2	Collagen type 1 alpha 2	120160
FN1	Fibronectin 1	135600
KCTD10	Potassium channel tetramerization domain containing protein 10	613421
MKRN2	Makorin 2	608426
MXRA7	Matrix remodelling associated 7	Veiga-Castelli *et al.,* 2010
RSU1	Ras suppressor protein 1	179555
SPARC	Osteonectin	182120
TGFB1	Transforming growth factor beta 1	190180
TRAM2	Translocation- associated membrane protein-2	608485
Cluster357		
ADAM19	ADAM metallopeptidase domain 19	603640
APPBP2	Amyloid beta precursor binding protein 2	605324
CCDC176	Coiled-coil domain containing 176	Ota *et al.,* 2004
GTF2H5	General transcription factor IIH polypeptide 5	608780

Table 3.2. Genes that co-expressed with *FBN1* in Cluster039 and Cluster357.

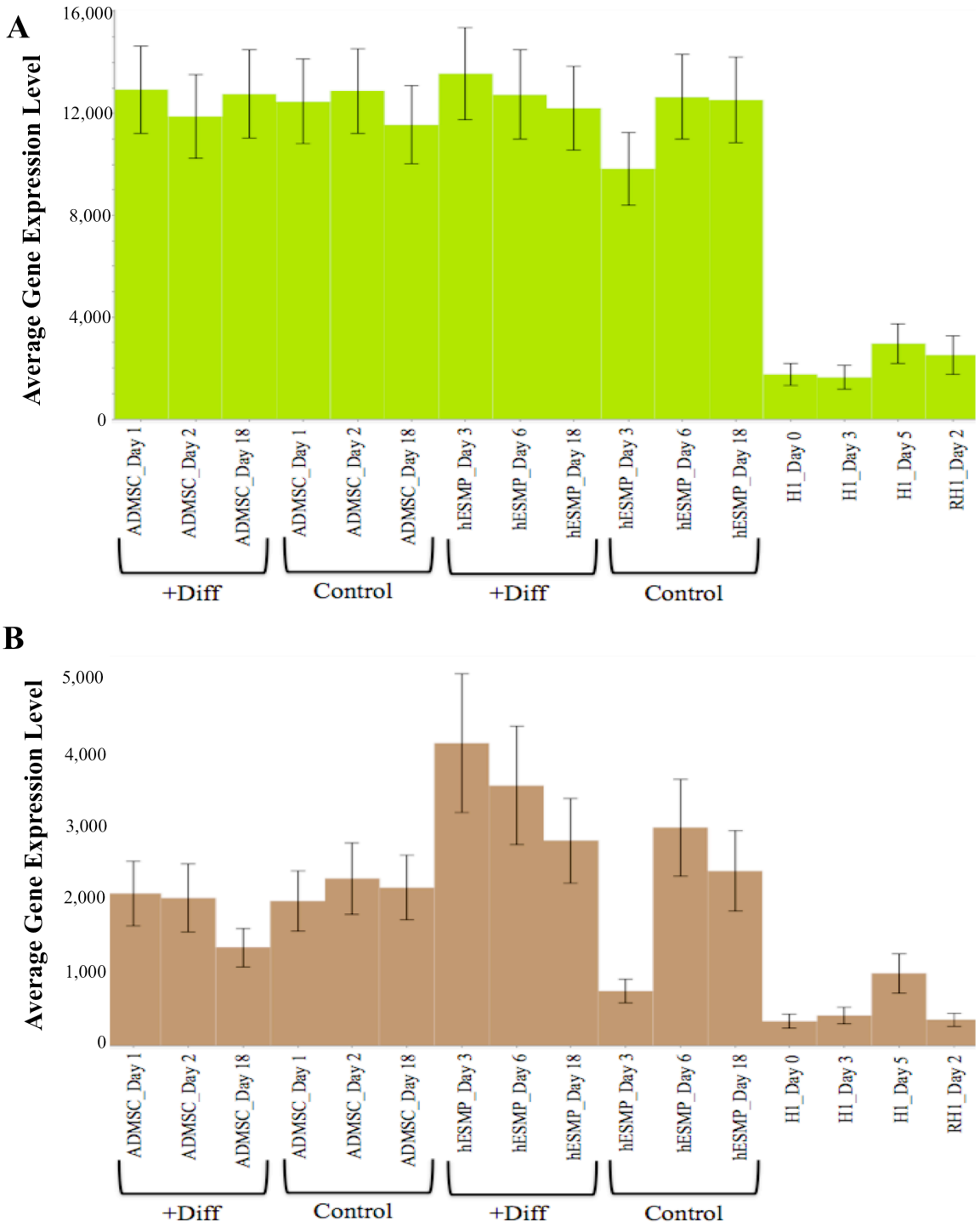

Figure 3.9. Plots of average expression profiles of genes in Cluster039 and Cluster357 following analysis using BioLayout *Express* [3D] (See *Figure 3.8)*. Y axis shows the normalised intensity value. X axis shows the samples from which the RNA was extracted. + Diff indicates cells undergoing adipose differentiation. Control indicates untreated cells. The last four samples on the histogram represent the expression patterns of differentiating H1 cells and the single RH1 cell sample at Day 2 of culture. (A) Cluster039 containing a total of 11 genes, including *FBN1*. (B) Cluster357 containing a total of 5 genes, including *FBN1*.

To further validate the expression patterns of *FBN1* in the ADMSC differentiating samples, qPCR analysis of *FBN1* mRNA expression across Day 1, Day 2 and Day 18 of adipose differentiated and undifferentiated samples was performed ***(Figure 3.10)***. The *FBN1* mRNA levels were not assessed for the hESMP timecourse because they did not differentiate to the adipose lineage (**See Section 3.3.2**). The qPCR results indicated a slight decrease in expression of *FBN1* during differentiation at Day 18 with an upregulation of expression at Day 18 in the undifferentiated culture ***(Figure 3.10A)***. These results were somewhat consistent with the *FBN1* mRNA probe intensity expression profiles ***(Figure 3.10B)*** and the protein staining ***(Figure 3.7)***. The mRNA levels differed between the qPCR and microarray analysis mainly at Day 18 in the undifferentiated samples ***(Figure 3.10)***.

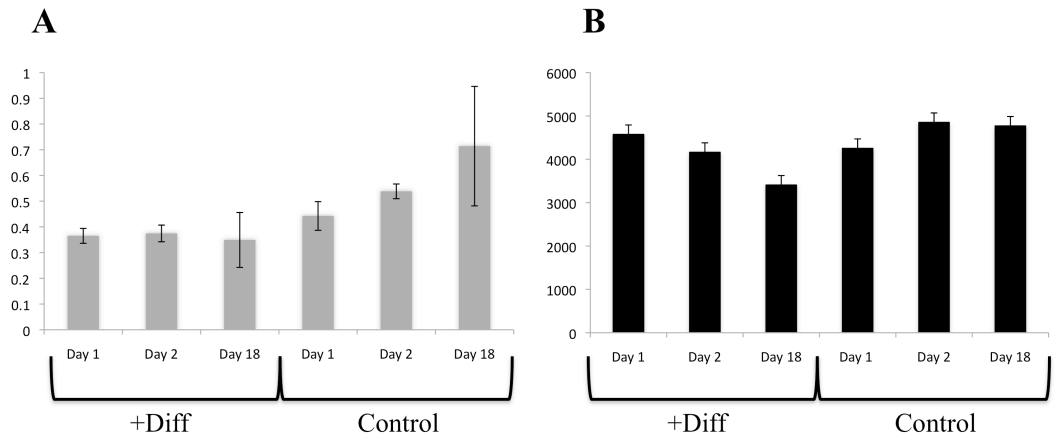

Figure 3.10. mRNA expression levels of *FBN1* during ADMSC differentiation to the adipose lineage. Expression patterns of *FBN1* at Day 1, Day 2 and Day 18 during differentiation (+Diff) and the control samples. (A) qPCR validation analysis. Expression levels were normalised using the housekeeping gene GAPDH and mean standard error is displayed (technical replicates=3). Y axis = target/housekeeping gene ratio. (B) Average of mRNA expression of the four *FBN1* probesets microarray data for ADMSC both differentiating and nondifferentiating to adipose lineage. The Y-axis represents the expression intensity detected by the U219 microarray analysis. The error bars represent standard errors determined in Microsoft excel across the average expression values.

3.4.2 *FBN2* is co-expressed with developmental genes in Cluster008

Cluster008 had a total of 232 nodes, representing 181 genes, and 4846 edges, with the highest overall expression of the genes in Day 3 of embryoid body development/differentiation ***(Figure 3.11)***. A single fibrillin-2 probe (FBN2: 11763384_a_at) was co-expressed with the cluster. The probe was designed to target

Chr5.127663780-127702115, which incorporates exon 23 through to exon 40 of transcript NM_001999. The high expression at Day 3 in H1 samples was consistent with the qPCR results ***(Figure 3.3)***, while there was very low and stable expression detected by FBN2: 11763384_a_at, across both hESMP and ADMSC adipose differentiation timecourses ***(Figure 3.11)***.

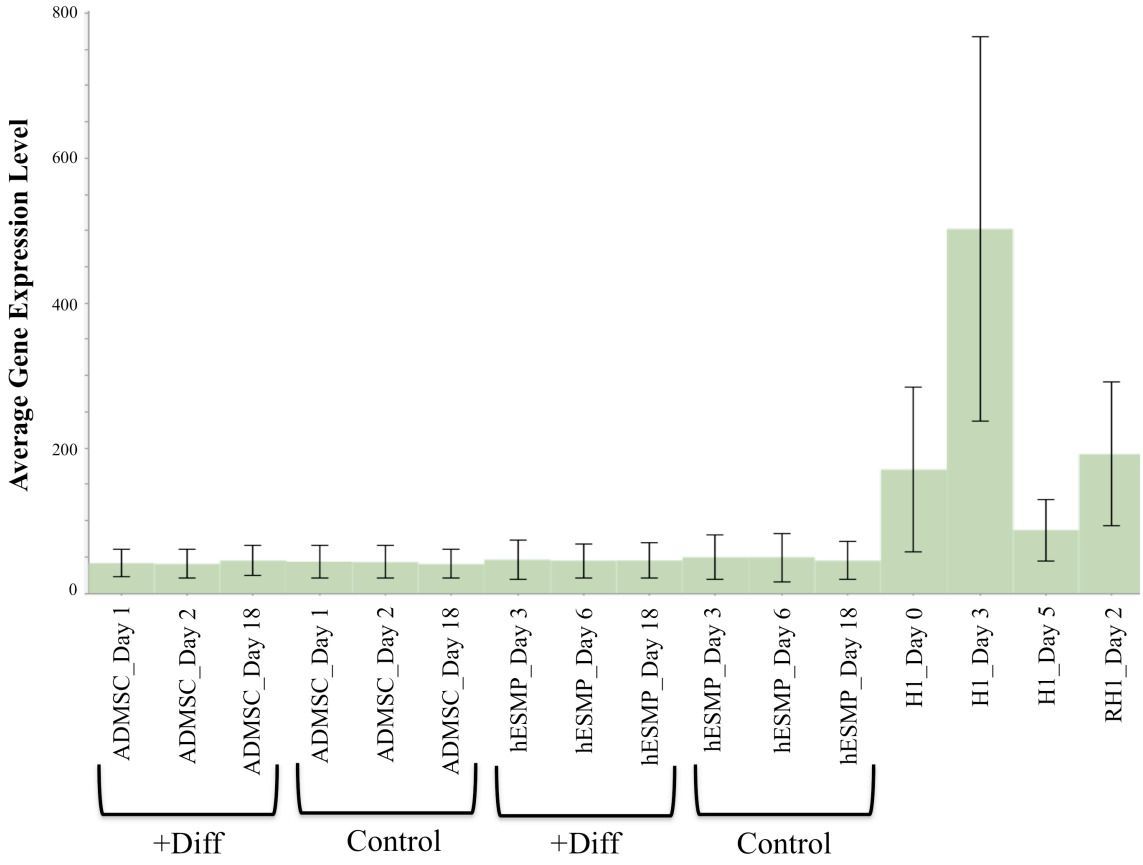

Figure 3.11. Plots of average expression profiles of genes in Cluster008 following analysis using BioLayout *Express* ^{3D} (See *Figure 3.8)*. Y axis shows the normalised intensity value. X axis shows the samples from which the RNA was extracted. + Diff indicates cells undergoing adipose differentiation. Control indicates untreated cells. The last four samples on the histogram represent the expression patterns of differentiating H1 cells and the single RH1 cell sample at Day 2 of culture (shown in bold). Cluster008 contained 181 genes.

DAVID GO terms analysis of the 181 genes within this fibrillin-2 early development cluster revealed the highest biological pathway GO terms associated with developmental process, multicellular organism development and anatomical structure development ***(Table 3.3)***. There were also multiple terms relating to embryogenesis as well as limb development ***(Table 3.3)***.

Cluster008		
Gene Ontology	**Number of Genes**	**P-value**
Biological Pathway (n=85)		
Developmental process	47	3.00E-3
Multicellular organismal development	46	7.40E-4
Anatomical structure development	41	1.40E-3
Embryonic Development	16	5.50E-4
Regulation of multicellular organismal process	15	8.50E-2
Embryonic morphogenesis	11	1.00E-3
Embryonic appendage morphogenesis	3	2.10E-1
Embryonic limb morphogenesis	3	2.10E-1
Appendage morphogenesis	3	2.10E-1
Limb morphogenesis	3	2.10E-1
Appendage development	3	2.10E-1
Limb development	3	2.10E-1
Cellular Compartment (n=7)		
Nucleus	58	5.20E-2
Microtubule cytoskeleton	10	7.10E-2
Occluding junction	4	3.10E-2
Tight junction	4	3.10E-2
Apical junction complex	2.2	6.50E-2
Disease (n=1)		
Psychiatric	12	5.10E-2

Table 3.3. A selection of GO terms associated with genes in Cluster008.

FBN2 was co-expressed with many genes associated with early embryogenesis and mesoderm formation ***(Table 3.4)***.

Cluster008		
Gene symbol	**Gene name**	**OMIM**
EOMES	Eomesodermin	604615
MESP1	Mesoderm posterior 1	608689
MESP2	Mesoderm posterior 2	605195
T	T, brachyury homolog	601397
WNT8A	Wingless-type MMTV integration site family member 8A	606360
NKD1	Naked cuticle drosophila homolog 1	607851
CFC1	Cryptic protein 1	605194

Table 3.4. Representative genes that co-expressed with *FBN2* in Cluster008.

Key early development genes co-expressing with *FBN2* included *EOMES*, an essential gene in mesoderm formation, *MESP1* and *MESP2,* important early developmental markers in cardiac development (Kitajima *et al.,* 2000), involved in early initiation of embryo segmentation (Saga *et al.,* 1997) and mesoderm development gene and mesoderm marker, *T* (brachyury) ***(Table 3.4)***. Furthermore, the cluster contained some genes involved in Wnt signalling, an important pathway in limb development. These genes included *WNT8A, NKD1* and *CFC1* ***(Table 3.4)***.

3.4.3 *FBN3* is co-expressed with early embryonic development, neurological and ECM related genes in Cluster003.

A single Affymetrix probe for *FBN3* was found in Cluster003 of the original clustering data ***(Figure 3.9)***. FBN3: 11732438_a_at detected the full NM_032447 transcript of *FBN3* from chr.19: 8130287- 8214730 though did not include the 5' or 3' UTR regions. Cluster003 consisted of 1326 nodes totalling 900 genes and 133,058 edges.

Consistent with initial qPCR results, *FBN3* and other genes in Cluster003 showed elevated expression levels at Day 0 with a steady decrease to Day 5 ***(Figure 3.3 and Figure 3.4 and Figure 3.12)***. RH1 untreated samples at Day 2 showed lower expression than H1 Day 1 and higher expression when compared to H1 Day 5 ***(Figure 3.12)***. There was very little expression of *FBN3* in the ADMSC or hESMP samples, regardless of their differentiated state.

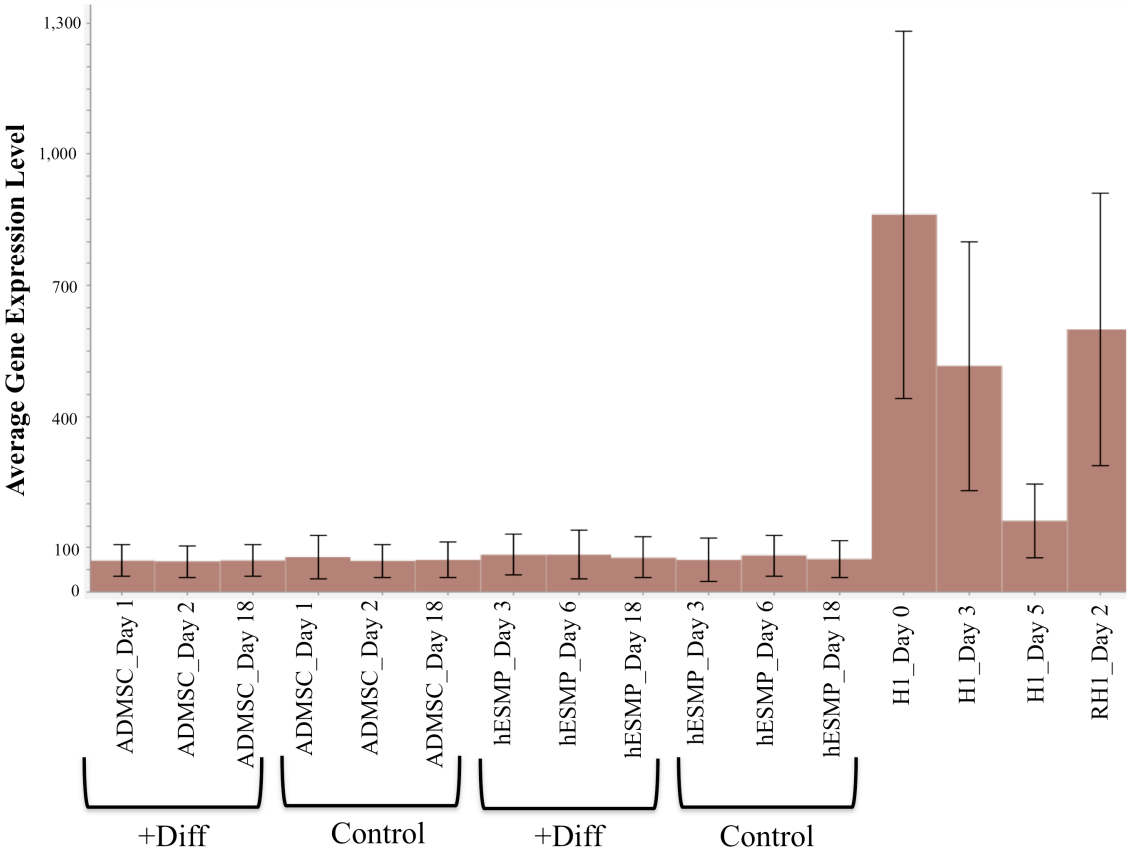

Figure 3.12 Plots of average expression profiles of genes in Cluster003 following analysis using BioLayout *Express* ^{3D} (See *Figure 3.8)*. Y axis shows the normalised intensity value. X axis shows the samples from which the RNA was extracted. + Diff indicates cells undergoing adipose differentiation. Control indicates untreated cells. The last four samples on the histogram represent the expression patterns of differentiating H1 cells and the single RH1 cell sample at Day 2 of culture. Cluster003 contained a total of 900 genes.

The 900 genes were subjected to DAVID GO term analysis, revealing multiple neuronal specific and embryonic biological pathway GO terms ***(Table 3.5)***. Though general cellular component terms such as nucleus and plasma membrane were associated with the highest number of genes, three extracellular matrix specific terms (extracellular region part, extracellular matrix and proteinaceous extracellular matrix) were also retrieved ***(Table 3.5)***. Two neurological diseases were associated with the cluster: neural tube defect and dementia ***(Table 3.5)***.

Gene Ontology (Fbn3)	Number of Genes	P-value
Biological Pathway (n=140)		
Nervous system Development	75	6.30E-4
Embryonic development	37	3.10E-2
Neuron Differentiation	33	7.20E-3
Neuron Development	27	8.10E-3
Neuron Projection Development	23	3.90E-3
Neural Crest cell differentiation	5	6.40E-2
Primary neural tube formation	5	6.40E-2
Neural crest development	5	6.40E-2
Cellular Components (n=23)		
Nucleus	259	1.10E-2
Plasma Membrane	193	3.20E-2
Plasma Membrane part	134	2.30E-4
Extracellular region part	56	4.00E-2
Cell junction	53	5.60E-8
Synapse	37	5.10E-6
Extracellular matrix	26	1.40E-2
Proteinaceous extracellular matrix	25	1.10E-2
Disease (n=4)		
Neural tube defect	5	9.20E-2
Dementia	4	6.00E-2
Cervical artery dissection, spontaneous	3	3.50E-2
Angina	3	7.90E-2

Table 3.5. A selection of GO terms associated with genes in Cluster003.

FBN3 co-expressed with many genes ($r \geq 0.95$) that were either ECM specific, active in early embryogenesis, markers of pluripotency or neuronal genes. This was further validated in the GO term ontology ***(Table 3.5)***. These genes are presented in ***Table 3.6***. The high correlation of the early developmental genes, especially pluripotency marker *NANOG,* suggests the possible importance for *FBN3* expression in early development.

Cluster003		
Gene Symbol	**Gene Name**	**OMIM**
ECM related		
ADAMTS16	A disintegrin-like and metalloproteinase with thromobospondin type 1 motif 16)	607510
ADAMTS19	A disintegrin-like and metalloproteinase with thromobospondin type 1 motif 19	607513
MMP9	Matrix metalloproteinase 9	120361
MMP15	Matrix metalloproteinase 15	602261
MMP25	Matrix metalloproteinase 25	608482
ENTPD2	Ectomucleoside triphosphate-diphosphohydrolase 2	602012
WNT3	Wingless type MMTV integration site family member 3	165330
LAMA5	Laminin alpha 5	601033
GPC2	Glypican 2	(Kurosawa *et al.,* 2001)
LAMC3	Laminin gamma 3	604349
Embryogenesis / pluripotency markers		
FOXH1	forkhead box H1	603621
NANOG	Nanog homeobox transcription factor	607937
OCT4	Octamer-binding transcription factor 4	164177
SOX2	Sry-box 2	184429
UTF1	Undifferentiated embryonic cell transcription factor 1	604130
NODAL	Nodal	601265
Neuronal associated		
CBS	Cystathionine beta-synthase	613381
CRABP1	Cellular retinoic acid binding protein 1)	180230
CYP26A1	Cytochrome P450 family 26 subfamily A polypeptide 1	602239

Table 3.6. Genes that co-expressed with *FBN3* in Cluster003.

3.4.4 ADMSC adipose differentiation, Cluster006

Cluster006 consisted of a total of 283 nodes, representing 167 unique genes, and 21,878 edges, with mean expression being the highest in Day 18 ADMSC differentiated mRNA samples ***(Figure 3.13)***.

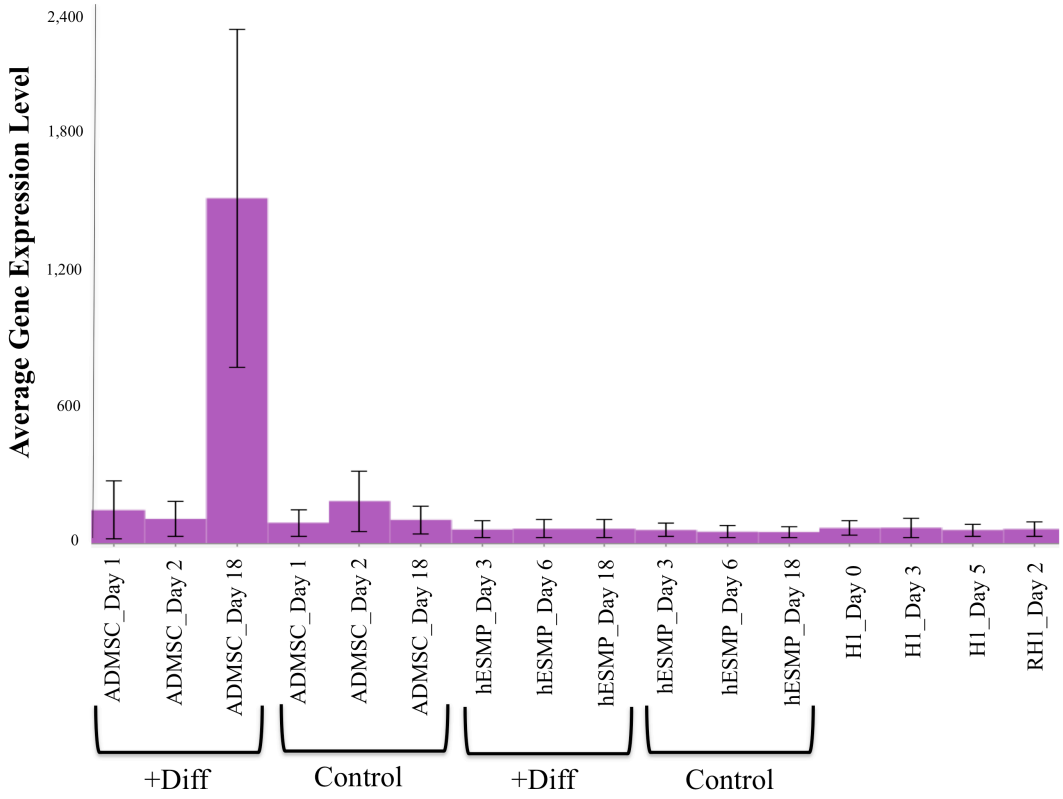

Figure 3.13. Plots of average expression profiles of genes in Cluster006 following analysis using BioLayout *Express* ^{3D} (See *Figure 3.8)*. Y axis shows the normalised intensity value. X axis shows the samples from which the RNA was extracted. + Diff indicates cells undergoing adipose differentiation. Control indicates untreated cells. The last four samples on the histogram represent the expression patterns of differentiating H1 cells and the single RH1 cells at Day 2 of culture. Cluster006 contained a total of 167 genes.

Most importantly the cluster contained adipocyte master regulatory genes, *PPARG* (encoding peroxisome proliferator-activated receptor gamma) and *CEBPA* (encoding CCAAT/enhancer-binding protein alpha). DAVID GO term analysis of the genes in cluster006 showed multiple lipid specific and differentiation terms, including lipid metabolic process and lipid localisation and several extracellular matrix terms ***(Table 3.7)***. Diseases association with the genes were diabetes and obesity ***(Table 3.7)***.

Go terms	Number of genes	P value
Biological pathway (n=419)		
Cellular process	116	4.7E-2
Lipid metabolic process	37	2.0E-14
Cellular lipid metabolic process	30	4.7E-14
Carbohydrate metabolic process	16	2.9E-4
Lipid localisation	6	2.1E-2
Cellular component (n=54)		
Cytoplasm	82	3.5E-2
Extracellular region	48	1.8E-9
Extracellular region part	35	1.6E-11
Extracellular space	24	1.3E-7
Extracellular matrix	15	5.3E-6
Disease (n=45)		
Diabetes, type 2	14	3.5E-3
Obesity	12	2.0E-5

Table 3.7. A selection of GO terms associated with genes in Cluster006.

Go terms for genes associated the lipid metabolic process and genes correlated with ECM are listed in ***Table 3.8***.

Cluster006		
Gene Symbol	**Gene Name**	**OMIM**
Lipid associated		
PPARG	Peroxisome proliferator-activated receptor gamma	601487
CEBPA	CCAAT/enhancer-binding protein alpha	116897
ADIPOQ	Adiponectin	605441
FABP4	Fatty acid binding protein 4- adipocyte	600434
GHR	Growth hormone receptor	600946
LEP	Leptin	164160
LIPE	Lipase, hormone sensitive	151750
LPL	Lipoprotein lipase	609708
PLIN1	Perlipin 1	170290
Extracellular matrix related		
TIMP4	Tissue inhibitor of metalloproteinase 4	601915
COMP	Cartilage oligomeric matrix protein	600310
COL5A3	Collagen type V alpha 3	120216
DPT	Dermatopontin	125597
MM19	Matrix metallopeptidase 19	601807

Table 3.8. Adipose and ECM specific genes in Cluster006.

The presence of these genes at Day 18 of the ADSMC differentiation is consistent with transformation into fat producing cells ***(Figure 3.5 and Figure 3.13)***. Their absence from the hESMP differentiation time course ***(Figure 3.13)*** confirms that those cells did not differentiate.

3.5 Discussion

This chapter examined the expression of the fibrillin gene family in early human embryonic development and in the differentiation of stem cells to the adipose lineage. The results for fibrillin-1 (Clusters039 and 357), fibrillin-2 (Cluster008) and fibrillin-3 (Cluster003) provided a detailed view of the fibrillins and co-expressing genes in the differentiation of the hESC (H1) cells to a mesoderm lineage. The mean expression patterns show that expression of genes in Cluster003 was highest at Day 0 and decreased over the time course, while Cluster008 genes were upregulated at Day 3 and Cluster039/357 expression was upregulated at Day 5, implying the differing functions of the fibrillin gene family during differentiation. Initial qPCR analysis validated the microarray findings of the H1 timecourse showing *FBN2* expression increased as *FBN3* levels declined, and *FBN1* mRNA expression was upregulated at Day 5 ***(Figure 3.3)***. These results were further validated through an analysis of data from publicly available database Functional Genomics of Embryonic Stem Cells (FunGenES, http://biit.cs.ut.ee/fungenes), a database containing microarray expression data in mice (Schulz *et al.,* 2004). Raw data file named "FungenES_UK0E-1" was downloaded and expression values for *Fbn1* and *Fbn2* were extracted. The file contained A-Affy-45 affymetrix geneChip mouse 430 .CEL files of mouse ES cells differentiating to embryoid bodies, with time points taken daily for 10 days. The results showed *Fbn1* levels to increase later than *Fbn2* levels ***(Figure 3.14)***. The *Fbn3* gene is degenerate in mice (**Chapter 1, Section 1.3**) and therefore *Fbn3* mRNA levels were not measurable.

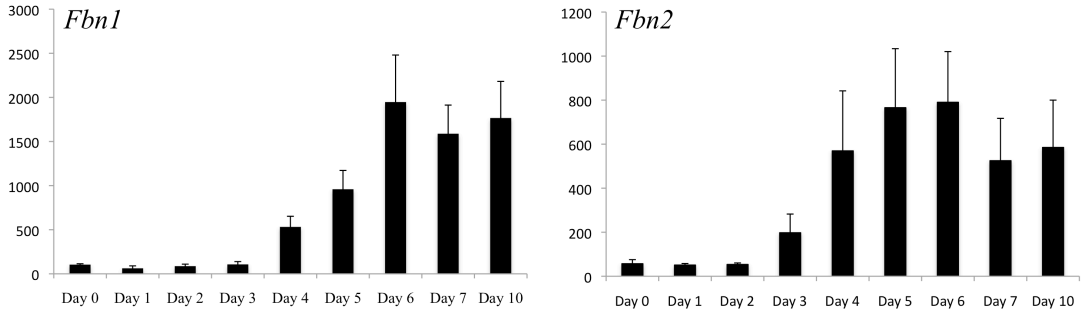

Figure 3.14. mRNA expression of *Fbn1* and *Fbn2* during mouse ESC differentiation to embryoid body formation. The graphs display microarray data from FunGenES, A-affy-45 affymetrix geneChip mouse 430 (2.0) analysis (See Section 3.4.1). The X-axis depicts the timepoints of the samples, and the y-axis shows the expression intensity.

3.5.1 Limitations of differentiation studies

The major limitation throughout the chapter was the low number of samples that could be assessed. The chapter illustrated preliminary results depicting the expression patterns of the fibrillin gene family and other key genes in adipose and early differentiation. To further support this chapters initial findings, the studies would need to be repeated (minimum of n=3 replicates) in the ES cell types. In addition, using multiple donors of ADMSC cells would assist in validating the observations of fibrillin expression patterns and developing the hypothesis about the role of fibrillin expression during adipose differentiation.

3.5.2 Fibrillin-1 in early differentiation and adipose differentiation

ADSMC were successfully differentiated to the adipose lineage, as demonstrated through both Oil Red O staining ***(Figure 3.5)*** and analysis of genes expressed at the end point (Day 18) **(Section 3.4.4)**. This differentiation study showed that *FBN1* was co-expressed with many genes associated with later development and mesenchymal lineage specific markers in ADMSC cells. There were slight differences in expression of the clusters containing *FBN1* ***(Figure 3.9)*** though overall the expression pattern remained stable. Quantification of *FBN1* mRNA through qPCR showed that at Day 1, Day 2 and Day 18 of both differentiating and control ADMSC samples, the mRNA expression remained unaltered ***(Figure 3.10)***, although the level of fibrillin-1 protein was very low after day 3

(Figure 3.7). This suggests upregulation of enzymes that degrade fibrillin-1 rather than down regulation of *FBN1* during differentiation, consistent with the upregulation of *MMP19* in Cluster006 at Day 18 of adipose differentiation ***(Figure 3.13)(Table 3.8)***. In humans with *FBN1* mutations there can be a generalized lack of adipocytes and fat deposition, indicating that normal fibrillin-1 is important in adipogenesis. The results here suggest that fibrillin-1 is present early in adipogenesis but is then possibly degraded as differentiation progresses. Therefore, further functional studies, such as knockdowns or genome editing, would need to be conducted to better understand the role of the fibrillin-1 protein in adipogenesis **(Chapter 8)**.

The study also showed that *FBN1* was co-expressed with many key ECM related genes during adipogenesis including *CAV1, COL1A2, FN1, SPARC, TGFB1* and *ADAM19* ***(Table 3.2)***. There is currently no evidence for a role of *ADAM19* in adipogenesis or any possible interactions with the fibrillin gene family. It is highly associated with embryogenesis (Yan *et al.,* 2011), neurological processes, cardiovascular development, inflammatory response and possibly with Alzheimer's disease (Qi *et al.,* 2009).

SPARC is a key protein in maintaining the structure and affecting the synthesis of the ECM (OMIM: 182120) (Bradshaw *et al.,* 2003) and in addition to *Col1a2*, the gene has been shown to co-express with *Fbn1* in mice (Summers *et al.,* 2010) **(Chapter 1, Section 1.4.2).** SPARC may play a key role in homeostasis of the adipose ECM. SPARC null mice have increased adipose tissue, suggesting that SPARC assists in maintaining normal adipose levels (Bradshaw *et al.,* 2003). The co-expression of both *FBN1* and *SPARC* demonstrated in this study is consistent with the involvement of both proteins in adipose maintenance.

FN1 is a key component of the ECM and provides essential functions in embryogenesis **(Chapter 1, Section 1.2.4)**. *FN1* null mice die *in utero* with multiple complications including defects of mesenchyme derived tissues, neural tube formation and heart vessel malformation (George *et al.,* 1993, Pankov and Yamada, 2002, Lee *et al.,* 2012). Decreased *FN1* mRNA levels have been demonstrated in severe (morbid) obesity (Lee *et al.,* 2012), suggesting that *FN1* and *FBN1* maybe be involved in adipose homeostasis. *COL1A2* is generally a key component of the ECM in bone and cartilage tissue, though

the gene is expressed in adipose (http://biogps.org), and mRNA of *COL1A2* increases following insulin induction in mouse adipocytes (Wang *et al.,* 2006). In the U219 microarray analysis described in this chapter, *FN1* and *COL1A2* levels remained stable, similar to *FBN1* levels across the timecourse (**Section 3.4.1**). It has been established that fibrillin-1 requires fibronectin to produce an ECM in fibroblasts (Kinsey *et al.,* 2008, Sabatier *et al.,* 2009)**(Chapter 1, Section 1.2.4),** and fibronectin may facility deposition of collagen 1 (Velling *et al.,* 2002), so the stability and co-expression of *FBN1*, *FN1* and *COL1A2* mRNA may be necessary to maintain the dynamic ECM composition required to adjust to the production of lipid within the cytoplasm.

CAV1 (OMIM: 601047) encodes the protein caveolin-1, which produces pits within the plasma membrane called caveolae, which are specialised "lipid rafts". *CAV1* is highly expressed in adipocytes and bronchial epithelial cells (http:/biogps.org) and mutations in *CAV1* have been associated with multiple adipose and lung specific disorders such as congenital generalized lipodystrophy type 3 (MIM: 612526), partial lipodystrophy, and primary pulmonary hypertension 3 (MIM: 615343) as well as congenital cataracts and neurodegenerative syndrome (MIM: 606721). Previous research suggests that *CAV1* may be a marker of later adipocyte development (Fernandez-Real *et al.,* 2010, Blouin *et al.,* 2008).

FBN1 and *CAV1* in the regulation of *TGFB* were further considered, given that *TGFB1* was also co-expressed with these genes. An increase in *TGFB1* levels has been associated with an increase in the adipose tissue (Choy and Derynck, 2003). In this study *TGFB* mRNA expression remained stable, in parallel to *FBN1* mRNA. As adipose differentiation occurs, TGFB receptors become less available, leading to a downregulation in SMAD signalling (Choy *et al.,* 2000).

When *CAV1* is upregulated, it suppresses TGFB signalling by binding to the TGFBR1, which inhibits the signal cascade of SMAD2 phosphorylation and SMAD4 activity (Razani *et al.,* 2001) (**Chapter 1, Section 1.3.3**). In addition, Razani *et al.,* (2001) showed that a decrease in *CAVI* transcription led to an increase in TGFB signalling. While fibrillin-1 has not been shown to interact with the TGFB receptors, it aids in sequestering TGFB, thereby preventing binding to the receptor **(Chapter 1, Section**

1.3.3). Both *FBN1* and *CAV1* mutations cause lipodystrophy, and the genes are co-expressed in adipose differentiation, suggesting that fibrillin-1 and CAV1 may be involved in regulating TGFB signalling in adipogenesis.

3.5.3 Fibrillin-2 in early differentiation

Cluster008 included multiple markers for formation of mesoderm, one of the three primary germ layers of the early embryo **(Section 3.1.2)**. These markers included *EOMES* (eomesodermin), *MESP1* (mesoderm posterior 1), *MESP2* (mesoderm posterior 2), and T (T, brachyury homolog), and some cell division genes, for example *CEP70* (centrosomal protein 70kDa).

T and *EOMES* are essential genes in mesoderm formation (Ninomiya *et al.,* 2004, Russ *et al.,* 2000). The embryonic development of *EOMES* deficient mice is halted at the blastocyst stage leading to spontaneous abortion (Russ *et al.,* 2000), demonstrating the gene's essential function in mesoderm formation. *T* mutant mice were found to be embryonic lethal, presenting with fragmented notochord and abnormal cardiac formation (Abe *et al.,* 2000). *MESP2* is highly involved in the NOTCH signalling pathway that leads to segmentation in early embryogenesis (Takahashi *et al.,* 2000, Morimoto *et al.,* 2005, Saga *et al.,* 1997). Mutations in *MESP2* also lead to autosomal recessive spondylocostal dysostosis 2 (MIM: 608681), a disorder that results in abnormal vertebral segmentation beginning *in utero* (Cornier *et al.,* 2008). *MESP1* is less well characterised but is also implicated in cardiac mesoderm development (Kitajima *et al.,* 2000).

The presence of *FBN2* in this cluster suggests that it is associated with mesoderm formation. This is consistent with previous reports that *FBN2* is activated before *FBN1*, leading to the hypothesis that fibrillin-2 provides a scaffold for elastin deposition while fibrillin- 1 maintains the homeostasis of the microfibrils into adult life (Zhang *et al.,* 1994, Mariencheck *et al.,* 1995, Quondamatteo *et al.,* 2002).

In addition to mesoderm formation, Cluster008 contained many genes involved in the WNT signalling pathway, including *WNT8A*, *NKD1*, *CFC1* and *PTCH1* **(Discussed in Section 3.4.2)**. This pathway is involved in limb development (reviewed in (Church and Francis-West, 2002)), and limb development related GO terms were highly correlated

with Cluster008 ***(Table 3.3)***. *PTCH1* (OMIM: 601309) had a direct edge to *FBN2* in the BioLayout *Express* ^{3D} network graph, and was grouped with *FBN2* and *PDX1* in multiple limb development GO terms ***(Table 3.3)***. *PTCH1* is the receptor for sonic hedgehog (SHH) (Ming *et al.,* 2002), the pathway that is crucial for limb development (Anderson *et al.,* 2012). *PTCH1* mutations are associated with many human diseases listed in OMIM including somatic basal cell carcinoma (MIM: 605492), basal cell nevus syndrome (MIM: 109400) and forebrain abnormality holoprosencephaly 7 (MIM: 610828).

In adult cells and tissues, fibrillin-2 is a mesenchyme specific gene, highly expressed in cells of bone and cartilage (**Chapter 1, Section 1.4.2**). Its expression level was low during adipogenesis ***(Figure 3.11)***. This BioLayout *Express* ^{3D} analysis further validates the known expression pattern trends of *FBN2* in early development and identified several *FBN2* co-expressing genes involved in limb development.

3.5.4 Fibrillin-3 in early differentiation

The 900 genes found to co-express with *FBN3* in the BioLayout *Express* ^{3D} analysis were associated with embryogenesis, neurological function, and ECM localization ***(Table 3.6)***. Fibrillin-3 has been characterized as an ECM gene and the gene is expressed early in development (Corson *et al.,* 2004), as well as in foetal lung and brain (http:/biogps.org). Cluster003 contained many pluripotency markers with decreasing expression across the time course ***(Figure 3.12)***. Well established pluripotency markers included *POU5F1* (POU class 5 homeobox 1 (also known as *OCT4*)), and *SOX2* (SRY sex determining region Y-box 2) (Niwa *et al.,* 2000, Rais *et al.,* 2013, Tay *et al.,* 2008)***(Table 3.6)***. In addition, *DPPA2/3/4/5* (developmental pluripotency associated 2/3/4/5), *JARID2/1C* (Jumonji, AT rich interactive domain 2/ domain containing 1C), *NODAL* (nodal growth differentiation factor), and *UTF1* (undifferentiated embryonic cell transcription factor 1) were included in Cluster003.

Two key embryonic marker genes were found to be highly correlated with *FBN3* and present within Cluster003. *NANOG* (OMIM: 607937) is a key gene marker for pluripotency (Tay *et al.,* 2008, Abranches *et al.,* 2014). *FOXH1* (OMIM: 603621) is involved in NODAL signalling, an important signal transduction pathway directly related

to differentiation during embryogenesis. The co-expression of *FBN3* with these pluripotency markers suggests that it is important early in development.

Cluster003 contained *TERF1* (telomeric repeat binding factor (NIMA-interacting) 1), and *TERT* (telomerase reverse transcriptase), which encode major proteins involved in maintenance of telomere length (OMIM: 600951)(OMIM: 187270). Key DNA methylation and cell division genes, for example *DNMT3A/3B* (DNA (cytosine-5)-methyltransferase 3 alpha / beta) (OMIM:602769)(OMIM: 602900)(Yanagisawa et al., 2002) and *MAP7* (microtubule-associated protein-7) (OMIM: 604108), were also in this cluster. The decreasing mRNA level for these pluripotency-associated genes demonstrated that the cells were switching from a pluipotent state to a lineage specific state.

There were multiple genes that were derived from the DAVID GO term analysis under neurological specific terms including *CBS* (OMIM: 613381), *CRABP1* (OMIM: 180230) and *CYP26A1* (OMIM: 602239). *CBS* is a gene that encodes cystathionine ß synthase that is involved in the transsulfuration pathway that converts methionine to cysteine in many cell types (OMIM: 613381)(McBean, 2011). *CBS* mutations are associated with B6-responsive and nonresponsive homocystinuria and thrombosis (OMIM: 236200). The phenotype associated with a deficiency in CBS includes some signs and symptoms similar to Marfan syndrome, including ectopia lentis (Sadiq and Vanderveen, 2013) and myopia (MIM: 236200) (Mudd, 2011, Perry, 1999, Lim and Lee, 2013), as well as developmental delay and other neurological manifestations. CRABP1 is a cellular retinoic acid binding protein (Kainov *et al.,* 2014). It has high mRNA expression in neuroblastoma cells (Plum and Clagett-Dame, 1995) though there were no specific neurological disorders associated with the gene. CYP26A1 is a retinoic acid inactivating protein essential to regulating retinoic acid levels during embryo development (Niederreither *et al.,* 2002) and *Cyp26a1* null mice exhibit many neural crest deformities (Maclean *et al.,* 2009). Retinoic acid (a derivative of vitamin A) is predicted to be involved in segmentation and hindbrain formation in mouse embryos (Rhinn *et al.,* 2011). The co-expression of these neural specific genes with *FBN3*, is consistent with the expression of *FBN3* in foetal brain and suggests a role for fibrillin-3 in neurological development.

MMP9, MMP15 and *MMP25* had direct edges to *FBN3*. MMPs are key ECM disassembly proteases required for ECM homeostasis. *MMP9* (OMIM: 120361) is a catalyst of ECM degradation and has been associated with connective tissue disease metaphyseal anadysplasia 2 (MIM: 120361), which affects both bone and cartilage formation (Lausch *et al.,* 2009). *MMP9* is also associated with bone and cartilage formation and repair (Huang *et al.,* 2014). *MMP15* (OMIM: 602261) is a widely expressed gene, and its product is involved in the EMT during early development **(Chapter 3, Section 3.1.2)**. *MMP25* (OMIM: 608482) encodes an ECM degradation protein involved in embryonic growth, tissue remodelling, ovulation and wound healing. More recently *MMP25* has been implicated in downstream interactions with *TGFB3* in early mouse embryonic development (Brown and Nazarali, 2010). While the MMP genes associated with *FBN3* have varying functions in embryonic development, they are all associated with maintaining ECM homeostasis and early ECM development.

There were several other genes encoding proteins involved in ECM synthesis and maintenance including *LAMA5* (OMIM: 601033)*, ENTPD2* (OMIM: 602012)*, ADAMTS16* (OMIM: 607510)*, ADAMTS19* (OMIM: 607513)*, LAMC3* (OMIM: 604349) and *GPC2*. *LAMA5* is a key laminin gene that was originally discovered in many adult mouse tissues and later identified in embryogenesis (Miner *et al.,* 1995, Miner *et al.,* 1998) (**Chapter 1, Section 1.2.3**). *Lama5* null mice have severe skeletal and neurological defects prior to premature embryonic death (Miner *et al.,* 1998). *LAMC3* is a widely expressed laminin gene and its product is predicted to be present in a stable ECM (Koch *et al.,* 1999). Expression was further identified within the retina (Cserhalmi-Friedman *et al.,* 2001) and mutations have been associated with occipital cortex malformations (MIM: 614115)(Barak *et al.,* 2011). *ADAMTS16* shows prominent expression in the kidney and has been linked to inherited hypertension (Joe *et al.,* 2009). Very little is known about low expressing *ADAMTS19,* though expression has been detected in foetal lung and it has more recently been identified as a possible candidate gene in premature ovarian failure (Cal *et al.,* 2002, Knauff *et al.,* 2009). Interestingly, both *FBN3* and *ADAMTS19* genes are candidates for ovarian disorders **(Chapter 1, Section 1.3.6)**. *ENTPD2* was associated with the proteinaceous ECM based on DAVID GO term analysis, and is also involved in

ocular development (Masse *et al.,* 2007). GPC2 is a heparan sulfate proteoglycan (Stipp *et al.,* 1994), involved in neurological growth (Kurosawa *et al.,* 2001).

The ECM genes found to co-express with *FBN3* had varying functions, but they all assist in maintaining ECM homeostasis. The function and predicted mechanisms of the co-expressed genes highlight the role of fibrillin-3 in the ECM, specifically in embryonic ECM development.

3.6 Conclusions

In summary, *FBN1* was predominant in early adipose differentiation and later embryogenesis, co-expressing with several genes involved in adipogenesis **(Section 3.4.1)**. *FBN2* was highly correlated with genes involved in mesoderm formation and limb development **(Section 3.4.2)**. Furthermore, *FBN3* was highly associated with genes in early embryogenesis, pluripotency, neuronal development and ECM maintenance **(Section 3.3.3)**. Therefore, this chapter has identified several key genes that co-express with *FBN1, FBN2* and *FBN3* in early differentiation and later differentiation of MSCs to adipose, though further studies will be required to support the relationships **(dicussed in Chapter 8)**. The studies described here focussed on two time courses of differentiation and development. As described in **Chapter 1, Section 1.1,** MSCs are capable of differentiating into multiple connective tissue lineages. The expression of the fibrillin gene family will be further explored in other connective tissue cell types in **Chapter 4**.

Chapter 4. Fibrillin expression in human connective tissue cell types

4.1 Introduction

In the previous chapter, the expression of the three fibrillin genes in two models of differentiation was examined. *FBN3* was strongly associated with pluripotency and its level declined in a model of early human development, while *FBN2* was associated with markers of mesoderm and *FBN1* appeared latest in embryonic development, but was strongly expressed in undifferentiated mesenchymal stem cells and in the early stages of adipogenesis. Since mesenchymal stem cells can differentiate in multiple other lineages, for example, chondrocytes, osteoblasts and fibroblasts (**Chapter 1, Section 1.1**), this chapter explores the expression of fibrillins in other mesenchyme derived cell types, using a number of human cell lines: neonatal fibroblasts (NHDF), chondrocyte cell lines (C20A4, C28I2 and TC28A2), osteosarcoma cell lines (SAOS2 and MG63), a human embryonic kidney cell line (HEK293) and human monocyte cell line (THP1)(**Chapter 2, Sections 2.1.1-2.1.5**).

Mutations in fibrillin-1 and fibrillin-2 affect multiple connective tissues outlined in **Chapter 1, Section 1.3.4 and 1.3.5**, including long bone, cartilage and dermal fibroblast formation. Marfan syndrome is the most frequent result of fibrillin-1 mutations and is diagnosed in patients based on the revised Ghent criteria, which include familial inheritance and *FBN1* mutations as well as physical abnormalities (Aalberts *et al.,* 2012, Loeys *et al.,* 2010, De Paepe *et al.,* 1996, Summers *et al.,* 2012). Both previous (De Paepe *et al.,* 1996) and current Ghent criteria (Loeys *et al.,* 2010) describe the skeletal and cartilage deformities as follows, pectus carinatum, pectus excavatum, increase long bone formation (upper and lower segments) arachnodaclyly, joint hypermobility, and facial appearance. This chapter will use osteosarcoma cell lines and chondrocyte cell lines to investigate the role of the fibrillin gene family in a bone and cartilage model system.

SAOS2 cells are capable of mineralisation and show upregulation of multiple osteoblast specific proteins such as, osteocalcin, bone sialoprotein (BSP), decorin, collagen 1,

collagen type III and osteoprotegerin **(Chapter 2, Section 2.1.1)**(Pautke *et al.,* 2004). Due to the lack of primary human bone cells available, SAOS2 cells were used as a model system for bone development and formation. The fibrillin gene family was also investigated in a non-mineralising human osteosarcoma cell line, MG63 **(Chapter 2, Section 2.1.1)**. While these cells are considered more immature in comparison to SAOS2, there was low but measurable expression of bone specific proteins osteocalcin, bone sialoprotein and decorin (Pautke *et al.,* 2004). The comparison of fibrillin expression in MG63 and SAOS2 cells could elucidate the role of fibrillins in calcifying tissues, by investigating expression in both mineralisation capable and non-capable cell lines.

Chondrocyte cell lines, C20A4, C28I2 and TC28A2 were used to better understand the role of the fibrillins in cartilage **(Chapter 2, Section 2.1.2)**. As previously described, the cells were derived from the costal cartilage of patients undergoing pectus excavatum repair (Goldring *et al.,* 1994). Furthermore, the cells behaved as typical chondrocytes, expressing expected levels of *COLII*, *COLIX* and *COLX1* (collagen type 2, type 9 and type 11, respectively), as well as responding to IL-1ß (interleukin 1-beta)(OMIM: 147720), which is essential for chondrocyte metabolism (Goldring *et al.,* 1994, Busschers *et al.,* 2010). Given the presence of key cartilage markers and the tissue region from which the cells were derived, these cell lines were to be used to look at expression in cartilage.

It has been established that patients with diagnosed MFS have abnormal dermal fibroblast assembly and structure (Kielty and Shuttleworth, 1994, Kielty *et al.,* 1994, Brenn *et al.,* 1996, Macek *et al.,* 1966) **(Chapter 1, Sections 1.3.4).** Human neonatal fibroblasts, NHDF, were used to better define the fibrillin gene family in nonmutant fibroblasts. The cells were obtained from Dr. Finn Grey **(Chapter 2, Section 2.1.3)**, and derived from neonatal circumcision material (Grey *et al.,* 2007). Driskell *et al.,* (2013) showed that *PDGFRA* (platelet-derived growth factor receptor, alpha) and *PDPN* (podoplanin) are candidate fibroblast markers, both of which were upregulated in the NHDF cells used in this thesis (obtained from the U219 microarray data (**Chapter 2, Section 2.3.5))**.

Given the controversy surrounding the use of HEK293 cells in the study of fibrillin **(Chapter 2, Section 2.1.4),** these cells were included to ascertain their origin and

suitability. The origin of the HEK293 cell line was introduced in **Chapter 2, Section 2.1.4** and will be discussed further in **Section 4.6** of this Chapter. THP-1 was analysed as a negative control **(Chapter 2, Section 2.1.5)**. THP-1 is a hematopoietic-derived cell line that has been used as a model system in macrophage and monocyte studies (Qin, 2011).

4.2 Aims of the Chapter

A survey was made of mRNA and protein expression of the fibrillin family and other extracellular matrix genes across various connective tissue types, aiming to identify co-expressed genes that could assist in the maintenance and development of a fibrillin-rich ECM. Expression microarray, qPCR and immunocytochemistry (ICC) techniques were used to determine key genes co-expressing with fibrillin-1 and fibrillin-2. Identifying genes co-expressed with fibrillins could provide further candidate modifier genes for Marfan syndrome and other connective tissue disease with similar phenotypes.

4.3 Materials and Methods

4.3.1 Cell culture and RNA extraction

RNA samples were obtained from Day 7 (seven days after plating) cell cultures of SAOS2, MG63, C20A4, TC28A2, C28I2, NHDF, THP1 and HEK293 **(Chapter 2, Section 2.2).** Single replicates were collected for C28I2, HEK293 and THP1. In addition, Ailsa Carlisle and Prof Kim Summers (The Roslin Institute) provided RNA samples of SAOS2 and MG63 cells after 14 days in calcification medium containing 50µg/ml ascorbic acid (Sigma-Aldrich) and 2.5mM ß-glycerophosphate (BGP) (Sigma-Aldrich). RNA was extracted and validated as described in **Chapter 2, Section 2.3.1).**

4.3.2 qPCR and ICC

Initial mRNA expression levels were quantified using qPCR techniques previously described in **Section 2.3.4 of Chapter 2**. All ICC technique was carried out as described in **Section 2.4.2 of Chapter 2**.

4.3.3 BioLayout *Express* ^{3D} analysis

Genome-wide expression profiles were obtained using the U219 human microarray and BioLayout Express ^{3D} analysis was completed on the dataset for the following Day 7 mRNA samples: SAOS2, MG63, C20A4, TC28A2, and NDHF (all n=2), C28I2, THP1, SAOS2 calcified, MG63 calcified and HEK293 (all n=1)**(Chapter 9, Appendix A)**. Microarray results and files for BioLayout *Express*^{3D} were subjected to quality control and filtering as described in **Chapter 2, Section 2.3.6**. Probes were removed from the data set if the normalised intensity value (equivalent to expression levels) was below 20 (unlogged), removing 13,613 probes (27.6%). The intensities for the remaining 35,772 probesets were loaded into BioLayout Express ^{3D}. The co-expression analysis was run at r≥0.92 and an MCL inflation value of 2.0 (**Chapter 9, Appendix B**).

4.3.4 DAVID GO term analysis

Cluster gene lists for Cluster001, Cluster002, Cluster003, Cluster004, Cluster005, Cluster008 and Cluster034 from the BioLayout *Express*^{3D} analysis were individually placed into the upload tool bar of DAVID 6.7 functional annotation tool (www.david.abcc.ncifcrf.gov/) and analysis was performed as described in **Chapter 2, Section 2.3.7.**

4.4 Results

4.4.1 ECM Gene expression in cell lines

Previous research suggested that *Fbn1* and *Fbn2* share the same expression patterns as *Ltbp2, Acta2, Bgn, Col1a1* and *Col1a2* in many mouse cell types (Summers *et al.,* 2010). Therefore, initially qPCR was performed on the human cell lines to examine expression patterns of these genes across human connective tissue cell types. The analysis also included *LTBP1*, *LTBP3* and *LTBP4*, the other members of the fibrillin-LTBP gene family (**Chapter 1, Section 1.3.2**). The qPCR analysis revealed varying levels of gene expression across the cell line samples ***(Figure 4.1)***.

The highest expression of *FBN1* was seen in chondrocyte line C20A4, while C28I2 displayed moderate levels ***(Figure 4.1A)***. Similarly, osteosarcoma MG63 had higher levels of *FBN1* expression when compared to mineralising osteosarcoma cell line SAOS2

(Figure 4.1A). Differing from *FBN1*, *FBN2* displayed the lowest overall expression in C20A4 and MG63 cell lines and measureable levels of expression in SAOS2 ***(Figure 4.1B)***. NHDF (fibroblasts) showed moderate expression of both *FBN1* and *FBN2* ***(Figure 4.1)***. The overall expression pattern of *FBN2* was similar across the cell types, other than MG63. *FBN3* expression was undetected in all cell types.

There was no measureable expression of *LTBP1* in either chondrocyte cell line (C20A4 and C28I2) ***(Figure 4.1C)***. ***Figure 4.1C-F*** shows that SAOS2 had the highest expression of *LTBP1*, though no measureable expression of *LTBP2,* very low levels of *LTBP3* and moderate levels of *LTBP4*. SAOS2 also had very low levels of *COL1A1* and *COL1A2* expression ***(Figure 4.1G and H)***. NHDF had the highest expression of *LTBP2* and *LTBP3*, with similar expression of *LTBP4* to MG63 ***(Figure 4.1D-F)***. NHDF and SAOS2 had the highest expression of *ACTA2,* while C20A4 showed considerably higher levels of *BGN* expression ***(Figure 4.1 I and J)***. C20A4 had the highest expression of *BGN* and *COL1A1* genes and very low expression in *ACTA2* ***(Figure 4.1G and J)***.

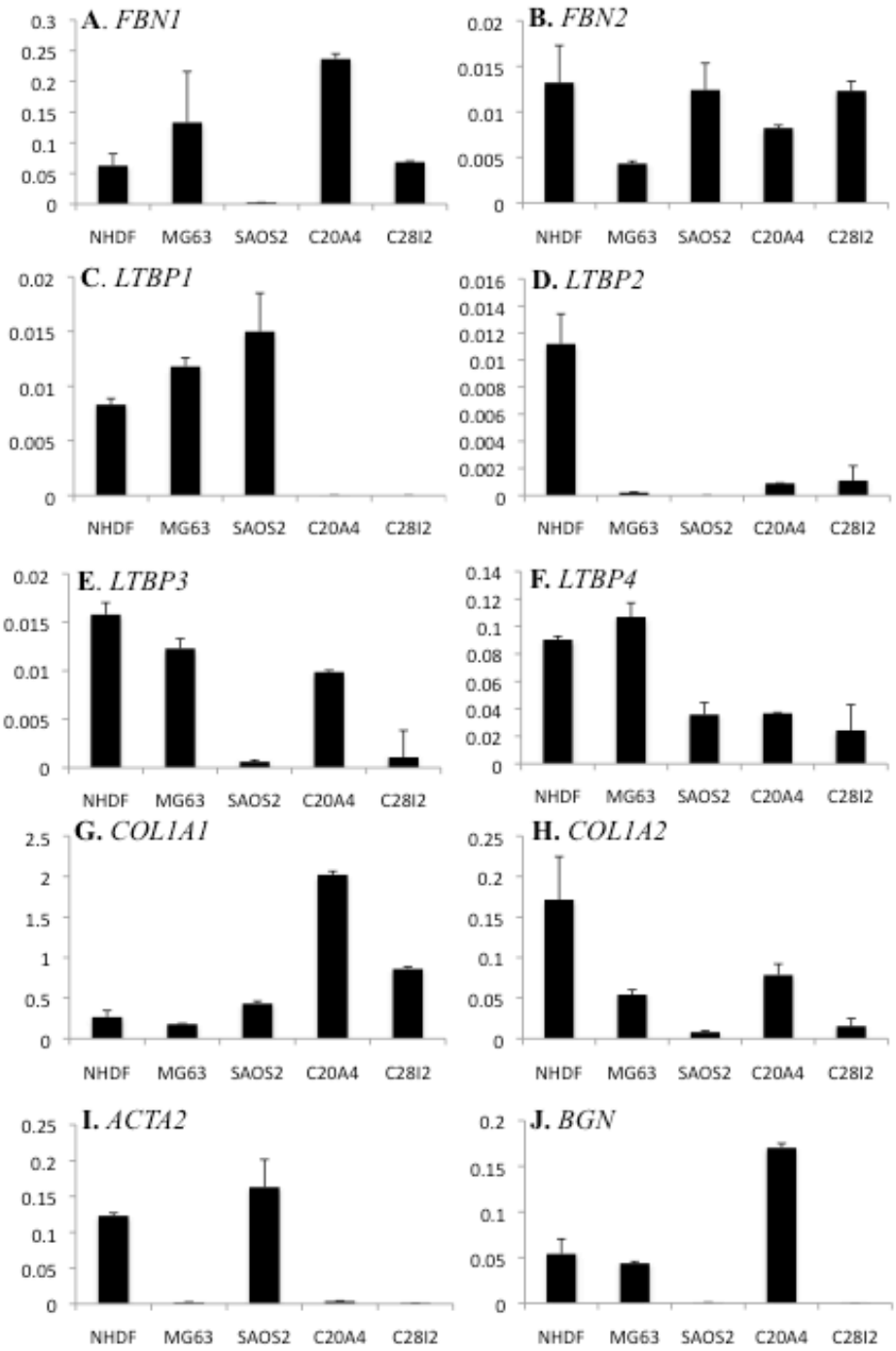

Figure 4.2. qPCR results for ECM gene expression in human cell lines. Expression patterns of (A) *FBN1,* (B) *FBN2,* (C) *LTBP1,* (D) *LTBP2,* (E) *LTPB3,* (F) *LTBP4,* (G) *COL1A1,* (H) *COL1A2,* (I) *ACTA2,* and (J) *BGN* in NHDF, (fibroblasts) MG63, SAOS2 (osteosarcoma cells), C20A4 and C28I2 (chondrocytes) at day 7 of culture. Expression levels were normalised using the housekeeping gene, *GAPDH*. Y-axis shows the ratio of target to housekeeping gene. (Chapter 2, Section 2.3.4) and mean standard error is displayed (N=3 biological replicates). Davis *et al.*, 2012.

4.4.2 Localisation of ECM and cytoskeletal proteins

ICC studies were performed to better define the nature and extent of the fibrillin matrix in the different cell lines **(Chapter 2, Section 2.4.2)**. Immunofluorescent staining of fibrillin-1 and fibillin-2 microfibrils in NHDF revealed extensive deposition of the proteins in the extracellular matrix ***(Figure 4.2A and B)***. Fibrillin-2 microfibrils formed linear, thin strands, while fibrillin-1 microfibrils appeared less organised and had more bundled fibres ***(Figure 4.2 A and B)***. Fibrillin-1 and -2 ICC images at 20x magnification illustrate the vast microfibril formation. ACTA2 staining displayed a rich network of intracellular actin filaments, possibly involved in cell-to-cell connections ***(Figure 4.2C)***. Biglycan and collagen type 1 staining was localised within the cell ***(Figure 4.2D and E)***. The intracellular staining of collagen 1 was likely due to the lack of ascorbic acid in culture, necessary for collagen secretion.

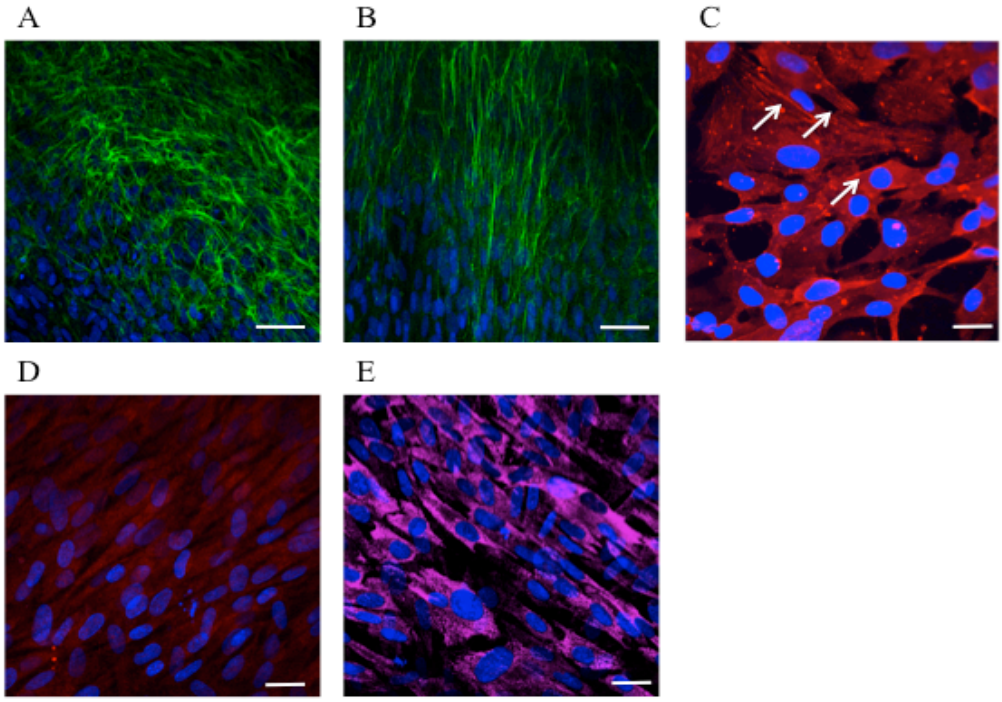

Figure 4.3. ICC of NHDF cells at Day 7 of culture. (A) Fibrillin-1 (20x) (green) n=3(B) Fibrillin-2 (20x) (green)n=3 (C) Smooth muscle actin (40x) (red) n=2, intracellular fibre formation is further highlighted with a white arrow (D) Biglycan (40x) (red) n=2 (E) Collagen type 1 (40x) (pink) n=2 . Antibody and technique information is given in Chapter 2, Section 2.4.2. The nuclei were counterstained with DAPI (blue). Images were captured using the Zeiss confocal microscope Scale bars (white) in A and B represent 50µm and scale bars in C, D and E represent 20µm.

The fluorescent ICC staining of fibrillin-1 protein revealed a vast fibrillin-1 microfibril matrix in MG63 at Day 7 and Day 14, while fibrillin-1 was intracellular within SAOS2 at both Day 7 and Day 14 ***(Figure 4.3)***. The extracellular fibrillin-1 matrix of MG63 cells became denser with time and fibrillin-1 staining of SAOS2 cells was more intense at Day 14, indicating increased protein, though no extracellular fibres had developed. These results are consistent with the relative mRNA levels measured by qPCR **(*Figure 4.1A and B*, Section 4.4.1)**.

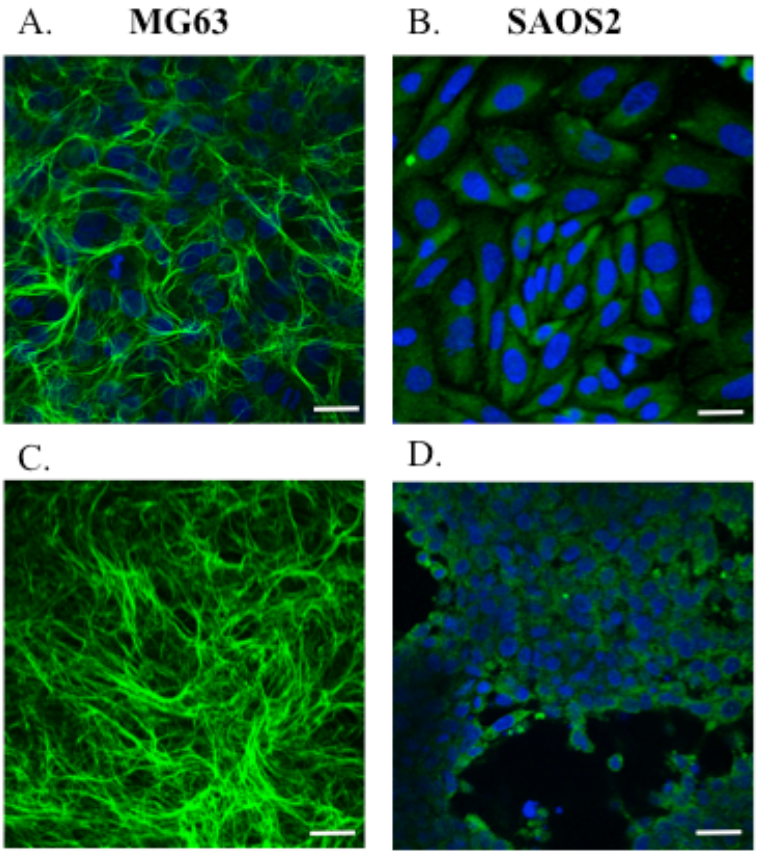

Figure 4.4. Fibrillin-1 ICC in osteosarcoma cell lines. (A) MG63 at Day 7, (B) SAOS2 at Day 7, (C) MG63 Day 14 (no DAPI), (D) SAOS2 at Day 14. (all x40) Green fluorescence shows fibrillin-1 protein, and nuclei were counterstained with DAPI, seen in blue. Antibody and technique information is given in Chapter 2, Section 2.4.2. Images were captured at 40x using the Zeiss confocal microscope (Chapter 2, Section 2.4.2). Scale bars (white) represent 20µm.

Like the osteosarcoma cell lines, chondrocyte cell lines C20A4 and C28I2 had differing expression levels of *FBN1* mRNA ***(Figure 4.1A)***. Fibrillin-1 ICC showed that C20A4 created a rich, thick and structurally organised fibrillin-1 microfibril matrix ***(Figure 4.4A)***. In comparison, C28I2 ***(Figure 4.4B)*** and the derived cell line TC28A2 ***(Figure***

4.4C) did not produce a fibrillin-1 matrix, though protein was detected in the intracellular region ***(Figure 4.4)***.

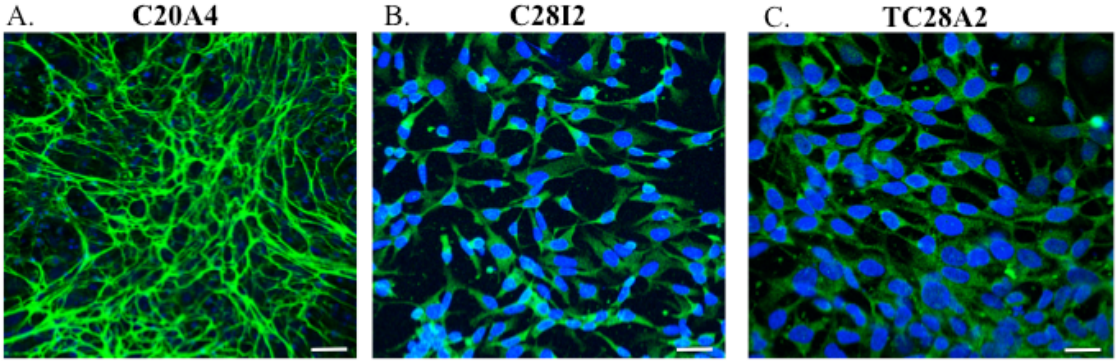

Figure 4.5. Fibrillin-1 ICC in chondrocyte cell lines. (A) C20A4 at Day 7, (B) C28I2 at Day 7, (C) TC28A2 at Day 7. Green fluorescence shows fibrillin-1 protein, nuclei were counterstained with DAPI. Antibody and technique information is given in Chapter 2, Section 2.4.2. Images were captured at 40x using the Zeiss confocal microscope (Chapter 2, Section 2.4.2). Scale bars (white) represent 20μm.

4.5 Microarray analysis

mRNA and protein analysis **(Sections 4.4.1 and 4.4.2)** showed that the two osteosarcoma lines were discordant for fibrillin expression as were the three chondrocyte lines. This suggested that there might be differential associations with other genes, which could provide insight into the interactions of the fibrillins in ECM formation. The Affymetrix human gene expression microarray platform U219 was therefore used to define the expression of key extracellular matrix genes in NHDF, MG63, SAOS2, C20A4, TC28A2, C28I2, THP1 and HEK293 cell lines at day 7 after plating (**Chapter 2, Section 2.3.5**)(**Chapter 9, Appendix A)**.

To identify gene co-expression patterns, a total of 35,772 probes and their expression (intensity) values were placed into network clustering analysis software BioLayout *Express*^{3D} (**See Section 4.3.3**). The analysis was run at r ≥0.92 and clustering was performed at an MCL of 2.0. At this relatively high P-value there were a total of 24,149 nodes (probes) and 627,371 edges included in the final graph ***(Figure 4.5)***. A total of 1,842 clusters were defined by the analysis. Seven clusters had high levels of expression in specific cell lines (Cluster001, Cluster002, Cluster003, Cluster004, Cluster005, Cluster008 and Cluster034)***(Figure 4.5)***. Two unique clusters contained probesets

(nodes) for the *FBN1* gene (Cluster022 and Cluster700) and Cluster704 had the same expression pattern as Clusters022 and 700, with a direct link to Cluster022. Fibrillin-2 did not cluster, and fibrillin-3 did not remain in the data set following filtering to remove low expression probes and those that were uncorrelated with any other probe (**Section 4.3.3**).

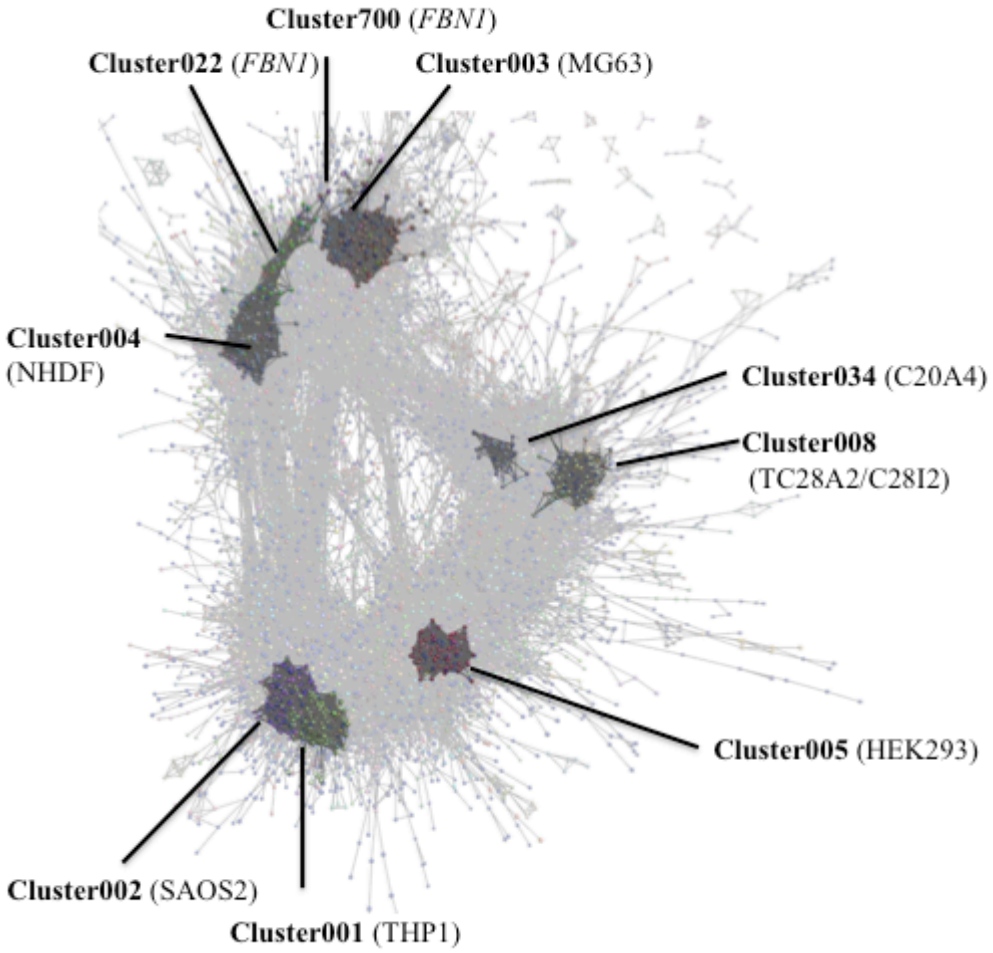

Figure 4.6. Network visualization and clustering of the transcriptomes of the cell lines (Day 7)(Section 4.3.5)(Appendix A). The image depicts the network diagram produced by BioLayout *Express*^{3D} using data from the Affymetrix U219 gene expression microarray platform. Spheres (nodes) represent individual probesets and the lines between them (edges) show correlations in expression pattern of $r \geq 0.92$. The nodes were clustered using an MCL inflation value 2.0 (Chapter 2, Section 2.3.6). The background of the image displays the whole network and clusters discussed in the text are highlighted and labelled.

4.5.1 Analysis of BioLayout *Express* ^{3D} derived cell line specific clusters

In addition to identifying two clusters containing *FBN1* probesets, the BioLayout*Express*^{3D} analysis yielded clusters where the set of genes had highest expression in a single cell line ***(Figure 4.6)***. For example, for genes in the largest cluster, Cluster001 (835 nodes) ***(Figure 4.6A),*** the highest overall expression was seen in THP1 macrophage cell line, and the genes identified contained macrophage and immune markers such as *CSF1R* (encoding colony stimulating factor receptor 1)*, CD33* and *CD4* ***(Figure 4.6A)***. GO terms for Cluster001 confirmed the high incidence of immune and defence response genes and general cell component terminology ***(Table 4.1)***.

Gene Ontology	Number of Genes	P-value
Biological Pathway (n=271)		
Regulation of biological process	254	5.6E-2
Regulation of cellular process	245	5.1E-2
Immune system process	79	6.5E-13
Immune response	61	5.7E-12
Defence response	45	1.1E-3
T cell activation	13	9.7E-4
Disease classification (n=2)		
Immune	58	4.8E-6
Infection	21	2.6E-2

Table 4.2. A selection of GO terms associated with genes in Cluster001-THP1. Biological pathways terms were identified for 80.9% of genes within the cluster.

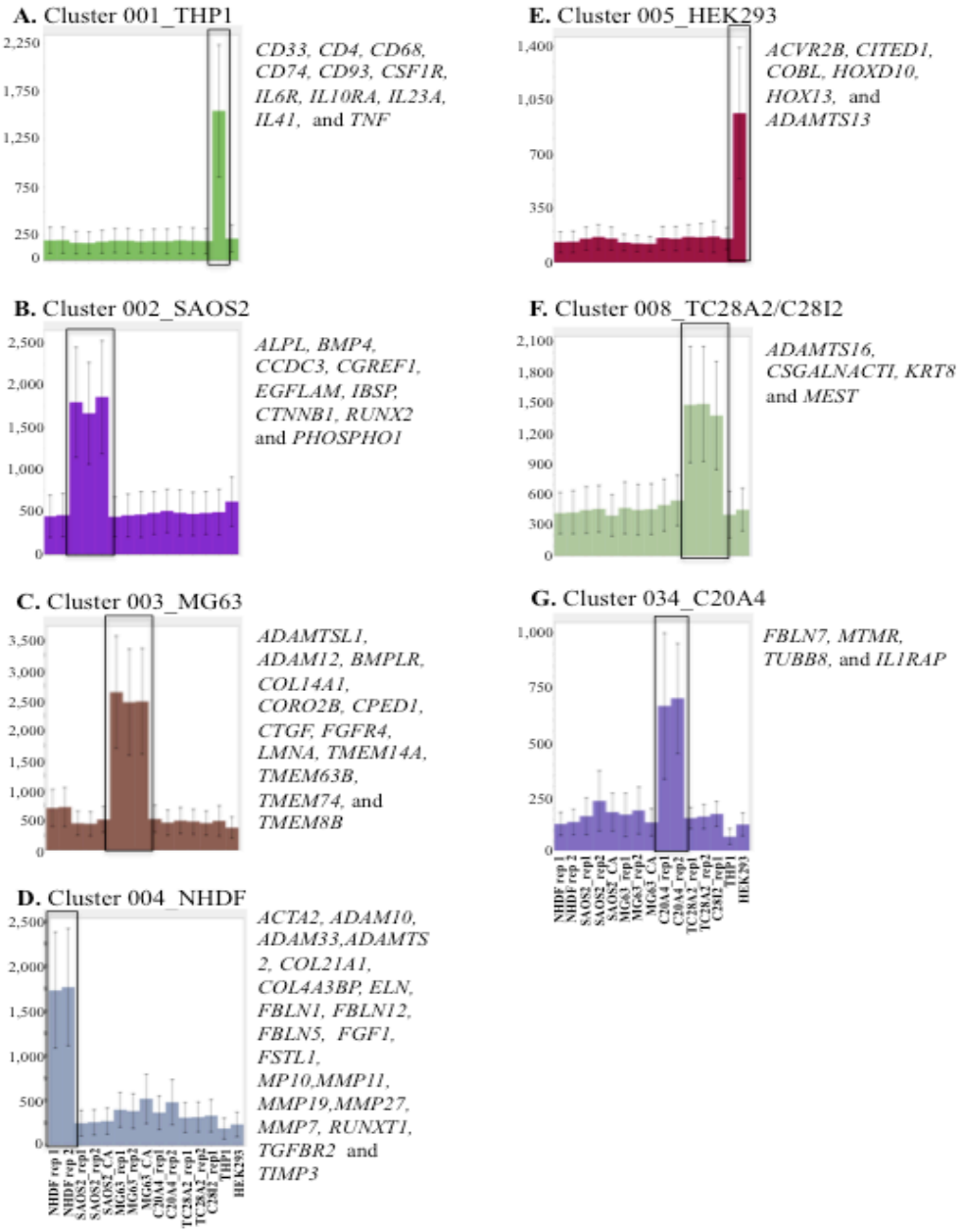

Figure 4.7. Plots of average expression profiles of genes in cell line specific clusters following analysis using BioLayout *Express* [3D] (See *Figure 3.8)*. Y axis shows the normalised intensity value. X axis shows the samples from which the RNA was extracted. Characteristics of each cluster was determined using the class viewer tool in BioLayout *Express* [3D]. (A) Cluster001- THP1, (B)Cluster002-SAOS2,(C) Cluster003-MG63, (D)Cluster004-NHDF, (E) Cluster005-HEK293, (F) Cluster008-TC28A2/C28I2, and (G) Cluster034- C20A4. The colors were arbitrarily assigned to clusters during the BioLayout*Express*[3D] MCL clustering (p≥0.92, MCL inflation value 2.0). Each cluster contains genes with high expression only in a specific cell line (boxed in). The genes listed are representative examples of ECM related genes, except for Cluster001 where representative genes reflect the hematopoietic lineage of THP1 cells.

Cluster003 and Cluster004 were in close proximity in the network graph to the more generally expressed fibrillin-1 clusters (Cluster022 and Cluster700, see ***Figures 4.5***). Cluster003 and Cluster004 contained many genes that are involved with the structure, function or maintenance of the ECM, in addition to some genes implicated in connective tissue disease, similar to the phenotype produced by fibrillin-1 and fibrillin-2 mutations ***(Figure 4.6CandD)***. Cluster003 contained a total of 567 nodes that were highly expressed in MG63 cells ***(Figure 4.6C)***. There were no edges with Cluster022 or Cluster700 genes. Cluster003 included ECM related genes such as *COL14A1* (encoding collagen, type XIV, alpha 1), *FGFR4* (fibroblast growth factor receptor 4), nuclear membrane gene *LMNA* (lamin A/C), and several transmembrane genes (*TMEM14A, TMEM63B, TMEM74* and *TMEM8B*) ***(Figure 4.6C)***. Multiple GO terms were identified for the genes in Cluster003, including muscle development and tooth development (odontogenesis) ***(Table 4.2)***. Surprisingly there were no GO terms associated with bone formation, consistent with the observation that this is an immature osteoblast phenotype.

Gene Ontology	Number of Genes	P-value
Biological Pathway (n=83)		
Biological regulation	136	5.5E-2
Organ development	40	2.5E-2
Anatomical structure morphogenesis	29	3.5E-2
Regulation of growth	11	5.4E-2
Muscle development	8	5.8E-2
Odontogenesis	4	5.8E-2
Cellular Component (n=20)		
Cell part	246	3.8E-3
Cell	246	3.8E-3
Intracellular	187	5.8E-2
Membrane	134	1.3E-2
Neuron projection	10	9.5E-2

Table 4.2. A selection of GO terms associated with genes in Cluster003-MG63. Biological pathways were identified in 75.3% of genes and cellular component terms were identified in 82.1% of genes within the cluster.

Cluster004 had 556 nodes highly expressed in NHDF cells ***(Figure 4.6D)***. A single gene, *VIM* (vimentin), highly characteristic of fibroblasts, shared an edge with a *FBN1* node in Cluster022 ***(Figure 4.7)***. There were many ECM related genes in Cluster004, including three different ADAM metallopeptidase domain genes *(ADAM10, ADAM33, ADAMTS2),* genes encoding collagen type XX1, alpha 1 (*COL21A1*) and elastin (*ELN*), three fibulin genes (*FBLN1, FBLN12, FBLN5*) and several matrix metallopeptidase genes ***(Figure 4.6D)***. GO terms associated with extracellular functions were overrepresented ***(Table 4.3)***. Cluster004 also showed co-expression of *ACTA2* and *TGFBR2* (encoding transforming growth factor beta receptor 2).

Gene Ontology	Number of Genes	P-value
Biological Pathway (n=231)		
Multicellular organism process	111	1.5E-4
Developmental process	105	9.4E-10
Tissue development	29	7.6E-5
Cell adhesion	29	1.8E-4
Skeletal system development	20	1.2E-5
Wound healing	13	3.1E-4
Cellular component (n=52)		
Membrane	156	2.7E-2
Extracellular region	81	4.4E-11
Extracellular region part	54	1.6E-12
Extracellular space	32	7.0E-6
Extracellular matrix	30	2.0E-11
Disease classification (n=0)		

Table 4.3. A selection of GO terms associated with genes in Cluster004-NHDF. Biological pathways were identified for 78.6% of genes and cellular component terms were identified for 89.3% of genes within the cluster.

Cluster002 (725 nodes) was highly expressed in the SAOS2 cell line ***(Figure 4.6B)***. It was located in close proximity to the THP1 Cluster001 and distant from the other osteosarcoma MG63 ***(Figure 4.5)***, although it contained multiple osteoblast lineage markers such as *IBSP* (integrin-binding sialoprotein), *RUNX2* (runt-related transcription factor 2), and *PHOSPHO1* (phosphatase, orphan 1) ***(Figure 4.6B)***. In addition, multiple

bone and cartilage specific GO terms were correlated with Cluster002, including osteoblast differentiation, skeletal and cartilage development ***(Table 4.4)***.

Gene Ontology	Number of Genes	P-value
Biological Pathway (n=132)		
Cellular process	272	2.2E-4
Metabolic Process	194	4.2E-2
Phosphorylation	29	2.0E-2
Skeletal system development	20	1.7E-4
Cartilage development	7	7.3E-3
Osteoblast differentiation	7	3.8E-4
Cellular Component (n=30)		
Cell part	337	4.8E-3
Cell	337	4.9E-3
Intracellular	275	3.3E-5
Intracellular membrane –bounded organelle	190	6.6E-2
Transcription factor complex	10	4.2E-2
Disease classification (n=1)		
Developmental	15	5.8E-3

Table 4.4. A selection of GO terms associated with genes in Cluster002-SAOS2. Biological pathways were identified for 77.9% of genes and cellular component terms were identified for 82.9% of genes within the cluster.

Cluster008 (192 nodes) and Cluster034 (35 nodes) showed the highest expression in the chondrocyte cell lines, TC28A2/C28I2 and C20A4 ***(Figure 4.6F and G)***, though they did not have any edges between them or any other analysed cluster. Both contained very few ECM associated genes, listed in ***Figure 4.6F and G***. GO analyses of Cluster008 and Cluster034 are shown in ***Table 4.5*** and ***Table 4.6***, respectively.

Gene Ontology	Number of Genes	P-value
Biological Pathway (n=30)		
Developmental process	28	6.2E-2
Anatomical structure development	24	4.9E-2
System development	22	6.5E-2
Nervous system development	14	2.2E-2
Regulation of signal transduction	11	5.6E-2
Cellular component (n=8)		
Intracellular part	82	4.1E-2
Intracellular organelle	70	7.0E-2
Organelle	70	7.2E-2
Membrane bound organelle	63	8.0E-2
Disease database (n=1)		
Cerebral infarct, atherothrombotic	2	6.7E-2

Table 4.5. A selection of GO terms associated with genes in Cluster008-TC28A2/C28I2. Biological pathways were identified for 75.4% of genes and cellular component terms were identified for 89.3% of genes within the cluster.

Gene Ontology	Number of Genes	P-value
Biological Pathway (n=13)		
Protein complex assembly	4	4.2E-2
Intracellular transport	4	4.2E-2
Dephosphorylation	3	2.4E-2
Cellular component (n=10)		
Membrane part	17	3.0E-2
Extracellular region part	5	6.8E-2
Proteinaceous extracellular matrx	4	1.5E-2
Extracellular matrix	4	1.8E-2

Table 4.6. A selection of GO terms associated with genes in Cluster034-C20A4. Biological pathways were identified for 39.7% of genes and cellular component terms were identified for 45.9% of genes within the cluster.

Cluster005 contained 308 nodes highly expressed in HEK293, with the majority of genes representing early differentiation, particularly of neuronal systems, and a small number of ECM related genes ***(Table 4.7)*** such as transcription factors homeobox D10 (*HOXD10),* homeobox D13 (*HOXD13*) and ECM protease *ADAMTS13* ***(Figure 4.6E)***.

Gene Ontology	Number of Genes	P-value
Biological Pathway (n=131)		
Cellular process	145	4.5E-3
Nervous system development	31	2.1E-5
Embryonic development	16	4.3E-3
Neurogenesis	16	7.1E-3
Generation of neurons	16	3.7E-3
Neuron differentiation	13	7.8E-3
Cellular component (n=4)		
Ion channel complex	8	6.3E-3
Cation channel complex	5	5.2E-2
Cytosolic part	5	7.9E-2
Microtubule associated complex	4	9.5E-2
Disease classification (n=2)		
Psychiatric	11	9.0E-2
Developmental	7	6.8E-2

Table 4.7. A selection of GO terms associated with genes in Cluster005-HEK293. Biological pathways were identified for 74.4% of genes and cellular component terms were identified for 81.2% of genes within the cluster.

4.5.2 Fibrillin-1 co-expression clusters

The human Affymetrix microarray U219 platform contained five probesets for *FBN1*, all mapping to transcript NM_00138 **(Chapter 3, *Table 3.1*)**. Four of the five clustered in the analysis. Cluster022 contained a total of 54 nodes, two of which were *FBN1* probesets, FBN1: 11720509_a_at and FBN1: 1175368_a_at. Cluster700 contained a total of 5 nodes, and had lower expression in comparison to Cluster022 (***Figure 4.7 and 4.8)***. Two of the nodes were *FBN1* probesets, FBN1: 11720507_at and FBN1: 11758093_s_at (**Chapter 3, *Table 3.1*).**

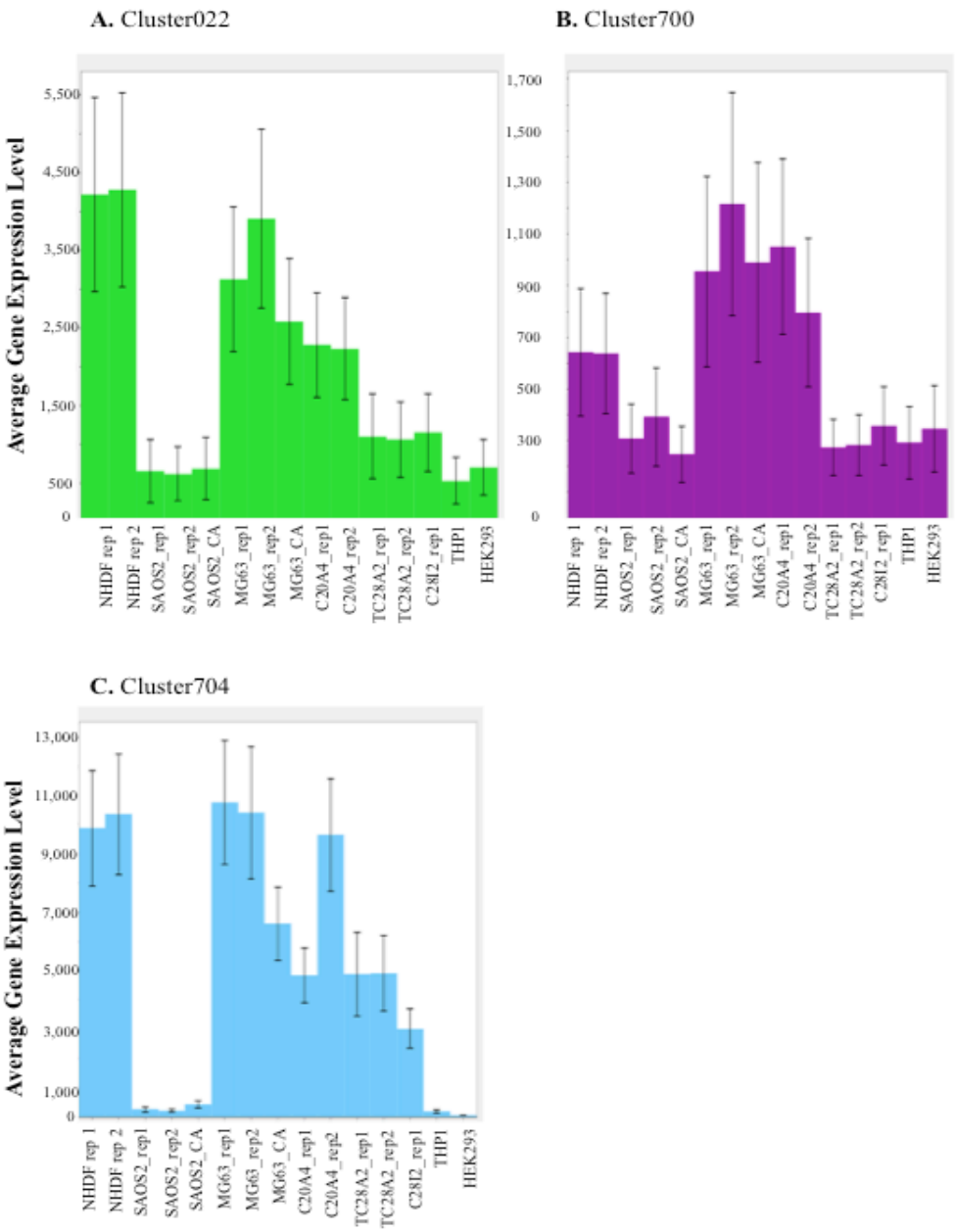

Figure 4.7. Plots of average expression profiles of genes in Cluster022, Cluster700 and Cluster704 following analysis using BioLayout *Express* [3D] (See *Figure 4.5)*. Y axis shows the normalized intensity value. X axis shows the samples from which the RNA was extracted. Characteristics of each cluster was determined using the class viewer tool in BioLayout *Express* [3D]. (A) 54 nodes in Cluster022, (B) 5 nodes in Cluster700, (C) 5 nodes in Cluster704. The bars depict the standard error of the mean.

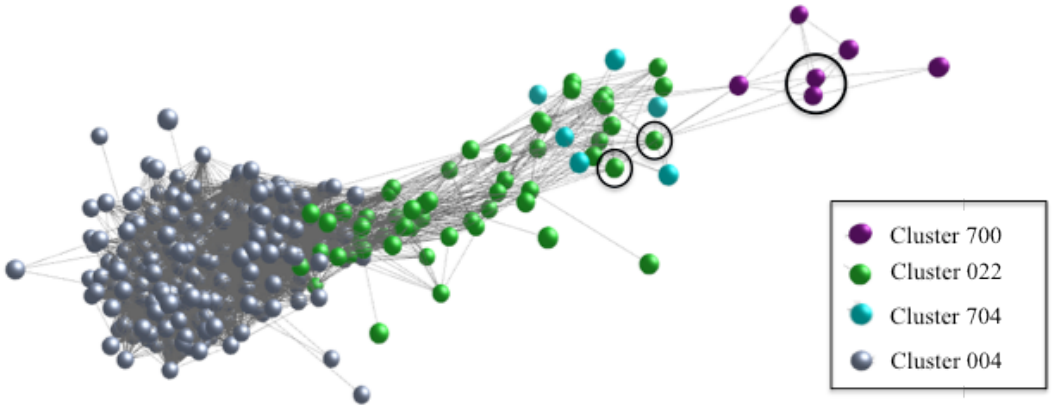

Figure 4.8. Visualization of clusters containing *FBN1* probes and related clusters. Cluster700, Cluster022, Cluster704 and Cluster004 were selected and reoriented for ease of interpretation from Section 4.5.1, *Figure 4.5. FBN1* probesets are outlined in black.

There were edges that directly connected Cluster022 to Cluster700 ***(Figure 4.8)*** including connections between nodes for fibrillin-1 probes, FBN1: 11758093_s_at (Cluster700) and FBN1: 1175368_a_at (Cluster022) ***(Figure 4.8)***.

Cluster022, Cluster700 and Cluster704 had similar expression patterns ***(Figure 4.7)***, being high in NHDF, MG63 and C20A4 cell lines, that had been shown to have high levels of *FBN1* mRNA and protein ***(Figures 4.1, 4.2, 4.3 and 4.4)*** and were located quite close to each other in the network ***(Figure 4.5)***. Cluster004 was the NHDF-specific cluster ***(Figure 4.6D)***, though it was highly correlated with Clusters022, 700 and 704 ***(Figure 4.8)***. The co-expressed genes were down regulated in SAOS2, TC28A2, C28I2, THP1 and HEK293 cell lines. The edges (connections) between the clusters suggested that though the expression of both Cluster022 and Cluster700 varied slightly, they had a correlated expression pattern ***(Figure 4.7)***. Cluster022 and Cluster700 contained multiple genes with ECM function ***(Table 4.8)***.

Cluster	Gene	Gene Name	Function / Disease Associated
Cluster022			
	ARHGAP29	Rho GTPase activating protein 29	Activator of cytoskeleton, RHO (OMIM: 600582) / Cleft Lip (Leslie *et al.,* 2012)
	ASPH	Aspartate beta-hydroxylase	Post- translational modifier of proteins / Traboulsi syndrome (OMIM: 600582)
	CAV1	Caveolin 1	Caveolae formation (OMIM: 601047) / Lipodystrophy (OMIM: 612526, 606721) Pulmonary hypertension (OMIM:615343)
	CAV2	Caveolin 2	Involved in adipose stabilisation (Scherer *et al.,* 1996) / NA
	COL6A3	Collagen, type VI, alpha 3	Extracellular matrix gene / Bethlem myopathy, Ullrich Congential muscular dystrophy (OMIM:120250)
	KIAA1033		Actin polymerization / Wiskott-Aldrich Syndrome (Ropers *et al.,* 2011)
	LOX	Lysyl oxidase	ECM copper enzyme, crosslinking to collagen and elastin (Hamalainen *et al.,* 1991) / NA
	MYOF	Myoferlin	Calcium and phospholipid-binding protein (OMIM: 604604) / Muscular dystrophy and cardiomyopathy (Davis *et al.,* 2000)
	NDST1	N-deacetylase/N-sulfotransferase (heparan glucosaminyl) 1	Heparan sulphate biosynthesis (Thompson *et al.,* 2008) / NA
	PXDN	Peroxidasin homolog (Drosophila)	ECM organisation (Horikoshi *et al.,* 1999) / Corneal opacification and other ocular anomalies (MIM: 269400)
	TWF1	Twinfilin actin-binding protein 1	Actin binding gene (Bockhorn *et al.,* 2013) / NA
Cluster700			
	ARRDC3	Arrestin domain containing 3	Implicated function in adipocyte differentiation and function (OMIM: 612466) / Obesity implications (gender specific) (Patwari *et al.,* 2011)
	EPG5	Ectopic P-granules autophagy protein 5	Regulation of Autophagy pathway (OMIM: 615068)(He and Klionsky, 2009) / Vici disease (OMIM: 242840)

Table 4.8. A selection of co-expressed genes in Cluster022 and Cluster700 from BioLayout*Express*^{3D}. The gene functions and disease associations are listed. If the gene function or disease association are unknown, it is marked as NA.

The majority of the genes in Clusters022 and 700 were associated with disease phenotypes that present with phenotypes also associated with fibrillin-1 and fibrillin-2

mutations **(Chapter 1, Section 1.3.4 and 1.3.5)**. For example, *CAV1* mutations are common in lipodystrophy **(Chapter 3, Section 3.5.1)**, *MYOF* mutations cause severe cardiac abnormalities (Davis *et al.,* 2000), *ARHGAP29* mutations can cause craniofacial abnormalities (Leslie *et al.,* 2012), and *ASPH* mutations can cause Tranoulsi syndrome, which presents with lens dislocation, craniofacial and segment formation abnormalities (MIM: 601552)***(Table 4.8)***. The remainder of the identified genes have an association either directly (*PXDN, COL6A3 and CAV1*) or indirectly (*LOX, NDST1* and *TWF1*) with the function or stabilisation of the ECM ***(Table 4.8)***. Cluster704 had the same average expression pattern as Cluster022 and was similar to Cluster700 ***(Figure 4.7)***. It contained a total of four genes (6 probes) of which two genes had ECM associations: *COL3A1* (collagen type 111, alpha 1) and *SPARC*.

4.6 Discussion

This chapter surveyed gene expression in human cell lines of mesenchymal origin. Both mRNA and protein levels were shown to be variable across the cell types, for a number of genes previously shown to co-express with *Fbn1* in mouse cell types (Summers *et al.,* 2010)***(Figure 4.1-4.4)***. Transcriptomic analysis of gene expression revealed that the cell lines were quite distinct, even those originating from the same primary cell type. A cluster of genes co-expressed with *FBN1* was identified and these genes are discussed further below.

Fibroblast cell line NHDF, MG63 osteosarcoma line and C20A4 chondrocyte line produced a vast and rich fibrillin-1 matrix ***(Figure 4.2-4.4)*** mimicking a phenotypically normal cellular system (Godfrey *et al.,* 1990). Previous studies on the fibrillin-1 matrix in developing cartilage detected a loose network of fibrillin fibres in human foetal tissue as early as 20 weeks and this was maintained throughout adulthood within the perichondrium (Keene *et al.,* 1997). The chondrocytes used in this study were retrieved form the costal cartilage of one patient aged 5 and the other 15 years (Goldring *et al.,* 1994). C20A4 maintained a more mesenchyme like cell phenotype by producing an extensive and organised fibrillin-1 matrix, while C28I2 and its subclone TC28A2 did not. Developing bone was represented by osteosarcoma lines MG63 and SAOS2. This study and others have shown that MG63 produces a fibrillin-1 matrix (Summers *et al.,* 2009),

similar to primary human osteoblast fibrillin-1 matrices (Kitahama *et al.,* 2000). In contrast, this study showed that SAOS2, considered to be a more mature bone cell type (Pautke *et al.,* 2004), did not produce an extracellular fibrillin-1 matrix. Thus immortalised cells deriving from the same primary cell type (osteoblasts or chondrocytes) do not necessarily retain the ability to form fibrillin-1 microfibrils (Alberts B *et al.*, 2002). Previous work had shown that HEK293 cells do not produce a fibrillin-1 matrix (Summers *et al.,* 2009), although these cells have been used to examine *FBN1* gene expression and promoters (Guo *et al.,* 2008)(**Chapter 2, Section 2.1.4**).

4.6.1 Description of fibrillin-1 clusters

The transcriptome-wide microarray analysis identified two clusters of genes co-expressed with *FBN1*, Cluster022 (32 genes) and Cluster700 (4 genes). According to the GO terms, 11 of the genes in Cluster022 ***(Table 4.8)*** were relevant to ECM maintenance and function or had been associated with connective tissue diseases presenting with similar phenotypes to those seen with *FBN1* mutations **(Section 4.5.2).** These ECM specific genes were found to be upregulated in MG63, NHDF and C20A4 cell lines, while expression levels remained low for SAOS2, TC28A2, C28I2, HEK293 and THP1.

One Cluster022 gene was *ARHGAP29,* encoding a protein associated with the regulation of small GTP binding proteins, including Ras homology gene family member A (RhoA) (OMIM: 610496)(Saras *et al.,* 1997). RhoA is a downstream effecter of TGFB signalling and involved in cytoskeleton remodelling (Kardassis *et al.,* 2009). *ARHGAP29* depletion in endothelial cell culture inhibited blood vessel lumen formation through increased RhoA expression and decreased integrin binding potential (Xu *et al.,* 2011). Adhesion between endothelial cells and ECM was disrupted, associated with low levels of integrin activation and dissociation of the endothelium in developing blood vessels from the underlying mesenchymal cells. *ARHGAP29* had been recently implicated in the development of cleft lip following mutation screening in over 1000 cases, consistent with the localization of gene expression to craniofacial structures in the mouse (Leslie *et al.,* 2012). Cleft lip and palate are not a feature of *FBN1* mutation phenotypes, although facial dysmorphism is common, but have been reported for other connective tissue conditions

with disrupted TFGß signalling, such as *TGFB3* mutation (Takahashi *et al.,* 1987), and Loeys-Dietz syndrome (mutation in *TGFBR1* or *TGFBR2*)(Tan *et al.,* 2009, Loeys *et al.,* 2006, Okamura and Matsumoto, 1984) as well as some forms of Ehlers- Danlos syndrome (mutations in genes for collagen molecules and other connective tissue proteins).

FBN1 was co-expressed with the two members of the caveolin gene family (*CAV1* and *CAV2*) in Cluster022. *FBN1* was also shown to co-express with *CAV1* during adipogenesis as discussed in **Chapter 3**. *CAV1* and *CAV2* encode components of the caveolae, modified lipid rafts that form in membrane of multiple cell types including fibroblasts, adipocytes, endothelial and smooth muscle cells (Briand *et al.,* 2011, Razani and Lisanti, 2001). *CAV1* has been implicated in lipodystrophy, pulmonary hypertension and lipotrophic diabetes (OMIM: 612526)(OMIM: 615343) (Briand *et al.,* 2011) and involved in TGFß signalling **(Chapter 3, Section 3.5.1)(Chapter 1, *Figure 1.5*)**. This suggests that if *CAV1* transcription is downregulated, *TGFB* levels will increase (Razani *et al.,* 2001), similar to the effect of *FBN1* mutation increasing active TGFß protein levels. The co-expression analysis along with previously published research indicates that *CAV1* and *ARHGAP29* (through RhoA interactions) along with fibrillin-1 may play a vital role in maintaining TGFβ homeostasis, and further studies would be necessary to determine a co-functional mechanism of action for these genes.

In addition to *ARHGAP29* (discussed above), Cluster022 contained several other genes involved in maintaining cytoskeletal structural integrity. *TWF1* binds to actin monomers that inhibit actin filament formation and *KIAA1033* is involved in actin polymerisation through interactions with integrin molecules ***(Table 4.8)***. These two genes could control the balance of actin monomers (G-actin) and actin polymers (F-actin), thereby assisting in the maintenance of actin fibre formation in the cytoskeleton (Dominguez and Holmes, 2011). The maintenance of actin is vital to communication between the ECM and the cytoskeleton (Bockhorn *et al.,* 2013, Ropers *et al.,* 2011) **(Chapter 1, *Figure 1.3* and Section 1.2.6)**.

COL6A3 was also co-expressed with fibrillin-1 within Cluster022. *COL6A3* is a connective tissue gene, mainly expressed in cells/tissue of mesenchyme origin

(http://fantom.gsc.riken.jp/zenbu/). Mutations cause moderate to severe Bethlem myopathy and Ullrich congenital muscular dystrophy (OMIM: 120250)(Bushby *et al.,* 2014, Demir *et al.,* 2002). Ullrich congenital muscular dystrophy is a connective tissue disorder that causes hyper-mobility, muscle weakness, joint contractures, and spinal defects (including scoliosis and rigid spine) leaving many patients immobile (OMIM: 254090). Bethlem myopathy is a less severe phenotype presenting with similar but milder symptoms (OMIM: 158810). These connective tissue disorders mimic some aspects of the Marfan syndrome phenotype **(Chapter 1, Section 1.3.4)**, reflecting the similar expression patterns of *COL6A3* and *FBN1* in Cluster022.

Also present in Cluster022 was myoferlin (*MYOF*), a gene associated with skeletal and cardiac muscle development (OMIM: 604603) (Davis *et al.,* 2000, Doherty *et al.,* 2005) and more recently implicated in the regulation of epidermal growth factor receptors (EGFR) in breast cancer models (Turtoi *et al.,* 2013). Demonbreun *et al.,* (2009) demonstrated that *Myof* null mice were unresponsive to insulin-like growth factor-1 (*Igf1*) stimulation, compared to the control mice which had a 25% increase in muscle fibre diameter when treated with myoferlin, suggesting that *MYOF* may be important in muscle growth and maintenance. Muscle weakness and change in muscle fibre integrity are seen in patients with Marfan syndrome (Behan *et al.,* 2003), consistent with co-expression of *MYOF* and *FBN1*.

Two additional genes found within Cluster022 have known functions in maintaining collagen structure in the ECM. Lysyl oxidase (*LOX*) is involved in collagen crosslinking to collagen (Hamalainen *et al.,* 1991), elastin to elastin **(Chapter 1, Section 1.2.2)** and peroxidasin (*PXDN*) is involved in collagen crosslinking to the ECM (Peterfi *et al.,* 2013). *LOX* was found in the same cluster as *FBN1* in the previous analysis of gene expression in mouse cells (Summers *et al.,* 2010). Another structurally important gene, *NDST,* is involved in heparan sulphate biosynthesis. Fibrillin-1 has heparan sulphate binding sites throughout the protein (Ritty *et al.,* 2003, Tiedemann *et al.,* 2001, Cain *et al.,* 2005) and interruption of heparan sulphate binding has been associated with connective disease, such as Weill Marchesani Syndrome (Cain *et al.,* 2012).

4.6.2 Transcriptomic characterisation of cell lines

In conjunction with the results for specific genes and proteins, transcriptomic analysis showed that each cell line had a unique set of highly expressed genes. Cluster003, Cluster004, and Cluster034 contained genes highly expressed in the osteosarcoma cell line MG63, fibroblast cell line NHDF and chondrocyte cell line C20A4, respectively ***(Figure 4.6)*** and included many genes involved in ECM assembly and function or implicated in multiple connective tissue disorders ***(Section 4.5.1)***. All three of these cell lines showed high expression of *FBN1* ***(Figure 4.1)***. Cluster004 displayed a different average expression pattern to the *FBN1* specific clusters, though it was located close by ***(Figure 4.6 and 4.7)***. *ACTA2* (OMIM: 102620) and *TGFBR2* (OMIM: 190182) were located within Cluster004 and both have been implicated in thoracic aortic aneurysm leading to acute aortic dissections (TAAD), a common and lethal phenotype in Marfan syndrome patients (Guo *et al.,* 2007, Pannu *et al.,* 2005). In addition mutations in *TGFBR2* have been identified in Loeys-Dietz syndrome, which shares many features with Marfan syndrome (Loeys *et al.,* 2006, Pannu *et al.,* 2005, Loeys *et al.,* 2005, Mizuguchi *et al.,* 2004). The high expression of these genes in NHDF cells suggests that fibroblast cell types are of primary importance in establishing and maintaining aortic structure, and that it is the impact of *FBN1* mutation on fibroblasts that contributes the high risk of aortic aneurysm (in the elastic medial layer) in Marfan syndrome patients.

Multiple members of the ADAM metallopeptidase domain gene family were in Cluster003 and Cluster004. ADAM genes are transmembrane proteases, while *ADAMTS* genes are specific to ECM protease activity (Primakoff and Myles, 2000). *ADAMTS2* (OMIM: 604539) co-expressed with genes in Cluster004 and has been implicated in connective tissue disease Ehlers-Danlos syndrome type VII (Colige *et al.,* 2004, Colige *et al.,* 1999). *ADAMTSL1* (OMIM: 609198), in Cluster003, encodes the ECM protein punctin found in skeletal muscle (Hirohata *et al.,* 2002).

Cluster004 had multiple members of the matrix metallopeptidase gene family including *MMP10, MMP11, MMP19, MMP27* and *MMP7*. These genes are involved in degrading ECM proteins and are regulated by the tissue inhibitor of metalloproteinases (TIMP) gene family, (reviewed by (Primakoff and Myles, 2000)) of which *TIMP3* was co-expressed

with Cluster004. MMPs are thought to degrade fibrillin-1 and fibrillin-2 either before or after microfibril formation (Hindson *et al.,* 1999). The co-expression of these genes in fibroblasts suggests possible mechanism that maintains fibrillin microfibril homeostasis.

There were multiple fibulin genes in Cluster004 including *FBLN1*, *FBLN12* and *FBLN5*. Recessive mutations in *FBLN1* have been implicated in synpolydactyly (webbed fingers) and mutations in *FBLN5* are implicated in cutis laxa (OMIM: 614434)(OMIM: 219100). Fibulins are ECM specific glycoproteins that bind to collagen and/or elastin (encoded by the *ELN* gene) (Argraves *et al.,* 1989, Argraves *et al.,* 1990, Xie *et al.,* 2007). *ELN* and collagen-related genes *COL21A1* and collagen binding protein gene, *COL4A3BP* were also found in Cluster004 and had the same expression pattern as the fibulin genes described above. Cluster004 also contained follistatin –like 1 (*FSTL1),* which had been previously identified in the *Fbn1*-associated cluster identified using in mouse cells (Summers *et al.,* 2010).

Similar to Cluster004, Cluster003 contained some genes involved in ECM maintenance, repair (*ADAMSTL1* described above) and connective tissue disease including *COL14A1*, *FGFR4*, and *LMNA*. *COL14A1* (OMIM: 120324) is an integral component of collagen fibrillogenesis, affecting formation of skin and collagenous tendons and recently implicated in myocardium formation (Ansorge *et al.,* 2009, Tao *et al.,* 2012). Due to the nature of MG63 cells that lack the ability to form a calcified matrix, the upregulation of *COL14A1* could indicate that they have a phenotype more closely resembling fibroblasts, consistent with the close proximity of the MG63 and NHDF clusters in the network layout ***(Figure 4.5)***.

In addition, nuclear intermediate filament gene, *LMNA* (OMIM: 150330), was upregulated in the MG63 cell line. *LMNA* has been implicated in multiple biological pathways. For example, it has been found as a key component in adipocyte differentiation (Lloyd *et al.,* 2002) and myotube formation and differentiation (Favreau *et al.,* 2004, Ho *et al.,* 2013), as well as inhibition of fibroblast proliferation through interactions with TGFβ1 (Van Berlo *et al.,* 2005). The gene is involved in 10 connective diseases. Several diseases caused by *LMNA* mutations mimic similar phenotypes of fibrillin-1 and fibrillin-2 associated diseases, such as Emery-Dreifuss muscular dystrophy (OMIM: 181350),

Hutchinson-Gilford progeria (OMIM: 176670), and restrictive dermopathy, lethal (OMIM: 275210). The disorders cause destructive phenotypes in multiple connective tissue systems including skeletal, cardiovascular, skin and cartilage formation. As discussed in **Chapter 3**, *LMNA* mutations are also associated with lipodystrophy (Capanni *et al.,* 2005).

Though Cluster034, which showed high expression in chondrocyte cell line C20A4, was noticeably smaller and more distant from the fibrillin-1 clusters in the network ***(Figure 4.5)***, it contained some ECM specific genes such as *FBLN7* and *MTMR2* ***(Figure 4.6)***. *FBLN7* is a fibulin gene required for tooth formation (de Vega *et al.,* 2007), and the cluster was highly correlated with ECM related GO terms ***(Table 4.6)*** possibly relating to the collagen in the periodontal ligament that gives an association with tooth formation. Myotubularin- related protein 2 (*MTMR2)* is associated with one form of demyelinating neuropathy (Bolino *et al.,* 2000) and is involved in production and function of normal myelin by Schwann cells, cells in the nervous system that support neurons. There has been evidence to suggest that chondrogenic activity supports the formation of epibranchial ganglia in the central nervous system (CNS)(Culbertson *et al.,* 2011). The epibranchial ganglia transmit important signals to the CNS and are developed in early embryogenesis. Therefore, upregulation of *MTMR2* in C20A4 cell lines could be suggestive of a role for cartilage in CNS development.

In contrast to NHDF, C20A4 and MG63 there were five cell lines analysed that did not show high levels of *FBN1* mRNA or fibrillin-1 protein expression ***(Figure 4.1 and 4.8)***. Human monocyte derived cell line, THP1, was expected to have very little or no fibrillin-1 expression, which was verified following the BioLayout *Express* ^{3D} overall clustering analysis ***(Figure 4.7)***. There was a high level of hematopoietic specific lineage markers, high incidence of DAVID determined GO terminology associated with immune/ defence response or T cell activation, and a large portion of genes associated with the THP1 specific cluster were related to immune and infectious diseases ***(Table 4.1)***. The lack of ECM related genes and the distance to the fibrillin-1 specific clusters, indicates that THP1 is a good negative control.

Surprisingly, mineralising human osteosarcoma cell line SAOS2 did not express *FBN1* mRNA or develop a fibrillin-1 ECM, similar to human chondrocyte cell lines TC28A2 and C28I2 ***(Figure 4.1, 4.3 and 4.4)***. The overall BioLayout Express ^{3D} analysis showed that the SAOS2 specific cluster was more closely related to THP1 ***(Figure 4.5)***. The relationship between SAOS2 and THP1 could be related to the process of bone regeneration. SAOS2 contained multiple osteoblast markers such as *IBSP*, *RUNX2* and *PHOSPHO1* ***(Figure 4.6),*** while cancerous cell line THP1, by nature, is derived from precursor cells that can also create osteoclasts (**Chapter 2, Section 2.1.5),** cells responsible for the degradation of bone (**Chapter 1, Section 1.1.4**). The close expression profiles between these cell lines could represent the need of macrophages for osteoblasts to calcify (Chang *et al.,* 2008). While both MG63 and SAOS2 human osteosarcoma cell lines were of mesenchyme origin, the expression of fibrillins varied between the two cell lines. As shown in ***Figure 4.1*** and ***Figure 4.3***, *FBN1* mRNA was extremely low in SAOS2 cells, and there were no visible SAOS2 fibrillin-1 microfibrils, in comparison to the high levels of both mRNA and fibrillin-1 microfibrils in MG63. This is consistent with the observation in **Chapter 3** that fibrillin 1 was associated with the less mature state during adipogenesis and disappeared as the lineage differentiated further. The lack of bone-associated GO terms for the MG63 cluster and its distance from SAOS2 in the network supports the concept that MG63 is a more immature (or dedifferentiated) cell line than SAOS2.

The chondrocyte cell line TC28A2 and its derivative C28I2 (Cluster008) were in close proximity to the chondrocyte cell line C20A4 cluster (Cluster034), as shown in ***Figure 4.5***, though the lack of a fibrillin-1 matrix in TC28A2 and C28I2 ***(Figure 4.4)*** could suggest that they originated from an undiagnosed Marfan syndrome patient. As described previously **(Section 4.1)**, C20A4 and TC28A2 were derived from the costal cartilage of patients undergoing corrective surgery for pectus excavatum (Goldring *et al.,* 1994), a common symptom of Marfan syndrome (OMIM: 154700)(Summers *et al.,* 2012). Pectus excavatum is described as a skeletal and cartilage deformity resulting in a hollow chest. The 5 year old male whose tissue yielded the cell line C20A4 may have had a sporadic deformity of pectus excavatum, while the donor of TC28A2 and subsequently C28I2 may have had Marfan syndrome with an undiagnosed *FBN1* mutation, explaining the lack of a

fibrillin-1 ECM. Further experiments such as exon sequencing would be needed to confirm this.

The human U219 microarray analysis revealed low levels of *FBN1* mRNA expression in HEK293 cell line, consistent with past research (Summers *et al.,* 2009, Guo *et al.,* 2013, Wang *et al.,* 2012)***(Figure 4.7)***. BioLayout *Express* ^{3D} analysis revealed that Cluster005 contained genes that were highly upregulated in HEK293 ***(Figure 4.6)***. As described previously, there were a few ECM related genes in this HEK293 cluster, including *ADAMTS16, HOXD10* and *HOXD13*. *ADAMTS16* mutations are commonly associated with thrombotic thrombocytopenic purpura (MIM: 274150) a disorder involving mainly cells of neonatal epithelial origin, consistent with the derivation of HEK293 from human embryonic kidney. *HOXD10* mutations have been implicated in a foot deformity, vertical congenital talus. It encodes a transcription factor linked to limb development (OMIM: 192950). HOXD13*,* like HOXD10, is a transcription factor associated with limb development and mutations cause multiple forms of both brachydactyly and synpolydactyly (OMIM: 142989). HEK293 was not expected to have high expression of many ECM related genes, since it was derived from embryonic epithelial cells. This is consistent with genes found in the cluster to be associated with the GO term embryonic development ***(Table 4.7)***. In addition, the DAVID GO term analysis produced several differential terms including nervous system development, neurogenesis, generation of neurons and neuron differentiation. A previous study suggested that HEK293 may have had a neuronal origin (Shaw *et al.,* 2002) which is supported by the presence of genes associated with these GO terms.

4.6.3 Limitations of cell line expression studies

This chapter demonstrated the expression patterns of the fibrillin gene family across a variety of connective tissue cell lines. Future expression arrays on primary cell types would need to be performed to validate the cell line findings outlined above.

4.7 Conclusions

Given the severe multisystem phenotype associated with *FBN1* mutations it was possible that fibrillin-1 was a central regulator of ECM formation. The analysis presented in this chapter showed that many ECM and cytoskeletal genes were co-regulated with *FBN1*. The co-expression of these genes implies possible co-operative functions between the ECM, cytoskeleton genes and fibrillin-1 in maintaining ECM homeostasis in C20A4 (chondrocyte cell line), MG63 (osteosarcoma cell line) and NHDFs (fibroblast primary line).

Therefore it was important to investigate whether fibrillin-1 controlled expression of any of these above defined genes. Based on the high expression of many ECM related genes including *FBN1* and association with ECM related GO terms, NHDF, C20A4 and MG63 were chosen for further studies.

Chapter 5. Investigating the functional role of fibrillin-1 in cell lines

5.1 Introduction

As discussed in **Chapter 1 (Section 1.3.4) a**nd **Chapter 4 (Section 4.1)**, mutations in *FBN1* cause major multisystemic phenotypic effects in humans, natural animal models and engineered mouse models. These include abnormalities in the bone, cartilage, adipose and skin formation. The study presented in **Chapter 3** demonstrated that fibrillin-1 protein was present in mesenchymal stem cells but declined rapidly when these cells were directed towards adipogenesis. The findings suggest that fibrillin-1 may be a regulator in mesenchyme type cells, as has been proposed previously (Summers *et al*., 2010). In **Chapter 4**, it was shown that C20A4 (chondrocyte), NHDF (neonatal fibroblast) and MG63 (osteosarcoma) cell lines produced a vast fibrillin-1 matrix and showed high levels of *FBN1* expression, co-expressed with genes implicated in ECM and cytoskeleton maintenance. These three cells lines were therefore chosen for a preliminary investigation of the effect of reducing *FBN1* using gene silencing by RNA interference (RNAi). Knocking down *FBN1* in these cells was expected to simulate the phenotype of MFS patients *in vitro* and therefore reveal genetic interactions important to the phenotype in this disease. Microarray analysis of RNA levels and ICC techniques using fluorescent tags for both fibrillin-1 and actin polymers were used to examine the effect on gene transcription and cell morphology of reducing the level of *FBN1* mRNA and hence fibrillin-1 protein.

RNAi is a technique for post-transcriptional gene silencing, shown to be effective in mammalian cells (Elbashir *et al.,* 2001). It involves introducing a double stranded RNA (dsRNA) that contains a sequence homologous to the targeted gene into the cells ***(Figure 5.1A)***. The dsRNA is cleaved within the cell into small interfering RNA (siRNA) and the antisense strand is integrated into the RNA induced silencing complex (RISC). The complex is recruited to the sense strand of the targeted mRNA, interfering with translation and causing premature degradation of the mRNA. The gene is therefore said to be silenced ***(Figure 5.1B)***(Birmingham *et al.,* 2006, Anderson *et al.,* 2008). This

process of reducing gene expression through inactivation of the mRNA has been termed "knockdown" (KD)***(Figure 5.1)***.

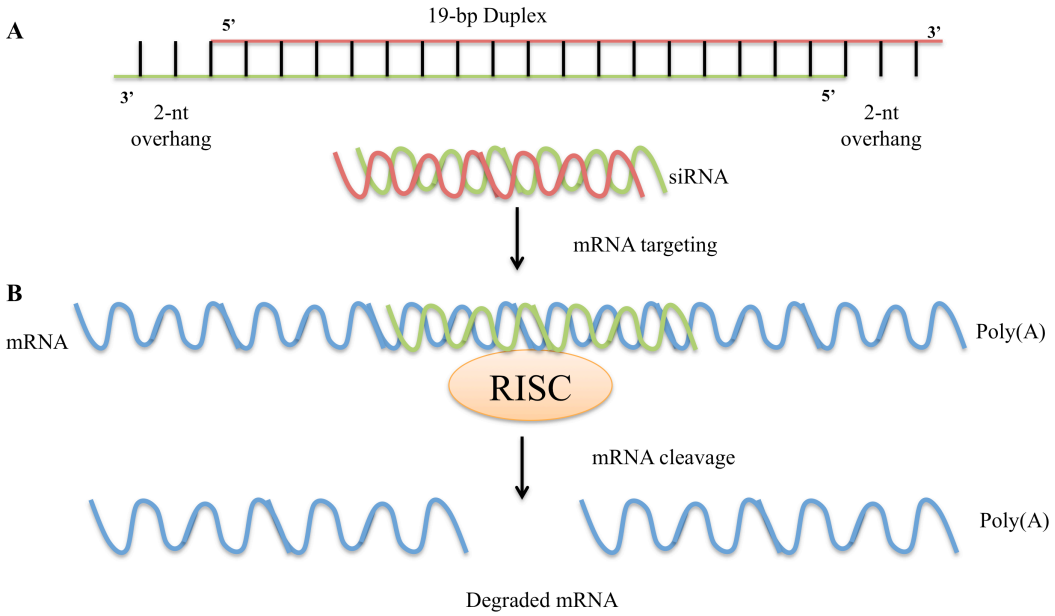

Figure 5.1. Gene knockdown (KD) mechanism using RNAi. (A) The overall structure of the siRNA duplex. The siRNA is constructed from the homologous sequence of the targeted gene to include both a 5' and 3' overhang. (B) Knockdown of gene expression. The dsRNA (siRNA) is unwound and the antisense strand is incorporated into the RISC (RNA induced silencing complex), initiating binding to the target mRNA strand and causing mRNA degradation. The passenger (sense) strand of the dsRNA is degraded. Image adapted from (Clark and Whitelaw, 2003).

Several studies have used this RNAi technique to examine the relationship between ECM molecules. For example, Choudhury *et al.,* (2009) used RNAi to study the role of ECM gene *FBLN4* (fibulin-4). They reduced *FLBN4* mRNA expression by 70% in a retinal pigmented epithelial cell line (ARPE19) and saw an increase in desmosine, a biomarker of elastin degradation (Choudhury *et al.,* 2009). Similar knockdown studies on *FBLN4* in neonatal foreskin fibroblasts (NHDF) showed that fibulin-4, considered a structural protein, also has a regulatory role and controls levels of tropoelastin via *ELN* (elastin) gene expression (Chen *et al.,* 2009). Knockdown studies of *MFAP4* (microfibril associated protein-4) in human dermal cell culture demonstrated that this protein could regulate levels of *FBN1* and *MMP1* (matrix metalloproteinase, a collagenase of the ECM) mRNA (Kasamatsu *et al.,* 2012)**(Chapter 3, Section 3.5.3)**. Furthermore, knockdown studies have been used to better understand the function of fibrillin-1 and fibronectin in

fibroblast cell cultures. Kinsey *et al.,* (2008) used RNAi to deplete *FN1* mRNA levels, showing little to no effect on *FBN1* mRNA expression. However, protein analysis performed on the KD samples showed a major depletion in fibrillin-1 microfibril formation.

5.1.1. Aims of the Chapter

In this chapter, the functions of *FBN1* were explored by using RNAi techniques to reduce the amount of *FBN1* mRNA and hence protein in the three cell lines with normally high levels of fibrillin-1, NHDF, MG63 and C20A4. The aim was to understand the interactions of fibrillin-1 with other ECM related genes in mesenchyme derived cells. Following the reduction of *FBN1* mRNA, gene and protein expression patterns as well as cell morphology were analysed to determine any downstream effects of fibrillin-1.

5.2 Materials and Methods

5.2.1 Transfection efficiency

Initially transfection efficiency was tested using Lipofectamine 2000 reagent (Invitrogen) and transfection indicator reagent siGLO (Thermo Scientific). EtOH treated glass cover slips (1.3mm, sterile, sonicated)(kindly supplied by Dr. Mark Barnett) were placed into three wells of a 24 well plate (NUNC), and allowed to air dry in a sterile hood. Once dried, the wells (with coverslips) were coated with 0.1% gelatin for 5 minutes. NHDF cells were seeded at 60% confluence (40,000 cells/well of a 24 well plate) and cultured overnight in normal media conditions **(Chapter 2, Section 2.2)**.

20µM siGLO (Thermo Scientific) was added to Opti-MEM 1x (Gibco) media for a final concentration of 1µM and incubated for 5 minutes. Simultaneously, Lipofectamine 2000 reagent (Invitrogen) was added to Opti-MEM 1x (at 1:10) and incubated for 5 minutes. The siGlo and Lipofectamine solutions were combined and incubated for 25 minutes at room temperature. DMEM + 10%FBS was added for a final concentration of siGlo/lipofectamine mixture of 90nM. 200µl of this solution was added to each well of the 24 well plate which was then placed at 37°C and 5% CO_2 for 5 hours. The transfection mix was removed and cells were incubated at 37°C in 5% CO_2 for 24 hours. The glass slides were fixed with 4% PFA for 20 minutes, washed 4 x for 5 minutes with

PBS, removed and mounted with Prolong GOLD + DAPI (Invitrogen) on Superfrost glass slides (Fischer Scientific). Samples were viewed using Zeiss LSM 710 confocal microscope and analyzed with ZEN software at standard settings (Zeiss)***(Figure 5.2)***.

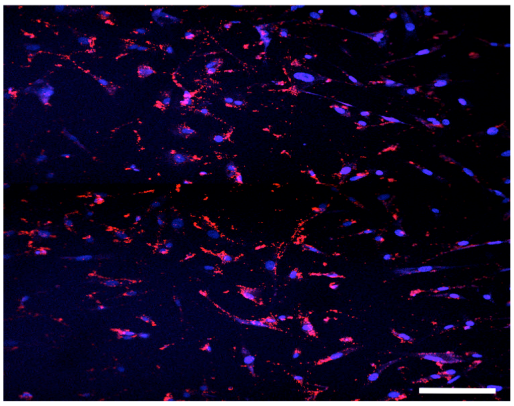

Figure 5.2. Transfection efficiency of Lipofectamine 2000 in NHDF cells. The image depicts the siGLO (red) tranfection indicator in NHDF cells. The nuclei are shown blue. The image was taken at 20x using a Zeiss confocal microscope (Section 5.2.1). The scale bar represents 50µm. The transfection efficiency was estimated at 90%.

5.2.2 *FBN1* knockdown with siRNA

MG63, C20A4 and NHDF cells were plated at 60% confluence: 10,000 cells/well in 8 well chamber slides (Thermo Scientific) which would be used later for ICC, and 60,000 per well in 6 well plates (NUNC) which would be used for RNA extraction, and cultured for 24 hours in conditions outlined in **Chapter 2, Section 2.2**. After 24 hours, the cells were checked using the inverted light microscope for 85-95% confluence. A 20µM working stock solutions was made of siGENOME SMART pool Human FBN1 siRNA (Thermo Scientific) and siGENOME SMARTpool non-targeting reagent (Thermo Scientific) and stored at -20°C. The siGENOME Human FBN1 siRNA SMART pool consists of four individual double-stranded RNA duplexes, D-011034-04, D-011034-03, D-011034-02 and D-011034-01 ***(Table 5.1)*** that are designed to target different regions of *FBN1* mRNA to silence gene expression ***(Table 5.1)***. Experiments were performed using all 4 duplexes targeting four regions.

Target Name	Target Sequence 5'-3'	Location of targeted sequence in FBN1
D-011034-01	CCAGAUAUGUCCUUAUGGA	Exon 52
D-011034-02	GAAUGAAGAUACACGAGUG	Exon 40
D-011034-03	AUACAACACUGCAAUAUUC	Exon 5
D-011034-04	CGAAUGAGCUACUGUUAUG	Exon 51

Table 5.1. FBN1 SMARTpool siRNA targets.

20µM siRNA targeting human *FBN1* mRNA (and non-targeting control) was added to Opti-MEM 1x media (final concentration of 2.5µM) and incubated for 5 minutes. Simultaneously, Lipofectamine 2000 was prepared and transfections were performed as described above **(Section 5.2.1)**. The siRNA reagent and Lipofectamine solutions were combined and incubated for 25 minutes at room temperature. DMEM + 10%FBS was added for a final concentration of 50nM (and both 50nM and 90nM for NHDF) of both the siRNA human *FBN1* and siRNA non-targeting control. 100µl of the appropriate transfection mix was added to a well of the 8 well chamber slides, and 200µl to a well of the 6 well plates and incubated as described in **Section 5.2.1** ***(Figure 5.3)*.**

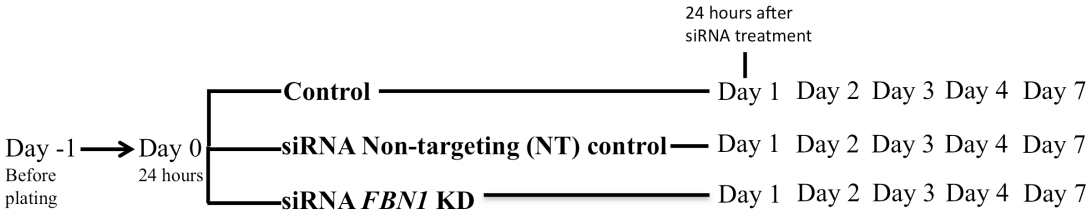

Figure 5.3. A schematic illustrating the experimental timeline and treatments used. The experiment was done using the following cells, MG63, C20A4 and NHDF. RNA was collected at all the timepoints shown (Chapter 2, Section 2.3.1), for all three treatments. ICC fluorescent staining (Section 5.2.4) was done at Day 4 and Day 7 for all cell types undergoing all three treatments.

The transfection reagent was removed from the well and replaced with normal culture media **(Chapter 2, Section 2.2)** and the cells were incubated until RNA extraction. RNA was extracted **(Chapter 2, Section 2.3.1)** at Day 1, Day 2, Day 3, Day 4 and Day 7 ***(Figure 5.3)***. RNA was also extracted from all cell types immediately prior to transfection, 24 hours after plating, (Day 0) and prior to culture in the 6 well plates (Day -1) ***(Figure 5.3)***. Two controls were included. Firstly, the non-targeting siGENOME SMARTpool (Invitrogen) was used at 50nM with Lipofectamine. Secondly, parallel cell cultures remaining in normal culture media throughout the time course were included.

RNA was collected for both controls as outlined above ***(Figure 5.3)***. *FBN1* knockdown experiments (50nM FBN1 SMARTpool) were replicated for RNA extraction as follows, NHDF n=2, MG63 n=1 and C20A4 n=1.

5.2.3 qPCR

mRNA expression levels were quantified using qPCR techniques previously described in **Section 2.3.4 of Chapter 2**. Statistical significance was calculated by using a standard student two-sample t-test. The analysis used the mean ΔCT of the technical replicates **(Chapter 2, Section 2.3.4.1)**, comparing for example Day 1 NT values to Day 1 *FBN1* knock down (FBN1KD) values.

5.2.4 ICC

The fibrillin-1 fluorescent staining was carried out as described in **Section 2.4.2 of Chapter 2**. ICC experiments were repeated at n=2.

5.2.4.1 Actin Staining

MG63, NHDF and C20A4 cells cultured in 8 well chamber slides **(Chapter 2, Section 2.2)** were fixed through the timecourse ***(Figure 5.3)*** with 4% PFA for 10 minutes then washed 3 x for 5 minute with PBS. Fixed cells were permeabilized with 0.1% Triton X-100 (Sigma-Aldrich) in PBS for 20 minutes at room temperature then washed 3 x for 5 minutes and blocked with 1% BSA in PBS for 1.5 hours at room temperature. 40x Texas Red X- Phallodin (Invitrogen) was added to the cells for 30 minutes at room temperature. The cells were then washed with PBS, and mounted with ProGold + DAPI (Invitrogen). Samples were viewed using Zeiss LSM 710 confocal microscope and analyzed with ZEN software at standard settings (Zeiss).

5.2.5 BioLayout *Express* ^{3D}

Gene expression levels in RNA samples were determined using the U219 human microarray platform **(Chapter 2, Section 2.3.5)** for FBN1KD, normal media (control) and non-targeting siRNA (NT control) at Day -1, Day 0, Day 1, Day 2, Day 3, Day 4 and Day 7 for MG63, C20A4 and NHDF samples (**Chapter 9, Appendix B**). Probes were removed from the data set that had expression intensity values under 16 **(Chapter 2, Section 2.3.6)**, removing 12, 811 of the low expressing probes, including the *FBN3* probe

(25.6%). Intensity results for the remaining 36,574 probeset were loaded into BioLayout *Express* ^{3D}. The clustering analysis was run at $r \geq 0.87$ at an MCL inflation value of 2.2, producing 951 clusters **(Chapter 2, Section 2.3.6)**.

Fold change of expression was determined using the U219 microarray expression values obtained from BioLayout *Express*^{3D} . The average expression of all the probes within a cluster at a specific time point was obtained. The ratio between the NT control and FBN1KD treated sample was used to demonstrate difference in expression between the two samples. A fold change of >1.5 (upregulated) or < -1.5 (downregulated) was considered to show differential gene expression.

5.2.6 GO terms

The gene list for large Cluster002 **(Section 5.3.3)** was placed into the upload tool bar of DAVID 6.7 functional annotation tool (www.david.abcc.ncifcrf.gov/)**(Chapter 2, Section 2.3.6)**.

5.3 Results

5.3.1 siRNA reduced *FBN1* mRNA levels in cell lines

Initial transfection efficiency was calculated at 90% using siGLO and Lipofectamine 2000 reagents **(Section 5.2.1).** Therefore, *FBN1* knockdown studies were performed on chondrocyte cell line (C20A4), fibroblasts (NHDF), and osteosarcoma cell line (MG63). The RNAi construct was introduced into the cells 24 hours after plating (D0)***(Figure 5.3)***. qPCR analysis at specific time points throughout the timecourse was used to determine if the levels of *FBN1* had been depleted compared with both the NT control and normal media control samples ***(Figure 5.4)***.

There was an estimated 83% knockdown when comparing Day 1 *FBN1* knockdown and NT samples in C20A4 cells. The results of the qPCR analysis of *FBN1* mRNA in C20A4 cells are shown in ***Figure 5.4A***. While control and NT samples maintained relatively high levels of *FBN1* mRNA, with a peak at Day 4, the *FBN1* knockdown samples revealed a decrease in *FBN1* mRNA expression at Day 4 and Day 7. In addition, the Day 7 FBN1KD sample was significantly lower ($p = 0.009$) than Day 7 NT control in this cell

line ***(Table 5.2)***. The results demonstrated that *FBN1* mRNA levels had been reduced by the siRNA transfection. Based on similar nucleotide and amino acid sequences of *FBN1* and *FBN2* (http://www.ensemble.org; see **Chapter 7**), off-target effects would most likely have affected fibrillin-2. qPCR analysis showed that even within the *FBN1* knockdown samples, *FBN2* mRNA levels remained relatively unchanged, demonstrating that *FBN2* expression was not altered in the *FBN1* knockdown system ***(Figure 5.4B)***. Furthermore there was no statistically significant variation calculated ($p \leq 0.1$) between the NT control and FBN1KD samples for *FBN2* expression.

As for C20A4, *FBN1* mRNA decreased after siRNA treatment of MG63 cells ***(Figure 5.4C)***. Day 1 of the knockdowns was the most affected (approximately 51% decrease when comparing knockdown and NT samples), with *FBN1* levels increasing at Day 2 and remaining static at Day 3 and Day 7, different to the control and NT control samples ($p \leq 0.1$)***(Figure 5.4C)(Table 5.2)***. Though expression levels varied between the control and NT control samples, the *FBN1* knockdown samples showed a consistent decrease in *FBN1* expression to less than half that in untreated cells. *FBN2* expression showed no significant differences across the control, NT control and FBN1KD sample time courses, though it did show a non significant increase of expression at Day 3 in the *FBN1* knockdowns ($p \leq 0.1$)***(Figure 5.4D)***.

The impact of the *FBN1* siRNA treatment was most obvious in the fibroblast cells, NHDF ***(Figure 5.4E)***. *FBN1* levels decreased in the knockdown samples at Day 1 by approximately 82% and the expression pattern across the knockdowns shows that *FBN1* mRNA level remained low throughout the timecourse when compared to both the control and NT control samples ***(Figure 5.4E)***. A two-sample t-test analysis comparing the NT control and FBN1KD samples showed statistical significance in the reduction of *FBN1* ***(Table 5.2).*** *FBN2* mRNA expression was unaffected in the *FBN1* knockdowns ($p \leq 0.1$)***(Figure 5.4F)***.

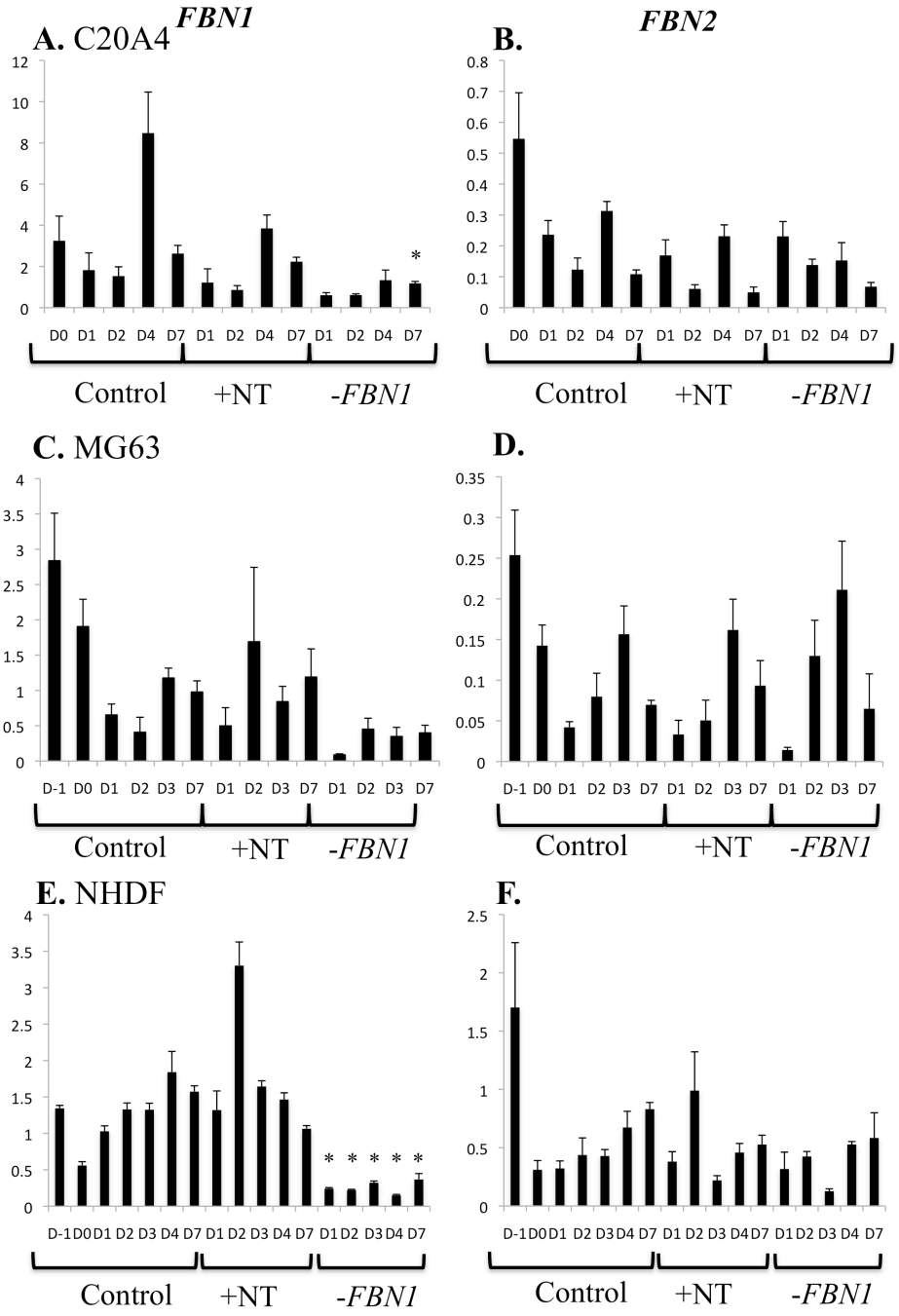

Figure 5.4. qPCR results for *FBN1* (A, C and E) and *FBN2* (B, D and F) expression in C20A4 (A and B), MG63 (C and D) and NHDF (E and F) cells after *FBN1* knockdown. The y-axis represents the expression values calculated by advanced relative quantification, Target/Reference ratio (LightCycler480, ROCHE, Chapter 2, Section 2.3.4). The reference was human *GAPDH* (Qiagen). Control samples were left untreated, +NT samples were treated with non-targeting (NT) siRNA and –*FBN1* samples were treated with siRNA human FBN1 SMARTpool(Thermo Scientific). Day 1 describes samples 24 hours after transfection (Figure 5.3). (A and B: Day 3 was omitted from qPCR analysis due to low total RNA yield, C and D: Day 4 was omitted from qPCR analysis due to low RNA yield.) The * over the FBN1KD samples depicts statistical significance p≤0.01 using a standard two sample student t-test, compared with the NT control sample at that specific time point (Section 5.2.5)(Table 5.2).

Comparison	P-value
C20A4	
Day 7 NT control and Day 7 FBN1KD	0.0099
NHDF	
Day 1 NT control and Day 1 FBN1KD	0.007
Day 2 NT control and Day 2 FBN1KD	0.0002
Day 3 NT control and Day 3 FBN1KD	0.001
Day 4 NT control and Day 4 FBN1KD	0.0152

Table 5.2. Values of statistically significant qPCR results for FBN1KD experiments (Figure 5.4). The samples not shown in the above table were found to not be statistically significant ($p \leq 0.05$).

5.3.2 FBN1 mRNA knockdown reduces fibrillin-1 protein expression

Fluorescent staining of fibrillin-1 and Texas Red X- phallodin (phallodin) staining of F-actin molecules was done on C20A4, NHDF and MG63 cultures at Day 4 and Day 7 (**Section 5.2.4)**. The time points for fibrillin-1 staining were chosen because the control samples revealed that a fibrillin-1 matrix was visible by Day 4 after plating (**Chapter 4, Section 4.4.2**).

The beginnings of a rich fibrillin-1 matrix were seen in the control and NT control samples of C20A4 cells at Day 4, while there appears to be very little production of fibrillin-1 microfibrils in the FBN1KD (-*FBN1*) samples ***(Figure 5.5)***. This was consistent with the reduced levels of *FBN1* mRNA at early time points ***(Figure 5.4A)***. Phallodin staining at Day 4 showed some indication of a disruption in actin fibre formation in the fibrillin-1 knockdowns where the actin fibres appear less organised and slightly degraded compared with controls ***(Figure 5.5)***. There was also a reduction in actin fibres in the NT control, possibly related to the established reduction in proliferation induced by Lipofectamine2000[2].

At Day 7 after fibrillin-1 knockdown, microfibrils had developed in the FBN1KD cultures ***(Figure 5.5)***. The fibres resemble those seen in the Day 4 control samples of C20A4 cells, suggesting that the cells were recovering from the effects of the siRNA.

[2] Personal communication with Dr. Mark Barnett, The Roslin Institute, University of Edinburgh

Interestingly, the phallodin staining shows that the cytoskeletal actin had regained the organisation seen in the controls at Day 7 ***(Figure 5.5, lower panel)***.

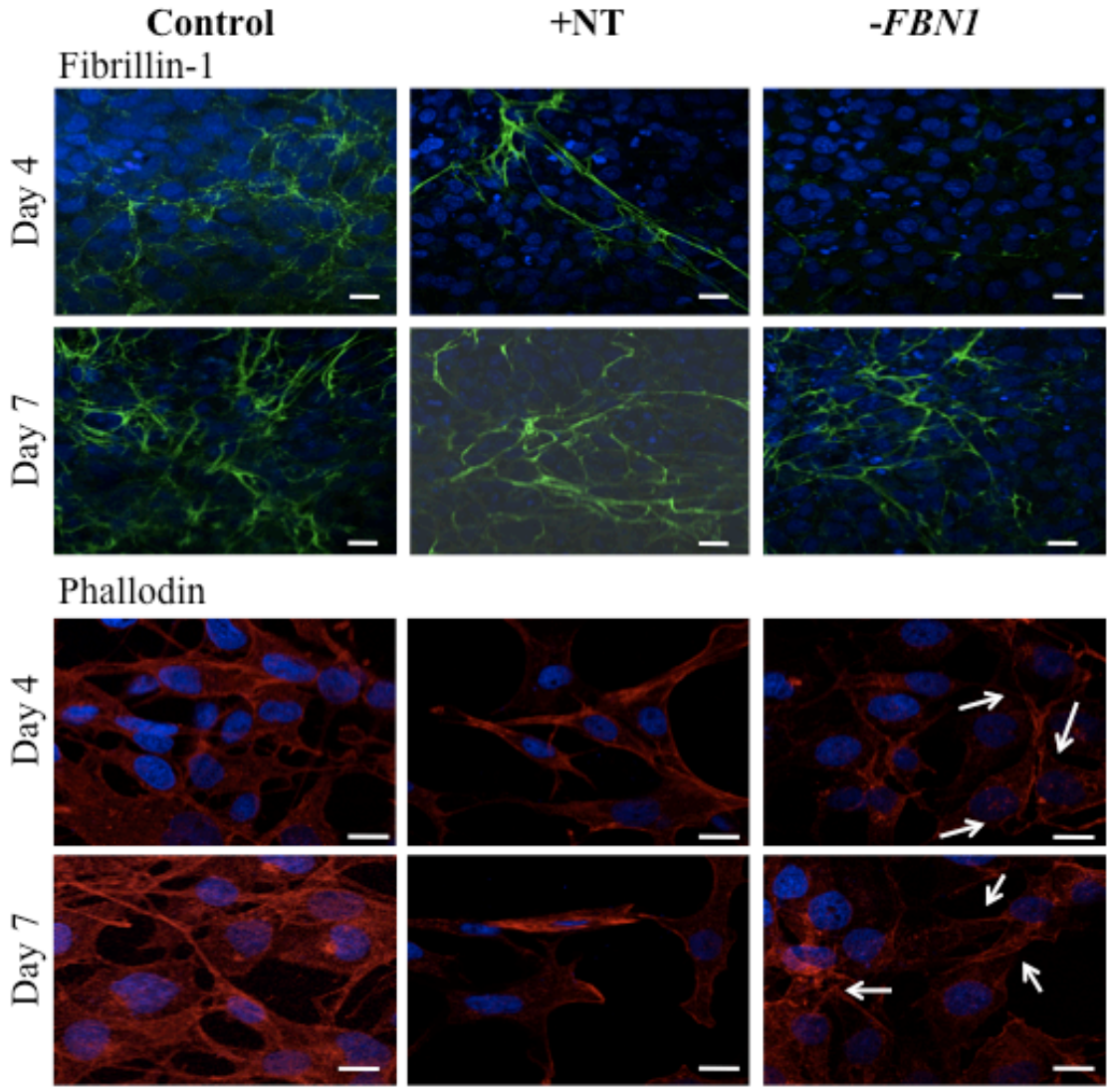

Figure 5.5. C20A4 cultures at Day 4 and Day 7. The green staining (upper panels) shows fibrillin-1detected with a monoclonal antibody (n=3)(Chapter 2, Section 2.4.2), imaged at 40x and the red staining (lower panels) shows cytoskeletal actin detected with Texas Red X-phalloidin (Section 5.2.4.1)(n=2), imaged at 63x. The white arrows depict specific actin fibres (see above text). The blue depicts DAPI stained nuclei. The fibrillin-1 and phalloidin stained images were captured using a Zeiss confocal microscope and images were adjusted using Zeiss software. The scale bars represent 20µm, n=2.

The beginnings of a rich fibrillin-1 matrix were visible at Day 4 in MG63 control and NT control samples, while there was no fibrillin-1 matrix in the *FBN1* knockdowns ***(Figure 5.6)***. The phallodin staining showed organised intracellular actin formation in the

controls. However, the actin staining in the *FBN1* knockdowns revealed disruptions in the actin fibres ***(Figure 5.6)***.

An extensive fibrillin-1 matrix was seen at Day 7 in MG63 control and NT control samples, while there were few fibrillin-1 microfibrils in the knockdown sample indicating that the cells had not recovered from the siRNA treatment ***(Figure 5.6)***. The staining that was seen could be evidence of early fibrillin-1 matrix formation. The phallodin staining of cytoskeleton actin showed that the actin fibres were beginning to form the structures seen in the controls of both Day 4 and Day 7 and the intensity of the actin fibre stain had increased since Day 4 ***(Figure 5.6, lower panel)***.

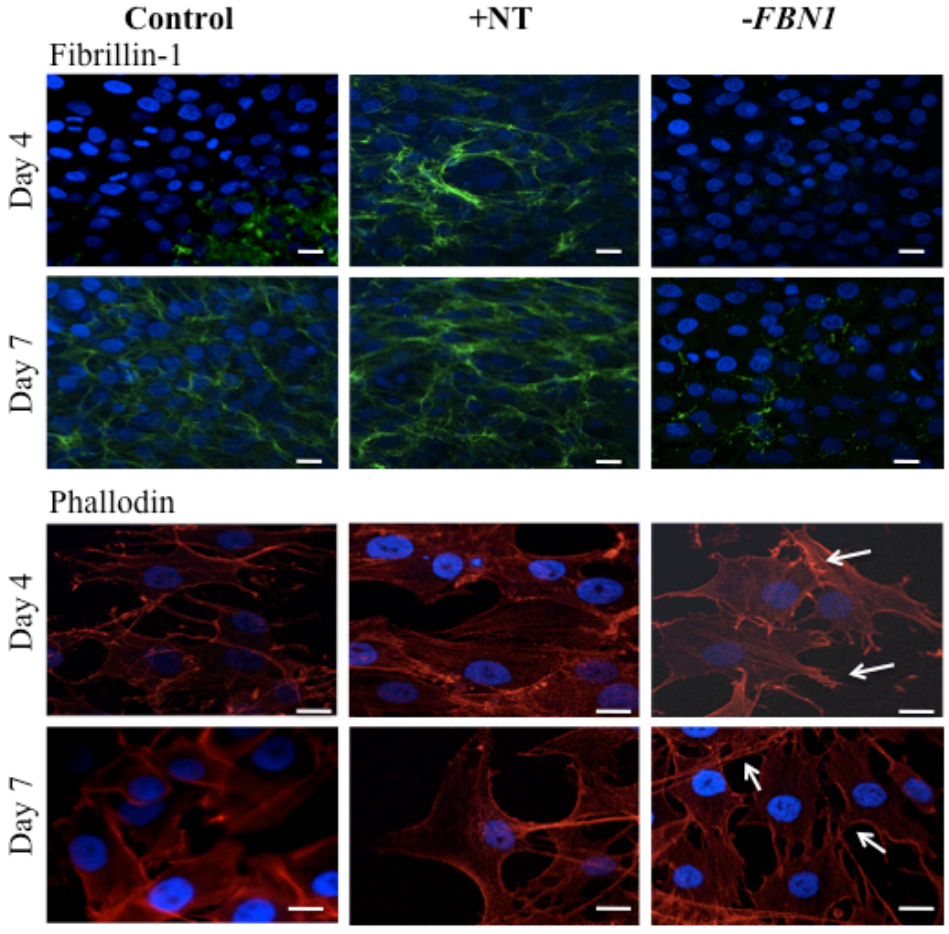

Figure 5.6. MG63 cultures at Day 4 and Day 7. The green staining (upper panels) shows fibrillin-1detected with a monoclonal antibody (Chapter 2, Section 2.4.2), imaged at 40x and the red staining (lower panels) shows cytoskeletal actin detected with Texas Red X phalloidin (Section 5.2.4.1), imaged at 63x. The white arrows depict specific actin fibres (see above text). The blue depicts DAPI stained nuclei. The fibrillin-1 and phalloidin stained images were captured using a Zeiss confocal microscope and images were adjusted using Zeiss software. The scale bars represent 20µm, n=2.

The initiation of a fibrillin-1 microfibril matrix was seen in the control NHDF samples at Day 4, while no visible fibrillin-1 matrix was detected in the knockdowns ***(Figure 5.7)***. The phallodin staining of cytoskeletal actin showed a highly organised, linear and rich actin fibre composition in NHDF control cells, while in the fibrillin-1 knockdown samples the actin fibres appeared less linear, and showed increased intensity when compared to the controls ***(Figure 5.7)***.

The fibrillin-1 results of Day 7 show the controls had developed dense fibrillin-1 microfibrils ***(Figure 5.7)*** as seen in **Chapter 4**. However, the fibrillin-1 matrix of the knockdown samples appeared scarce and fragmented.

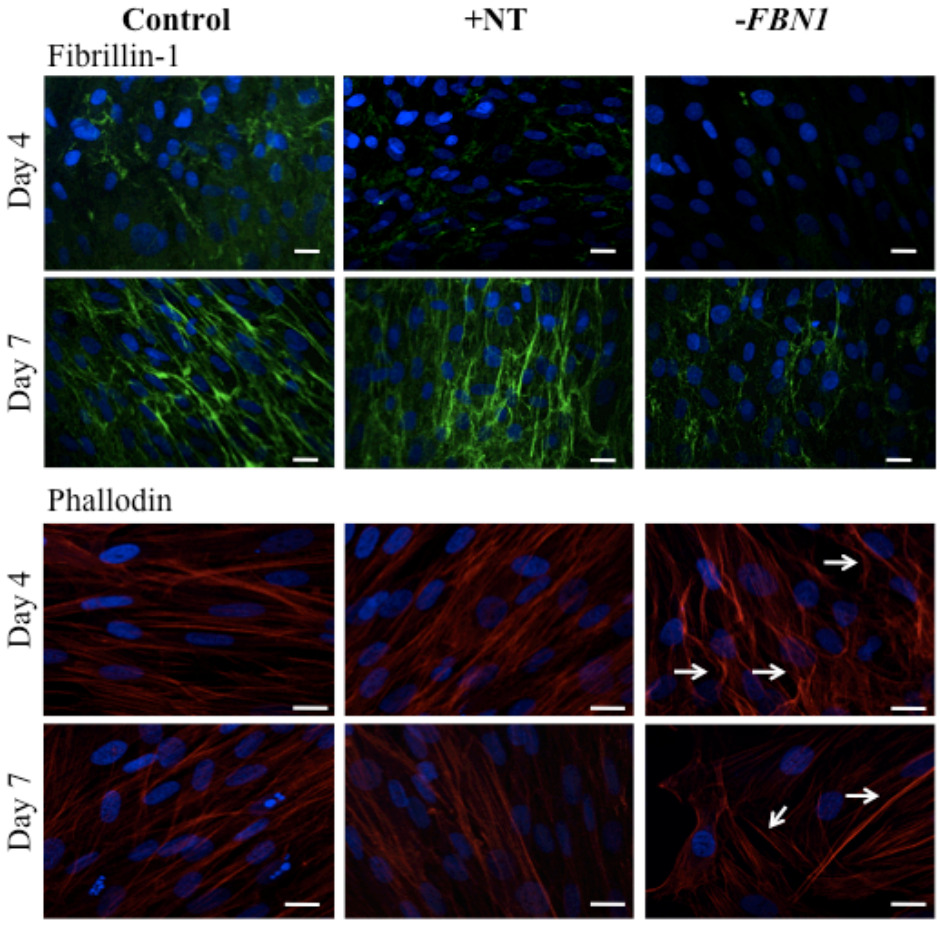

Figure 5.7. NHDF cultures at Day 4 and Day 7. The green staining (upper panels) shows fibrillin-1 detected with a monoclonal antibody (Chapter 2, Section 2.4.2), imaged at 40x and the red staining (lower panels) shows cytoskeletal actin detected with Texas Red X phalloidin (Section 5.2.4.1), imaged at 63x. The blue depicts DAPI stained nuclei. The fibrillin-1 and phalloidin stained images were captured using a Zeiss confocal microscope and images were adjusted using Zeiss software. The scale bars represent 20µm. n=2.

5.3.3 General gene expression analysis of fibrillin-1 knockdowns

The BioLayout *Express* ^{3D} analysis of U219 microarray data (**See Section 5.2.5**) collected from NHDF, C20A4 and MG63 knockdown timecourse experiments at $r \geq 0.87$ had a total of 19,363 nodes and 784,011 edges ***(Figure 5.8)***. *FBN1* probsets did not cluster with any other genes ***(Figure 5.8)*** and nor did *FBN2*. The fibrillin-1 cluster (Cluster 763) contained only four fibrillin-1 probes (11731230_a_at, 11736217_at, 11745470_x_at and 11746201_a_at). Cluster002 contained probesets for genes that were highly mesenchyme specific.

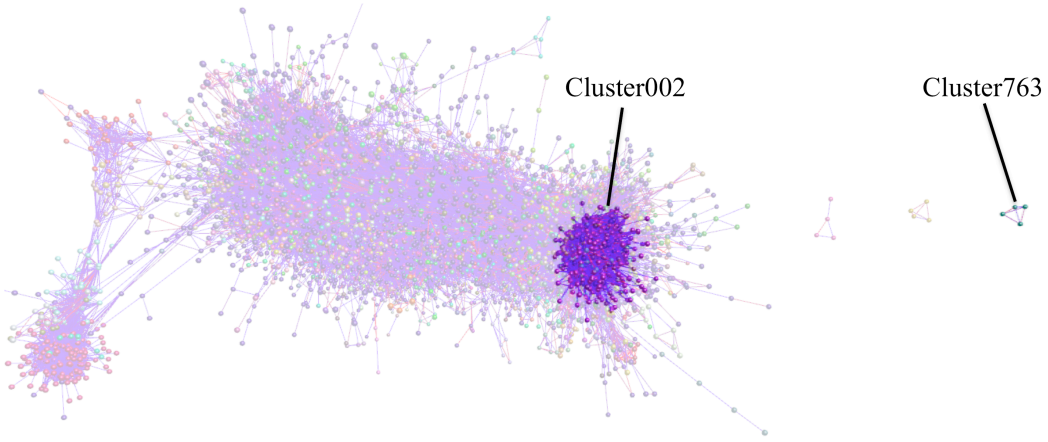

Figure 5.8. Network visualization and clustering of the NHDF, C20A4 and MG63 transcriptomes. The image depicts the network diagram produced by BioLayout *Express* ^{3D} using data from the Affymetrix U219 gene expression microarray platform on knockdown experiments across Day -1, Day 0, Day 1, Day 2, Day 3, Day 4 and Day 7. Spheres (nodes) represent individual probesets and the lines between them (edges) show correlations in expression pattern of $r \geq 0.87$. The nodes were clustered using an MCL inflation value 2.2 (Chapter 2, Section 2.3.6). The background of the image displays the whole network and clusters discussed in the text are highlighted. Cluster002 was the largest mesenchyme specific cluster and Cluster763 contained *FBN1* probes.

Cluster763 revealed distinct expression of *FBN1* throughout the timecourses, not surprising given the artificial manipulation of the *FBN1* mRNA ***(Figure 5.9)***. No other gene had the same expression pattern, suggesting that there were no off target effects. The control and NT control time course samples for NHDF, C20A4 and MG63 showed varying but high levels of *FBN1* expression across the time course with slight down regulation of *FBN1* at Day 1 and Day 2 of C20A4 ***(Figure 5.9)***. *FBN1* expression levels within the *FBN1* knockdown timecourse showed steady downregulation of the gene

across all time points in the NHDF, for both replicates, while gradually increasing in expression levels within MG63 and C20A4 ***(Figure 5.9)***, similar to the initial qPCR results ***(Figure 5.4)*** The fold change comparing the NT control and FBN1KD expression intensity values are shown in ***Table 5.3***.

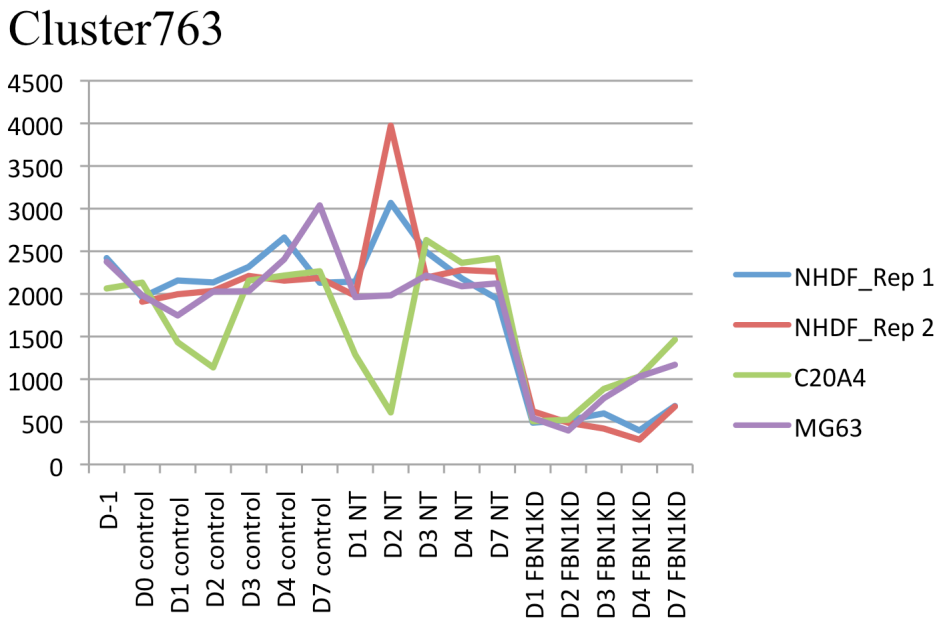

Figure 5.9. Plots of average expression profiles of genes in Cluster763 following analysis using BioLayout *Express* ^{3D} (See *Figure 5.8)*. Y axis shows the normalised intensity value. X axis shows the samples from which the RNA was extracted. Characteristics of the cluster were determined using the class viewer tool in BioLayout *Express* ^{3D} and plots were created in Microsoft Excel. Cluster763 contained only the *FBN1* gene probes.

Sample	C20A4	MG63	NHDF
Day 1 NT &FBN1KD	2.54	3.6	3.70
Day 2 NT &FBN1KD	1.16	4.98	6.97
Day 3 NT &FBN1KD	2.97	2.85	4.59
Day 4 NT &FBN1KD	2.29	2.02	6.47
Day 7 NT &FBN1KD	1.65	1.81	3.08

Table 5.3. The calculated fold change (Section 5.2.5) of the expression values obtained from the U219 microarray data. Fold change over 1.5 was considered a differential change in gene expression.

In total, Cluster002 consisted of 1593 nodes (888 unique genes) and 194,428 edges, and showed similar expression patterns across the timecourses in all three systems, with the highest expression in NHDF ***(Figure 5.10)***. Cluster002 contained multiple ECM related

genes as well as mesenchyme specific markers. Many ECM cellular component GO terms were associated with Cluster 002 ***(Table 5.4)***.

GO terms	Gene count	% of Cluster	P value
Cellular component			
Extracellular region	136	15.3%	6.4E-6
Extracellular region part	91	10.2%	1.4E-10
Extracellular space	53	6%	4.04E-4
Extracellular matrix	48	5.4%	3.9E-11

Table 5.4. A selection GO terms associated with genes in Cluster002. 86.4% of Cluster002 genes were included in the analysis.

The cluster contained genes that previously co-expressed with *FBN1* in the static samples (**Chapter 3 and Chapter 4**) including *CAV1* (caveolin 1), *CAV2* (caveolin 2), *LOX* (lysyl oxidase) and *MYOF* (myoferlin), though these genes remained unchanged in the *FBN1* knockdowns. In addition, Cluster002 had several mesenchyme specific genes (ECM related terms) such as *COL1A1* (collagen type 1 alpha), *DCN* (decorin), three fibulin genes *FBLN1, FBLN2, FBLN5, LTBP2, TGFBR3* and *TGFBR2.*

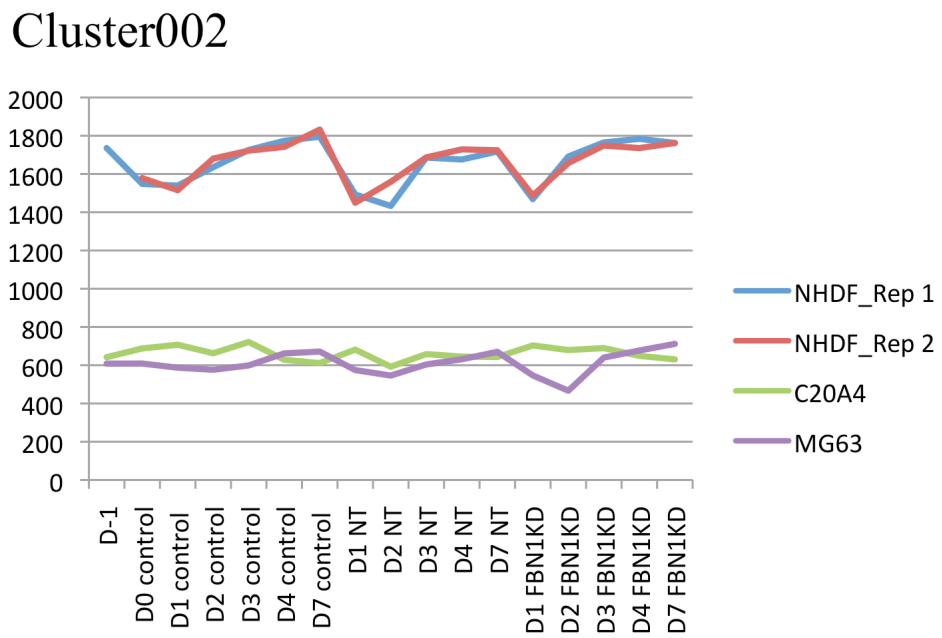

Figure 5.10. Plots of average expression profiles of genes in Cluster002 following analysis using BioLayout *Express* ^{3D} (See *Figure 5.8)*. Y axis shows the normalised intensity value. X axis shows the samples from which the RNA was extracted. Characteristics of the cluster were determined using the class viewer tool in BioLayout *Express* ^{3D} and plots were created in Microsoft Excel. Cluster002 contained 888 genes.

There was no clear effect of *FBN1* knockdown based on the average expression patterns of Cluster002 ***(Figure 5.10)***. However, after observing individual probe expression patterns in Cluster002, 19 genes showed upregulation in the FBN1KD NHDF cultures, although there were no obvious expression changes in the C20A4 or MG63 timecourse experiments ***(Figure 5.11)(Figure 5.12)(Table 5.5)***. The genes with this expression pattern were localised throughout the cluster ***(Figure 5.11)***. The upregulated genes from Cluster002 will be referred to as subcluster002 for the remainder of the thesis.

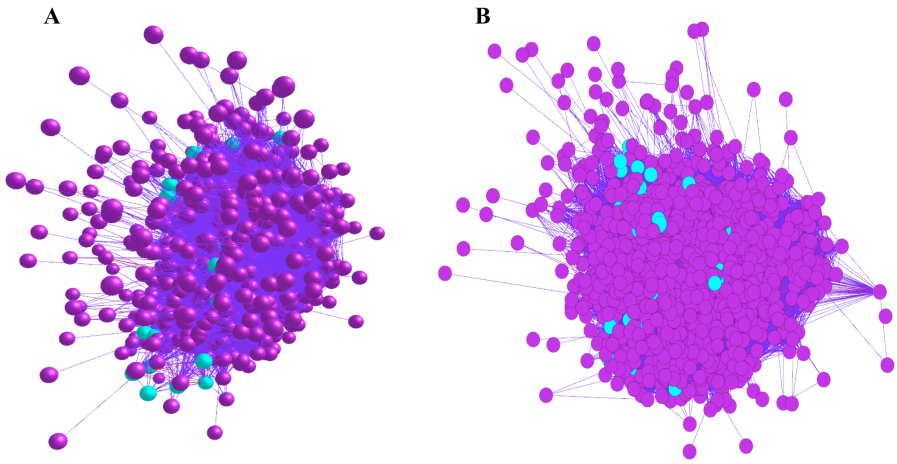

Figure 5.11. A zoomed in view of cluster002 (see *Figure 5.8*). (A) Three dimensional image, (B) Two-dimensional image. Purple nodes display expression patterns consistent with the average pattern seen in *Figure 5.10*, and the blue nodes show subcluster002. The expression pattern of subcluster002 is shown in *Figure 5.12*.

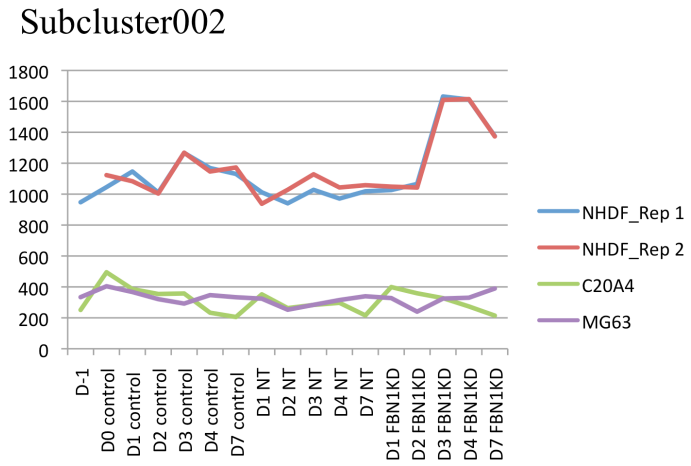

Figure 5.12. Plots of average expression profiles of genes in subcluster002 (See *Figure 5.11)*. Y axis shows the normalised intensity value. X axis shows the samples from which the RNA was extracted. Characteristics of the cluster were determined using the class viewer tool in BioLayout *Express* [3D] and plots were created in Microsoft Excel. Subcluster002 contained 19 genes.

Gene	Gene Name	Function/Disease Association
ACTA2	Actin, alpha-2, smooth muscle, aorta	OMIM:102620
ACTG2	Actin, gamma-2, smooth muscle, enteric	OMIM:102545
ACTR1B	Actin related protein, 1B	OMIM:605144
ADAM23	A disintegrin and metalloproteinase domain 23	OMIM:603710
AGTR1	Angiotensin receptor 1	OMIM:106165
ANGPT1	Angiopoietin 1	OMIM:601667
CAPN2	Calpain	OMIM:114230
CCDC81	coiled-coil domain containing 81	Strausberg *et al.,* 2002
CLND22	Claudin 22	Heiskala *et al.,* 2001
CNN1	Calponin 1	OMIM:600806
FLT	FMA-related tyrosine kinase	OMIM:165070
GNA14	Guanine nucleotide binding protein, alpha 14	OMIM:604397
GNAI1	Guanine nucleotide binding protein, alpha inhibiting activity polypeptide 1	OMIM:139310
IGF2	Insulin like growth factor-2	OMIM:147470
MAMDC2	Mam domain- containing 2	OMIM:612879
NEXN	Nexilin	OMIM: 613121
OPN3	Opsin,3	OMIM: 606695
PARVA	Parvin alpha	OMIM: 608120
STMN2	Stathmin- like 2	OMIM: 600621

Table 5.5. Genes showing upregulated expression in Cluster002, forming subcluster002.

Subcluster002 showed an increase of expression at Day 3 (average fold change:1.5) , Day 4 (average fold change 1.6) and Day 7 (average fold change: 1.32) in NHDF cells, though these genes were unaltered in C20A4 and MG63 cell lines ***(Figure 5.12)***. Fold change over 1.5 was considered to have a differential change in gene expression when the NT and FBN1KD samples were analysed. The sub-cluster (summarized in ***Table 5.5***) contained three different actin-related genes, *ACTG2* (enteric smooth muscle actin), *ACTR1B* (actin related protein 1B) and *ACTA2* (aortic smooth muscle actin). *ACTA2* had been previously shown to be co-expressed with fibrillin-1 in mouse cells (Summers et al., 2009) **(Chapter 4)**. qPCR analysis of *ACTA2* across the NHDF timecourse experiment

showed upregulated expression of *ACTA2* at Day 4 and Day7 ($p \leq 0.1$) when compared to the NT controls ***(Figure 5.13)***, and there appeared to be increased intensity of actin fibre staining at Day 4 ***(Figure 5.7)*** thus further validating the microarray results ***(Figure 5.12)***.

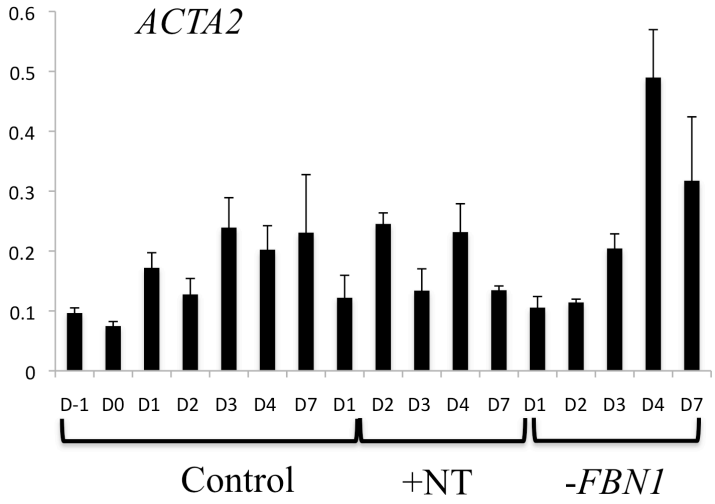

Figure 5.13. qPCR results for *ACTA2* across NHDF time course. The y-axis represents the expression values calculated by advanced relative quantification, target/reference ratio (LightCycler480 Roche). The reference was human *GAPDH*. Technical replicates=3

In addition to *ACTA2*, other genes implicated in cardiovascular function were upregulated at Day 4 and Day 7 of the fibrillin-1 knockdowns in the fibroblasts ***(Figure 5.12)(Table 5.5)***. These genes included *AGTR1* (angiotensin receptor 1), *NEXN* (nexilin), and *MAMDC22* (Mam domain-containing 22). The upregulated genes within subcluster002 also contained *PARVA* (parvin alpha) and *CNN1* (calponin 1), which encode smooth muscle maintenance proteins and several genes with neurological functions were in this group, including *STMN2* (stathmin-like 2) and *OPN3* (opsin 3). Furthermore, *IGF2* (insulin like growth factor 2), as well as metabolic control genes *GNA14* and *GNAI1* (encoding guanine nucleotide binding protein alpha subunit and guanaine nucleotide binding protein alpha subunit inhibiting, respectively) and *CLND22* (claudin 22) were in the subcluster. The genes are summarized in ***Table 5.5***.

5.3.4 Gene expression in the NHDF *FBN1* knockdown timecourse.

There were little to no differences detected in the chondrocyte or osteosarcoma cell lines following the reduction of *FBN1* using siRNA, but changes were detected in the NHDF (fibroblasts) cells ***(Figure 5.12)***. Therefore, a detailed BioLayout *Express* ^{3D} analysis was performed on the results of the NHDF timecourse alone. The NHDF samples were clustered at a r≥ 0.85 and at an MCL inflation value of 3.0. This is a more stringent analysis with greater granularity in the clusters. The analysis consisted of 11,790 nodes and 411,151 edges producing 2,709 clusters ***(Figure 5.14)***. The clustering analysis revealed two clusters containing genes with altered expression following reduction in *FBN1* mRNA ***(Figure 5.14)***.

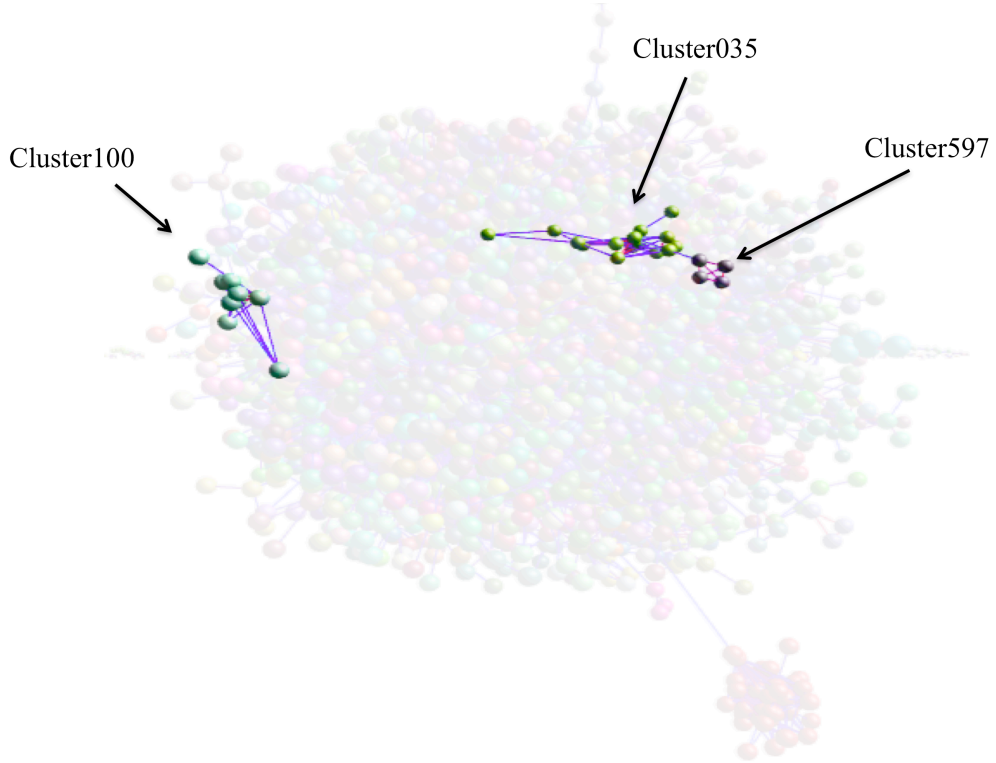

Figure 5.14. Network visualisation and clustering of the NHDF transcriptome. The image depicts the network diagram produced by BioLayout *Express* ^{3D} using data from the Affymetrix U219 gene expression microarray platform on knockdown experiments across Day -1, Day 0, Day 1, Day 2, Day 3, Day 4 and Day 7. Spheres (nodes) represent individual probesets and the lines between them (edges) show correlations in expression pattern of r ≥ 0.85. The nodes were clustered using an MCL inflation value 3.0 (Chapter 2, Section 2.3.6). The background of the image displays the whole network and clusters discussed in the text are highlighted. Cluster597 contained *FBN1* probes and the remaining clusters are discussed in detail in Section 5.3.4.

Cluster597 contained only fibrillin-1 probes which were reduced in expression (***Figure 5.9)***. ***Figure 5.15*** shows these results for NHDF alone.

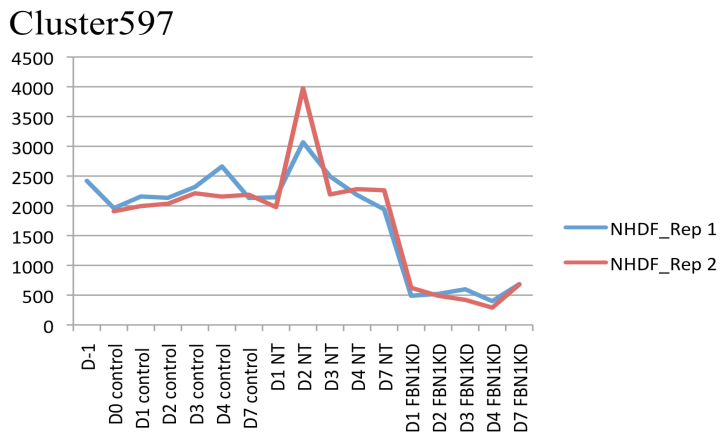

Figure 5.15. Plot of average expression profiles of *FBN1* probes (Cluster597) following analysis of NHDF time course results using BioLayout *Express* [3D] (See *Figure 5.14)*. Y axis shows the normalised intensity value. X axis shows the samples from which the RNA was extracted. Characteristics of the cluster were determined using the class viewer tool in BioLayout *Express*[3D] and plots were created in Microsoft Excel.

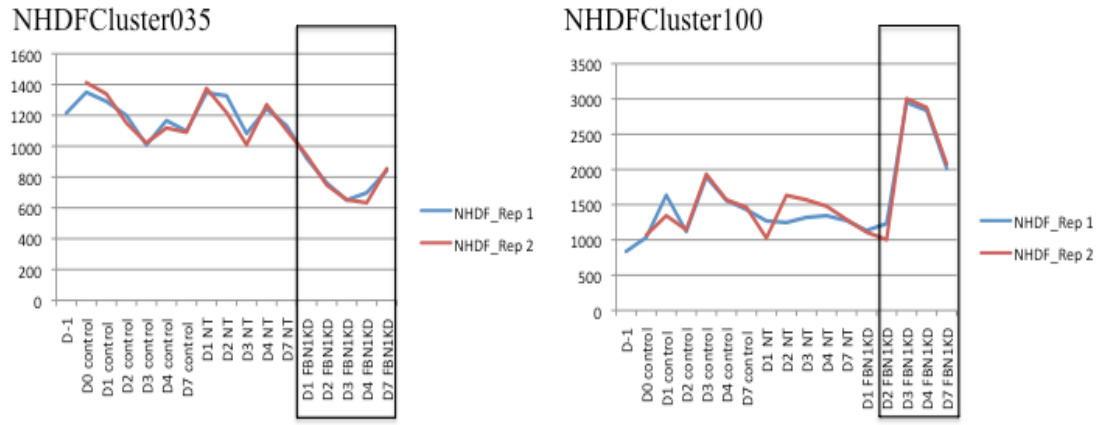

Figure 5.16. Plots of average expression profiles of genes in NHDFCluster035 and NHDFCluster100 following analysis using BioLayout *Express* [3D] (See *Figure 5.14)*. Y axis shows the normalised intensity value. X axis shows the samples from which the RNA was extracted. Characteristics of the cluster were determined using the class viewer tool in BioLayout *Express* [3D] and plots were created in Microsoft Excel. The genes within both clusters are shown in *Table 5.7* and fold change is shown in *Table 5.6*.

NHDFCluster035 was located very close to NHDFCluster597, the cluster containing probes for *FBN1* in the network layout ***(Figure 5.14)***. This cluster contained a total of 9 genes ***(Table 5.7)*** that were downregulated 24 hours after *FBN1* mRNA expression decreased ***(Figure 5.16)(Table 5.6)***. The genes included scaffolding gene *GIPC1* (OMIM: 605772), involved in actin binding. NHDFCluster035 showed a gradual decrease in gene expression from Day 1 and Day 2, with increasing expression following Day 3 ***(Figure 5.16)(Table 5.6)***.

Sample	NHDFCluster035 (downregulated)	NHDFCluster100 (upregulated)
Day 1	-1.46	0.97
Day 2	-1.68	1.29
Day 3	-1.6	2.06
Day 4	-1.88	2.02
Day 7	-1.31	1.59

Table 5.6. Fold Change in NHDFCluster035 and NHDFCluster100. See *Figure 5.16* . A fold change of >1.5 (upregulated) or <-1.5 (downregulated) was considered to show differential gene expression.

NHDFCluster 100 had a very similar expression pattern to the previously identified subcluster002 of Cluster002 from the overall analysis ***(Figure 5.12)(Figure 5.16)***, and included six genes, three of which were included in subcluster002, actin genes *ACTA2* and *ACTG2* as well as *CNN1* encoding basic smooth muscle calponin 1 ***(Table 5.5)(Table 5.7)***. The other three genes in NHDFCluster100 of this stringent analysis were *GALNT18* (OMIM: 615316)*, IMPA2* (OMIM: 605922) and *ITGA1* (OMIM: 192968). The overall expression of the genes within the cluster showed upregulation of expression at Day 3, Day 4 and Day 7 within NHDF FBN1KD samples ***(Table 5.6)(Figure 5.16)***.

Gene Symbol	Gene Name	Disease Association/Reference
NHDFCluster035		
DERL1	DER1-Like Domain Family, Member 1	OMIM: 608813 (Chen *et al.,* 2013)
EIF5A2	Eukaryotic Translation Initiation Factor 5a2	OMIM: 605782
GIPC1	GIPC PDZ Domain-Containing Family, Member 1	OMIM: 605072
GMFB	Glia Maturation Factor, Beta	OMIM:601713
HIATL1	SLC Gene	(Sreedharan *et al.,* 2010)
MRPS21	Mitochondrial Ribosomal Protein S21	OMIM: 611984 (McGivney *et al.,* 2010)
REEP5	Receptor Expression-Enhancing Protein 5	OMIM: 125265
SDHAF2	Succinate Dehydrogenase Complex Assembly Factor 2	OMIM: 613019
UBL3	Ubiquitin-Like 3	OMIM: 604711 (Huang *et al.,* 2012)
NHDFCluster100		
ACAT2	See ***Table 5.5***	
ACTG2	See ***Table 5.5***	
CNN1	See ***Table 5.5***	
GALNT18	UDP-N-Acetyl-Alpha-D-Galactosamine:Polypeptide N-Acetylgalactosaminyltransferase 18	OMIM: 615136 (Li *et al.,* 2011)
IMPA2	Myo-Inositol Monophosphatase 2	OMIM: 605922
ITGA1	Integrin, Alpha-1	OMIM: 192968 (Zemmyo *et al.,* 2003, Ekholm *et al.,* 2002) (Maher, 1970)

Table 5.7. A list of all the genes in NHDFCluster035 and NHDFCluster100 with altered expression following *FBN1* mRNA KD in NHDF cells *(See Figure 5.16)*

5.4 Discussion

5.4.1 Limitations of siRNA approach

Using siRNA tools to reduce the level of a specific mRNA has become common in studies of gene function. Reduction in the level of mRNA can have three outcomes: there may be no change in other genes (suggesting that the target gene is an end point of regulation rather than a regulator of those genes), expression of other genes may go up (indicating that there is a negative feedback loop between the target and the genes) or expression of other genes may go down (consistent with a positive feedback loop). When *FBN1* was knocked down, all three outcomes were seen.

One limitation of the approach is that the reduction in mRNA is transient so it is not possible to analyze the impact of a sustained depletion of the target protein. The lack of response of the osteosarcoma and chondrocyte lines may be due to their ability to degrade the siRNA construct quickly and therefore prevent the full impact of the transient knockdown. Secondly, the process involves use of cell transfection which can cause cell death and/effect proliferation. Lipofectamine2000, used in this study, can reduce cell proliferation (Dr Mark Barnet, Roslin Institute, University of Edinburgh, personal communication) and hence some effects seen may be due to removal of cells from the cell cycle and then their return during the recovery period. The differences in actin staining between the normal control and both transfected cultures (with the non-targeting construct or the *FBN1* siRNA) could be attributed to differences in the number of cells that were cycling over the time course. Thirdly, there may be off target effects, where the siRNA molecules bind to related mRNAs as well as the target. Given the sequence conservation between the human fibrillin genes **(**discussed further in **Chapter 7)** this could have been a problem with the present study. However, there was no apparent effect on *FBN2* mRNA **(Section 5.3.1)**, and it is considered unlikely that this gene was impacted by the treatment.

Taking into account these limitations, it was clear that knock down of *FBN1* mRNA resulted in upregulation and downregulation of a limited number of genes. These groups of genes are discussed below.

5.4.2 Actin and actin related genes were upregulated following depletion of *FBN1* mRNA levels

There were many cytoskeleton actin filament synthesis and processing genes found to be upregulated after *FBN1* mRNA levels were reduced in fibroblast cell line, NHDF ***(Table 5.5)(Table 5.7)(Figure 5.13)(Figure 5.16)***. The genes identified have specific functions in sustaining a healthy cytoskeleton in connective tissue, thereby maintaining cellular homeostasis. As previously described in **Chapter 1**, the ECM interacts with integrin proteins within the plasma membrane, which connect with intercellular actin fibres and hence the cytoskeleton **(Chapter 1, Section 1.2, *Figure 1.3*)**.

ACTA2 mutation is a cause of thoracic aortic aneurysms and aortic dissections **(Chapter 4)** (Guo *et al.,* 2007). Interestingly, microarray and qPCR analysis showed upregulation of *ACTA2* following the knockdown of fibrillin-1 in the fibroblast (NHDF) cell system, though not in chondrocyte (C20A4) or osteoblast (MG63) cell types ***(Figure 5.12)***. According to human microarray data available on http://biogps.org, *ACTA2* was highly expressed in cell and tissue types of mesenchyme origin including cardiac and skin types, while mouse microarray data (available at the same site) showed that *Acta2* is also strongly expressed in osteoblast cells. Previous BioLayout *Express* ^{3D} analysis of single time point samples placed *ACTA2* in Cluster004 with high levels of expression in the NHDF cells **(Chapter 4, Section 4.5.1, *Figure 4.6*)**. *ACTA2* was the only gene from static sample Cluster004 to show increased expression when fibrillin-1 expression was decreased, contrary to its parallel expression pattern with *Fbn1* in mouse cell lines (Summers *et al.,* 2009). *ACTA2* is upregulated in primary rat liver stellate cells following hepatic injury, demonstrating a potential role in wound healing (Rockey *et al.,* 2013). It is possible that one signal of wounding is the disruption of the normal fibrillin-1 ECM microfibrils, leading to perturbation of the intracellular *ACTA2* cytoskeleton. This action may trigger the production of smooth muscle actin via *ACTA2* upregulation, and the knockdown of *FBN1* in NHDF cells may mimic this effect.

Additional actin-related genes, *ACTG2* and *ACTR1B,* were upregulated following the knockdown of fibrillin-1 ***(Figure 5.12)(Table 5.5)(Table 5.7)***. *ACTG2* is an isoform of actin that is primarily expressed in tissue of both adult and foetal gastrointestinal tract, and has very low expression in skin (http://.biogps.org)(Szucsik and Lessard, 1995).

ACTG2 mutations have been associated with familial visceral myopathy, a disorder involving the inability of the intestines to contract normally leading to severe obstructions (Lehtonen *et al.,* 2012, Thorson *et al.,* 2013)(MIM: 155310). This is consistent with abnormalities of the muscle cells of the intestine, a cell type which expresses *FBN1*, again highlighting links between the intracellular cytoskeleton and the extracellular milieu. *ACTR1B* is an actin related protein that is expressed in a variety of cell types including mesenchyme derived and neurological tissues and had low expression in eye tissue (http://biogps.org).

In the results presented in this chapter, the knockdown of fibrillin-1 in NHDF led to some disorganisation of actin filaments at Day 4, though this appeared to be repaired by Day 7 ***(Figure 5.7)***. This decrease in organisation could have instigated the upregulation of *ACTA2*, *ACTG2* and *ACTR1B* mRNA levels by Day 3 ***(Section 5.3.3)(Table 5.6)***. Therefore, a decrease in fibrillin-1 mRNA and protein in fibroblasts may stimulate a wound repair response, leading to an increase in *ACTA2*, *ACTG2* and *ACTR1B* ***(Figure 5.17)***.

NEXN was also found to be upregulated following the knockdown of fibrillin-1 ***(Table 5.5)(Figure 5.17)***. The gene encodes nexilin, a Z-disk protein (Ohtsuka *et al.,* 1998). Z-disk proteins are linear, dense fibres that bind repeated sections of sarcomeres in myofibrils (Luther, 2009), ultimately forming muscle tissue. Nexilin was associated with F-actin filaments in heart and skeletal muscle (Lee *et al.,* 2013). HeLa cells stably transfected with the *NEXN* gene showed an increase of cellular migration and adhesion (Wang *et al.,* 2005). Inactivation of *NEXN* in zebrafish led to heart failure (Hassel *et al.,* 2009)(MIM: 613122) and studies involving 121 patients diagnosed with hypertrophic cardiomyopathy (MIM: 192600) identified several novel *NEXN* mutations (Wang *et al.,* 2010). Muscle F-actin binding protein, *PARVA* (alpha parvin), which mediates cellular adherence (Olski *et al.,* 2001), also showed upregulation in the fibrillin-1 knockdown samples of NHDF ***(Table 5.5)(Figure 5.17)***. *PARVA* is a highly conserved gene across vertebrates. Based on northern blot analysis in mouse tissue, it is highly expressed in kidney, heart, liver and skeletal muscle and co-localised with actin in strong bundle formations of mouse fibroblasts (Tanaka *et al.,* 1975). Calponin 1 (encoded by the *CNN1* gene) is a smooth muscle protein thought to have a role in the regulation of smooth

muscle contractions (Winder and Walsh, 1990) and has been shown to bind and induce conformational changes in F-actin (Noda *et al.,* 1992). It was found in Cluster002 of the initial analysis and in Cluster100 of the more stringent analysis of NHDF only ***(Table 5.7)(Figure 5.16)(Figure 5.17)***. While mice with the gene inactivated do not show any direct smooth muscle phenotypes, there was a significant decrease of actin in the bladder and vas deferens (Matthew *et al.,* 2000). The upregulation of these actin supporting genes could be attributed to the increase in actin mRNA (*ACTA2* and *ACTG2),* therefore an indirect response to *FBN1* depletion ***(Figure 5.17)***.

This cluster also revealed upregulated expression of *ITGA1* at Day 3, Day 4 and Day 7 ***(Figure 5.16)(Figure 5.17)(Table 5.7)***. ITGA1 (integrin alpha 1)(OMIM: 192968) is an integrin that binds to ITGB1 (integrin beta 1) to form a heterodimer that interacts with laminin and/or collagen allowing for communication of the ECM with cytoskeletal actin. Therefore the increase of actin protein resulting from the increase in actin related mRNAs could have upregulated the expression of integrin binding receptors, like *ITGA1* ***(Figure 5.17)***.

GIPC1 (OMIM: 605072) is an ECM scaffolding protein that has been implicated in actin filament binding in embryogenesis through growth factor signalling (through integrin binding sites) and cell adhesion (Katoh *et al.*, 2002). *GIPC1* is thought to have direct interactions with a range of *FBN1* binding integrins such as *ITGA6* and *ITGA5* (Tani and Mercurio, 2001). This gene was found to be downregulated along with *FBN1* in NHDF *FBN1*KD samples ***(Table 5.7)(Figure 5.16)(Figure 5.17)***.

Figure 5.17 summarises the proposed interactions of the actin related genes and fibrillin-1 through a schematic of protein activity. The model shows a normal fibrillin-1 ECM and cytoskeleton in response to reduced *FBN1* mRNA. *GIPC1* levels decrease at Day 2 (24 hours after depletion of *FBN1*) while the integrins and actin related genes are upregulated at Day 3, outlined in ***Figure 5.17.***

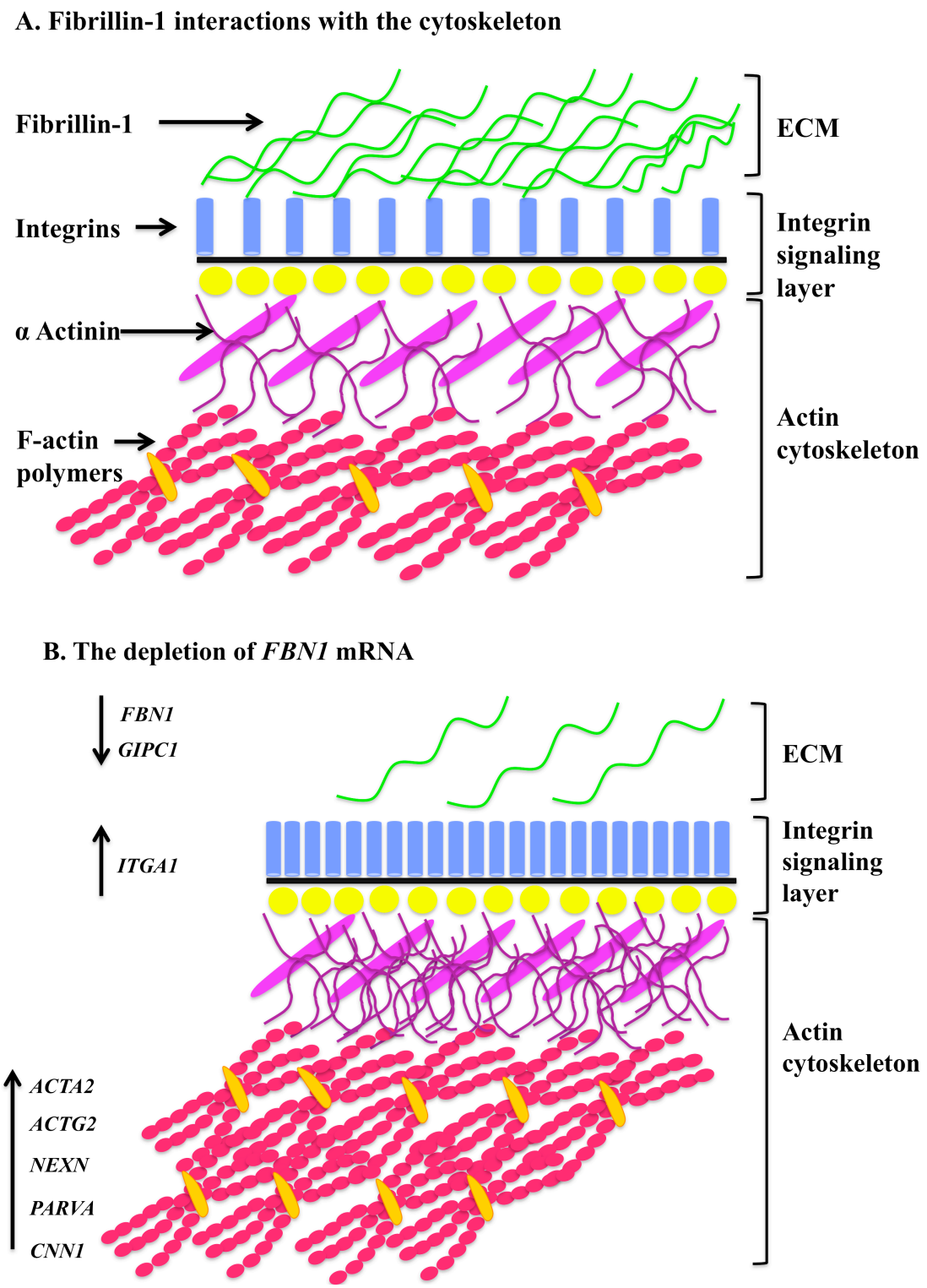

Figure 5.17. The effect of *FBN1* mRNA depletion in NHDF cells, an actin model. (A) This figure shows the cytoskeleton and ECM with normal fibrillin-1 protein levels. (B) The proposed model of interactions of cytoskeleton and ECM related proteins following *FBN1* mRNA and consequently protein depletion. The individual genes are discussed in Section 5.4.1.

5.4.3 Other genes that co-express with fibrillin-1

There were several growth factors that were upregulated in the FBN1 knockdown NHDF cells. One example was insulin-like growth factor-2 (*IGF2* gene)***(Figure 5.12)(Table 5.5)***. IGF2 is an insulin family member involved in cell proliferation and maintaining growth hormone action and functional in prenatal development (OMIM: 147470). Although *IGF2* has not been implicated in any experimental interactions with the fibrillin family, it was expressed at high level in mouse mesenchymal cells in a previous analysis, and clustered with *Fbn1* and *Fbn2* (Summers *et al.,* 2009). Furthermore, *IGF2* has been used to initiate osteogenic differentiation in human parthenogenetic ESCs (Kang *et al.,* 2011). The upregulation of *IGF2* following the depletion of *FBN1* mRNA suggests that it would be interesting to examine the relationship between fibrillins and IGF2 further, particularly in light of the bone overgrowth in Marfan syndrome.

ATGR1 (angiotensin receptor 1),was upregulated in NHDF cells with reduced *FBN1* ***(Figure 5.12)(Table 5.5)(Section 5.3.2)***. The pharmaceutical Losartan, an angiotensin receptor 1 antagonist, is effective in preventing aortic aneurysm and dissection in fibrillin-1 mutant mouse models. Losartan inhibits the binding of angiotensinII (ANGII) to ATGR1(Matt and Eckstein, 2012, Chiu *et al.,* 2013, Groenink *et al.,* 2013) **(Chapter 1, Section 1.3.4).** Habashi *et al.,* (2006) showed that Losartan reduced aortic wall thickening in $Fbn1^{C1039G/+}$ mice. These are phenotypically similar to human MFS patients and $Fbn1^{C1039G/+}$ mice present with a dilated aortic root developing as early as 2 weeks of age, that becomes more pronounced over time (Habashi *et al.,* 2006). Histology of the mice at 14 weeks further indicated abnormal thickening of the aortic root in $Fbn1^{C1039G/+}$ mice and increased fragmentation of elastic fibres, when compared to normal mice. They also noted an increase in collagen fibre formation and SMAD2 level within the nucleus (Loeys *et al.,* 2005) suggesting an increase in TGFB activity (Rossi *et al.,* 1988, Schlumberger *et al.,* 1991)(***Figure 5.18***). Losartan treated mice showed a significant decrease in elastic fibre fragmentation, a decrease in SMAD2 signalling and repair of the aortic root, correcting defects to comparable levels with the normal mice. The depletion of *FBN1* mRNA and fibrillin-1 microfibrils in the fibroblasts could have induced upregulation of *ATGR1* due to the possible increase in free TGF*β*. This would require further functional protein analysis for validation.

Stathin-like 2 (*STMN2)* is a neuronal specific protein involved in neurogenesis (OMIM: 600621). *STMN2* is highly expressed in foetal brain, with slight expression in adipocytes. Opsin 3 (*OPN3)* is a G-protein- coupled retinoid receptor. In mice, northern blot studies showed that *Opn3* expression was high in the cerebellum, frontal cortex and testes of adults. *In situ* hybridisation experiments on embryonic and foetal mice showed high expression in the spinal cord, pachytene spermatids, retina and pineal photosensitive regions (Blackshaw and Snyder, 1999). The rational for increased expression of neural genes following a decrease in fibrillin-1 is not obvious, though the KD of *FBN1* mRNA and actin reorganisation could take the fibroblasts back to a less differentiated neuronal state (Neuhuber *et al.,* 2004).

There were five additional genes that were upregulated following fibrillin-1 knockdown in NHDF cells: *CCDC81, CLND22, GNA14, GNAI1 and MAMDC2* whose precise functions are relatively uncharacterised. ***(Figure 5.13)(Table 5.5)*** GNA14 is a guanine nucleotide binding protein and GNA1I appears to inhibit polypeptide-binding activity in guanine nucleotide binding proteins (OMIM: 604397)(OMIM: 139310). Claudin 22 (*CLND22)* was described as a transmembrane protein involved in maintaining tight junction interactions across the membranes in paracellular transport (Bloom *et al.,* 1976). *MAMDC2* was mapped during a search for genes involved in Kabuki syndrome (MIM: 147920), though no disease association has been determined (Contento, 1991).

Genes in NHDFCluster035 from the more stringent BioLayout *Express* ^{3D} analysis showed a sharp decline in expression 24 hours after *FBN1* mRNA levels had been manipulated ***(Table 5.6)(Figure 5.16)***. This cluster contained several relatively undefined genes including *DERL1, HIATL1, MRPS21, REEP5, SDHAF2* and *UBL3* ***(Table 5.7)***. However, there were three genes, *EIF5A2, GIPC1* and *GMFB* that are regulated by, or regulate, TGF*ß* activity ***(Table 5.7)***. *EIF5A2* is a translation initiating factor (OMIM: 605782) that has recently been implicated in indirectly activating TGFß activity through interactions with *STAT3* (signal transducer and activator of transcription factor 3), in bladder cancer (Wei *et al.,* 2014). *GIPC1* (discussed in **Section 5.3.4)** is proposed to interact with endoglin (type 1 membrane glycoprotein) enhancing TGFß1 and thereby increasing phosphorylation of the SMAD pathway ***(Figure 5.18)*** in endothelial cells (Lee *et al.,* 2008*)*. In addition, *GMFB* was shown to be not only an inhibitor of the signal

transduction ERK pathway (extracellular signal-regulated kinases)(Zaheer and Lim, 1996), but also an enhancer of cell cycle pathway p38/MAPK (Lim and Zaheer, 1996). Both the pathways non-canonical (non-SMAD inducing) TGF*ß* pathways (reviewed in (Zhang, 2009). Since *FBN1, EIF5A2, GIPC1* and *GMFB* all have proposed functions in regulating TGF*ß*, it can be proposed that the more undefined genes within the cluster may also have a role in TGF*ß* activity.

This discussion has focused on the response to *FBN1* depletion in human neonatal fibroblast cells, NHDF. However, the FBN1KD transfections in the chondrocyte and osteosarcoma cell lines did not have any changes in gene expression other than *FBN1* ***(Figure 5.9)*** This could mean that *FBN1* mRNA was insufficiently reduced in the MG63 and C20A4 cell lines. While *FBN1* mRNA knock down appeared equivalent to the NHDF cells in MG63 at Day 1, and more depleted in C20A4, both MG63 and C20A4 cells showed recovery of *FBN1* mRNA levels within the seven-day time course, while the NHDF cells showed little increase in *FBN1* mRNA ***(Table 5.3)(Figure 5.9)***. In addition, only a single replicate was used for these cells, which limited the power of the study. Therefore, the experiment would need to be repeated with at least two replicates. Potentially genome editing (with the CRISPR-Cas9 or TALEN systems (reviewed in (Wei *et al.,* 2013, Gaj *et al.,* 2013)) could be used to create a stable knock out of the *FBN1* gene, resulting in sustained loss of *FBN1* mRNA, in these cells. Another explanation for the variation in *FBN1* siRNA effect could be related to the immortal nature of these cell lines. MG63 is a cancer line and C20A4 was created by adenovirus treatment of primary chondrocytes. This means they are culture-adapted and may have altered requirements for cellular homeostasis that do not need the full repertoire of gene expression that is seen in the parent tissues. Therefore, the initial results obtained from the work outlined above would need to be repeated on primary chondro and osteo tissue/cell types for validation.

5.5 Conclusions

In conclusion, through siRNA manipulation of *FBN1* mRNA in NHDF cells, this study was able to determine a set of genes that were affected by *FBN1* depletion. These results led to a model for fibrillin-1 interaction with the cytoskeleton in wound healing. Furthermore, due to the lack of change seen in *FBN2* ***(Figure 5.4)(Section 5.3.3)*** and *FBN3* (***Section 5.2.5***) following the reduction of *FBN1* mRNA, it appears that there is no compensatory mechanism to upregulate an alternative fibrillin gene in the absence of fibrillin-1. This further supports the notion that there is a clear developmental and functional distinction between the members of the fibrillin gene family, and that they are regulated independently. Therefore, a study of the promoters of the three fibrillin genes was undertaken to assess key factors involved in this differential regulation ***(Chapter 6)***.

Chapter 6. Identification and expression of promoters of the fibrillin gene family

6.1 Promoter identification and regulation

Previous chapters **(Chapter 3-5)** have shown that the fibrillin gene family is differentially expressed. Expression is driven by gene transcription and transcriptional regulation. Transcription of genes is controlled by proximal and distal DNA sequences as well as trans-acting protein factors (transcription factors; TF). The core promoter consists of the region where the RNA polymerase enzyme and core TFs bind, which lies immediately upstream of the transcript start site (TSS). Beyond this region there can be additional TF binding motifs which modulate transcription and more remote up- and downstream elements that act as enhancers or silencers of transcription. The same gene in different cell types within the body can be under different regulation, depending on the TFs that are present in a specific cell type. Most genes have more than one TSS, with different regulatory elements and activity (Lenhard *et al.,* 2012). This chapter will present bioinformatics data to investigate TSS regions and TF networks of the fibrillin gene family.

Recently, advances in genomics and transcriptome biology have lead to the creation of worldwide consortia using various techniques to uncover the regulatory factors of the human genome. For example, widescale transcriptome studies including FANTOM (Functional Annotation of Mammals) and ENCODE (Encyclopedia for DNA elements) have established DNA elements that regulate gene expression. ENCODE is a world wide consortium sponsored by the US National Human Genome Research Institute, that used many high throughput sequence analysis methods (including promoter assays and computational TFBS prediction methods (RFBR (Yale ChIP-chip Regulatory Factor Binding Regions Analysis (Zhang *et al.,* 2007)), to predict TSS across the human genome (Birney *et al.,* 2007, Birney *et al.,* 2012, de Souza, 2013). However, this chapter will investigate the data generated through the FANTOM projects.

Recent projects by the FANTOM consortium **(Chapter 1, Section 1.4.3)** have delineated the structure and regulation of mammalian promoters (Hayashizaki and Carninci, 2006,

Ravasi *et al.,* 2010, Suzuki *et al.,* 2009, Carninci *et al.,* 2005). The FANTOM5 project utilized deepCAGE technology (a form of genome-wide 5'RACE) to identify multiple promoters (Forrest *et al.,* 2014). Furthermore, using deepCAGE they created a human cell-type specific transcriptome consisting of 975 samples (573 primary cell types, 152 tissues, 250 cell lines) that provided detailed promoter specific expression patterns, as well as determining promoter structure (Forrest *et al.,* 2014). CAGE traps the 5'end of mRNA via the modified guanine cap, followed by sequencing the first 20-27nt. These 20-27nt CAGE tags are then mapped back to the whole genome sequence and identify the TSS of the gene (Forrest *et al.,* 2014).

Past FANTOM collaborations have shown that for the majority of genes, transcription was initiated across a broad DNA sequence rather than on a single nucleotide. TSS tend to be found in CpG islands and the majority are not associated withi a TATA box. Genes can have a number of TSS clusters, associated with different promoters, which can show differential expression across tissues or cell states (promoter switching) (Carninci *et al.,* 2005). The FANTOM4 project highlighted promoter switching and TF variation in the activation of a monocyte cell line (THP1)**(Chapter 2, Section 2.1.5)**(Suzuki *et al.,* 2009). THP1 cells were differentiated to macrophages using PMA (phorbol myristate acetate), and samples were collected at 0, 1, 4, 12, 24 and 96 hours. CAGE analysis using 454 sequencing demonstrated time-dependent promoter switching and distinguishable promoter expression profiles as well as TF networks associated with specific time points and TSS regions.

The current FANTOM5 project aims to look at gene expression both in single time points across many cell and tissue types and in a number of dynamic time courses of activation and differentiation (Forrest *et al.,* 2014).

6.1.1 Promoter identification and expression

The FANTOM consortium mapped CAGE tags across the whole genome using single-molecule sequencing (Kanamori-Katayama *et al.,* 2011). DPI (decomposition- based peak identification) was used to identify a set of transcription start sites (TSS), at permissive and robust levels (containing at least one nucleotide position with > 2 or > 10

independent single molecule observations respectively in a single library) (Forrest *et al.,* 2014). Expression levels were normalised using relative log expression (RLE) in edgeR (Robinson *et al.,* 2009, Sillar and Plint, 1989). The counts of the CAGE tags that mapped to each promoter region (Schug *et al.,* 2005), referred to as normalised tags per million (TPM), reflected the expression level of the gene/promoter. Promoters were then numbered by expression rank at the permissive level (Forrest *et al.,* 2014). At the more stringent robust level some of these promoters were lost and this accounts for gaps in the numbering of robust promoters. The full permissive set can be seen on the ZENBU browser (http://fantom.gsc.riken.jp/zenbu/) (Severin *et al.,* 2014). Composite promoters are those where two or more robust peaks occur within 100 bp of each other (Forrest *et al.,* 2014).

Figure 6.1 illustrates the format of the data available from FANTOM5, using as an example the gene profile of *ACTA2* in humans.

Figure 6.1. Example of selected tracks on the FANTOM5 ZENBU browser showing *ACTA2* promoter usage and expression level in humans. (A) Displays the direction of the transcript and the location on the chromosome. This shows that *ACTA2* is transcribed off the reverse strand (3'-5') and located at Chr10: 90694830-90751146. (B) Depicts the two reference sequences for this gene, the shorter NM_001613 and the longer transcript NM_001141945. (C) Displays the track identifying CpG islands, imported from the UCSC browser (http://genome.ucsu.edu/). The *ACTA2* gene contains one CpG island, CpG:62 associated with NM_001141945. (D) Illustrates the promoters associated with *ACTA2*, based on CAGE analysis. There are 11 in total, three supporting transcript NM_ 001613 and eight supporting NM_001141945 (outlined in black). (E) Shows histograms of the corresponding CAGE tags associated with the identified promoters (outlined in black). The purple vertical lines are proportional to the number of CAGE tags associated with the promoters and hence to expression of the gene from that promoter.

Figure 6.1 illustrates selected tracks that will be used in this chapter, identifying promoters and expression data for the fibrillin gene family. *ACTA2* is transcribed on the reverse strand of chromosome 10, in humans, and has two reference sequences (RefSeqs) for transcripts, NM_001613 and NM_001141945 ***(Figure 6.1A & 6.1B)***. There were 11 promoters identified by CAGE analysis, labelled pX@ACTA2 with the X depicting the promoter number given by the FANTOM5 consortium. The highest expressing promoter (determined by CAGE tag technology) begins with the number one or p1@ACTA2 while

p14@ACTA2 displays the lowest number of tags ***(Figure 6.1D)***. Promoters are defined as the region immediately upstream of TSSs. In addition, the browser reveals which transcription initiation sites are in CpG islands, visualized on a single track ***(Figure 6.1C)***. The quantitative nature of the CAGE data is illustrated by the histogram rendering of the number of tags supporting the identified promoters ***(Figure 6.1E)***. The FANTOM5 data show promoter expression across many human primary cells, tissue and cultured cell lines. *ACTA2* has two major TSS regions ***(Figure 6.1D and 6.1E)***, which are supported by the two different RefSeqs. These transcripts are expressed in different tissues at different expression levels. For example the TSS region (three promoters in total) supporting NM_001613 was most highly expressed in fibroblast-like synoviocytes, adipocytes, aorta, smooth muscle and umbilical cord. In addition this TSS region was more highly expressed overall, based on the peak height in comparison to the alternate TSS region associated with NM_001141945, where there were eight promoters identified ***(Figure 6.1)***. This TSS region was most highly expressed in MSCs, fibroblasts, cord blood, adipocytes and smooth muscle. Therefore, FANTOM5 defined alternate promoters and TSS regions and supported two major transcripts of *ACTA2* across approximately 900 human samples.

The data provided by the FANTOM5 project via the Zenbu browser will be used to analyze promoters of the fibrillin gene family to determine alternate promoter usage and transcript specific expression patterns within the family.

6.1.2 Identifying TFs

As part of the FANTOM5 project, the whole-genome alignment of the human genome along with 45 other vertebrate genomes was downloaded from the UCSC Genome Browser database (Meyer *et al.,* 2012). Alignments between the human, macaque, mouse, rat, cow, horse, dog, opossum, and chicken genomes, were done using the T-Coffee alignment tool (Notredame *et al.,* 2000). Members of the FANTOM5 consortium, then ran MotEvo (Arnold *et al.,* 2012) on the genome alignments to predict the TF binding sites (TFBSs) in the human genome, using a background prior probability of 0.98, a UFE

(unidentified functional element) motif length of 8bp, and a uniform background sequence probability.

In addition, Motif Activity Response Analysis (MARA) was applied on these TFBS predictions to infer the regulatory network (Suzuki *et al.,* 2009). MARA is an analysis technique that operates on the assumption that TFs will bind to specific DNA sequence elements close to the TSS of the gene (Suzuki *et al.,* 2009). The expression of the TSS is then assumed to be correlated with the number of TF binding motifs within the region. A linear based model is then applied to infer the regulators of the promoters (Suzuki *et al.,* 2009).

6.1.3 Aims of the Chapter

The FANTOM5 data will be used to explore the promoter activity and regulation of the three fibrillin genes in single time point samples. The aim of the study in this chapter was to identify major promoters, alternate (tissue-specific) promoters and regulatory elements that could support the differential expression of the fibrillin gene family.

6.2 Materials and Methods

6.2.1 Analysis of TSSs

The FANTOM5 database was used to identify TSS yielding promoters for the fibrillin gene family. Using the publicly available genome browser, ZENBU (http://fantom.gsc.riken.jp/zenbu) the TSS regions and expression patterns across the human samples were determined. The terms FBN1, FBN2 and FBN3 were entered, separately, into the search bar yielding the results of deepCAGE analysis. Tracks were selected as follows: (1) *Entrez gene hg19* ***(Figure 6.1A)*** (position on the chromosome), (2) *UCSU_RefSeq_hg19* ***(Figure 6.1B)*** (transcript structure), (3) *UCSC_CpGislands_hg19* ***(Figure 6.1C)*** (CpG island identification), (4) *FANTOM5 PHASE 1 FREEZE DPI Clusters human (robust)****(Figure 6.1D)*** (robust promoter location and identification) and *(*5) *FANTOM5 CAGE Phase 1 CTSS human tracks pooled filtered with 3 or more tags per library and RLE normalised* ***(Figure 6.1E)*** (expression peak).

Expression profiles were extracted by manually highlighting the area of the cage peaks within the browser using the track, *FANTOM5 CAGE Phase 1 CTSS human tracks pooled filtered with 3 or more tags per library and RLE normalised*. Once the area was highlighted, an expression profile track was automatically generated within the browser yielding expression values quantified as RLE normalised tags per million (TPM)(Balwierz *et al.,* 2009)(Forrest *et al.,* 2014). The expression data was organized using Microsoft excel.

6.2.2 Identifying TFs controlling fibrillin genes

The MARA and MotEvo analyses were downloaded from the FANTOM5 database (prior to public release) to infer regulators of the promoters. The files were acquired and TF predictions were collected for *FBN1*, *FBN2* and *FBN3*.

Because of its low expression level, the single promoter for FBN3 was not associated with TFs in the MARA and MotEvo analysis. Therefore TFBS were predicted for *FBN3* using the ECR browser (Evolutionary Conserved Regions)(htt://ecrbrowser.dcode.org/)(Ovcharenko *et al.,* 2004). The analysis was completed in October 2012. FBN3 was entered into the search term gateway and the following link was selected for analysis: FBN3 at chr19: 8130287-8212385 (NM_032447) fibrillin-3 precursor RefSeq. The FANTOM5 determined promoter region was manually highlighted within the human genome track (region chr19: 8213992-8215010), and the "conserved TF binding sites" link was selected, generating rVISTA (regulatory VISTA) analysis (http://rVISTA.dcode.org) (Loots and Ovcharenko, 2004). The following was selected within the rVISTA analysis: (1) TRANSFAC professional V10.2 library, (2) selected species: vertebrates, (3) Matrix similarities "optimized for function" (Ovcharenko *et al.,* 2005) and (5) run on all TF families. The alignment analysis was performed across the following species, dog, mouse, opossum, chicken, fish and frog. The analysis generated a list of TFBS conserved across the species within the confines of fibrillin-3 described above.

6.3 Promoter Identification using FANTOM5 data

6.3.1 *FBN1* has a single major promoter region

The promoter sequence for *FBN1* in human and mouse was identified previously through analysis of FANTOM3 data (Summers *et al.,* 2009). FANTOM5, which included many more human samples, confirmed that *FBN1* had a major promoter (p1@FBN1) associated with transcript NM_000138 ***(Figure 6.2)***, with transcription initiating on one of two purine nucleotides 12 nucleotides apart.

Figure 6.2. Identification of the major *FBN1* promoters in human. (A) The full fibrillin-1 transcript, CpG island location and robust promoters at the 5' end (outlined in black). (B) Detailed view of the outlined region, showing the architecture of the broad promoter, with multiple TSSs all within a single CpG island, CpG_174. Below is the expression peak. The height of the peak is proportional to the CAGE tags mapped to that region. The figure is further explained in Section 6.3.1. The image was obtained from http://fantom.gsc.riken.jp/zenbu/.

The region of this promoter contained several additional robust peaks of transcription initiation (p2@FBN1, p3@FBN1, p6@FBN1, p9@FBN1 and p11@FBN1), defining an extensive composite promoter (Forrest *et al.,* 2014)***(Figure 6.2B)***. As previously reported (Summers *et al.,* 2009, Guo *et al.,* 2008, Singh *et al.,* 2008) this *FBN1* promoter region was GC rich and contained a characteristic pyrimidine stretch, about 70 nucleotides upstream of the TSS associated with p1@FBN1. Four additional TSS regions were identified by CAGE analysis. Initiation from any of these promoter regions would result in alternative 5' UTR sequences spliced to the same first coding exon ***(Figure 6.2B)***. p11@FBN1 is probably associated with the rarely used Exon B of previous reports (Guo *et al.,* 2008, Corson *et al.,* 1993), while p7@FBN1/p25@FBN1 may be associated with the previously described Exon C (Corson *et al.,* 1993)***(Figure 6.2B)***. p8@FBN1 and p13@FBN1 were singleton low expressing broad promoters. p13@FBN1 was located within the first coding exon, immediately downstream of the start codon. All identified robust promoter regions were located within the CpG island, CpG_174 and all, excluding p13@FBN1, were located upstream the first start codon of NM_000138 ***(Figure 6.2A)***.

6.3.2 FBN2 has two promoter regions

As shown in ***Figure 6.3,*** a total of 10 significant TSS clusters were detected in human *FBN2*, eight located in or upstream of the 5' noncoding region of the gene and two appearing within intron 25 of the gene ***(Figure 6.3A)***.

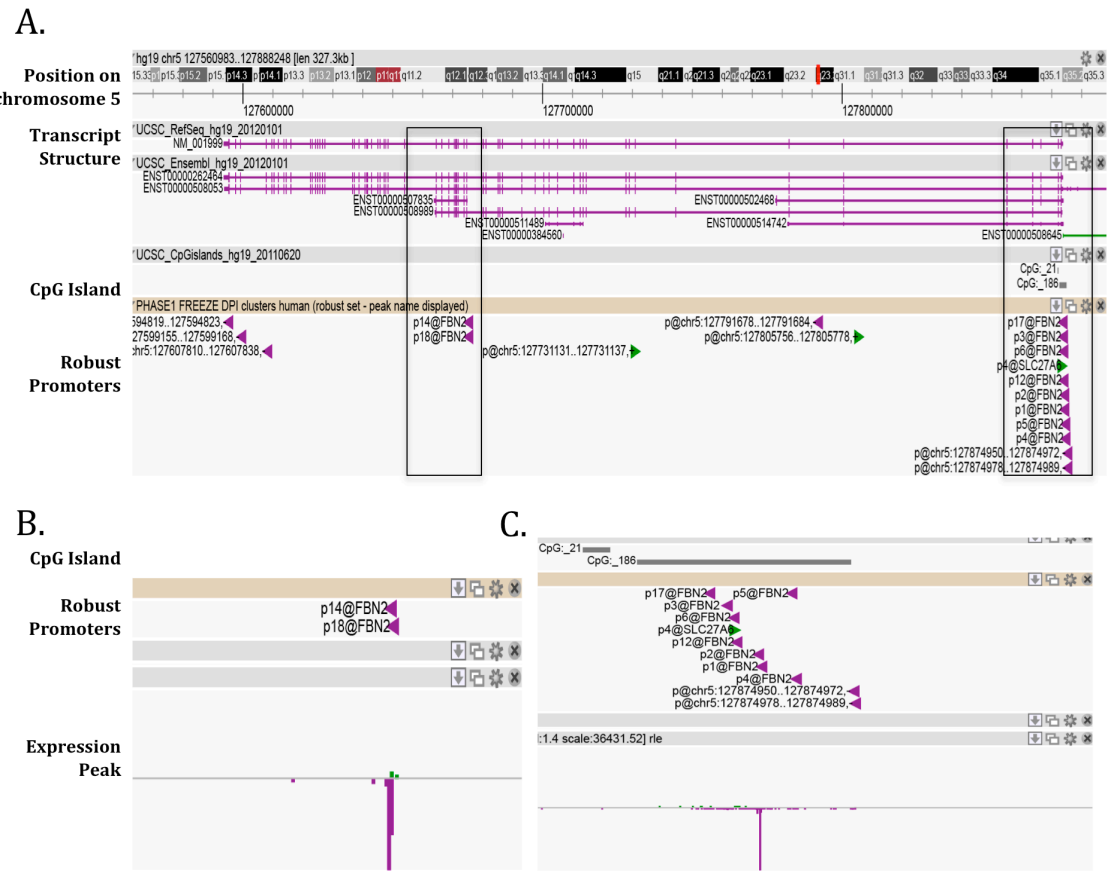

Figure 6.3. Identification of the major *FBN2* promoters in human. (A) The full fibrillin-2 transcript, CpG island location and a set of robust promoters at the 5' end (outlined in thick black line), and two additional TSS, p14@FBN2 and p18@FBN2 within intron 25 (outlined in thin black line). (B) Detailed view of the outlined region of p14@FBN2 and p18@FBN2, showing the architecture of the promoters, with multiple TSSs. Below is the CAGE expression peak. (C) Detailed view of the major TSS region consisting of 8 robust promoters. This figure is further explained in Section 6.3.2. The image was obtained from http://fantom.gsc.riken.jp/zenbu/.

The two main TSS clusters (p1@FBN2 and p2@FBN2) were approximately 40 base pairs apart and formed a composite promoter ***(Figure 6.3C)***. The highest expressed promoter, p1@FBN2, showed initiation on two guanines separated by a CC dinucleotide. The region of these TSSs was within a CpG island ***(Figure 6.3A)*** but showed no

sequence homology with the *FBN1* promoter region. This promoter region was characterized by a stretch of four adenines followed by a very cytosine-rich sequence. A number of other TSS regions were detected for *FBN2*. p17@FBN2, p3@FBN2, p6@FBN2 and p12@FBN2 were located within the first exon, downstream of p1@FBN2 ***(Figure 6.3C)***. p4@FBN2 and p5@FBN2 made up a composite promoter that lies upstream of p1@FBN2 and probably splice to the same first coding exon ***(Figure 6.3C)***. p14@FBN2 and p18@FBN2 were found in intron 25 and were associated with the short transcript ENST00000507835.1 ***(Figure 6.3A)***. Initiation of this transcript occurs over approximately 70 nucleotides (characteristic of a broad promoter), followed by an AT rich sequence. CAGE tags did not support some published transcripts. For example, there was no support at the robust level for a promoter for the long *FBN2* transcript ENST00000508053.1 which has an additional six 5′ non-coding exons (available at http://fantom.gsc.riken.jp/zenbu/).

6.3.3 FBN3 has a single robust promoter

Fibrillin-3 expression is restricted to foetal and embryonic tissue types (Corson *et al.,* 2004; confirmed in **Chapter 3 and Chapter 4**). FANTOM5 had extensive representation of human cells and tissues from early developmental stages allowing for the identification of the promoter region and the most common starting nucleotide for human *FBN3.* There is a single broad promoter, p2@FBN3 and the major TSS is 2126 nucleotides upstream from the ATG start codon of transcript NM_032447 ***(Figure 6.4A)***.

Figure 6.4. Identification of the major *FBN3* promoters in human. (A)The full fibrillin-3 transcript, CpG island location and the single robust promoter at the 5' end (outlined in black). (B) Detailed view of the outlined region showing the architecture of the single promoter, with multiple CAGE tag peaks all within a single CpG island, CpG_46. Below is the CAGE expression peak. There are several peaks associated with the single TSS. This figure is further explained in Section 6.3.3. The image was obtained from http://fantom.gsc.riken.jp/zenbu/.

This region is pyrimidine rich and associated with CpG_46. Expression from this promoter was very low after RLE normalisation ***(Table 6.3)***. There was no homology with any of the *FBN1* or *FBN2* promoter regions **(Chapter 7)**. A second, sharp promoter region (p1@FBN3) was located further away from the start codon and was associated with a TATA box 30 nucleotides upstream. This promoter was annotated only at the permissive level (http://fantom.gsc.riken.jp/zenbu/). In addition, CAGE tags did not support previously published transcripts (AY203940 and AK022050), for two long transcripts which overlap *FBN3* (Corson *et al.,* 2004). Due to the low expression of *FBN3*, the promoter definition will require confirmation.

6.3.4 FANTOM5 determined expression of the fibrillin family

The analysis of promoter sequences using CAGE technology provided quantitative as well as qualitative information about gene expression from the different promoters. RLE-normalised tag counts (Robinson *et al.,* 2009, Forest *et al.,* 2014) were used to determine the level of expression of the three fibrillin genes in the 975 tissues and cell lines.

Both *FBN1* and *FBN2* showed a high level of expression in cells of mesenchymal origin in human, as previously reported for mouse (Summers *et al.,* 2010). However, the highest expression was seen in different cell types for the two genes ***(Table 6.1 & 6.2)***.

For *FBN1*, the 10 robust promoter regions ***(Figure 6.2)***, in general displayed the highest expression levels in the samples of mesenchymal origin including smooth muscle cells, fibroblasts, preadipocytes and adipocytes, chondrocytes, mesenchymal stem cells and cardiac myocytes ***(Table 6.1)***(http://fantom.gsc.riken.jp/zenbu/). Outside the main compound promoter, p11@FBN1 was expressed in multiple different fibroblast tissue samples, but displayed the highest expression levels in chorionic and amniotic membrane cells. p7@FBN1 showed peak levels of expression in neural tissue ***(Table 6.1)***.

FANTOM5 promoter ID	Highest expression tissue/cell types	Total number of samples showing expression	Highest expression value (RLE normalised TPM)
p1@FBN1	Smooth muscle cells (Aorta)	714	2563
	Fibroblast (Aorta)		
	Fibroblast (Skin)		
p2@FBN1	Smooth muscle cells (aortic)	573	376
	Fibroblasts (aortic)		
	Sertoli cells		
p3@FBN1	Smooth muscle cells	386	31
	Fibroblasts (aortic)		
	Fibroblast (skin)		
p6@FBN1	Smooth muscle cells (pulmonary artery)	419	13
	Fibroblast (aortic)		
	Fibroblast (skin)		
p9@FBN1	Smooth muscle cells (pulmonary artery)	299	12
	Fibroblast (aortic)		
	Fibroblast (skin)		
p11@FBN1	Amniotic membrane cells	314	10
	Chorionic membrane cells		
	Fibroblast (skin)		
p8@FBN1	Fibroblast (aorta)	326	9
	Chorionic membrane cells		
	Amniotic membrane cells		
p7@FBN1	Cholangiocellular carcinoma cell line – HuH-28	345	7
	Corpus callosum		
	Fibroblast (aorta)		
p13@FBN1	Fibroblasts (aortic)	236	5

	Chorionic membrane cells		
	Basal cell carcinoma cell line TE354		
p25@FBN1	Diencephalon (adult)	135	4
	Corpus callosum		
	Smooth muscle cells (aorta)		

Table 6.1. *FBN1* promoter expression determined from FANTOM5 analysis. The table displays all the promoters identified for *FBN1* and highlights the tissue/cell types where the promoters showed highest expressed, the total number of samples that expressed the promoter and the highest TPM associated with the promoter. Order of the promoters is presented based on the highest expression value (TPM).

For *FBN2*, more embryonic and foetal tissues showed high expression than for *FBN1,* with the maximum normalised tag count seen in a range of cells from foetal tissues, fibroblasts, osteoblasts, placenta, hair follicle and lens epithelial cells (http://fantom.gsc.riken.jp/zenbu/).

FANTOM5 promoter ID	**Highest expression tissue/cell type**	**Total number of samples showing expression**	**Highest expression value (RLE normalised TPM)**
p1@FBN2	Normal embryonic palatal mesenchyme stem cell lines HEPM	682	1548
	Fibroblast (skin)		
	Sacrococcigeal teratoma cell line HTST		
p2@FBN2	Fibroblasts (skin)	586	82
	Extraskeletal myxoid chondrosarcoma cell line HEMC SS		
	Normal embryonic palatal mesenchyme stem cell lines HEPM		
p3@FBN2	Placenta (adult)	579	37
	Pancreatic carcinoma cell line NORP1		

	Adipocyte		
p6@FBN2	Prostate Stromal Cells	234	15
	Osteoblast		
	Extraskeletal myxoid chondrosarcoma cell line HEMC SS		
p14@FBN2	Testis (adult)	4	8
p4@FBN2	Lens epithelial cells	358	7
	Testicular germ cells embryonal carcinoma cell line NEC-15		
p18@FBN2	Testis (adult)	3	6
p5@FBN2	Extraskeletal myxoid chondrosarcoma cell line HEMC SS	267	5
	Placenta (adult)		
	Teratocarcinoma cells		
p17@FBN2	Extraskeletal myxoid chondrosarcoma cell line HEMC SS	52	4.6
	Hair follicle dermal papilla cells		
	Fibroblast		
p12@FBN2	Fibroblast (Skin) 3 donors	71	5

Table 6.2. *FBN2* promoter expression determined from FANTOM5 analysis. The table displays all the promoters identified for *FBN2* and highlights the tissue/cell types where the promoters showed highest expresison, the total number of samples that expressed the promoter and the highest TPM associated with the promoter. Order of the promoters is presented based on the highest expression value (TPM).

The major significant promoters p1@FBN2 and p2@FBN2 displayed similar expression values and peaked in the same cell types ***(Figure 6.3)(Table 6.2)*** while p3@FBN2 peaked in hematopoietic cell types. p14@FBN2 and p18@FBN2, located in intron 25, displayed highest expression in testis. The transcript deriving from these promoters, ENST00000507835.1, covers coding exons 26 to 34 of the full length *FBN2* and the

polypeptide would consist of eight cbEGF domains with short N- and C-terminal flanking sequences (http://www.ensembl.org).

As expected, *FBN3* was almost exclusively expressed in cells of foetal and embryonic origin in human ***(Table 6.3)*** (Corson *et al.,* 2004) **(Chapter 3)**.

FANTOM5 promoter ID	Highest expression tissue/cell type	Total number of samples showing expression	Highest expression value (RLE normalised TPM)
p2@FBN3	Occipital lobe (foetal)	66	6
	H9 embryonic stem cell line Rep 1		
	H9 embryonic stem cell line Rep2		

Table 6.3. *FBN3* Promoter Expression determined from FANTOM5 analysis. The table displays the promoter identified for *FBN3* and highlights the tissue/cell types where the promoter showed highest expression, the total number of samples that expressed the promoter and the highest TPM associated with the promoter.

This expression pattern was further observed in the more limited BioGPS data (http://biogps.org) (**Chapter 1, *Figure 1.6***). p2@FBN3, was expressed at the highest level in foetal brain and embryonic cells ***(Figure 6.3)***.

6.4.5 Transcriptional Regulation

A total of 21 robust promoters were identified for *FBN1, FBN2* and *FBN3*. MARA analysis was able to infer possible TF regulation for 13 of the robust promoters ***(Table 6.4)***. The promoters noted in ***Table 6.4*** are given in order along the chromosome to highlight the relationship between promoters within one composite promoter region.

Name	Transcript ID	CpG island	Composite	Transcription factors
Fibrillin 1 (*FBN1*)				
p13@FBN1	NM_000138	CpG:_174	SINGLETON	None
p8@FBN1	NM_000138	CpG:_174	SINGLETON	None
p25@FBN1	NM_000138	CpG:_174	p7, p25	None
p7@FBN1	NM_000138	CpG:_174	p7, p25	FOXD3, HOXA9_MEIS1, MAZ, PATZ1, TFAP4, TFDP1
p3@FBN1	NM_000138	CpG:_174	p1, p2, p3, p6, p9, p11	GTF2I, NKX3-1, TBX4-5,TFAP4
p2@FBN1	NM_000138	CpG:_174	p1, p2, p3, p6, p9, p11	GTF2I, NKX3-1, TBX4-5,TFAP4
p1@FBN1	NM_000138	CpG:_174	p1, p2, p3, p6, p9, p11	GTF2I, NKX3-1, TBX4-5,TFAP4
p6@FBN1	NM_000138	CpG:_174	p1, p2, p3, p6, p9, p11	GTF2I, NHLH1-2, NKX3-1, PRDM1, TBX4-5, TFAP4
p9@FBN1	NM_000138	CpG:_174	p1, p2, p3, p6, p9, p11	GTF2I, NKX3-1, PRDM1, TBX4-5
p11@FBN1	NM_000138	CpG:_174	p1, p2, p3, p6, p9, p11	PRDM1
Fibrillin-2 (*FBN2*)				
p14@FBN2	ENST00000507835.1	None	p14, p18	None
p18@FBN2	ENST00000507835.1	None	p14, p18	None
p17@FBN2	NM_001999	CpG:_186	SINGLETON	TOPORS
p3@FBN2	NM_001999	CpG:_186	SINGLETON	KLF4
p6@FBN2	NM_001999	CpG:_186	p6, p12	HIC1, HIF1A, KLF4, PAX5, TFAP2B, TOPORS

p12@FBN2	NM_001999	CpG:_186	p6, p12	HIF1A, KLF4, TFDP1, TOPORS
p2@FBN2	NM_001999	CpG:_186	p1, p2	GFI1, GTF2I, HIF1A, MZF1, SP1, TRAP2B, TFDP1
p1@FBN2	NM_001999	CpG:_186	p1, p2	GFI1, GTF2I, HIF1A, MZF1, SP1, TRAP2B, TFDP1
p5@FBN2	NM_001999	CpG:_186	p4, p5	None
p4@FBN2	NM_001999	CpG:_186	p4, p5	None
Fibrillin-3 (*FBN3*)				
p2@FBN3	NM_032447	CpG:_46	SINGLETON	None

Table 6.4. TF motifs association with fibrillin gene promoters. The table displays the promoters identified for fibillin-1, fibrillin-2 and fibrillin-3. This table highlights the transcripts associated with the promoters, the presence of CpG islands, promoter architecture (composite vs. single) and the MARA-identified TF regulation. Order of the promoters is presented in the table based on the promoter location. All three fibrillin genes are transcribed from the reverse strand.

Seven of the 10 *FBN1* promoters were associated with potentially regulating TFs. Motifs associated with GTF2I, NKX3-1, TBX4-5 and TFAP4 TFs were found to regulate five fibrillin-1 promoters ***(Table 6.4)***. PRMD1, associated with p9@FBN1, was also a putative regulator of p11@FBN1.

Of the 10 robust *FBN2* promoter regions, a total of six were associated with TFs. p1@FBN2 and p2@FBN2 were regulated by the same TF motifs GFIT1, MZF1, SP1, TRAP2B , TFDP1, HIF1A and GFIT21 ***(Table 6.4)***. In addition, motifs associated with HIF1A regulated p6@FBN2 and p12@FBN2. There was a high prevalence of motifs for TOPORS and KLF4 TFs associated with broad promoter region consisting of p3@FBN2, p6@FBN2, p12@FBN2 and p17@FBN2 ***(Table 6.4)*** although there were no TFs associated with p14@FBN2 or p18@FBN2.

There were no MARA determined motifs associated with p2@FBN3, though TF binding motifs for MAZ, PATZ1, RREB1, SP1 and TFAP4 were detected in an analysis performed through the ECR Browser (http://ecrbrowser.dcode.org/)**(Section 6.2.3)**.

6.4 Discussion

This chapter presents a study of the TSS and predicted TFs associated with the fibrillin gene family using FANTOM5 deepCAGE data. A total of 10 novel TSSs for *FBN1* were identified, expanding from previous promoter analysis of *FBN1* (Summers *et al.,* 2009). The broad promoter region consists of both composite and single promoter structures, all associated with a single CpG island (CpG_174). Expression of *FBN1* was mainly in cell and tissue types of mesenchymal origin (Summers *et al.,* 2010)**(Chapter 4)**, with the exception that p7@FBN1 showed high neuronal expression and p11@FBN1 was expressed in extra-embryonic membranes. Seven of the ten robust promoters were associated with identified TF motif by MARA analysis. The major composite promoter region ***(Figure 6.2)*** shared similar TFs ***(Table 6.1)***, while p7@FBN1 had differing motifs assigned. p7@FBN1 was associated with FOXD3, consistent with expression peaks in neural tissue/ cell types. FOXD3 (OMIM: 611539) is a regulator in embryonic neural crest formation. In addition there were several other early development motifs, for example PATZ1, MEIS1 and HOXA9 ***(Table 6.4)***. Five promoters had motifs for limb development, including TF TBX4-5 (OMIM: 601719)(OMIM: 601620)(Takeuchi *et al.,* 1999, Minguillon *et al.,* 2005), consistent with the abnormalities of limb development in the presence of *FBN1* mutations (**Chapter 1, Section 1.3.4**). While there was not a single TF motif shown to regulate all promoters within the fibrillin family, general TF, GTF2I (Orphanides *et al.,* 1996) was associated with the high expressing promoters in both *FBN1* and *FBN2* ***(Table 6.4)***.

A total of 10 novel TSSs were identified for *FBN2* ***(Figure 6.3)***. *FBN2* was highly expressed in mesenchyme cell types and early development. Some of the promoters were regulated by epithelial and pluripotency associated motifs, KLF4, PAX5, TRAP2B, and early expression motif, SP1 ***(Table 6.4)***, consistent with expression patterns and the predicted role of *FBN2* in mesoderm formation **(Chapter 3)**. Furthermore, the HIF1A (OMIM: 603348) motif was coupled with four major fibrillin-2 promoters including, p1@FBN2, p2@FBN2, p6@FBN2 and p12@FBN2, and HIF1A has recently been implicated in osteoblast formation (Wang *et al.,* 2007). *FBN2* is highly expressed in cells of osteoblast lineage ***(Table 6.4)***(Summers *et al.,* 2009) and mutations in *FBN2*

phenotypically show disruption in bone and cartilage formation (**Chapter 1, Section 1.3.5**). The relationship between *FBN2* and *HIF1A* will need to be further validated as a potential target for therapy in CCA.

One TSS was identified in *FBN3,* associated with a single CpG island (CpG_46)***(Figure 6.4)***. While the MARA analysis did not reveal motifs regulating p2@FBN3, several TF binding motifs, SP1, TRAF4, PATZ1, MAZ, and RREB1, were identified through the ECR browser conserved TFBS function (http://ecrbrowser.dcode.org/)**(Section 6.2.1)**. Conservation of a motif across species is considered to be an indication of likely biological function (Ovcharenko *et al.,* 2004). All these factors are involved in embryogenesis and development. For example, general TF, SP1 (OMIM: 189906), has been shown to be involved in blastocyst segmentation (Wimmer *et al.,*1993), TRAF4 (OMIM: 602464) was shown to be a crucial factor in skeletal, tracheal and neural tube development in the embryo (Regnier *et al.,* 2002), and PATZ1 is a general TF in embryogenesis (Valentino *et al.,* 2012). These findings are consistent with *FBN3* expression patterns in early development and foetal neural cells **(Chapter 3)(Section 6.3.3)**.

6.5 Conclusions

In summary, this chapter presented evidence of the promoter and TSS region architecture for the fibrillin gene family as well as possible regulatory motifs associated with specific promoter expression. *FBN1* and *FBN2* shared similar promoter architecture, presenting with a large broad promoter containing many TSS within the region as well as singleton TSS regions appearing outside the major broad promoter. Though both *FBN1* and *FBN2* were highly expressed in cells of mesenchyme origin, the level of expression and tissue specificity varied between the two genes. In addition, the low expressing singleton promoters identified indicated further specific expression differences between the genes. The promoter region of *FBN3* showed one major TSS (singleton) with tissue specific expression, mainly in foetal and embryonic cell types. There were no consistent TF identified for all three fibrillin genes. The variation in the promoter architecture and regulatory elements of the fibrillin gene family supports the concept of differential roles for *FBN1*, *FBN2* and *FBN3*. Since in humans there is no one central regulator of the

fibrillin family, and the TSS regions show varying expression patterns (tissue specific) between the fibrillin genes, it was important to examine if this phenomenon also occurred in other species. This will be explored in **Chapter 7** by looking at the sequence conservation of the promoters and other key fibrillin gene family regions across vertebrates.

Chapter 7. Evolutionary conservation of the fibrillin gene family

7.1 Introduction

Fibrillin-1 -and -2 are expressed across many cell types, mainly mesenchyme derived, and fibrillin-3 is highly expressed in early and fetal tissues, as outlined in this thesis. The genes have independent expression patterns, so each gene appears to have a specific and different function **(Chapters 3-6)** and they are controlled by different regulatory sequences **(Chapter 6)**. The multiple deleterious phenotypes associated with mutations in *FBN1* and *FBN2* suggest that these genes are important and likely to be conserved across species. The inactivation of the *FBN3* gene in mice and rats (Corson *et al.,* 2004) leaves open the question of potential redundancy of this gene in other mammals. Gene conservation and major evolutionary events are thought to have led to the development of the three fibrillin genes in humans (Piha-Gossack *et al.,* 2012, Robertson *et al.,* 2010).

Comparative sequence analysis is a powerful tool that can be used to understand the evolutionary significance of (for example) conserved promoter regions, protein domains and mutation regions, across species, within a gene family. **Chapter 6** identified key TSS regions within the fibrillin gene family. Investigating the sequence conservation of promoter regions has been previously used to predict 5' regulatory regions within a gene, across various cell types (Sato *et al.,* 2001), and across species (Rostas *et al.,* 1986, Bashyam *et al.,* 1996). Furthermore, studying promoter conservation can identify key regions that could be used in gene therapy to target gene expression (Li and Zhang, 2014, Summers *et al.,* 2009, De Mey *et al.,* 2010). This chapter examines the sequence conservation of the previously identified TSS regions in the fibrillin gene family. This was done to understand the evolutionary trends in transcriptional regulation.

Mutations in amino acids that are critical to the function of a protein are likely to have major phenotypic consequences and such amino acids tend to be conserved across species (Strachen T., 2004). This chapter reports sequence homology studies on the sites of severe mutations in MFS and CAA, to determine the likely significance of the regions for protein function across the fibrillin family. As introduced in **Chapter 1, Section 1.3.4 and 1.3.5**, the majority of neonatal MFS and CCA cases present with mutations in a

region containing many cbEGF-like domains and a single TB (TGFβ binding protein like) domain in both fibrillin-1 and -2. The region stretches from exon 24 to exon 33, consisting of TB5 domain in exon 24, followed by several cbEGF-like domains **(Chapter 1, Section 1.3.2)**. The severity of the phenotypes caused by mutations in this region in both genes, suggests that it plays an important role in the function of the encoded proteins. There were no mutations reported in fibrillin-3 for that region. In addition, four mutations resulting in truncation of fibrillin-1 at exon 64 have been shown to cause severe lipid depletion in patients diagnosed with MFS, extensively discussed in **Chapter 3**. A study of the conservation of the amino acid sequence in the regions covering the severe phenotypes and the lipodystrophy phenotype both within and among fibrillins across vertebrates will help to understand the importance of the protein domains where these severe mutations reside within the fibrillin gene family.

7.1.1. Aims of the Chapter

This chapter reports a wide scale bioinformatics search to identify conservation of gene sequence and structure across vertebrates containing transcripts and/or annotated genes for *FBN1, FBN2* and *FBN3*. The study examined the conservation of the main promoter regions of fibrillin gene family identified by the FANTOM5 project **(Chapter 6)**. In addition, the analysis explored the conservation of various protein domains and amino acid regions of interest across species and among the fibrillin gene family, specifically addressing exons 24 – 32 where mutations are associated with the most severe phenotypes and exon 64 where mutations present with a high incidence of MFS with lipodystrophy. The overall aim of the study was to understand the functional significance of the different regions of the fibrillin genes through the conservation of key amino acids.

7.2 Materials and Methods

7.2.1 Conservation across vertebrates

The search terms *FBN1*, *FBN2* and *FBN3* were entered into the search facility of Ensembl (http://www.ensembl.org) and all genes retrieved were examined for chromosome/scaffold location, flanking genes, and number of annotated exons. Amino acid sequences were obtained for those species that had sequence homologous to the start

sites annotated for the human genes **(Chapter 9, Appendix C)**. Amino acid sequence alignments were conducted by ClustalW analysis (DNASTAR, Lasergene, Madison, WI, USA). Percent identity was determined based on sequence displacement values determined by the ClustalW alignment (DNASTAR, Lasergene). All analysis was performed on genome builds available in Ensembl in 2013 **(Table 7.1)**.

7.2.2. Promoter conservation

The promoter sequences for human *FBN1, FBN2* and *FBN3* were obtained from FANTOM5 human dataset (http://fantom.gsc.riken.jp/zenbu/)**(Chapter 6).** The promoters with the highest expression across all cell types were considered to identify the major transcription start site for each gene (p1@FBN1, p1@FBN2 and p2@FBN3). Nucleotide sequences from approximately 200bp upstream and 100bp downstream of these transcription start sites were obtained ***(Table 7.1)***.

Gene name	Gene symbol	Genome Location	Number of nucleotides (nt)
Fibrillin-1	*FBN1*	Chr.15: 48645593- 48645905	312
Fibrillin-2	*FBN2*	Chr.5: 127873797-127874203	406
Fibrillin-3	*FBN3*	Chr.19: 8214401-8214701	300

Table 7.1. The human nucleotide regions used in the BLAT (BLAST-like alignment tool) searches for promoter conversation studies.

The retrieved human sequences were then entered into the BLAT search engine within Ensembl and equivalent sequences were recovered for *FBN1, FBN2* and *FBN3* in the following species, *Mus musculus* (mouse), *Sus scrofa* (pig), *Ovis aries* (sheep), *Mustela putorius furo* (ferret), *Otolemur garnettii* (bushbaby), *Ailuropoda melanoleuca* (panda) and *Dasypus novemcinctus* (armadillo) (www.ensembl.org). These species were selected for the promoter conservation analysis because they had mostly adequate sequencing of the 5'regions for all three fibrillin genes, excluding *Fbn3* in mouse.

7.2.3 Conservation of amino acids associated with MFS, CCA and lipodystrophy

Amino acid sequences **(Chapter9, Appendix C)** of exon 24-33 and exon 64 (based on the human sequence) of fibrillin-1, -2 and -3 were extracted for the following species: human, mouse, pig, sheep, ferret, bushbaby, armadillo, *Gallus gallus* (chicken), *Ficedula albicollis* (flycatcher), *Meleagris gallopavo* (turkey), *Latimeria chalumnae* (coelacanth), and *Pelodiscus sinensis* (Chinese softshell turtle). The sequences were aligned and percent identity was determined as outlined in **Section 7.2.1.** Conserved amino acid residues were visually identified within the alignments.

7.3 Results: Conservation of fibrillins across vertebrates

7.3.1 Conservation of Fibrillin-1

The *FBN1* gene in humans contained 66 annotated coding exons and one 5' non-coding exon, and was flanked by *CEP152* and *SHC4* at the 5' end and *DUT* and *SLC12A1* at the 3' end. It was located on chromosome 15 and transcribed from the minus strand. The human *FBN1* gene covered more than 237,000bps and the longest transcript consisted of 11,695bps. A total of 58 species had a gene annotated as *FBN1* and where data was available the same flanking genes were detected, except for *Petromyzon marinus* (lamprey) where none of these genes were located in the same region ***(Table 7.2 and Table 7.3).***

Common Name	Chromosome/Scaffold	Flanking genes	Exons
Human*	Chr. 15	*DUT, CEP152, SHC4, SLC12A1*	66
Alpaca	Sc_1602	*DUT, SLC12A1*	76
Armadillo*	Sc_5300:	*DUT*	71
Bushbaby*	GL: 873530	*DUT,CEP152, SLC12A1*	65
Cat*	ChrB3	*DUT, SLC12A1*	67
Chimpanzee*	Chr.15	*DUT, CEP152, SHC4, SLC12A1*	66
Cow*	Chr. 10	*CEP152, SHC4, DUT, SLC12A1*	65
Dog*	Chr. 30	*DUT, CEP152, SHC4, SLC12A1*	65
Dolphin*	Sc_275	*DUT, SLC12A1*	71
Elephant*	Sc_80	*DUT, CEP152, SLC12A1*	65
Ferret*	Gl: 896926	*DUT, CEP152, SHC4, SLC12A1*	69
Gibbon*	GL: 397306	*DUT, CEP152*	65
Gorilla*	Chr. 15	*DUT, CEP152, SHC4, SLC12A1*	66
Guinea Pig*	Sc_23	*Dut, Slc12a1*	65
Hedgehog	Sc_3407	*DUT*	69
Horse	Chr. 1	*CEP152, DUT, SLC12A1*	70
Hyrax*	Sc_5473	*Data not available*	72
Kangaroo rat	Sc_603	*Dut, Cep152, Slc12a1*	70
Lesser hedgehog tenrec	Sc_6197	*Data not available*	86
Macaque*	Chr. 7	*DUT, SLC12A1*	65
Marmoset*	Chr. 10	*DUT, CEP152, SHC4, SLC12A1*	67
Megabat*	Sc_2805	*Data not available*	66
Microbat	GL:42970	*DUT, SLC12A1*	91
Mouse	Chr. 2	*Cep152, Shc4, Dut, Slc12a1*	66
Mouse Lemur	Sc_401	*DUT, SLC12A1*	68
Opossum*	Chr. 1	*CEP152, SHC4, DUT, SLC12A1*	66
Orangutan*	Chr. 15	*DUT, CEP152, SHC4*	73
Panda*	GL: 192544	*DUT, CEP152, SLC12A1*	65
Pig*	Chr. 1	*CEP152, SCL12A1, SHC4*	71
Pika	Sc_2374	*DUT, SLC12A1*	69
Platypus*	UltracontigUltra 375	*CEP152, SLC12A1*	60
Rabbit*	Chr. 17	*DUT, CEP152, SHE4*	67
Rat	Chr. 3	*Dut, Cep152, Shc4, Slc12a1*	65
Sheep*	Chr. 7	*CEP152, SLC12A1*	65
Shrew*	Sc_5245	*Data not available*	80
Sloth	Sc_5856	*Data not available*	68
Squirrel*	JH: 393281	*SLC12A1, DUT*	71
Tarsier	Sc_6131	*Data not available*	67
Tree Shrew	Sc_4047	*CEP152*	75
Wallaby	Sc_7349	*Data not available*	70

Table 7.2 Fibrillin-1 genes in mammals. The mapped location and number of exons of the fibrillin-1 gene among mammalian species is shown. The * signifies that the mammal has annotated genes for fibrillin-1, -2 and -3. Information was obtained from http://www.ensembl.org (See Section 7.2.1).

Common Name	Chromosome/Scaffold	Flanking genes	Exons
Birds			
Chicken*	Chr. 10	*DUT, CEP152, SLC12A1*	69
Duck*	KB743097.1	*DUT, CEP152, SHC4, SLC12A1*	64
Flycather*	JH603201.1	*DUT, CEP152, SHC4, SLC12A1*	64
Turkey*	Chr. 12	*DUT, CEP152, SHC4*	64
Fish			
Cod	Sc_2886	*dut, slc12a1*	92
Coelacanth*	JH127003	*cep152,slc12a1, shc4*	66
Fugu	Sc_1	*dut, slc12a1*	67
Lamprey	GL:476354	*yjefn3, mtfmt*	67
Medaka	Chr.3	*dut, slc12a1*	66
Platyfish	JH55670	*shc4*	44
"	AGAJ01039647	*dut, slc12a1*	21
Spotted gar*	LG3	*dut, slc12a1, shc4*	67
Stickleback	GroupII	*dut, slc12a1, shc4*	79
Tetraodon	Chr. 5	*slc12a1, dut*	67
Tilapia	GL831355	*dut, slc12a1, shc4*	85
Zebrafish	Chr. 18	*dut, slc12a1*	4
Reptiles and amphibians			
Anole lizard	Sc_GL343806	*dut*	52
Chinese softshell turtle*	JH212494	*dut, cep152, slc12a1*	65
Xenopus	GL172857	*cep152, slc12a1, shc4*	66

Table 7.3 Fibrillin-1 genes in other vertebrates. The mapped location and number of exons of the fibrillin-1 gene in birds, fish, reptiles and amphibians is shown. The * signifies that the species has annotated genes for fibrillin-1, -2 and -3. The information was obtained from http://www.ensembl.org (See Section 7.2.1).

Fibrillin-1 transcripts were well represented in the available mammal, bird, reptile and amphibian genomes ***(Table 7.2 and 7.3)***. The fibrillin-1 sequence for *Procavia capensis* (hyrax), *Echinops telfairi* (lesser hedgehog tenrec), *Pteropus vampyrus* (megabat), *Sorex araneus* (shrew), *Choloepus hoffmanni* (sloth), *Tarsius syrichta* (tarsier) and *Macropus eugenii* (wallaby) had been mapped to scaffolds that did not have the flanking genes

present ***(Table 7.2)***. The identified *fbn1* in *Xiphophorus maculates* (platyfish) was divided across two scaffolds, JH55670 and AGAJ01039647, though located near the flanking genes ***(Table 7.3)***. The lamprey sequence also mapped to two scaffolds, one showing flanking genes that map approximately 20 Mb distal to *FBN1* on chromosome 15 in humans.

The first half of the gene, in humans, contained three very long introns and only seven of the exons, with the second half having the majority of the exons interspersed with short introns. ***Figure 7.1*** highlights this architecture of human *FBN1* compared with the intron/exon architecture for species where the amino acid sequence at the beginning of the gene shows high similarity to the human sequence (mouse, sheep, ferret and Chinese softshell turtle). For many species, the first annotated exon did not contain the start codon or did not contain sequence matching the first human coding exon, suggesting that annotation of the 5' end of many *FBN1* genes is incomplete. For example in pig, the first long intron was present but the longest intron absent and many more exons were identified. The first exon after this long intron in pig was found by BLAT analysis to map to the middle of the human gene, and it is likely that the intervening exons are artefacts of sequence annotation or assembly.

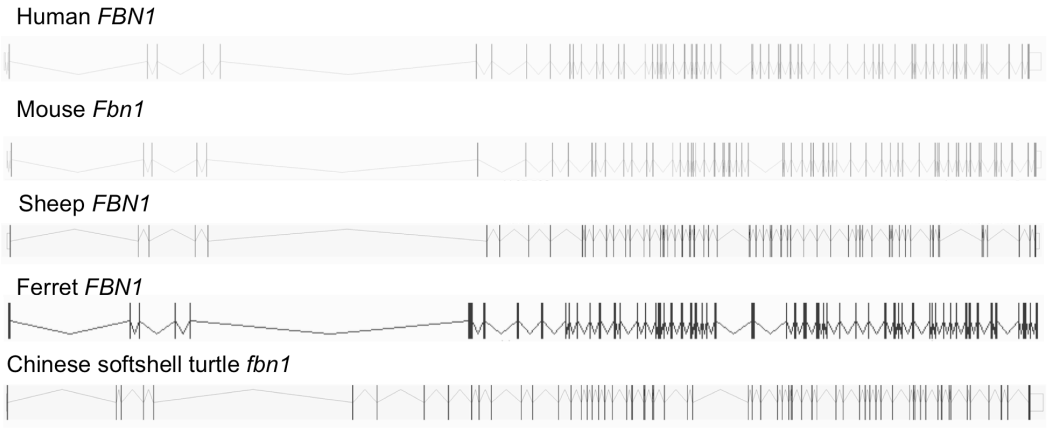

Figure 7.1. Fibrillin-1 gene architecture. *FBN1* gene structure (Chapter 6) of species discussed in Section 7.3.1 is shown. The vertical lines depict exons, and the horizontal (v-shaped) lines represent introns. These images were obtained from http://www.ensembl.org.

Mouse, sheep, ferret and Chinese softshell turtle showed the 5' long intron and sparse exon distribution characteristic of the first half of the gene ***(Figure 7.1)***. Alignments of the total amino acid sequence of the species indicated that the first coding exon was homologous across these species, indicating high levels of similarity in the architecture of the gene ***(Table 7.4)***.

A total of 19 mammals, birds and fish were selected for additional sequence analysis (MegAlign, DNstar) ***(Table 7.4)***. When compared with the complete human fibrillin-1 amino acid sequence, bushbaby had the highest percent identity at 97.9%, but all the mammals were close to this value ***(Table 7.4)***. In birds, the fibrillin-1 sequence was more diverse at around 87% ***(Table 7.4)***. While the Chinese softshell turtle showed a high level of homology at 87.4%, the fish were the most divergent with the highest amino acid percent identity in coelacanth at 76.8% ***(Table 7.4)***.

Common Name	FBN1	FBN2	FBN3
Mammals			
Mouse	96.3	96.6	X
Pig	96.5	94.7	86.5
Sheep	97.5	97.7	82.6
Ferret	96.8	97.7	84
Bushbaby	97.9	97.5	82
Panda	97.4	X	85.4
Armadillo	96.7	91	82.9
Birds			
Chicken	86.9	91.4	71.1
Flycatcher	87.3	87.8	67.9
Fish			
Coelacanth	76.8	80.8	X
Fugu	71.6	X	69.2
Medaka	72.3	X	68.7
Spotted gar	75	X	63.4
Stickleback	70.7	X	68.9
Tetraodon	71.3	X	68.8
Tilapia	73.3	X	68.3
Reptile			
Chinese softshell turtle	87.4	92	48.2

Table 7.4. Percent identity of amino acid sequences to the human fibrillin sequences across vertebrates. The percent identity was defined through a ClustalW alignment (DNASTAR) of the predicted amino acid sequences (Appendix C). Fibrillin-2 sequences for panda and spotted gar and fibrillin-3 sequence for coelacanth were omitted from the analysis due incomplete sequencing. The X depicts no mapped gene to the respective genome.

7.3.2 Conservation of Fibrillin-2

The *FBN2* gene was located on chromosome 5 in humans, between flanking genes *SLC12A2* (3' end) and *SLC27A6* (5' end). There were 65 annotated exons. The *FBN2* gene covered over 250,000 bps and the longest transcript was 11,132 bps. A total of 51 vertebrates with annotated *FBN2* genes were identified ***(Table 7.5 and 7.6)***. A gene annotated as encoding *FBN2* was present in most mammal and bird genomes available,

but it was missing from the majority of fish genomes, except coelacanth, spotted gar, *Astyanax mexicanus* (cavefish) and *Danio rerio* (zebrafish) ***(Table 7.6)***.

Many species lacked complete annotation, as measured by variations in the number of exons annotated, lack of synteny and lack of a start codon in the first coding exon, with respect to human. For example *fbn2* in zebrafish had only 17 exons annotated ***(Table 7.6)***. In addition, species including armadillo, coelacanth, lesser hedgehog tenrec, platypus, shrew, sloth, and *Dipodomys ordii* (kangaroo rat) were mapped to short contigs with no flanking genes ***(Table 7.5)***.

Common Name	**Chromosomal/Scaffold**	**Flanking genes**	**Exons**
Human	Chr. 5	*SLC12A2, SLC27A6*	65
Alpaca	Sc_3525	*SLC12A2*	70
Armadillo	Sc_3526	*Data not available*	84
Bushbaby	Sc_GL873522.1	*SLC12A2*	66
Cat	Chr. A1	**SLC12A2, *SLC27A6*	66
Chimpanzee	Chr. 5	*SCL12A2, SLC27A6*	64
Cow	Chr. 7	*SLC12A2, SLC27A6*	100
Dog	Chr. 11	*SLC12A2 , SLC27A6*	65
Dolphin	Sc_186	*SLC12A2*	76
Elephant	Sc_1	*SLC12A2, SLC27A6*	65
Ferret	GL896898.1	*SLC12A2*	65
Gibbon	GL397277.1	*SLC12A2*	64
Gorilla	Chr. 5	*Slc12a2*	63
Guinea Pig	Sc_6	*Slc12a2, Slc27a6*	71
Hedgehog	Sc_4310	*Data not available*	71
Horse	Chr. 14	*SLC12A2, SLC27A6*	68
Hyrax	Sc_3612	**SCL12A2, SLC27A6*	79
Kangaroo rat	Sc_3272	*Data not available*	73
Lesser hedgehog tenrec	Sc_4180	*Data not available*	77

Macaque	Chr. 6	*SLC12A2, SLC27A6*	69
Marmoset	Chr. 2	*SLC12A2, SLC27A6*	65
Megabat	Sc_253	*SCL12A2, *SCL27A6*	77
Microbat	GL429767	*SLC12A2, SLC27A6*	67
Mouse	Chr. 18	*Slc12a2, Slc27a6*	65
Mouse Lemur	Sc_2153	**SLC12A2, *SLC27A6*	74
Opussum	Chr. 3	**SLC12A2*	44
Orangutan	Chr. 5	*SCL12A2, SLC27A6*	65
Panda	GL192553.1	*SLC12A2 , SLC27A6*	68
Pig	Chr. 2	*SLC12A2, SLC27A6*	56
Pika	Sc_2449	**SLC12A2,* SLC27A6*	75
Platypus	Contig 4457	*Data not available*	
Rabbit	Chr. 3	*SCL12A2, SLC27A6*	65
Rat	Chr. 18	*Slc12a2, Slc27a6*	59
Sheep	Chr. 5	*SLC12A2*	65
Shrew	Sc_3494	*Data not available*	99
Sloth	Sc_3915	*Data not available*	74
Squirrel	JH393314.1	*SLC12A2*	66
Tarsier	Sc_4048	**SLC12A2,* SLC27A76*	83
Tree Shrew	Sc_2703	**SLC12A2*	76

Table 7.5. Fibrillin-2 genes in mammals. The mapped location and number of exons of the fibrillin-2 gene among mammalian species is shown. Information was obtained from http://www.ensembl.org (See Section 7.2.1).The * indicates the gene name varies on Ensembl.

Common Name	Chromosomal/Scaffold	Flanking genes	Exons
Birds			
Chicken	Chr. Z	*SLC12A2*	74
Duck	KB743087.1	*SLC12A2*	63
Flycatcher	JH603436.1	*SLC12A2*	66
Turkey	Chr. Z	*SLC12A2*	66
Zebra finch	Chr. Z	*SLC12A2*	67
Fish			
Cave fish	KB882157.1	*slc12a2 , slc27a6*	67
Coelacanth	JH128014.1	*Data not available*	62
Spotted gar	LG_2	*slc27a6, slc12a2*	65
Zebrafish	Chr. 10	*slc12a2*	17
Reptiles & amphibians			
Anole Lizard	Chr. 2	*slc12a2, slc27a6*	66
Chinese softshell turtle	JH211314.1	*scl12a2, slc27a6*	97
Xenopus	GL172643.1	*slc12a2 , slc27a6*	67

Table 7.6 Fibrillin-2 genes in other vertebrates. The mapped location and number of exons of the fibrillin-2 gene in birds, fish, reptiles and amphibians is shown. The information was obtained from http://www.Ensembl.org (See Section 7.2.1).

Human *FBN2* intron/exon architecture was compared with the structure of the *FBN2* gene in other species with a homologous first coding exon ***(Figure 7.2)***. Human, mouse, sheep, ferret and Chinese softshell turtle showed similar *FBN2* exon/intron boundaries with long introns in the 5'region, as also found for *FBN1* ***(Figure 7.1)***.

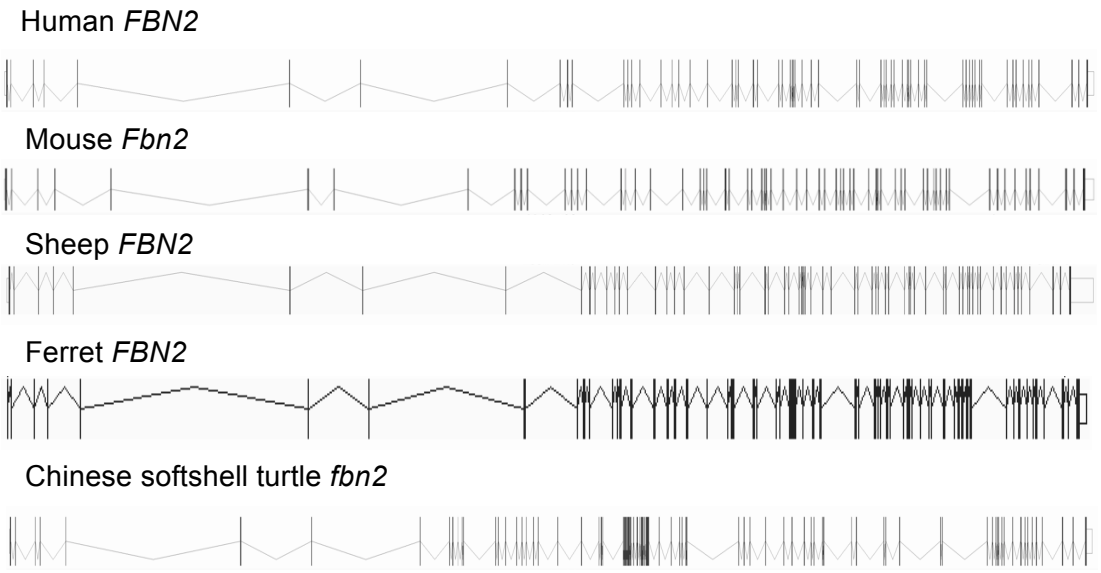

Figure 7.2. Fibrillin-2 gene architecture. *FBN2* gene structure (Chapter 6) of species discussed in Section 7.3.2 is shown. The vertical lines depict exons, and the horizontal (v-shaped) lines represent introns. These images were obtained from http://www.ensembl.org.

Amino acid sequence alignments were performed on a subset of vertebrate species to determine overall sequence homology to human fibrillin-2. The number of vertebrates in the alignment was depleted for fibrillin-2 in comparison to fibrillin-1 ***(Table 7.4)***. This was due to the lack of annotated fibrillin-2 genes in the fish species as well as incomplete sequencing of spotted gar and panda *FBN2* genes. The mammals showed the highest sequence homology, as high as 97.7% (sheep and ferret)***(Table 7.4)***. Similar to fibrillin-1 ***(Table 7.3)***, the Chinese softshell turtle had higher amino acid sequence conservation than the birds, showing a percent identity of 92%, though chicken *FBN2* had a percent identity of 91.4%. Of the fish with an identified fibrillin-2 gene, coelacanth had a complete amino acid sequence and had 80.8% sequence homology with human ***(Table 7.4)***.

7.3.3 Conservation of Fibrillin-3

Fibrillin-3 mapped to chromosome 19 in humans, and contained 64 exons. The gene was located between flanking genes *CERS4* (also known as *LASS4*) (upstream) and *CTXN1, TIMM44* and *CCL25* (downstream). The gene mapped within the annotated *ELAVL1* gene. Annotation and assembly of the *FBN3* genes for many species was incomplete, as seen for *FBN1* and *FBN2*. For example, *FBN3* in the hyrax, platypus, shrew, wallaby, lamprey and anole lizard genomes was mapped to short contigs with no information on flanking genes ***(Table 7.7 and 7.8)***.

Common Name	Chromosome/Scaffold	Flanking genes	Exons
Mammals			
Human	Chr. 19	*LASS4, (ELAVL1), CCL25, TIMM44*	64
Armadillo	JH583495.1	*CTNX1, ELAVL1*	23
Bushbaby	GL873590.1	*CCL25, ELAVL1, TIMM44*	68
Cat	Chr. A2	*ELAVL1, TIMM44*	72
Chimpanzee	Chr. 19	*CCL25, ELAVL1, TIMM44, LASS4*	62
Cow	Chr. 7	*LASS4, TIMM44*	66
Dog	Chr. 20	*LASS4, TIMM44, ELAVL1*	63
Dolphin	Sc_1255	*CCL25*	80
Elephant	Sc_114	*ELAVL1, TIMM44, LASS4, CCL25*	72
Ferret	GL897062.1	*CCL25, ELAVL1, TIMM44, LASS4*	71
Gibbon	GL397524.1	*CCL25, ELAVL1, TIMM44*	59
Gorilla	Chr. 19	*LASS4, TIMM44, ELAVL1*	68
Guinea Pig	Sc_195	*Lass4, Timm44, Elavl1*	67
Hyrax	Sc_3824	*Data not available*	86
Macaque	Chr. 19	*ELAVL1, TIMM44*	67
Marmoset	Chr. 22	*CCL25*	56
Megabat	Sc_1458	*CCL25, LASS4*	67
Opossum	Chr. 3	*ELAVL1, TIMM44*	64
Orangutan	Chr. 19	*CCL25, ELAVL1, TIMM44, LASS4*	66
Panda	GL192871.1	*CCL25, ELAVL1*	76
Pig	Chr. 2	*CCL25, ELAVL1, TIMM44, LASS4*	24
Platypus	Contig_4457	*Data not available*	60

Rabbit	GL018767	*LASS4, TIMM44, CCL25*	68
Sheep	Chr. 5	*CCL25, ELAVL1,*	73
Shrew	Sc_3690	*Data not available*	53
Squirrel	JH393398.1	*CCL25, ELAVL1*	63
Tasmanian devil	GL841426.1	*TIMM44, ELAVL1*	68
Wallaby	Sc_5231	*Data not available*	72

Table 7.7. Fibrillin-3 genes in mammals. The mapped location and number of exons of the fibrillin-3 gene among mammalian species is shown. Information was obtained from http://www.ensembl.org (See Section 7.2.1).

Common Name	**Chromosome/Scaffold**	**Flanking genes**	**Exons**
Birds			
Chicken	Chr. 28	*TIMM44, LASS4*	65
Duck	KB743016.1	*CTNX1, TIMM44*	59
Flycatcher	JH603387.1	*CTNX1, TIMM44*	71
Turkey	Chr. 30	*TIMM44, ELAVL1*	10
Zebra finch	Chr. 28	*TIMM44*	68
Fish			
Cave fish	KB882097.1	*ctnx1, timm44*	65
Cod	Sc_1986	*timm44*	68
Coelacanth	JH126613.1	*timm44*	72
Fugu	Sc_122	*timm44*	62
Lamprey	GL476354	*Data not available*	67
Medaka	Chr. 4	*timm44*	81
Platyfish	JH556710.1	*timm44*	68
Spotted gar	Chr. LG19	*ctnx1, timm44*	64
Stickleback	groupVIII	*ctnx1*	64
Tetraodon	Chr. 1	*timm44*	68
Tilapia	GL831140.1	*timm44*	65

Reptiles/amphibians			
Anole Lizard	GL344437.1	*Data not available*	56
Chinese softshell turtle	JH209348.1	*timm44*	56
Xenopus	GL173191.1	*timm44*	63

Table 7.8. Fibrillin-3 genes in birds, fish, reptiles and amphibians. The mapped location and number of exons of the fibrillin-3 gene in birds, fish, reptiles and amphibians is shown. Information was obtained from http://www.ensembl.org (See Section 7.2.1).

In addition, *FBN3* transcripts more often mapped to contigs and scaffolds rather than fully assembled chromosomes. *FBN3* was less represented in the mammals analysed, but it was identified in the ferret, *Cavia porcellus* (guinea pig), and *Ictidomys tridecemlineatus* (squirrel) genomes ***(Table 7.7)*** though not in mouse or *Rattus norvegicus* (rat). This is consistent with previous findings that the *Fbn3* gene is degenerate in mouse and rat (Corson et al., 2004).

As seen in ***Figure 7.3***, human *FBN3* lacked the long 5' intron regions found in *FBN1* and *FBN2* ***(Figure 7.1 & 7.2)***, with exons and introns relatively evenly dispersed throughout. This was also seen in *FBN3* genes of squirrel and ferret ***(Figure 7.3)***.

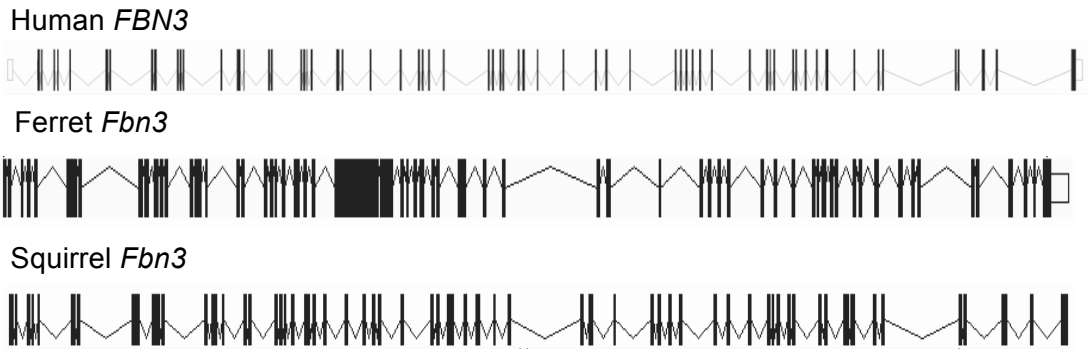

Figure 7.3 Fibrillin-3 gene architecture. *FBN3* gene structure (Chapter 6) of species discussed in Section 7.3.3 is shown. The vertical lines depict exons, and the horizontal (v-shaped) lines represent introns. These images were obtained from http://www.ensembl.org.

The predicted amino acid sequence was analysed to determine homology against several vertebrate species ***(Table 7.4)***. There was overall less homology than that seen for the other fibrillin family members. *Fbn3* in pig had the highest percent identity with human, at 86.5%, primate bushbaby showed the lowest overall sequence homology of the

mammals at 82% ***(Table 7.4)***. Interestingly, squirrel *Fbn3* had 85.1% homology with human. Chicken *Fbn3* had the highest homology with human of the birds at 71.1%. Chinese softshell turtle had the lowest sequence homology at 48.2% and coelacanth had the highest of the fish at 69.2% ***(Table 7.4)***.

7.3.4 Conservation of highest expressing promoter regions for fibrillin-1,-2 and -3

The major promoter regions for *FBN1*, *FBN2* and *FBN3* were identified using the FANTOM5 data for human and mouse **(Chapter 6)*(Table 7.9)***.

Gene	Promoter Name	Location	Sequence of TSS region (5'-3')
Human *FBN1*	p9@FBN1	chr15: 48,937,983-48,937,988	AAAAGT
	p6@FBN1	chr15: 48,937,954-48,937,964	CGCTGCGGGC
	p1@FBN1	chr15: 48,937,885-48,937,933	AAAGGAGGGGGCTGGGGAGCCGCGGCAGAGACTGTGGGTGCCACAAGC
	p2@FBN1	chr15: 48,937,854-48,937,881	CAGGAGCCACAGCTGGCACAGCTGCGAG
	p3@FBN1	chr15: 48,937,841-48,937,844	GCAG
Mouse *Fbn1*	p1@Fbn1	chr2:125,332,156-125,332,181	GGGCCGCAGAGTTGGGGCAGAGACTG
	p2@Fbn1	chr2:125,332,132-125,332,144	GGCGGCCACAG
Human *FBN2*	p1@FBN2	chr5: 127,873,926-127,873,945	CTCCACCGCCGCATCTTCTC
	p2@FBN2	chr5: 127,873,897-127,873,909	GCCCTCTCTCTTG
Mouse *Fbn2*	p1@Fbn2	chr18: 58,369,711-58,369,721	CACGTTGCATC
Human *FBN3*	p2@FBN3	chr19: 8,214,471-8,214,486	AGAGCTGCCACTCGGG

Table 7.9. Human and mouse high expressing transcription start sites (TSS; determined from FANTOM5 database). Conservation of the sequence from 200 bases upstream to 100 bases downstream of these TSSs, which contained the promoter and regulatory elements, was determined across available vertebrates. See *Figures 7.4 and 7.5*.

An analysis of the region flanking the major transcription start sites was performed to determine if the sequence of these promoter regions was conserved across species.

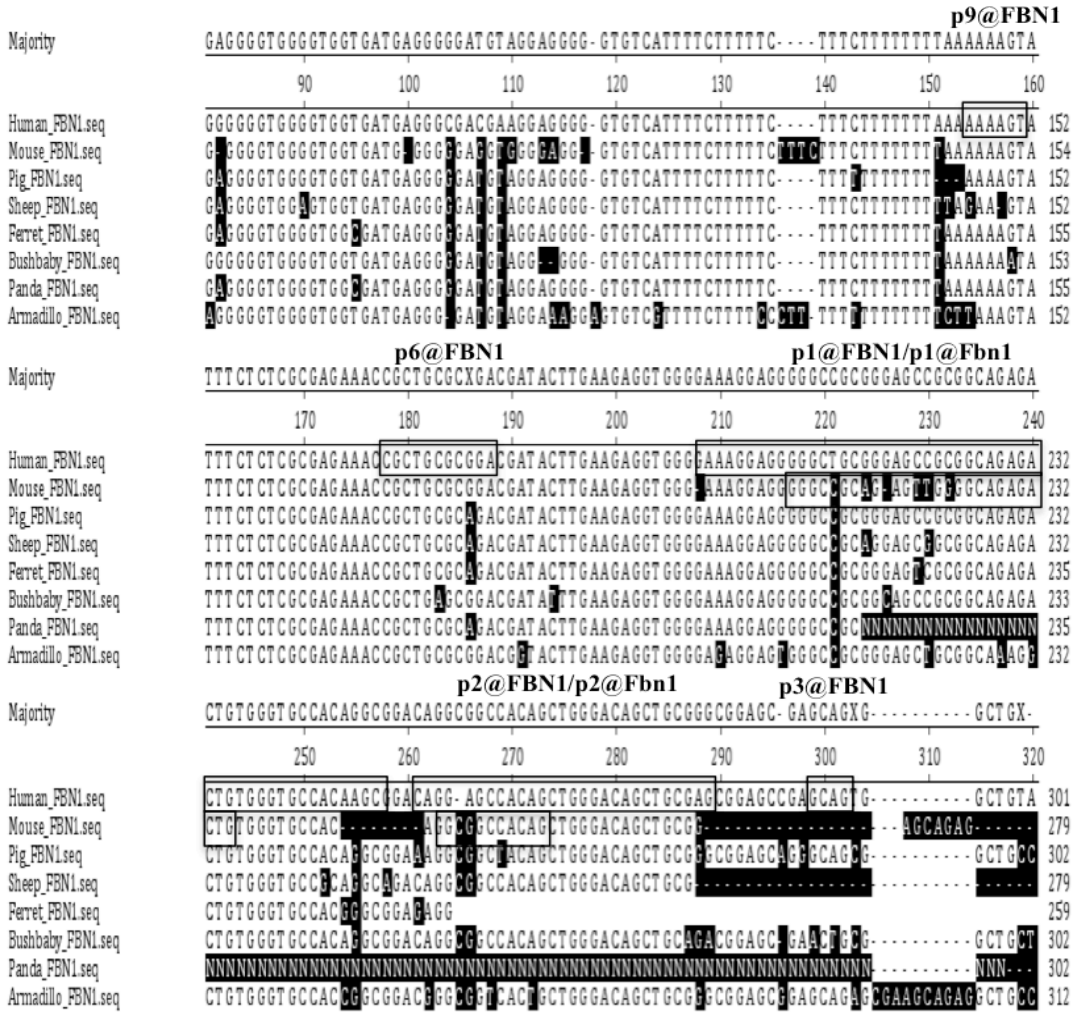

Figure 7.4. Sequence alignment of the promoter region of *FBN1*. The sequences are presented in 5'-3' direction showing the coding strand. Human promoters detected in the FANTOM5 data are boxed and labelled within the human sequence. p1@Fbn1 and p2@Fbn2 are outlined in the mouse sequence. Nucleotides that are different from the human sequence are marked with black shading, except in the 3' region of the panda where the sequence is not available (depicted with "N").

The alignment of the fibrillin-1 promoter region revealed a high level of conservation across the selected species. p1@FBN1, p2@FBN1 and p3@FBN1 showed sequence discrepancies in the ferret. p1@FBN1 was highly conserved, although a single nucleotide change was seen in all the non-human species, showing a pyrimidine switch (T→C) ***(Figure 7.4)***. p2@FBN1 also showed minor differences, with an insertion of C and a transition from an A to a G nucleotide in all species other than humans ***(Figure 7.4)***.

Sequence homology was high for p6@FBN1 and p9@FBN1, but concrete observations were unable to be made for p3@FBN1 due to incomplete sequencing. Directly upstream of the p9@FBN1 promoter region, the C/T rich region identified in (Guo *et al.,* 2008, Summers *et al.,* 2009) was found for all mammals examined ***(Figure 7.4)***.

Of the five promoters for fibrillin-1 of mouse (http://fantom.gsc.riken.jp/zenbu/), p1@Fbn1 and p2@Fbn2 had the highest overall expression, and aligned with p1@FBN1 and p2@FBN1 of human, respectively. p1@Fbn1 showed many sequence variations with the other species, while p2@Fbn2 was showed high sequence similarity ***(Figure 7.4)***. Overall, the transcription start site region of *FBN1* was highly conserved across species ***(Figure 7.4)***.

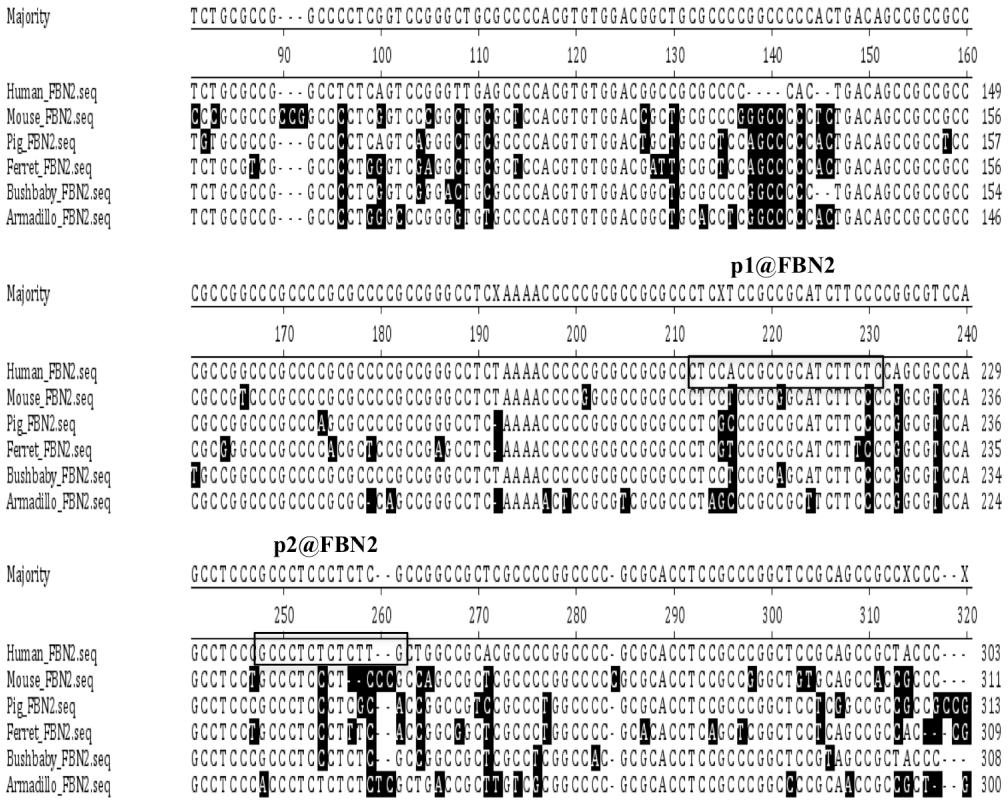

Figure 7.5. Sequence alignment of the promoter region of *FBN2*. The sequences are presented in 5'-3' direction showing the coding strand. Human promoters detected in the FANTOM5 data are boxed and labelled within the human sequence. Nucleotides that are different from the human sequence are marked with black shading.

The alignment of the human sequence containing p1@FBN2 and p2@FBN2 with other species showed high sequence similarity across the transcription start site region ***(Figure 7.5)***. p2@FBN2 showed two distinct sequence substitutions from T, in humans, to C in other species ***(Figure 7.5)***. There was a highly conserved G/C rich repeat region followed by a poly-A tail just upstream of p1@FBN2 ***(Figure 7.5)***. There was one robust promoter identified for *Fbn2* in mouse, p1@Fbn2, but it was located further upstream of the region analysed (http://fantom.gsc.riken.jp/zenbu/).

The alignment of the promoter region for *FBN3* was less obvious (data not provided). Because it is only expressed in a limited number of foetal tissues, and is not found in mouse, only the human sequence was detected in the FANTOM5 data. The 5' sequence was poorly annotated across the species examined; therefore concrete conservation of the region could not be determined. Further studies would be needed to determine the conservation of the *FBN3* promoter, including sequencing the 5' upstream region of *FBN3* in species with an annotated *FBN3* gene, then performing comparative studies.

7.3.5 Conservation of the region of severe mutations

Predicted amino acid sequences of exon 24-33 (www.ensembl.org) for human fibrillin-1, fibrillin-2 and fibrillin-3 were aligned (ClustalW), showing 75.1% homology between fibrillin-1/ fibrillin-2, 69.3% for fibrillin-2/ fibrillin-3 and 64.5% for fibrillin-1/fibrillin-3 ***(Figure 7.6)***. This was greater than the sequence similarity over the whole amino acid sequence (fibrillin-1/fibrillin-2 = 68.3%; fibrillin-2/fibrillin-3 = 67.4%; fibrillin-1/fibrillin-3 = 60.1%).

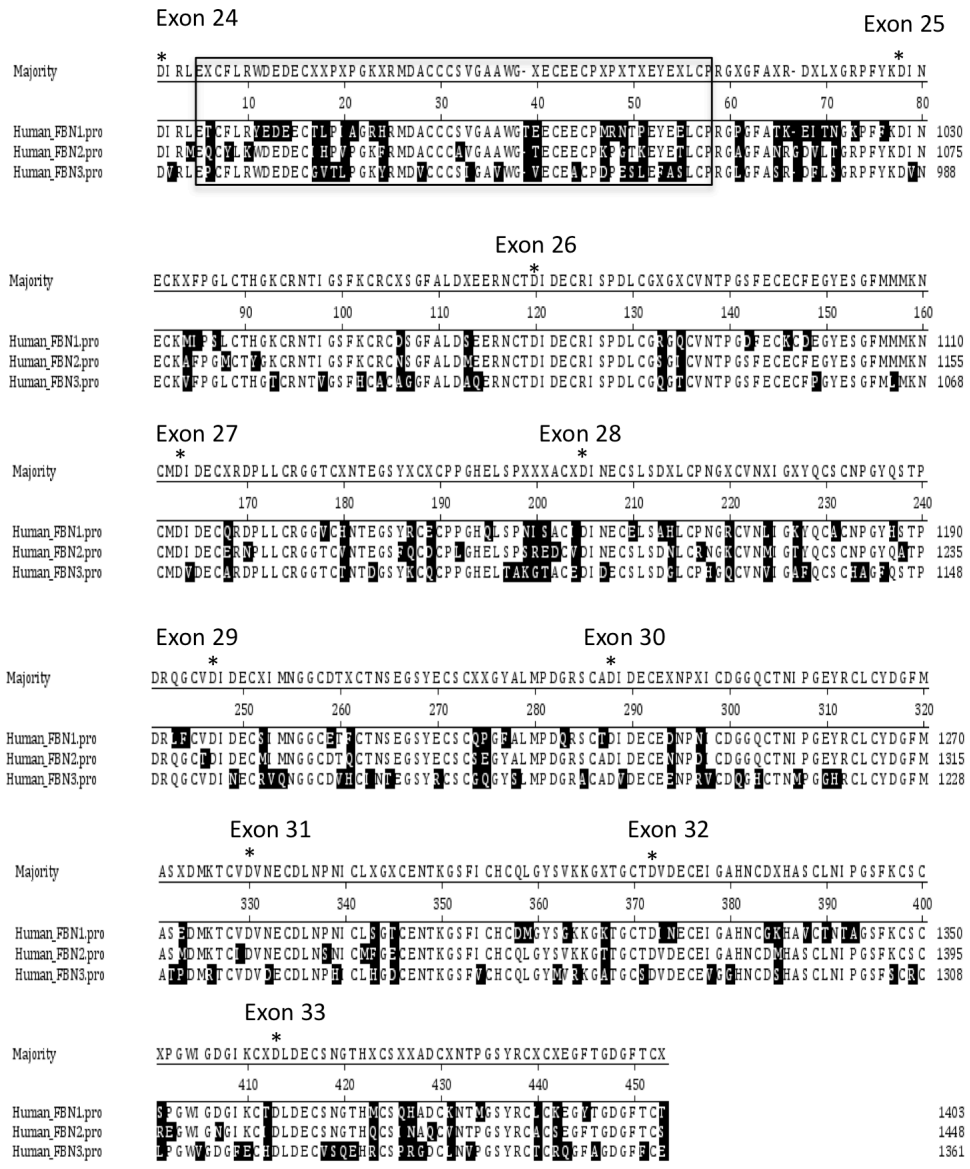

Figure 7.6. Predicted amino acid sequence of exons 24 to 33 in the three *FBN* genes. The conserved TB domain (TB5) is outlined. The * symbolises the beginning of the exons. Black shading shows sequence variation when compared to the majority sequence.

The sequence similarity of the region was higher than the overall amino acid conservation ***(Table 7.10)***. In addition, the eight cysteine residues associated with the TB5 (in exon 24), were conserved across all three fibrillins ***(Figure 7.6)*** consistent with earlier TB domain analysis (Piha-Gossack *et al.,* 2012). The region of severe *FBN1* mutations corresponding to the region of most *FBN2* mutations was highly conserved across several vertebrate species for both *FBN1* and *FBN2* ***(Table 7.10)***.

Common Name	Human FBN1 % identity with other FBN1 vertebrates	Human FBN2 % identity with other FBN2 vertebrates
Mouse	96.9	98.1
Pig	98	99.2
Sheep	98.3	98.7
Ferret	97.8	98.7
Bushbaby	98	95
Panda	98	X*
Armadillo	96.7	85.1
Chicken	86.7	92.9
Flycatcher	88.5	85.7
Turkey	87.1	43.2
Coelacanth	83.2	88.9
Fugu	73.2	X
Medaka	74.3	X
Spotted gar	80	X
Tetraodon	73.6	X
Turtle	86.7	94.1

Table 7.10. Percent Identity of predicted amino acid sequence for exons 24 to 33 of fibrillin-1 and fibrillin-2. The % identity was calculated from the Clustal W alignment (DNAStar, Lasergene, Madison, WI, USA) of the sequences against the human sequence. The X* signifies unannotated sequence in the region, while the X signifies that a transcript was not identified for that species.

This region showed extremely high similarity in mammalian fibrillin-1 and fibrillin-2, highest in pig at 98.3% and 99.2%, respectively. Chicken showed the highest percent identity of the birds (86.7% for fibrillin-1 and 92.9% for fibrillin-2), and coelacanth the highest for the fish species (83.2% for fibrillin-1 and 88.9% for fibrillin-2). Sequence homology was also high in the Chinese softshell turtle at 86.7% and 94.1% for fibrillin-1 and fibillin-2 respectively. Thus the region showed considerable sequence homology across the group of vertebrates that could be assessed ***(Table 7.10)***

The high degree of conservation of this region is consistent with the severe nature of the phenotype caused by mutations in the region. The conservation of amino acids affected by a number of mutations with phenotypes ranging from severe neonatal to mild adult MFS and CCA ***(Table 7.11)*** was examined across species.

Mutation	Exon Location	Domain Region	Mutation Type	Disease	Reference
Fibrillin-1					
p.Ile953_Asp1113del	24	TB5/cbEGF	In frame deletion of exons 24 to 26	Neonatal MFS	Apitz *et al.,* 2010
p.Gly1013Arg	24	TB5/cbEGF	Tv	Neonatal MFS	Nijbroek *et al.,* 1995
p.Ile1048Thr	25	cbEGF	Tv	Neonatal MFS	Lonnqvist *et al.,* 1996
p.Arg1137Pro	27	cbEGF	Missense	MFS	Dietz *et al.,* 1991
p.Cys1265Arg	30	cbEGF	Ts	MFS	Montgomery *et al.,* 1998
p.Gly1301Val	31	cbEGF	Ts	MFS	www.umd.be/FBN1/
p.Leu1364_Asp1404	33	cbEGF	In frame deletion	Neonatal MFS	Blyth *et al.,* 2008
p.His2685Ilefs*9	64	cbEGF	Splice site mutation leading to exon 64 skipping	Marfanoid phenotype and severe lipodystrophy	Jacquinet *et al.,* 2014
p.Lys2719Aspfs*18	64	cbEGF	2 nt. deletion/ frameshift	Marfanoid phenotype and severe lipodystrophy	Graul-Neumann *et al.,* 2010
p.Lys2719Thrfs*12	64	cbEGF	12 nt. deletion/ frameshift	Marfanoid phenotype and severe lipodystrophy	Goldblatt *et al.,* 2011
p.Arg2726Glufs*9	64	cbEGF	8 nt. deletion/ frameshift	Marfanoid phenotype and severe lipodystrophy	Takenouchi *et al.,* 2013
Fibrillin-2					
p.Gly1056Asp	24	TB5/cbEGF	Tv	CCA	Park *et al.,* 1998
p.Asp1115His	26	cbEGF	Tv	CCA	Babcock *et al.,* 1998

p.Cys1198Tyr	28	cbEGF	Ts	CCA	Gupta *et al.,* 2002
p.Cys1323Arg	31	cbEGF	Ts	CCA	www.umd.be/FBN2/
p.Cys1425Gly	33	cbEGF	Tv	CCA	Callewaert *et al.,* 2009

Table 7.11 Mutations affecting amino acids examined for conservation. The mutations analysed were within the severe MFS region (exon 24-33) and those with a lipid depletion phenotype (Exon 64) (Section 7.1 and 7.3.5). Transitions (purine to purine or pyrimidine to pyrimidine) are depicted with Ts and transversions (switch from a purine to a pyrimidine or vice versa) with Tv.

Mutation p.Ile953_Asp1113del was discovered in fibrillin-1 of a patient presenting with severe neonatal MFS, ultimately leading to premature death (Apitz *et al.,* 2010)***(Table 7.11)***. The mutation results in an in frame deletion of exon 24 to 26. The deletion begins at Ile953, which is located upstream of TB5 of fibrillin-1 and amino acid Ile 953 is conserved in fibrillin-1 and fibrillin-2 ***(Figure 7.6)***, highly conserved across vertebrates, along with exons 24-26 ***(Figure 7.7)***. p.Leu1364_Asp1404del of fibrillin-1, was also identified in a patient with severe neonatal MFS, resulting in an in frame deletion of exon 33 (Blyth *et al.,* 2008)(***Table 7.11)***. Exon 33 contains a cbEGF binding domain and N-glycosylation site (NGT) and is highly conserved across the vertebrates, with slight sequence differences in the fish species ***(Figure 7.8)***. Leu1364 is homologous across the three fibrillin proteins ***(Figure 7.6)***. Amino acids associated with mild forms and phenotypes of human MFS (Ile1048, Arg1137, Cys1265, and Gly1301 (Lonnqvist *et al.,* 1996, Dietz *et al.,* 1991, Blyth *et al.,* 2008, Montgomery *et al.,* 1998))***(Table 7.11)*** are also highly conserved across vertebrate species ***(Figure 7.8)*** and conserved across the fibrillin protein family ***(Figure 7.6)***.

The recurrent mutation p.Gly1013Arg in fibrillin-1 has been associated with severe adult MFS, including cardiovascular complications (Nijbroek *et al.,* 1995)***(Table 7.11)***. The glycine residue at that position in fibrillin-1 is highly conserved across the vertebrates ***(Figure 7.7)***. Interestingly, a mutation at the glycine residue residing in the same location on fibrillin-2, Gly1056, has been implicated in a mild form of CCA ***(Table 7.11)*** and is fully conserved across the selected vertebrates ***(Figure 7.8)***. Both mutations are located within highly conserved cbEGF-like binding domains of fibrillin-1 and fibrillin-2 ***(Figure 7.7 & 7.8)***. Furthermore, the glycine amino acid residue at that position is conserved in fibrillin-3 ***(Figure 7.6)***. Amino acid substitution mutation p.Asp1115His in fibrillin-2

was identified in a patient presenting phenotypically with CCA, located in exon 26 and Asp1115 was found to be fully conserved across the selected vertebrates ***(Figure 7.8)***. Fibrillin-2 amino acid residues, Cys1198, Cys1323 and Cys1425 (Gupta *et al.,* 2002, Callewaert *et al.,* 2009) (http://www.umd.be/FBN2/) have been associated with CCA, and were also highly conserved amino acid residues across the selected vertebrates ***(Figure 7.8)***.

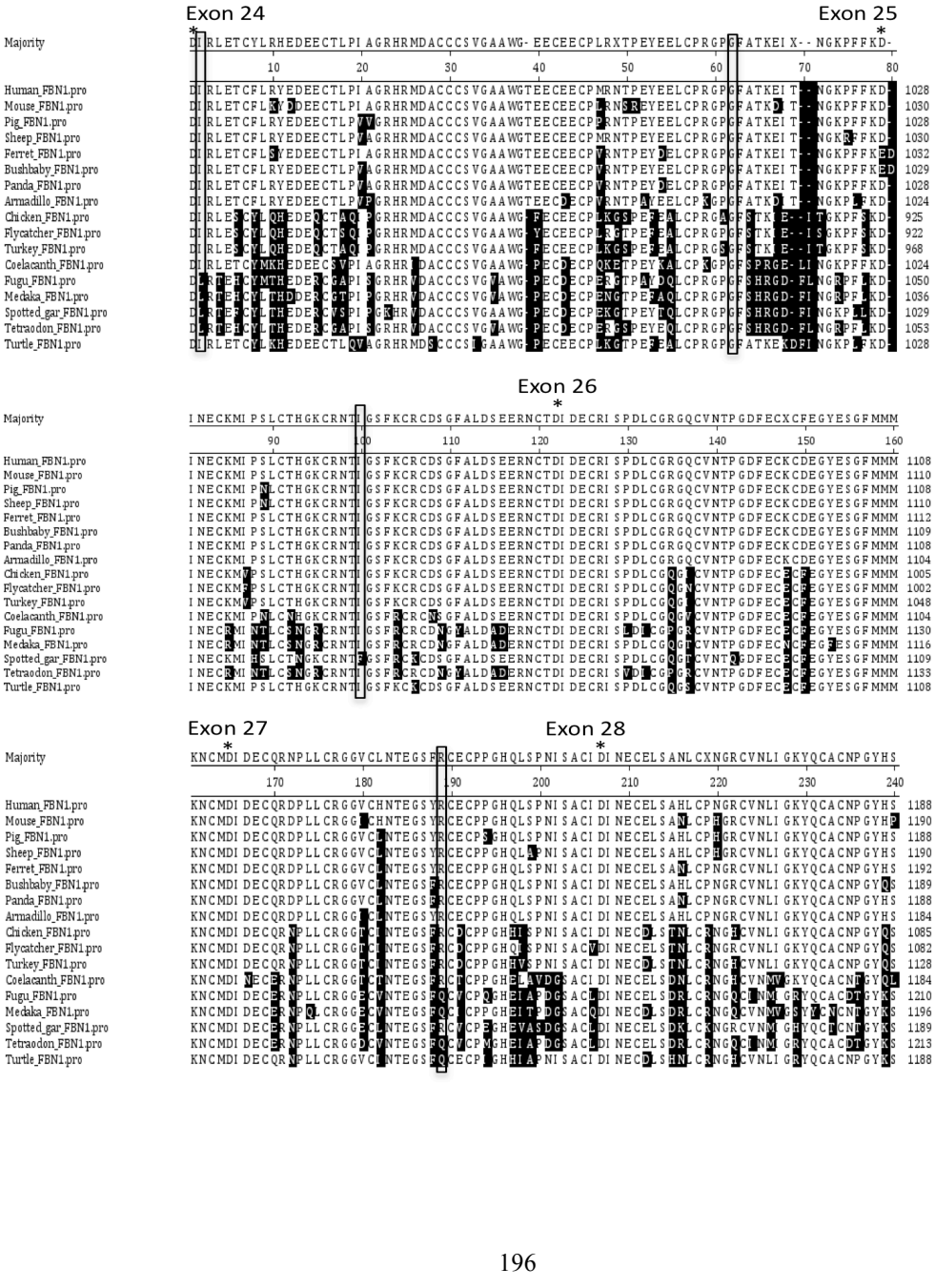

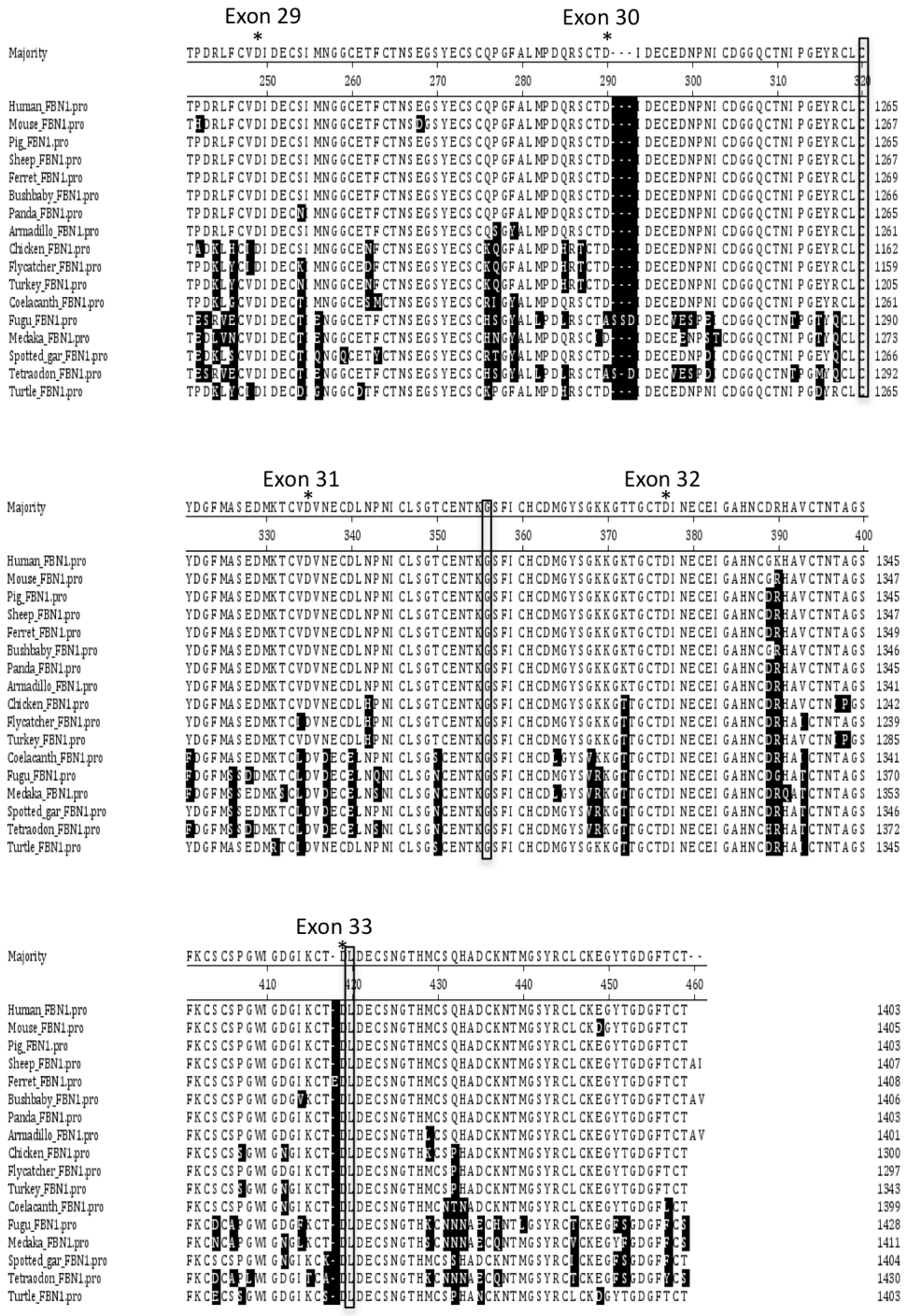

Figure 7.7 The region of fibrilin-1 where mutations causing severe phenotypes occur. Clustal W alignment (DNAStar, Lasergene, Madison, WI, USA) of exon 24-33 across vertebrates. The amino acids analysed are outlined and sequence differences from the human sequence are shaded in black.

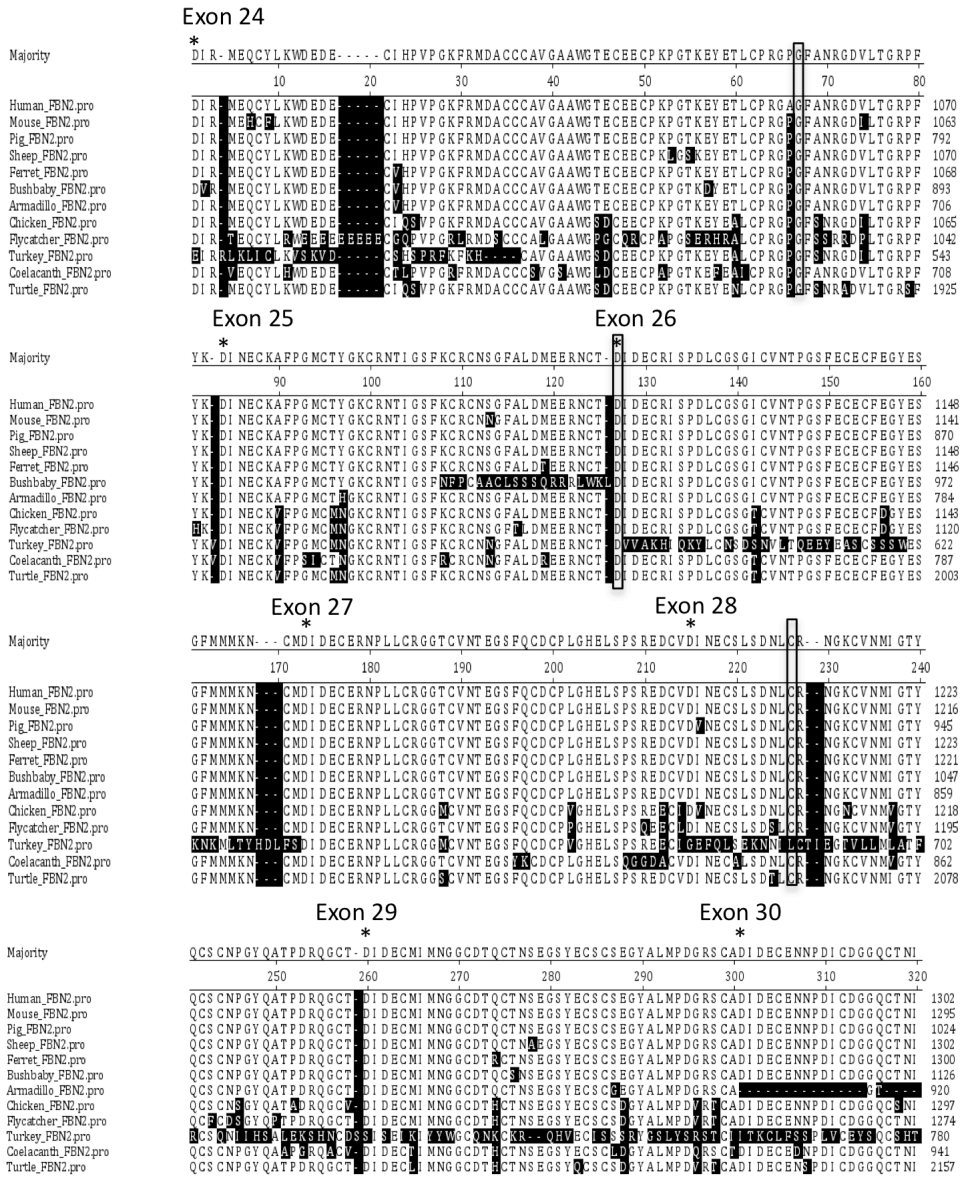
Exon 24
Exon 25
Exon 26
Exon 27
Exon 28
Exon 29
Exon 30
Majority
Human_FBN2.pro
Mouse_FBN2.pro
Pig_FBN2.pro
Sheep_FBN2.pro
Ferret_FBN2.pro
Bushbaby_FBN2.pro
Armadillo_FBN2.pro
Chicken_FBN2.pro
Flycatcher_FBN2.pro
Turkey_FBN2.pro
Coelacanth_FBN2.pro
Turtle_FBN2.pro

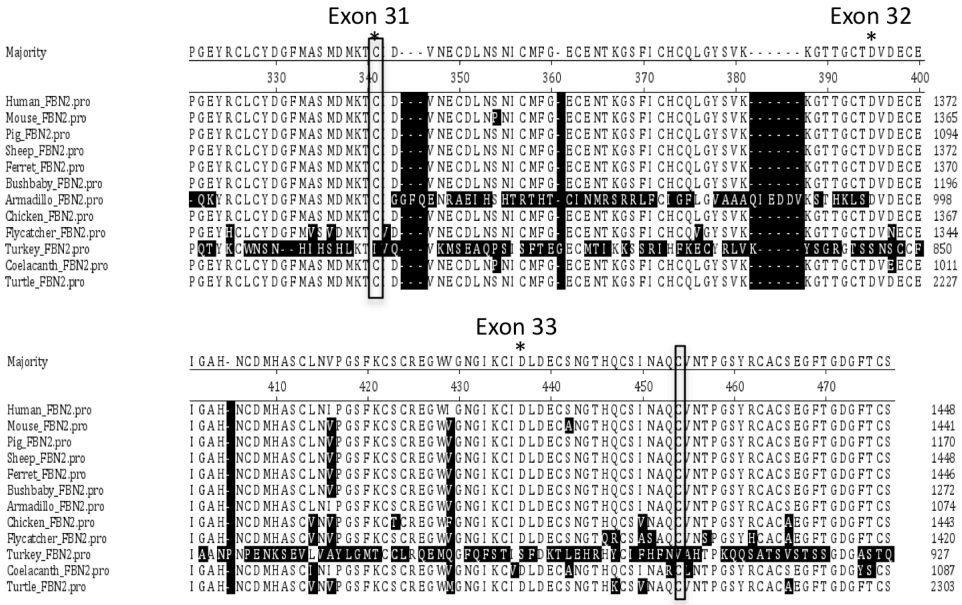

Figure 7.8. The region of fibrilin-2 where mutations causing CCA occur. Clustal W alignment (DNAStar, Lasergene, Madison, WI, USA) of exon 24-33 across vertebrates. The amino acids analysed are outlined and sequence differences from the human sequence are shaded in black.

7.3.6 Fibrillin-1 mutations associated with lipid depletion

As discussed in **Chapter 3, Section 3.1.4,** severe generalised lipodystrophy was recently identified in four patients diagnosed with MFS or marfanoid habitus (Jacquinet *et al.,* 2014, Graul-Neumann *et al.,* 2010, Goldblatt *et al.,* 2011, Takenouchi *et al.,* 2013). All four cases had mutations affecting exon 64, at the C terminus of fibrillin-1 ***(Table 7.11)(Figure 7.9)***. All the mutations coded for premature stop codons resulting in a truncated protein. The mutations universally removed the amino acid sequence N'RGRKRRSTNETDASNIE C' (which will be referred to as the exon 64 lipid region) within exon 64, highlighted in ***Figure 7.9***. Furthermore, the mutations subsequently deleted exon 65.

Exon 64 is not highly conserved among fibrillin-1, -2 and -3 in humans and there are no known mutations in the aligning regions of exon 64 in fibrillin-2 or fibrillin-3. In addition, the exon 64 lipid region of fibrillin-1 was not conserved across the fibrillin gene family ***(Figure 7.10)***. The conservation of exon 64 in fibrillin-1 was analysed across the selected vertebrates ***(Figure 7.11)***. It was well conserved across mammals with sequence

discrepancies in bird, reptile and fish species, not only within the N' terminus of the exon but also in the last five amino acids of the lipid region ***(Figure 7.11)***. Furthermore the 15 amino acid residues upstream of the exon 64 lipid region were highly conserved across all the vertebrates analysed ***(Figure 7.11)***.

A. Reference Sequence exon 64 (fibrillin-1)

2685 HCVSGMGMGRGNPEPPVSGEMDDNSLSPEACYECKINGYPK**RGRKRRSTNETDASNIE**

B. c.8155_8156del (2 nt. deletion)

2685 HCVSGMGMGRGNPEPPVSGEMDDNSLSPEACYEC|DQWLPQTGQETEKHKRNX

C. c.8156_8175del (12 nt. deletion)

2685 HCVSGMGMGRGNPEPPVSGEMDDNSLSPEACYEC|TGQETEKHKRNX

D. c.8175_8182del 8 nt. deletion

2685 HCVSGMGMGRGNPEPPVSGEMDDNSLSPEACYECKINGYPK|ETEKHKRNX

E. c.8226+1G-T Exon 64 deletion

2685 |X

Figure 7.9. Identifying the amino acid sequence of the exon 64 lipid region of fibrillin-1. This figure outlines the four fibrillin-1 mutations associated with a lipodytrophy phenotype *(Table 7.11)*. (A) Shows the reference sequence for exon 64 in an unaffected phenotype, (B) shows the sequence of a patient with a c.8155_8156del mutation, (C) shows the sequence of a patient with a c.8156_8175del mutation, (D) shows the sequence of a patient with a c.8175_8182del and (E) shows the sequence of a patient with a c.8226+1G-T mutation, resulting in the deletion of exon 64. (B-E) result in a truncated protein. The amino acid sequences highlighted in pink share homology with the reference sequence. The blue line represents where the mutation occurs. The amino acids depicted after the blue line are those that are incorporated in the protein as a result of the frame shift. The X represents the stop codon. The exon 64 lipid region is shown in bold in the reference sequence (A). This figure was adapted from (Jacquinet *et al.,* 2014).

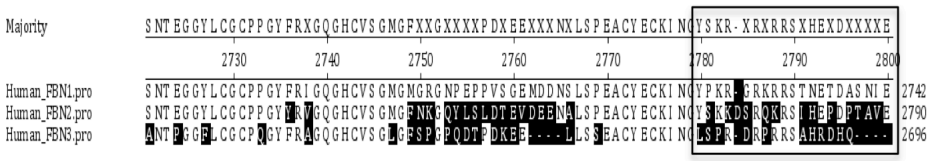

Figure 7.10 Exon 64 alignment of fibrillin-1, -2 and -3, in human. A ClustalW alignment (DNAStar, Lasergene, Madison, WI, USA), shows the exon 64 lipid region (boxed in amino acids black; Section 7.3.6), and sequence differences from the fibrillin-1 sequence are shaded in black.

Figure 7.11 Conservation of exon 64 of fibrillin-1 across vertebrates. A ClustalW alignment (DNAStar, Lasergene, Madison, WI, USA), shows exon 64 lipid region (boxed in amino acids black; Section 7.3.6), and sequence differences from the human sequence are shaded in black.

7.4 Discussion

7.4.1 Fibrillin conservation

This chapter presented evidence that the fibrillin gene family is well conserved across vertebrate species. This was based on the presence of annotated fibrillin genes/transcripts, chromosomal synteny, gene architecture and amino acid sequence homology seen across a wide range of vertebrates. *FBN1*, *FBN2* and *FBN3* genes were present in the majority of annotated genomes in the Ensembl database, including high representation across mammals, fish, birds and reptile species. Interestingly, there was a noticeable absence of annotated *fbn2* genes in fish species, while the *fbn3* identified in fish species had the intron/exon architecture expected for *fbn2* genes ***(Table 7.6)(Figure 7.3)***. This could indicate the degeneration of *fbn2* in some fish species (similar to *Fbn3* in mouse and rat), although this seems unlikely since four fish species did have a *fbn2* gene ***(Table 7.6)***. The

annotated *fbn3* gene could represent an ancestral *fbn*2/3 gene. Alternatively, this result could reflect incomplete sequencing and annotation of these genomes.

During the course of this research, two studies emerged proposing the evolutionary history of the fibrillin family based on the unique protein domain architecture (Piha-Gossack *et al.,* 2012, Robertson *et al.,* 2010). Roberston *et al*. (2010) concluded that a single fibrillin gene emerged first based on the unique protein domain organisation **(Chapter 1, Section 1.3.2)** and the presence of a single fibrillin gene in early Cnidarians (Jelly fish) (Reber-Muller *et al.,* 1995). Piha-Gossack *et al.* (2012) proposed that the ancestral fibrillin gene underwent a gene duplication event at the point when jawed vertebrate species emerged, yielding *fbn1* and *fbn*2/3. Through the evolution of tetrapods, the *fbn*2/3 gene split into separate and functionally relevant genes, known as *fbn2* and *fbn*3. This is most likely the reason for the lack of identified *fbn2* genes in fish, and the *fbn3* genes identified may be the merged *fbn*2/3.

Though the emerging evolutionary research supported the findings of this study, the loss of a functional *Fbn3* gene in mice and rats is still not understood. Since the duplication event occurred prior to mammal and bird evolution, *FBN3* should be present in all mammals, including mice and rats (Corson *et al.,* 2003). Corson *et al.* (2003) demonstrated that a functional *Fbn3* was not present in mice or rats though *Fbn1* and *Fbn2* are present. They speculate that the *Fbn*3 gene may have been disrupted during mouse evolution because remnants of the gene are still present between the flanking genes. This present study was able to identify a total of 47 vertebrates with annotated *FBN3* genes, including members of the rodent family, guinea pig and squirrel, which also contained annotated genes for *Fbn1* and *Fbn2.* The evidence that *Fbn3* is present and associated with transcripts in other rodent family members could help to provide further information about the role of *Fbn3*. Future work could be done to knock down or knockout the *Fbn3* gene in the other rodent family members to examine whether the gene is redundant in rodents.

Extensive work on the *FBN1* promoter region had been previously done (Summers *et al.,* 2009). The 5' UTR region of *FBN1* was shown to be highly conserved in primates (Singh

et al., 2008) and in multiple vertebrate species including mouse and pig (Summers, *et al.,* 2009, Singh *et al.,* 2006). The present study provides evidence that the specific transcription start sites in *FBN1* might be shared across species ***(Figure 7.4)***. This study included an analysis of conservation of the promoter regions of *FBN2* and *FBN3*. The *FBN2* promoter region was highly conserved across the selected species, and it was inferred that TSS determined by FANTOM5 CAGE analysis ***(Table 7.9),*** identified high expressing promoters in sequence that was conserved across the species analysed ***(Figure 7.5)***. Furthermore, this study identified a conserved G/C region upstream of the major transcription start site of *FBN2* ***(Figure 7.5)***. There was very poor sequence homology for *FBN3* across the selected species, including the promoter region defined by p2@FBN3, and hence it seems likely that this region is not strongly conserved.

This study also demonstrated high homology across regions of the *FBN1* and *FBN2* genes associated with severe mutations, indicating the importance of specific amino acids, in the fibrillin family. The regions contained exon 24-33 in *FBN1* and *FBN2*. The conservation analysis showed overall amino acid sequence homology across these regions, that was higher than for the total protein, even in fibrillin-3 ***(Figure 7.6)***. In addition, there was high conservation of reported single amino acid residues across vertebrates ***(Figure 7.7 and 7.8)*** and the fibrillin protein family **(Section 7.3.5)**. A study done on the factor IX gene, involved in the development of hemophilia B, recognised that the more conserved the amino acid, the more likely mutation of that amino acid would lead to disease (Popat *et al.,* 1991), a widely accepted theory in the scientific community (Strachen T., 2004). While the mutations examined were all already implicated in disease, the conservation and consensus sequences indicate regions of fibrillin-3 that may harbour mutations with phenotypic effect.

In contrast, the proposed exon 64 lipid region was not highly conserved across the fibrillin family, though it was conserved across *FBN1* genes in mammals ***(Figure 7.10 and 7.11)***. Exon 64 is located downstream the final cbEGF binding domain in fibrillin-1. The exon 64 lipid region amino acid sequence that was removed as a result of the mutations ***(Figure 7.9)(Table 7.11)*** consisted of 50% polar and acidic amino acids, and was replaced ***(Figure 7.9B,C and D)*** in three cases with a highly charged amino acid sequence ETEKHKRN (Jacquinet *et al.,* 2014). Since mutation c.8226+G-T does not

add the highly charged amino acid sequence, it may not be the only factor in the development of adipose depletion in with exon 64 fibrillin-1 mutations. Classic MFS caused by mutations in other exons generally presents with fat depletion along with symptoms that are recognised by the Ghent criteria (Summers *et al.,* 2012), for example an exon 25 missense mutation (Summers *et al.,* 2006). It is likely that mutations found in exon 64 and 65 that result in classic MFS will also involve a lipodystrophy-like phenotype (Collod-Beroud *et al.,* 2003), possibly due to protein missfolding (Jensen *et al.,* 2014). Therefore the exon 64 lipid region and the whole of the unaffected exon 65 sequence may be important in adipose maintenance.

7.4.2 Conclusions

This chapter has shown results consistent with available literature supporting the evolutionary trends and conservation of the fibrillin gene family. The long 5' introns of *FBN1* and *FBN2* are consistent with slower production of mature mRNA than *FBN3* which lacks these long introns (Singh and Padgett, 2009) and may reflect the different functions of the genes. In addition, preliminary results showed that the TSS regions of *FBN1* and *FBN2* are conserved across vertebrates, although very different from each other. This suggests that other species would also show differential expression of the two genes (**Chapters 3 and 4**), mediated through the different transcription factor binding motifs associated with the conserved promoter region (**Chapter 6**). Future studies (suggested in **Section 7.3.5)** will need to be conducted to examine the conservation of the TSS region in *FBN3.* Finally, the chapter has proposed a highly conserved amino acid sequence within exon 64 of *FBN1* that may be important in adipose development.

Chapter 8. General Discussion and Future Studies

8.1 Summary of Results

The underlying hypothesis to be tested by the research reported in this thesis was that fibrillin-1 is a central regulator of mesenchymal cell differentiation (Summers *et al.,* 2010). The results showed that the three fibrillin genes are expressed at different developmental stages and in different mature cell types **(Chapters 3 and 4)**, in spite of the high level of conservation of the protein three sequences across a wide evolutionary spectrum **(Chapter 7)**. The different roles were reflected in both the genes with which each fibrillin gene was co-expressed **(Chapters 3 - 5)** and the sequences of their regulatory regions (promoters) **(Chapters 6 and 7)**. However, when *FBN1* was knocked down in fibroblasts **(Chapter 5)**, only a small number of genes were up and downregulated, suggesting that fibrillin-1 may be an endpoint rather than key regulator of mesenchymal cells.

8.1.1 Fibrillins are differentially expressed.

The first aim of this study **(Chapter 1, Section 1.5)** was to analyse the expression of the three fibrillin genes at different stages of development and differentiation. Previous studies using animal models and human tissues had shown that each fibrillin was present at different developmental stages. Zhang *et al.,* (1995) performed *in situ* hybridization assays on mouse embryos at several stages and first proposed that fibrillin-1 was expressed in late embryogensis and involved in structural support of developing tissues. Also, fibrillin-2 was a possible regulator of early elastic fibre formation and highly present in early morphogenesis (Zhang *et al.,* 1995). Quondamatteo *et al.,* (2002) showed that fibrillin-1 and fibrillin-2 have different developmental roles based on variability in levels of the proteins in different human foetal tissues and organs (weeks 5-12 of gestation). Fibrillin-3 was later characterised by (Corson *et al.,* 2004) and proposed to have specific functions in human development (Sabatier *et al.,* 2010). Corson *et al.* (2004) demonstrated that fibrillin-3 was not present within rodents, though expressed in human foetal tissues such as fibroblasts, brain, and lung (gestation weeks 6-12).

In the present study, the expression of fibrillins in various human cell lines was examined. The results presented in **Chapters 3 and 4** showed that *FBN3* was the earliest fibrillin to be expressed during ES cell differentiation to mesoderm, followed by *FBN2* and then *FBN1*. *FBN3* was associated with the pluripotent state and its unique role was highlighted by the fact that it was not expressed in any of the other cell lines examined, which represent more mature mesenchymal states. *FBN2* was expressed at the stage of mesoderm formation, suggesting *FBN2* maybe a mesoderm marker. *FBN1* was expressed later than either *FBN2* or *FBN3*, in cells already predetermined to go to mesenchymal lineages, but it was minimal at the highest level of differentiation suggesting that it may be a marker for relatively plastic mesenchymal cells prior to commitment to a specific lineage. Surprisingly, given the lipodystrophic phenotype associated with Marfan syndrome and other *FBN1* mutations, fibrillin-1 was apparently required only at the early stages of adipogenic differentiation, and degraded once the process was established. The presence of fibrillin-1 in early adipose differentiation **(Chapter 3, Section 3.3.3)** may be evidence that it assists in preadipocyte scaffold formation. The mRNA was also expressed in adult adipocytes **(Chapter 6)** so may be involved in the constant turnover of adipose ECM. In addition, fibrillin-1 was not required to sustain the ECM of cells in culture, since one chondrocyte lineage and one osteosarcoma line could proliferate in the absence of extracellular fibrillin-1 protein. Consistent with the hypothesis that fibrillin-1 is a marker for early mesenchymal stages, the osteosarcoma line MG63, with a relatively immature osteoblast phenotype, had a high level of *FBN1* mRNA and fibrillin-1 protein while the more mature osteosarcoma SAOS2 had very low levels.

8.1.2 Fibrillins are co-expressed with genes characteristic of different roles

As shown in **Chapter 3**, expression of *FBN3* was highly correlated with genes involved in early embryogenesis, ECM formation, neuronal development and importantly with markers of pluripotency. *FBN3* mRNA has been detected in meiosis stage II oocytes (Kocabas *et al.,* 2006) suggesting that it may be one of the maternal mRNAs that populate the oocyte to support the early development of the zygote. Co-expressed genes in later foetal stages (Sabatier *et al.,* 2010) were not assessed here but would likely be a

different set of genes, possibly associated with development of the foetal mesenchyme. Alternatively this later expression of *FBN3* might reflect maintenance of a small population of pluripotent cells within foetal tissues. These hypotheses could be tested using the co-expression analysis outlined here on RNA from foetal tissues. The origin (maternal or embryonic) of the *FBN3* mRNA in very early embryos could be tested using genetic variation in the *FBN3* gene.

FBN2 was co-expressed with genes involved in mesoderm formation (notably *EOMES*) and limb development, suggesting *FBN2* maybe a mesoderm marker. In fact, there were no genes that co-expressed with *FBN2* in the later differentiated samples and the mRNA levels remained at a low level in all the cell types (**Chapter 4**). This is consistent with observations that *FBN2* may have a role in guiding the formation of the elastin associated microfibrils during development (Quondamatteo *et al.,* 2002). Similarly, *FBN2* mRNA levels remained unaltered despite the depletion of *FBN1* in siRNA experiments discussed in **Chapter 5**, supporting differential roles for the fibrillin gene family.

The co-expression analyses presented in **Chapters 3, 4** and **5** provided further evidence of the distinct role of *FBN1*. Its expression was highly correlated with ECM specific genes and genes associated with connective tissue diseases. One association that was strongly supported by the co-expression studies was the link between the ECM and the cytoskeleton. Recent studies suggest changes within the ECM, whether through collagen reorganisation or mechanosensing, can alter cellular mobility by causing disruptions in cytoplasmic actin fibres (Starke *et al.,* 2014, Provenzano and Keely, 2011). Therefore, it is suggested that ECM shape can dictate the plasticity and adaptive response of the cytoskeleton ***(*Chapter 5, *Figure 5.17).*** This is important since fibrillin-1 microfibrils are valuable structural components of the ECM and this was highlighted by the frequent appearance of cytoskeleton genes in the ECM clusters containing *FBN1* probesets in unaltered adult mesenchyme cells **(Chapter 4)** and upregulation of actin / actin related genes in siRNA treated fibroblasts **(Chapter 5)**. Since the studies presented in the thesis were performed in cell culture systems, whether cancer, transformed or primary cells types, the need for communication between the cytoskeletal actin and ECM fibrillin microfibrils was limited and further studies should be conducted using tissues or mixed cell type models. Future work within *in vivo* animal model systems that have all three

fibrillin genes, for example pig, would greatly improve the study across tissue types (Lunney, 2007). For instance, creating a *FBN1* knockdown pig would allow for further studies on actin response in many mesenchyme tissue types.

8.1.3 Fibrillin genes use alternative promoters in different cell types

In **Chapter 6** it was shown that the fibrillin gene family has differentially regulated transcription start sites, different promoter structures and no identifiable consistent transcription factors **(Chapter 6)**. This was determined using deepCAGE data obtained from FANTOM5. Both *FBN1* and *FBN2* shared similar broad promoter structures, with transcription initiation occurring at different nucleotides depending on the cell/ tissue type. Promoters for both genes were highly active in cells of mesenchyme origin, for example fibroblasts. The major *FBN1* promoters maintained high expression in adult mesenchyme cells, consistent with the presence of motifs for transcription factors TBX4 and TBX5, which are involved in later limb development **(Chapter 6, Section 6.5)**. Alternate promoter usage was evident with p7@FBN1, showing high levels of expression in neuronal tissues and regulation by neuronal transcription factor, *FOXD3*. Conversely, *FBN2* promoters were shown to be regulated by transcription factors highly correlated with mesoderm formation, for example *KLF4, PAX5* and *TRAP2B* **(Chapter 6, Section 6.4.5)**. Furthermore, several *FBN2* promoters showed high expression in osteoblast cell types, which was consistent with predicted regulation by osteoblast formation transcription factor *HIF1A* **(Chapter 6, Section 6.5)**. In contrast, the promoter structure of *FBN3* showed a single major TSS with tissue expression mainly within foetal and embryonic cell types. The promoter was predicted to be regulated by key embryogenesis transcription factors, *SP1*, *TRAF4* and *PATZ1* **(Chapter 6, Section 6.4.5)**.

8.1.4 Fibrillins are highly conserved across vertebrates

There are significant phenotypes associated with mutations of *FBN1* and *FBN2* **(Chapter 1)**. Mutation of *FBN3* has not been described and the study of its role is hampered by the lack of a functional *Fbn3* gene in mouse and rat (Corson *et al.,* 2004). However, the present study identified *Fbn3* transcripts in other rodents, for example squirrel **(Chapter**

7), though the functional nature of the gene will need to be addressed in the future. The different times of expression and varying sets of co-expressed genes suggested that the fibrillins have different roles in the multicellular eukaryote. Therefore a study of the evolutionary conservation of the fibrillins, focussing on promoters because of their role in gene regulation and two regions of significant mutations, was performed **(Chapter 7)**. The promoter regions for *FBN1* and *FBN2* were well conserved across vertebrates. Conservation in the promoter region of *FBN3* was unable to be determined due to poor annotation of the 5'UTR region of the gene across vertebrates. In addition, high levels of conservation of the "neonatal region" (where severe *FBN1* mutations and almost all *FBN2* mutations map) were shown across vertebrates. This represents a key candidate for inactivating mutations of *FBN3*. Finally, conservation of the lipodystrophy region at the 3' end of the genes was observed. It is likely that this region of *FBN1* is critical for adipose development and a strong candidate for disease-causing mutations in *FBN2* and *FBN3*. Future work to determine the importance of the region in the fibrillin family could include upregulation of the truncated region in fibrillin-1 to determine if adipose cells can recover. This could be achieved by creating a *FBN1* mutant pig as proposed in **Section 8.1.2.** In addition, truncating the 3' lipodystrophy region in both *FBN2* and *FBN3* in early development could determine if development is altered or unaffected in an *in vivo* model system or in appropriate primary cell types. Therefore the conservation of fibrillin sequence across vertebrates shows the importance of this gene family. It contrasts with the differing expression patterns and roles of the fibrilllins and shows that relatively subtle changes in amino acid sequence can make major differences to protein function.

8.2 Fibrillins as cellular regulators

Summers *et al* (2010) showed the high correlation of *Fbn1* expression in mouse mesenchymal cells advanced the hypothesis that fibrillin-1 might be a central regulator of mesenchymal state, suggesting that fibrillin-1 levels might control the expression of a suite of mesenchymal genes during development of connective tissue types. Given their structural similarity, fibrillin-2 and fibrillin-3 could also be major regulators of different stages of differentiation.

8.2.1 Is fibrillin-1 a master regulator of mesenchymal state?

In this thesis several lines of evidence indicate that fibrillin-1 is unlikely to be a key regulator of mesenchymal function.

Firstly, cultures of cells from two mesenchymal lineages grew satisfactorily in the absence of a fibrillin-1 microfibril matrix **(Chapter 4)**. If fibrillin-1 is a key regulatory protein in mesenchymal cells, it would be expected that these cells might show phenotypic abnormalities or fail to grow. It could be explained by the fact that these lines represent more mature differentiation (where fibrillin-1 may be less important) and this is validated for the osteosarcoma SAOS2 **(Section 8.1.1)**. Alternatively, since these are both immortal cell lines adapted for culture they may not need the full repertoire of mesenchymal genes that are necessary for a solid tissue in a multicellular organism.

Secondly, knocking down *FBN1* mRNA to about 20% of its normal level in primary fibroblasts **(Chapter 5)** did not result in failure of the culture or in major phenotypic abnormalities of the cells, even though slight cytoskeleton actin fibre alterations were visible. In addition, knocking down *FBN1* mRNA in the chondrocyte and osteosarcoma lines which showed high levels of fibrillin-1 protein had no impact on cell function and showed no concomitant up or down regulation of any genes.

Thirdly, in the NHDF cell line, knockdown of *FBN1* only affected a small number of genes. Although some of these were in *FBN1* co-expression clusters, many other co-expressed genes were unaffected by FBN1KD, suggesting that it only interacts with a minimal set of ECM related genes.

However, the severe connective tissue phenotype that results from *FBN1* mutations (**Chapter 1**) and the high level of *FBN1* conservation across vertebrates (**Chapter 7)** is consistent with a key role in mesenchymal tissues, manifested through both the structural function and the role in TFGβ regulation. In this thesis the role of fibrillin-1 in early embryogenesis, adipogenesis and mature cell types was examined. Due to the low levels of expression of *FBN1* in early development, high levels of fibrillin-1 protein in early adipogenesis and consistent *FBN1* expression levels in more mature cells types, *FBN1* may have broad regulatory properties in early mesenchyme lineage differentiation. The role of fibrillin-1 in later differentiation and mature cells types could be limited to

sequestering and inactivation of TGFB (single pathway regulation) and structural support of the ECM. Future work such as permanent knockdown of *FBN1* early in differentiation could provide evidence as to whether fibrillin-1 is required in early development, therefore indicating possible key regulatory characteristics. If *FBN1* were knocked down early in lineage progression (for example during embryoid body formation from H1 ES cells or at Day 1 of adipose differentiation in ADMSCs), would the MSCs continue to differentiate to the predetermined cell type, or would differentiation be negatively affected, or stunted? In addition, would any of the co-expressed genes determined in **Chapter 3** become up or downregulated, possibly indicating further targets for gene therapy treatment.

8.2.2 Are fibrillin-2 and fibrillin-3 regulatory genes?

The proposed early regulatory action by fibrillin-1 could be similar to what is seen in both fibrillin-2 and fibrillin-3. Fibrillin-2 failed to co-express with any genes in adipose differentiation or in more mature cells types, and had low levels of mRNA expression. However, *FBN2* was highly expressed prior to *FBN1* expression in early ES cell differentiation to mesoderm, and co-expressed with many key mesoderm specific markers. Therefore, *FBN2* could have regulatory properties in mesoderm formation but is likely an endpoint in mesenchyme lineage progression and adult cell types. *FBN3* mRNA appeared very early in ES cells, co-expressing with several key ES and pluirpotency markers, and is also expressed in foetal tissues during human development. Therefore, fibrillin-3 could be a key regulator of early differentiation, and an endpoint important for early connective tissue development in foetal tissues. Future knockdown studies during early ES cell differentiation and mesoderm development, either *in vitro* (human ES cells) or *in vivo* (pig) would be useful in determining whether depletion of *FBN3* would block development to embryoid body formation, or if depleted levels of *FBN2* in mesoderm differentiation would affect mesenchymal stem cell formation and progression. The knockdown of *FBN3* could also determine whether the gene is redundant as the functional transcript has been lost in certain rodents, or if the gene is embryonic lethal, therefore implying the role of fibrillin-3 must have been assumed by fibrillin-2 or another protein in mice and rats. In addition to permanent knockdown or knockout experiments,

conditional knockouts at specific points in ES development, for example mesoderm and embryonic body formation for *FBN2* and *FBN3,* respectively, could further determine the role of the fibrillin genes at specific developmental stages. As was shown in **Chapter 3**, there were multiple genes that co-expressed with *FBN2* and *FBN3* providing insight into the function of the genes. The proposed future knockdown/knockout studies (either permanent or conditional), along with performing widescale co-expression studies as described in this thesis, could determine whether any of the co-expressed genes are altered. This would then provide further evidence to the regulatory role of *FBN2* and *FBN3* in early development as well as propose genes targets that could assist in treating diseases with *FBN2* and possible *FBN3* mutations.

8.3 Role of fibrillin family members in differentiation and development

In **Section 8.2**, it is proposed the fibrillin-1, fibrillin-2 and fibrillin-3 have the potential to be key regulators at different points within early development, though their role in mature mesenchyme cell types could be classified as an endpoint. These studies have provided evidence for two waves of expression for each of these genes, one during the initial stages of embryo formation (exemplified by the pattern of expression in ES cells) and a second in maturing or mature connective tissues. A model is proposed where the early, precisely timed expression of the different fibrillins is essential to trigger appropriate signalling leading to the development of mesoderm and further differentiation into mesenchyme. The later wave of expression in foetal and adult tissues is involved in regulating local TGFß family member levels as well as providing structure to the connective tissues, but may not have the central regulatory role at these developmental stages. The proposed experiments in early embryogenesis and lineage progression described above would be important in uncovering the exact timing and importance of the regulatory roles.

Although extensive studies have been performed on *FBN1* and *FBN2* null or mutant mice, the lack of *FBN3* and the anatomical and physiological differences between mice and humans limit their relevance to human conditions. Large animals (for example pigs and sheep) have been used extensively to develop surgical techniques for use in humans

and to understand human physiology and pathology (Lunney, 2007, Hasenfuss, 1998, Dixon and Spinale, 2009, Meeusen EN, 2009). Recent developments in large animal genome modification and genome editing (Bruce *et al.,* 2013, Lillico *et al.,* 2013)(**Chapter 5, Section 5.4.3)** open the possibility of developing relevant models to investigate the fibrillin gene family. This will be particularly relevant in understanding the role and function of *FBN3*. In addition to large animal models, to further understand the evolutionary loss of *Fbn3* in rodents, introducing cDNA containing functional *Fbn3* (from other species, for example, squirrel) into mouse and/or rat ES cells could reveal the functional relevance of the gene in rodents.

This thesis has provided a better understanding of the fibrillin gene family (**Sections 8.1 and 8.2**) and dicusses their role in not only diseases with known mutations but also many other associated diseases such as thoracic aneurysm and dissections, obesity, lipodystrophy, and ovarian syndromes. The work presented in this thesis has contributed to the field of fibrillin research by proposing mechanisms by which the gene family participates in the development, differentiation and maintenance of mesenchyme cell types.

Chapter 9. Appendences

9.1 Appendix A

ARK_ID	Sample identifier	260/280 nm	RIN[e]
2195M0001	MG63 D-1	1.85	9.2
2195M0002	MG63 D0	1.73	9.6
2195M0003	MG63 D1 CONTROL	1.84	9.5
2195M0004	MG63 D1 NT	1.82	9.6
2195M0005	MG63 D1 FBN1KD	1.83	9.7
2195M0006	MG63 D2 CONTROL	1.76	9.6
2195M0007	MG63 D2 NT	1.83	9.8
2195M0008	MG63 D2 FBN1KD	1.74	9.7
2195M0009	MG63 D3 CONTROL	1.79	9.6
2195M0010	MG63 D3 NT	1.82	9.6
2195M0011	MG63 D3 FBN1KD	1.82	9.6
2195M0012	MG63 D4 CONTROL	1.9	9.5
2195M0013	MG63 D4 NT	1.84	9.6
2195M0014	MG63 D4 FBN1KD	1.85	9.7
2195M0015	MG63 D7 CONTROL	1.77	9.5
2195M0016	MG63 D7 NT	1.75	9.6
2195M0017	MG63 D7 FBN1KD	1.8	9.5
2195M0018	C20A4 D-1	1.93	7.7
2195M0019	C20A4 D0	1.47	9.1
2195M0020	C20A4 D1 CONTROL	1.83	9.6
2195M0021	C20A4 D1 NT	1.67	9.6
2195M0022	C20A4 D1 FBN1KD	1.83	9.8
2195M0023	C20A4 D2 CONTROL	1.76	9.7
2195M0024	C20A4 D2 NT	1.86	9
2195M0025	C20A4 D2 FBN1KD	1.83	9.7
2195M0026	C20A4 D3 CONTROL	1.7	8.9
2195M0027	C20A4 D3 NT	1.52	8.8
2195M0028	C20A4 D3 FBN1KD	1.32	8
2195M0029	C20A4 D4 CONTROL	1.76	9
2195M0030	C20A4 D4 NT	1.98	9
2195M0031	C20A4 D4 FBN1KD	1.75	9.5
2195M0032	C20A4 D7 CONTROL	1.71	9.4

2195M0033	C20A4 D7 NT	1.71	9.5
ARK_ID	**Sample identifier**	**260/280 nm**	**RIN[e]**
2195M0034	C20A4 D7 FBN1KD	1.71	9.6
2195M0035	NHDF D-1	2.07	9.4
2195M0036	NHDF D0	2.03	9.4
2195M0037	NHDFD1 control	2.06	9.4
2195M0038	NHDF D1 NT	2.08	9.54
2195M0039	NHDF D1 FBN1KD	2.07	9.1
2195M0040	NHDFD2 control	2.16	9.5
2195M0041	NHDF D2 NT	1.72	9.7
2195M0042	NHDF D2 FBN1KD	2.06	9.5
2195M0043	NHDF D3 CONTROL	1.82	9.6
2195M0044	NHDF D3 NT	1.89	9.2
2195M0045	NHDF D3 FBN1KD	1.85	9.2
2195M0046	NHDF D4 control	1.99	9.5
2195M0047	NHDF D4 NT	2.05	9.6
2195M0048	NHDF D4 FBN1KD	2	9.3
2195M0049	NHDF D7 control	2.06	9.4
2195M0050	NHDF D7 NT	2.05	9.5
2195M0051	NHDF D7 FBN1KD	2.06	9.4
2195M0052	NHDF D0	2.17	9.6
2195M0053	NHDFD1 control	2.15	9.5
2195M0054	NHDF D1 NT	2.13	9.5
2195M0055	NHDF D1 FBN1KD	2.18	9.5
2195M0056	NHDFD2 control	2.16	9.5
2195M0057	NHDF D2 NT	1.81	9.6
2195M0058	NHDF D2 FBN1KD	2.08	9.7
2195M0059	NHDF D3 CONTROL	1.86	9.4
2195M0060	NHDF D3 NT	1.81	8.7
2195M0061	NHDF D3 FBN1KD	1.84	9.3
2195M0062	NHDF D4 control	2.11	9.5
2195M0063	NHDF D4 NT	2.14	9.4
2195M0064	NHDF D4 FBN1KD	2.36	8.9
2195M0065	NHDF D7 control	2.12	9.4
2195M0066	NHDF D7 NT	2.18	9.5
2195M0067	NHDF D7 FBN1KD	2.1	9.5
2195M0068	ADMSC +1	1.93	9.3
2195M0069	ADMSC +2	1.87	6
2195M0070	ADMSC +18	1.95	8.8
2195M0071	ADMSC -1	1.85	9.1

2195M0072	ADMSC-2	1.92	9.2
2195M0073	ADMSC -18	1.99	9.5
ARK_ID	**Sample identifier**	**260/280 nm**	**RIN[e]**
2195M0074	hESMP +3	1.98	9.2
2195M0075	hESMP+6	1.89	9.1
2195M0076	hESMP+18	1.95	9.2
2195M0077	hESMP-3	1.95	9.5
2195M0078	hESMP-6	1.92	8.8
2195M0079	hESMP-18	2.01	9.3
2195M0080	H1 D0	2.02	8.7
2195M0081	H1 D3	2.06	9.6
2195M0082	H1 D5	2.04	9.6
2195M0083	SAOS2D7	1.85	9.2
2195M0084	SAOS2 D7	2.12	9.5
2195M0085	MG63 D7	1.91	9.2
2195M0086	MG63D7	2.13	9.5
2195M0087	C20A4 D7	1.81	9
2195M0088	C20A7 D7	2.13	8.8
2195M0089	TC28A2 D7	1.88	9.6
2195M0090	TC28A2D7	2.14	9.3
2195M0091	C28I2	2.13	9.2
2195M0092	RH1 (24hours)	1.99	9.5
2195M0093	THP1	1.76	6.8
2195M0094	HEK293	2.13	9.6
2195M0095	MG63 T16 (C3)	2.02	9.6
2195M0096	SAOS2 T16 (Ex9)	2.06	9.6

9.2 Appendix B

Files contained in C.D on the inside back cover of this thesis.

9.2.1 BioLayout Express ^{3D} Files for Chapter 3

9.2.2 BioLayout Express ^{3D} Files for Chapter 4

9.2.3 BioLayout Express ^{3D} Files for Chapter 5

9.3 Appendix C

Common Name	**Fibrillin-1**	**Fibrillin-2**	**Fibrillin-3**
Human	ENSP00000325527	ENSP00000424571	ENSP00000470498
Mouse	ENSMUSP00000099524	ENSMUSP00000025497	X
Pig	ENSSSCP00000005017	ENSSSCP00000015165	ENSSSCP00000014445
Sheep	ENSOARP00000022590	ENSOARP00000018461	ENSOARP00000003672
Ferret	ENSMPUP00000011768	ENSMPUP00000011697	ENSMPUP00000007296
Bushbaby	ENSOGAP00000008576	ENSOGAP00000007715	ENSOGAP00000011557
Panda	ENSAMEP00000001943	ENSAMEP00000005373	ENSAMEP00000009357
Armadillo	ENSDNOP00000005602	ENSDNOP00000012246	ENSDNOP00000026528
Chicken	ENSGALP00000007941	ENSGALP00000023620	ENSGALP00000000432
Flycatcher	ENSFALP00000012028	ENSFALP00000012882	ENSFALP00000001070
Turkey	ENSMGAP00000007192	ENSMGAP00000008154	ENSMGAP00000018726
Coelacanth	ENSLACP00000010136	ENSLACP00000002844	ENSLACP00000018340
Fugu	ENSTRUP00000043351	X	ENSTRUP00000032967
Medaka	ENSORLP00000003276	X	ENSORLP00000006743
Spotted gar	ENSLOCP00000005288	ENSLOCP00000010204	ENSLOCP00000016276
Stickleback	ENSGACP00000022153	X	ENSGACP00000013669
Tetraodon	ENSTNIP00000003762	X	ENSTNIP00000001525
Tilapia	ENSONIP00000016782	X	ENSONIP00000002223
Chinese softshell turtle	ENSPSIP00000014935	ENSPSIP00000017170	ENSPSIP00000016490

Table C1. Table of protein ID from http://ensembl.org.

Chapter 10. References

AALBERTS, J. J., THIO, C. H., SCHUURMAN, A. G., VAN LANGEN, I. M., VAN DER POL, B. A., VAN TINTELEN, J. P. & VAN DEN BERG, M. P. (2012) Diagnostic yield in adults screened at the Marfan outpatient clinic using the 1996 and 2010 Ghent nosologies. Am J Med Genet A, 158A, 982-8.

ABE, K., YAMAMURA, K. & SUZUKI, M. (2000) Molecular and embryological characterization of a new transgene-induced null allele of mouse Brachyury locus. Mamm Genome, 11, 238-40.

ABRANCHES, E., GUEDES, A. M., MORAVEC, M., MAAMAR, H., SVOBODA, P., RAJ, A. & HENRIQUE, D. (2014) Stochastic NANOG fluctuations allow mouse embryonic stem cells to explore pluripotency. Development, 141, 2770-9.

ABREU-VELEZ, A. M. & HOWARD, M. S. (2012) Collagen IV in Normal Skin and in Pathological Processes. N Am J Med Sci, 4, 1-8.

AKAGAWA, M. & SUYAMA, K. (2000) Mechanism of formation of elastin crosslinks. Connect Tissue Res, 41, 131-41.

ALBERTS, B., JOHNSON, A., LEWIS, J ET AL. (2002a) Molecular Biology of the Cell New York, Garland Science.

ALBERTS, B., JOHNSON, A., LEWIS, J ET AL. (2002b) Molecular Biology of the Cell, New York, Garland Science.

ALBERTS, J. J., THIO, C. H., SCHUURMAN, A. G., VAN LANGEN, I. M., VAN DER POL, B. A., VAN TINTELEN, J. P. & VAN DEN BERG, M. P. (2012) Diagnostic yield in adults screened at the Marfan outpatient clinic using the 1996 and 2010 Ghent nosologies. Am J Med Genet A, 158A, 982-8.

ALLOCCO, D. J., KOHANE, I. S. & BUTTE, A. J. (2004) Quantifying the relationship between co-expression, co-regulation and gene function. BMC Bioinformatics, 5, 18.

ANDERSON, E. M., BIRMINGHAM, A., BASKERVILLE, S., REYNOLDS, A., MAKSIMOVA, E., LEAKE, D., FEDOROV, Y., KARPILOW, J. & KHVOROVA, A. (2008) Experimental validation of the importance of seed complement frequency to siRNA specificity. RNA, 14, 853-61.

ANDERSON, E., PELUSO, S., LETTICE, L. A. & HILL, R. E. (2012) Human limb abnormalities caused by disruption of hedgehog signaling. Trends Genet, 28, 364-73.

ANNES, J. P., CHEN, Y., MUNGER, J. S. & RIFKIN, D. B. (2004) Integrin alphaVbeta6-mediated activation of latent TGF-beta requires the latent TGF-beta binding protein-1. J Cell Biol, 165, 723-34.

ANNES, J. P., MUNGER, J. S. & RIFKIN, D. B. (2003) Making sense of latent TGFbeta activation. J Cell Sci, 116, 217-24.

ANSORGE, H. L., MENG, X., ZHANG, G., VEIT, G., SUN, M., KLEMENT, J. F., BEASON, D. P., SOSLOWSKY, L. J., KOCH, M. & BIRK, D. E. (2009) Type XIV Collagen Regulates Fibrillogenesis: PREMATURE COLLAGEN FIBRIL GROWTH AND TISSUE DYSFUNCTION IN NULL MICE. J Biol Chem, 284, 8427-38.

APITZ, C., MACKENSEN-HAEN, S., GIRISCH, M., KERST, G., WIEGAND, G., STUHRMANN, M., NIETHAMMER, K., BEHRWIND, G. & HOFBECK, M. (2010) Neonatal Marfan syndrome: unusually large deletion of exons 24-26 of FBN1 associated with poor prognosis. Klin Padiatr, 222, 261-3.

ARBISER, J. L., ARBISER, Z. K. & MAJZOUB, J. A. (1991) Regulation of gene expression in choriocarcinoma by methotrexate and hydroxyurea. Endocrinology, 128, 972-8.

ARGRAVES, W. S., DICKERSON, K., BURGESS, W. H. & RUOSLAHTI, E. (1989) Fibulin, a novel protein that interacts with the fibronectin receptor beta subunit cytoplasmic domain. Cell, 58, 623-9.

ARGRAVES, W. S., TRAN, H., BURGESS, W. H. & DICKERSON, K. (1990) Fibulin is an extracellular matrix and plasma glycoprotein with repeated domain structure. J Cell Biol, 111, 3155-64.

ARNAOUT, M. A. (2004) The structural basis of elasticity in fibrillin-based microfibrils. Structure, 12, 734-6.

ARNOLD, P., ERB, I., PACHKOV, M., MOLINA, N. & VAN NIMWEGEN, E. (2012) MotEvo: integrated Bayesian probabilistic methods for inferring regulatory sites and motifs on multiple alignments of DNA sequences. Bioinformatics, 28, 487-94.

ARTEAGA-SOLIS, E., GAYRAUD, B., LEE, S. Y., SHUM, L., SAKAI, L. & RAMIREZ, F. (2001) Regulation of limb patterning by extracellular microfibrils. J Cell Biol, 154, 275-81.

AUMAILLEY, M., BRUCKNER-TUDERMAN, L., CARTER, W. G., DEUTZMANN, R., EDGAR, D., EKBLOM, P., ENGEL, J., ENGVALL, E., HOHENESTER, E., JONES, J. C., KLEINMAN, H. K., MARINKOVICH, M. P., MARTIN, G. R., MAYER, U., MENEGUZZI, G., MINER, J. H., MIYAZAKI, K., PATARROYO, M., PAULSSON, M., QUARANTA, V., SANES, J. R., SASAKI, T., SEKIGUCHI, K., SOROKIN, L. M., TALTS, J. F., TRYGGVASON, K., UITTO, J., VIRTANEN, I., VON DER MARK, K., WEWER, U. M., YAMADA, Y. & YURCHENCO, P. D. (2005) A simplified laminin nomenclature. Matrix Biol, 24, 326-32.

BABCOCK, D., GASNER, C., FRANCKE, U. & MASLEN, C. (1998) A single mutation that results in an Asp to His substitution and partial exon skipping in a family with congenital contractural arachnodactyly. Hum Genet, 103, 22-8.

BAIER, C., BAADER, S. L., JANKOWSKI, J., GIESELMANN, V., SCHILLING, K., RAUCH, U. & KAPPLER, J. (2007) Hyaluronan is organized into fiber-like structures along migratory pathways in the developing mouse cerebellum. Matrix Biol, 26, 348-58.

BALWIERZ, P. J., CARNINCI, P., DAUB, C. O., KAWAI, J., HAYASHIZAKI, Y., VAN BELLE, W., BEISEL, C. & VAN NIMWEGEN, E. (2009) Methods for analyzing deep sequencing expression data: constructing the human and mouse promoterome with deepCAGE data. Genome Biol, 10, R79.

BANDYOPADHYAY, A., TSUJI, K., COX, K., HARFE, B. D., ROSEN, V. & TABIN, C. J. (2006) Genetic analysis of the roles of BMP2, BMP4, and BMP7 in limb patterning and skeletogenesis. PLoS Genet, 2, e216.

BANEYX, G., BAUGH, L. & VOGEL, V. (2002) Fibronectin extension and unfolding within cell matrix fibrils controlled by cytoskeletal tension. Proc Natl Acad Sci U S A, 99, 5139-43.

BARAK, Y., NELSON, M. C., ONG, E. S., JONES, Y. Z., RUIZ-LOZANO, P., CHIEN, K. R., KODER, A. & EVANS, R. M. (1999) PPAR gamma is required for placental, cardiac, and adipose tissue development. Mol Cell, 4, 585-95.

BARAK, T., KWAN, K. Y., LOUVI, A., DEMIRBILEK, V., SAYGI, S., TUYSUZ, B., CHOI, M., BOYACI, H., DOERSCHNER, K., ZHU, Y., KAYMAKCALAN, H., YILMAZ, S., BAKIRCIOGLU, M., CAGLAYAN, A. O., OZTURK, A. K., YASUNO, K., BRUNKEN, W. J., ATALAR, E., YALCINKAYA, C., DINCER, A., BRONEN, R. A., MANE, S., OZCELIK, T., LIFTON, R. P., SESTAN, N., BILGUVAR, K. & GUNEL, M. (2011) Recessive LAMC3 mutations cause malformations of occipital cortical development. Nat Genet, 43, 590-4.

BARNES, J. L., TORRES, E. S., MITCHELL, R. J. & PETERS, J. H. (1995) Expression of alternatively spliced fibronectin variants during remodeling in proliferative glomerulonephritis. Am J Pathol, 147, 1361-71.

BARNETT, C. P., CHITAYAT, D., BRADLEY, T. J., WANG, Y. & HINEK, A. (2011) Dexamethasone normalizes aberrant elastic fiber production and collagen 1 secretion by Loeys-Dietz syndrome fibroblasts: a possible treatment? Eur J Hum Genet, 19, 624-33.

BARNETT, M. W., OLD, R. W. & JONES, E. A. (1998) Neural induction and patterning by fibroblast growth factor, notochord and somite tissue in Xenopus. Dev Growth Differ, 40, 47-57.

BASHYAM, M. D., KAUSHAL, D., DASGUPTA, S. K. & TYAGI, A. K. (1996) A study of mycobacterial transcriptional apparatus: identification of novel features in promoter elements. J Bacteriol, 178, 4847-53.

BEHAN, W. M., LONGMAN, C., PETTY, R. K., COMEGLIO, P., CHILD, A. H., BOXER, M., FOSKETT, P. & HARRIMAN, D. G. (2003) Muscle fibrillin deficiency in Marfan's syndrome myopathy. J Neurol Neurosurg Psychiatry, 74, 633-8.

BELL, D. M., LEUNG, K. K., WHEATLEY, S. C., NG, L. J., ZHOU, S., LING, K. W., SHAM, M. H., KOOPMAN, P., TAM, P. P. & CHEAH, K. S. (1997) SOX9 directly regulates the type-II collagen gene. Nat Genet, 16, 174-8.

BENJAMIN, M. & RALPHS, J. R. (1998) Fibrocartilage in tendons and ligaments--an adaptation to compressive load. J Anat, 193 (Pt 4), 481-94.

BERNSTEIN, E. F., CHEN, Y. Q., TAMAI, K., SHEPLEY, K. J., RESNIK, K. S., ZHANG, H., TUAN, R., MAUVIEL, A. & UITTO, J. (1994) Enhanced elastin and fibrillin gene expression in chronically photodamaged skin. J Invest Dermatol, 103, 182-6.

BHATTACHARJEE, A. & BANSAL, M. (2005) Collagen structure: the Madras triple helix and the current scenario. IUBMB Life, 57, 161-72.

BILLIAU, A., EDY, V. G., HEREMANS, H., VAN DAMME, J., DESMYTER, J., GEORGIADES, J. A. & DE SOMER, P. (1977) Human interferon: mass production in a newly established cell line, MG-63. Antimicrob Agents Chemother, 12, 11-5.

BIRMINGHAM, A., ANDERSON, E. M., REYNOLDS, A., ILSLEY-TYREE, D., LEAKE, D., FEDOROV, Y., BASKERVILLE, S., MAKSIMOVA, E., ROBINSON, K., KARPILOW, J., MARSHALL, W. S. & KHVOROVA, A. (2006) 3' UTR seed matches, but not overall identity, are associated with RNAi off-targets. Nat Methods, 3, 199-204.

BIRNEY, E., STAMATOYANNOPOULOS, J. A., DUTTA, A., GUIGO, R., GINGERAS, T. R., MARGULIES, E. H., WENG, Z., SNYDER, M., DERMITZAKIS, E. T., THURMAN, R. E., KUEHN, M. S., TAYLOR, C. M., NEPH, S., KOCH, C. M., ASTHANA, S., MALHOTRA, A., ADZHUBEI, I., GREENBAUM, J. A., ANDREWS, R. M., FLICEK, P., BOYLE, P. J., CAO, H., CARTER, N. P., CLELLAND, G. K., DAVIS, S., DAY, N., DHAMI, P., DILLON, S. C., DORSCHNER, M. O., FIEGLER, H., GIRESI, P. G., GOLDY, J., HAWRYLYCZ, M., HAYDOCK, A., HUMBERT, R., JAMES, K. D., JOHNSON, B. E., JOHNSON, E. M., FRUM, T. T., ROSENZWEIG, E. R., KARNANI, N., LEE, K., LEFEBVRE, G. C., NAVAS, P. A., NERI, F., PARKER, S. C., SABO, P. J., SANDSTROM, R., SHAFER, A., VETRIE, D., WEAVER, M., WILCOX, S., YU, M., COLLINS, F. S., DEKKER, J., LIEB, J. D., TULLIUS, T. D., CRAWFORD, G. E., SUNYAEV, S., NOBLE, W. S., DUNHAM, I., DENOEUD, F., REYMOND, A., KAPRANOV, P., ROZOWSKY, J., ZHENG, D., CASTELO, R., FRANKISH, A., HARROW, J., GHOSH, S., SANDELIN, A., HOFACKER, I. L., BAERTSCH, R., KEEFE, D., DIKE, S., CHENG, J., HIRSCH, H. A., SEKINGER, E. A., LAGARDE, J., ABRIL, J. F., SHAHAB, A., FLAMM, C., FRIED, C., HACKERMULLER, J., HERTEL, J., LINDEMEYER, M., MISSAL, K., TANZER, A., WASHIETL, S., KORBEL, J., EMANUELSSON, O., PEDERSEN, J. S., HOLROYD, N., TAYLOR, R., SWARBRECK, D., MATTHEWS, N., DICKSON, M. C., THOMAS, D. J., WEIRAUCH, M. T., GILBERT, J., et al. (2007) Identification and analysis of functional elements in 1% of the human genome by the ENCODE pilot project. Nature, 447, 799-816.

BIRNEY, E., STAMATOYANNOPOULOS, J. A., DUTTA, A., GUIGO, R., GINGERAS, T. R., MARGULIES, E. H., WENG, Z., SNYDER, M., DERMITZAKIS, E. T., THURMAN, R. E., KUEHN, M. S., TAYLOR, C. M., NEPH, S., KOCH, C. M., ASTHANA, S., MALHOTRA, A., ADZHUBEI, I., GREENBAUM, J. A., ANDREWS, R. M., FLICEK, P., BOYLE, P. J., CAO, H.,

CARTER, N. P., CLELLAND, G. K., DAVIS, S., DAY, N., DHAMI, P., DILLON, S. C., DORSCHNER, M. O., FIEGLER, H., GIRESI, P. G., GOLDY, J., HAWRYLYCZ, M., HAYDOCK, A., HUMBERT, R., JAMES, K. D., JOHNSON, B. E., JOHNSON, E. M., FRUM, T. T., ROSENZWEIG, E. R., KARNANI, N., LEE, K., LEFEBVRE, G. C., NAVAS, P. A., NERI, F., PARKER, S. C., SABO, P. J., SANDSTROM, R., SHAFER, A., VETRIE, D., WEAVER, M., WILCOX, S., YU, M., COLLINS, F. S., DEKKER, J., LIEB, J. D., TULLIUS, T. D., CRAWFORD, G. E., SUNYAEV, S., NOBLE, W. S., DUNHAM, I., DENOEUD, F., REYMOND, A., KAPRANOV, P., ROZOWSKY, J., ZHENG, D., CASTELO, R., FRANKISH, A., HARROW, J., GHOSH, S., SANDELIN, A., HOFACKER, I. L., BAERTSCH, R., KEEFE, D., DIKE, S., CHENG, J., HIRSCH, H. A., SEKINGER, E. A., LAGARDE, J., ABRIL, J. F., SHAHAB, A., FLAMM, C., FRIED, C., HACKERMULLER, J., HERTEL, J., LINDEMEYER, M., MISSAL, K., TANZER, A., WASHIETL, S., KORBEL, J., EMANUELSSON, O., PEDERSEN, J. S., HOLROYD, N., TAYLOR, R., SWARBRECK, D., MATTHEWS, N., DICKSON, M. C., THOMAS, D. J., WEIRAUCH, M. T., GILBERT, J., et al. (2012) An integrated encyclopedia of DNA elements in the human genome. Nature, 489, 57-74.

BLACKSHAW, S. & SNYDER, S. H. (1999) Encephalopsin: a novel mammalian extraretinal opsin discretely localised in the brain. J Neurosci, 19, 3681-90.

BLAKE, J. A., BULT, C. J., EPPIG, J. T., KADIN, J. A. & RICHARDSON, J. E. (2014) The Mouse Genome Database: integration of and access to knowledge about the laboratory mouse. Nucleic Acids Res, 42, D810-7.

BLOOM, G. P., FROMM, D., ROSENBERG, S. & GOLDMAN, H. (1976) Attempted retrograde cannulation of the ampulla: a probable cause of mass in the pancreas. Ann Surg, 183, 107-8.

BLOUIN, C. M., LE LAY, S., LASNIER, F., DUGAIL, I. & HAJDUCH, E. (2008) Regulated association of caveolins to lipid droplets during differentiation of 3T3-L1 adipocytes. Biochem Biophys Res Commun, 376, 331-5.

BLYTH, M., FOULDS, N., TURNER, C. & BUNYAN, D. (2008) Severe Marfan syndrome due to FBN1 exon deletions. Am J Med Genet A, 146A, 1320-4.

BOCHICCHIO, D., COMELLINI, M., LAMBERTINI, P., MARCHETTO, G. & DELLA CASA, G. (2014) Selective mobilization of fatty acids in adipose tissue of heavy pigs. Animal, 1-8.

BOCHICCHIO, B. & TAMBURRO, A. M. (2002) Polyproline II structure in proteins: identification by chiroptical spectroscopies, stability, and functions. Chirality, 14, 782-92.

BOCKHORN, J., DALTON, R., NWACHUKWU, C., HUANG, S., PRAT, A., YEE, K., CHANG, Y. F., HUO, D., WEN, Y., SWANSON, K. E., QIU, T., LU, J., PARK, S. Y., DOLAN, M. E., PEROU, C. M., OLOPADE, O. I., CLARKE, M. F., GREENE, G. L. & LIU, H. (2013) MicroRNA-30c inhibits human breast tumour chemotherapy resistance by regulating TWF1 and IL-11. Nat Commun, 4, 1393.

BODAS, M. & VIJ, N. (2010) The NF-kappaB signaling in cystic fibrosis lung disease: pathophysiology and therapeutic potential. Discov Med, 9, 346-56.

BODINE, P. V. & KOMM, B. S. (2006) Wnt signaling and osteoblastogenesis. Rev Endocr Metab Disord, 7, 33-9.

BOLINO, A., MUGLIA, M., CONFORTI, F. L., LEGUERN, E., SALIH, M. A., GEORGIOU, D. M., CHRISTODOULOU, K., HAUSMANOWA-PETRUSEWICZ, I., MANDICH, P., SCHENONE, A., GAMBARDELLA, A., BONO, F., QUATTRONE, A., DEVOTO, M. & MONACO, A. P. (2000) Charcot-Marie-Tooth type 4B is caused by mutations in the gene encoding myotubularin-related protein-2. Nat Genet, 25, 17-9.

BOSKEY, A. L. & ROY, R. (2008) Cell culture systems for studies of bone and tooth mineralisation. Chem Rev, 108, 4716-33.

BRADSHAW, A. D., GRAVES, D. C., MOTAMED, K. & SAGE, E. H. (2003) SPARC-null mice exhibit increased adiposity without significant differences in overall body weight. Proc Natl Acad Sci U S A, 100, 6045-50.

BRENN, T., AOYAMA, T., FRANCKE, U. & FURTHMAYR, H. (1996) Dermal fibroblast culture as a model system for studies of fibrillin assembly and pathogenetic mechanisms: defects in distinct groups of individuals with Marfan's syndrome. Lab Invest, 75, 389-402.

BRIAND, N., LE LAY, S., SESSA, W. C., FERRE, P. & DUGAIL, I. (2011) Distinct roles of endothelial and adipocyte caveolin-1 in macrophage infiltration and adipose tissue metabolic activity. Diabetes, 60, 448-53.

BROWN, G. D. & NAZARALI, A. J. (2010) Matrix metalloproteinase-25 has a functional role in mouse secondary palate development and is a downstream target of TGF-beta3. BMC Dev Biol, 10, 93.

BRUCE, A., CASTLE, D., GIBBS, C., TAIT, J. & WHITELAW, C. B. (2013) Novel GM animal technologies and their governance. Transgenic Res, 22, 681-95.

BRUDER, S. P., FINK, D. J. & CAPLAN, A. I. (1994) Mesenchymal stem cells in bone development, bone repair, and skeletal regeneration therapy. J Cell Biochem, 56, 283-94.

BURNETTE, D. T., SHAO, L., OTT, C., PASAPERA, A. M., FISCHER, R. S., BAIRD, M. A., DER LOUGHIAN, C., DELANOE-AYARI, H., PASZEK, M. J., DAVIDSON, M. W., BETZIG, E. & LIPPINCOTT-SCHWARTZ, J. (2014) A contractile and counterbalancing adhesion system controls the 3D shape of crawling cells. J Cell Biol, 205, 83-96.

BUSHBY, K. M., COLLINS, J. & HICKS, D. (2014) Collagen type VI myopathies. Adv Exp Med Biol, 802, 185-99.

BUSSCHERS, E., HOLT, J. P. & RICHARDSON, D. W. (2010) Effects of glucocorticoids and interleukin-1 beta on expression and activity of aggrecanases in equine chondrocytes. Am J Vet Res, 71, 176-85.

CAIN, S. A., BALDOCK, C., GALLAGHER, J., MORGAN, A., BAX, D. V., WEISS, A. S., SHUTTLEWORTH, C. A. & KIELTY, C. M. (2005) Fibrillin-1 interactions with heparin. Implications for microfibril and elastic fiber assembly. J Biol Chem, 280, 30526-37.

CAIN, S. A., BALDWIN, A. K., MAHALINGAM, Y., RAYNAL, B., JOWITT, T. A., SHUTTLEWORTH, C. A., COUCHMAN, J. R. & KIELTY, C. M. (2008) Heparan sulfate regulates fibrillin-1 N- and C-terminal interactions. J Biol Chem, 283, 27017-27.

CAIN, S. A., MCGOVERN, A., BALDWIN, A. K., BALDOCK, C. & KIELTY, C. M. (2012) Fibrillin-1 mutations causing Weill-Marchesani syndrome and acromicric and geleophysic dysplasias disrupt heparan sulfate interactions. PLoS One, 7, e48634.

CAL, S., OBAYA, A. J., LLAMAZARES, M., GARABAYA, C., QUESADA, V. & LOPEZ-OTIN, C. (2002) Cloning, expression analysis, and structural characterization of seven novel human ADAMTSs, a family of metalloproteinases with disintegrin and thrombospondin-1 domains. Gene, 283, 49-62.

CALLEWAERT, B. L., LOEYS, B. L., FICCADENTI, A., VERMEER, S., LANDGREN, M., KROES, H. Y., YARON, Y., POPE, M., FOULDS, N., BOUTE, O., GALAN, F., KINGSTON, H., VAN DER AA, N., SALCEDO, I., SWINKELS, M. E., WALLGREN-PETTERSSON, C., GABRIELLI, O., DE BACKER, J., COUCKE, P. J. & DE PAEPE, A. M. (2009) Comprehensive clinical and molecular assessment of 32 probands with congenital contractural arachnodactyly: report of 14 novel mutations and review of the literature. Hum Mutat, 30, 334-41.

CAMELLITI, P., BORG, T. K. & KOHL, P. (2005) Structural and functional characterisation of cardiac fibroblasts. Cardiovasc Res, 65, 40-51.

CAPANNI, C., MATTIOLI, E., COLUMBARO, M., LUCARELLI, E., PARNAIK, V. K., NOVELLI, G., WEHNERT, M., CENNI, V., MARALDI, N. M., SQUARZONI, S. & LATTANZI, G. (2005)

Altered pre-lamin A processing is a common mechanism leading to lipodystrophy. Hum Mol Genet, 14, 1489-502.

CAPLAN, A. I. (1991) Mesenchymal stem cells. J Orthop Res, 9, 641-50.

CARNINCI, P., KASUKAWA, T., KATAYAMA, S., GOUGH, J., FRITH, M. C., MAEDA, N., OYAMA, R., RAVASI, T., LENHARD, B., WELLS, C., KODZIUS, R., SHIMOKAWA, K., BAJIC, V. B., BRENNER, S. E., BATALOV, S., FORREST, A. R., ZAVOLAN, M., DAVIS, M. J., WILMING, L. G., AIDINIS, V., ALLEN, J. E., AMBESI-IMPIOMBATO, A., APWEILER, R., ATURALIYA, R. N., BAILEY, T. L., BANSAL, M., BAXTER, L., BEISEL, K. W., BERSANO, T., BONO, H., CHALK, A. M., CHIU, K. P., CHOUDHARY, V., CHRISTOFFELS, A., CLUTTERBUCK, D. R., CROWE, M. L., DALLA, E., DALRYMPLE, B. P., DE BONO, B., DELLA GATTA, G., DI BERNARDO, D., DOWN, T., ENGSTROM, P., FAGIOLINI, M., FAULKNER, G., FLETCHER, C. F., FUKUSHIMA, T., FURUNO, M., FUTAKI, S., GARIBOLDI, M., GEORGII-HEMMING, P., GINGERAS, T. R., GOJOBORI, T., GREEN, R. E., GUSTINCICH, S., HARBERS, M., HAYASHI, Y., HENSCH, T. K., HIROKAWA, N., HILL, D., HUMINIECKI, L., IACONO, M., IKEO, K., IWAMA, A., ISHIKAWA, T., JAKT, M., KANAPIN, A., KATOH, M., KAWASAWA, Y., KELSO, J., KITAMURA, H., KITANO, H., KOLLIAS, G., KRISHNAN, S. P., KRUGER, A., KUMMERFELD, S. K., KUROCHKIN, I. V., LAREAU, L. F., LAZAREVIC, D., LIPOVICH, L., LIU, J., LIUNI, S., MCWILLIAM, S., MADAN BABU, M., MADERA, M., MARCHIONNI, L., MATSUDA, H., MATSUZAWA, S., MIKI, H., MIGNONE, F., MIYAKE, S., MORRIS, K., MOTTAGUI-TABAR, S., MULDER, N., NAKANO, N., NAKAUCHI, H., NG, P., NILSSON, R., NISHIGUCHI, S., NISHIKAWA, S., et al. (2005) The transcriptional landscape of the mammalian genome. Science, 309, 1559-63.

CARNINCI, P., KVAM, C., KITAMURA, A., OHSUMI, T., OKAZAKI, Y., ITOH, M., KAMIYA, M., SHIBATA, K., SASAKI, N., IZAWA, M., MURAMATSU, M., HAYASHIZAKI, Y. & SCHNEIDER, C. (1996) High-efficiency full-length cDNA cloning by biotinylated CAP trapper. Genomics, 37, 327-36.

CARNINCI, P., SANDELIN, A., LENHARD, B., KATAYAMA, S., SHIMOKAWA, K., PONJAVIC, J., SEMPLE, C. A., TAYLOR, M. S., ENGSTROM, P. G., FRITH, M. C., FORREST, A. R., ALKEMA, W. B., TAN, S. L., PLESSY, C., KODZIUS, R., RAVASI, T., KASUKAWA, T., FUKUDA, S., KANAMORI-KATAYAMA, M., KITAZUME, Y., KAWAJI, H., KAI, C., NAKAMURA, M., KONNO, H., NAKANO, K., MOTTAGUI-TABAR, S., ARNER, P., CHESI, A., GUSTINCICH, S., PERSICHETTI, F., SUZUKI, H., GRIMMOND, S. M., WELLS, C. A., ORLANDO, V., WAHLESTEDT, C., LIU, E. T., HARBERS, M., KAWAI, J., BAJIC, V. B., HUME, D. A. & HAYASHIZAKI, Y. (2006) Genome-wide analysis of mammalian promoter architecture and evolution. Nat Genet, 38, 626-35.

CARTA, L., PEREIRA, L., ARTEAGA-SOLIS, E., LEE-ARTEAGA, S. Y., LENART, B., STARCHER, B., MERKEL, C. A., SUKOYAN, M., KERKIS, A., HAZEKI, N., KEENE, D. R., SAKAI, L. Y. & RAMIREZ, F. (2006) Fibrillins 1 and 2 perform partially overlapping functions during aortic development. J Biol Chem, 281, 8016-23.

CATALAN, V., GOMEZ-AMBROSI, J., RODRIGUEZ, A. & FRUHBECK, G. (2012) Role of extracellular matrix remodelling in adipose tissue pathophysiology: relevance in the development of obesity. Histol Histopathol, 27, 1515-28.

CHANET, S. & MARTIN, A. C. (2014) Mechanical force sensing in tissues. Prog Mol Biol Transl Sci, 126, 317-52.

CHANEY, W. G., HOWARD, D. R., POLLARD, J. W., SALLUSTIO, S. & STANLEY, P. (1986) High-frequency transfection of CHO cells using polybrene. Somat Cell Mol Genet, 12, 237-44.

CHANG, M. K., RAGGATT, L. J., ALEXANDER, K. A., KULIWABA, J. S., FAZZALARI, N. L., SCHRODER, K., MAYLIN, E. R., RIPOLL, V. M., HUME, D. A. & PETTIT, A. R. (2008) Osteal tissue macrophages are intercalated throughout human and mouse bone lining tissues and regulate osteoblast function in vitro and in vivo. J Immunol, 181, 1232-44.

CHAPMAN, A. B., KNIGHT, D. M. & RINGOLD, G. M. (1985) Glucocorticoid regulation of adipocyte differentiation: hormonal triggering of the developmental program and induction of a differentiation-dependent gene. J Cell Biol, 101, 1227-35.

CHARBONNEAU, N. L., ONO, R. N., CORSON, G. M., KEENE, D. R. & SAKAI, L. Y. (2004) Fine tuning of growth factor signals depends on fibrillin microfibril networks. Birth Defects Res C Embryo Today, 72, 37-50.

CHARBONNEAU, N. L., CARLSON, E. J., TUFA, S., SENGLE, G., MANALO, E. C., CARLBERG, V. M., RAMIREZ, F., KEENE, D. R. & SAKAI, L. Y. (2010) In vivo studies of mutant fibrillin-1 microfibrils. J Biol Chem, 285, 24943-55.

CHAUHAN, A. K., KISUCKA, J., COZZI, M. R., WALSH, M. T., MORETTI, F. A., BATTISTON, M., MAZZUCATO, M., DE MARCO, L., BARALLE, F. E., WAGNER, D. D. & MURO, A. F. (2008) Prothrombotic effects of fibronectin isoforms containing the EDA domain. Arterioscler Thromb Vasc Biol, 28, 296-301.

CHEN, G., DENG, C. & LI, Y. P. (2012) TGF-beta and BMP signaling in osteoblast differentiation and bone formation. Int J Biol Sci, 8, 272-88.

CHEN, Q., ZHANG, T., ROSHETSKY, J. F., OUYANG, Z., ESSERS, J., FAN, C., WANG, Q., HINEK, A., PLOW, E. F. & DICORLETO, P. E. (2009) Fibulin-4 regulates expression of the tropoelastin gene and consequent elastic-fibre formation by human fibroblasts. Biochem J, 423, 79-89.

CHEN, S. F., WU, C. H., LEE, Y. M., TAM, K., TSAI, Y. C., LIOU, J. Y. & SHYUE, S. K. (2013) Caveolin-1 interacts with Derlin-1 and promotes ubiquitination and degradation of cyclooxygenase-2 via collaboration with p97 complex. J Biol Chem, 288, 33462-9.

CHEVALLIER, A., KIENY, M. & MAUGER, A. (1977) Limb-somite relationship: origin of the limb musculature. J Embryol Exp Morphol, 41, 245-58.

CHIKUDA, H., KUGIMIYA, F., HOSHI, K., IKEDA, T., OGASAWARA, T., SHIMOAKA, T., KAWANO, H., KAMEKURA, S., TSUCHIDA, A., YOKOI, N., NAKAMURA, K., KOMEDA, K., CHUNG, U. I. & KAWAGUCHI, H. (2004) Cyclic GMP-dependent protein kinase II is a molecular switch from proliferation to hypertrophic differentiation of chondrocytes. Genes Dev, 18, 2418-29.

CHIU, H. H., WU, M. H., WANG, J. K., LU, C. W., CHIU, S. N., CHEN, C. A., LIN, M. T. & HU, F. C. (2013) Losartan added to beta-blockade therapy for aortic root dilation in Marfan syndrome: a randomized, open-label pilot study. Mayo Clin Proc, 88, 271-6.

CHRIST, B., JACOB, H. J. & JACOB, M. (1977) Experimental analysis of the origin of the wing musculature in avian embryos. Anat Embryol (Berl), 150, 171-86.

CHRIST, B. & WILTING, J. (1992) From somites to vertebral column. Ann Anat, 174, 23-32.

CHOO, A. & LIM, S. K. (2011) Derivation of mesenchymal stem cells from human embryonic stem cells. Methods Mol Biol, 690, 175-82.

CHOUDHURY, R., MCGOVERN, A., RIDLEY, C., CAIN, S. A., BALDWIN, A., WANG, M. C., GUO, C., MIRONOV, A., JR., DRYMOUSSI, Z., TRUMP, D., SHUTTLEWORTH, A., BALDOCK, C. & KIELTY, C. M. (2009) Differential regulation of elastic fiber formation by fibulin-4 and -5. J Biol Chem, 284, 24553-67.

CHOY, L. & DERYNCK, R. (2003) Transforming growth factor-beta inhibits adipocyte differentiation by Smad3 interacting with CCAAT/enhancer-binding protein (C/EBP) and repressing C/EBP transactivation function. J Biol Chem, 278, 9609-19.

CHOY, L., SKILLINGTON, J. & DERYNCK, R. (2000) Roles of autocrine TGF-beta receptor and Smad signaling in adipocyte differentiation. J Cell Biol, 149, 667-82.

CHURCH, V. L. & FRANCIS-WEST, P. (2002) Wnt signalling during limb development. Int J Dev Biol, 46, 927-36.

CIRULIS, J. T., BELLINGHAM, C. M., DAVIS, E. C., HUBMACHER, D., REINHARDT, D. P., MECHAM, R. P. & KEELEY, F. W. (2008) Fibrillins, fibulins, and matrix-associated glycoprotein modulate the kinetics and morphology of in vitro self-assembly of a recombinant elastin-like polypeptide. Biochemistry, 47, 12601-13.

CIRUNA, B. & ROSSANT, J. (2001) FGF signaling regulates mesoderm cell fate specification and morphogenetic movement at the primitive streak. Dev Cell, 1, 37-49.

CLARK, R. A., MCCOY, G. A., FOLKVORD, J. M. & MCPHERSON, J. M. (1997) TGF-beta 1 stimulates cultured human fibroblasts to proliferate and produce tissue-like fibroplasia: a fibronectin matrix-dependent event. J Cell Physiol, 170, 69-80.

CLARK, J. & WHITELAW, B. (2003) A future for transgenic livestock. Nat Rev Genet, 4, 825-33.

COLIGE, A., NUYTINCK, L., HAUSSER, I., VAN ESSEN, A. J., THIRY, M., HERENS, C., ADES, L. C., MALFAIT, F., PAEPE, A. D., FRANCK, P., WOLFF, G., OOSTERWIJK, J. C., SMITT, J. H., LAPIERE, C. M. & NUSGENS, B. V. (2004) Novel types of mutation responsible for the dermatosparactic type of Ehlers-Danlos syndrome (Type VIIC) and common polymorphisms in the ADAMTS2 gene. J Invest Dermatol, 123, 656-63.

COLIGE, A., SIERON, A. L., LI, S. W., SCHWARZE, U., PETTY, E., WERTELECKI, W., WILCOX, W., KRAKOW, D., COHN, D. H., REARDON, W., BYERS, P. H., LAPIERE, C. M., PROCKOP, D. J. & NUSGENS, B. V. (1999) Human Ehlers-Danlos syndrome type VII C and bovine dermatosparaxis are caused by mutations in the procollagen I N-proteinase gene. Am J Hum Genet, 65, 308-17.

COLLOD-BEROUD, G., LE BOURDELLES, S., ADES, L., ALA-KOKKO, L., BOOMS, P., BOXER, M., CHILD, A., COMEGLIO, P., DE PAEPE, A., HYLAND, J. C., HOLMAN, K., KAITILA, I., LOEYS, B., MATYAS, G., NUYTINCK, L., PELTONEN, L., RANTAMAKI, T., ROBINSON, P., STEINMANN, B., JUNIEN, C., BEROUD, C. & BOILEAU, C. (2003) Update of the UMD-FBN1 mutation database and creation of an FBN1 polymorphism database. Hum Mutat, 22, 199-208.

CONTENTO, I. R. (1991) Children's dietary knowledge, skills, and attitudes: measurement issues. J Sch Health, 61, 208-11.

COOPER, G. (2000) The Cell: A Molecular Approach., Sunderland, MA, Sinauer Associates.

CORNIER, A. S., STAEHLING-HAMPTON, K., DELVENTHAL, K. M., SAGA, Y., CAUBET, J. F., SASAKI, N., ELLARD, S., YOUNG, E., RAMIREZ, N., CARLO, S. E., TORRES, J., EMANS, J. B., TURNPENNY, P. D. & POURQUIE, O. (2008) Mutations in the MESP2 gene cause spondylothoracic dysostosis/Jarcho-Levin syndrome. Am J Hum Genet, 82, 1334-41.

CORSON, G. M., CHALBERG, S. C., DIETZ, H. C., CHARBONNEAU, N. L. & SAKAI, L. Y. (1993) Fibrillin binds calcium and is coded by cDNAs that reveal a multidomain structure and alternatively spliced exons at the 5' end. Genomics, 17, 476-84.

CORSON, G. M., CHARBONNEAU, N. L., KEENE, D. R. & SAKAI, L. Y. (2004) Differential expression of fibrillin-3 adds to microfibril variety in human and avian, but not rodent, connective tissues. Genomics, 83, 461-72.

CSERHALMI-FRIEDMAN, P. B., OLSON, P. F., KOCH, M., CHAMPLIAUD, M. F., BRUNKEN, W. J., BURGESON, R. E. & CHRISTIANO, A. M. (2001) Structural analysis and mutation detection strategy for the human LAMC3 gene. Biochem Biophys Res Commun, 280, 39-44.

CULBERTSON, M. D., LEWIS, Z. R. & NECHIPORUK, A. V. (2011) Chondrogenic and gliogenic subpopulations of neural crest play distinct roles during the assembly of epibranchial ganglia. PLoS One, 6, e24443.

DALLAS, S. L. & BONEWALD, L. F. (2010) Dynamics of the transition from osteoblast to osteocyte. Ann N Y Acad Sci, 1192, 437-43.

DANIELS, K. & SOLURSH, M. (1991) Modulation of chondrogenesis by the cytoskeleton and extracellular matrix. J Cell Sci, 100 (Pt 2), 249-54.

DAS, U. N. (2006) Essential Fatty acids - a review. Curr Pharm Biotechnol, 7, 467-82.

DAVIS, D. B., DELMONTE, A. J., LY, C. T. & MCNALLY, E. M. (2000) Myoferlin, a candidate gene and potential modifier of muscular dystrophy. Hum Mol Genet, 9, 217-26.

DAVIS, M. R. & SUMMERS, K. M. (2012) Structure and function of the mammalian fibrillin gene family: implications for human connective tissue diseases. Mol Genet Metab, 107, 635-47.

DAVIS, M. R., ANDERSSON, R., SEVERIN, J., DE HOON, M., BERTIN, N., BAILLIE, J. K., KAWAJI, H., SANDELIN, A., FORREST, A. R. & SUMMERS, K. M. (2014) Transcriptional profiling of the human fibrillin/LTBP gene family, key regulators of mesenchymal cell functions. Mol Genet Metab, 112, 73-83.

DELWEL, G. O., DE MELKER, A. A., HOGERVORST, F., JASPARS, L. H., FLES, D. L., KUIKMAN, I., LINDBLOM, A., PAULSSON, M., TIMPL, R. & SONNENBERG, A. (1994) Distinct and overlapping ligand specificities of the alpha 3A beta 1 and alpha 6A beta 1 integrins: recognition of laminin isoforms. Mol Biol Cell, 5, 203-15.

DE MEY, M., MAERTENS, J., BOOGMANS, S., SOETAERT, W. K., VANDAMME, E. J., CUNIN, R. & FOULQUIE-MORENO, M. R. (2010) Promoter knock-in: a novel rational method for the fine tuning of genes. BMC Biotechnol, 10, 26.

DE PAEPE, A., DEVEREUX, R. B., DIETZ, H. C., HENNEKAM, R. C. & PYERITZ, R. E. (1996) Revised diagnostic criteria for the Marfan syndrome. Am J Med Genet, 62, 417-26.

DE ROOIJ, J. (2014) Cadherin adhesion controlled by cortical actin dynamics. Nat Cell Biol, 16, 508-10.

DE SOUZA, N. (2013) The ENCODE project. Nat Methods, 9, 1046.

DE VEGA, S., IWAMOTO, T., NAKAMURA, T., HOZUMI, K., MCKNIGHT, D. A., FISHER, L. W., FUKUMOTO, S. & YAMADA, Y. (2007) TM14 is a new member of the fibulin family (fibulin-7) that interacts with extracellular matrix molecules and is active for cell binding. J Biol Chem, 282, 30878-88.

DEMIR, E., SABATELLI, P., ALLAMAND, V., FERREIRO, A., MOGHADASZADEH, B., MAKRELOUF, M., TOPALOGLU, H., ECHENNE, B., MERLINI, L. & GUICHENEY, P. (2002) Mutations in COL6A3 cause severe and mild phenotypes of Ullrich congenital muscular dystrophy. Am J Hum Genet, 70, 1446-58.

DEMONBREUN, A. R., POSEY, A. D., HERETIS, K., SWAGGART, K. A., EARLEY, J. U., PYTEL, P. & MCNALLY, E. M. (2009) Myoferlin is required for insulin-like growth factor response and muscle growth. FASEB J, 24, 1284-95.

DERYNCK, R., JARRETT, J. A., CHEN, E. Y., EATON, D. H., BELL, J. R., ASSOIAN, R. K., ROBERTS, A. B., SPORN, M. B. & GOEDDEL, D. V. (1985) Human transforming growth factor-beta complementary DNA sequence and expression in normal and transformed cells. Nature, 316, 701-5.

DIAB, M., WU, J. J. & EYRE, D. R. (1996) Collagen type IX from human cartilage: a structural profile of intermolecular cross-linking sites. Biochem J, 314 (Pt 1), 327-32.

DIETZ, H. C., CUTTING, G. R., PYERITZ, R. E., MASLEN, C. L., SAKAI, L. Y., CORSON, G. M., PUFFENBERGER, E. G., HAMOSH, A., NANTHAKUMAR, E. J., CURRISTIN, S. M. & ET AL. (1991) Marfan syndrome caused by a recurrent de novo missense mutation in the fibrillin gene. Nature, 352, 337-9.

DIXON, J. A. & SPINALE, F. G. (2009) Large animal models of heart failure: a critical link in the translation of basic science to clinical practice. Circ Heart Fail, 2, 262-71.

DOHERTY, K. R., CAVE, A., DAVIS, D. B., DELMONTE, A. J., POSEY, A., EARLEY, J. U., HADHAZY, M. & MCNALLY, E. M. (2005) Normal myoblast fusion requires myoferlin. Development, 132, 5565-75.

DOMINGUEZ, R. & HOLMES, K. C. (2011) Actin structure and function. Annu Rev Biophys, 40, 169-86.

DRISKELL, R. R., LICHTENBERGER, B. M., HOSTE, E., KRETZSCHMAR, K., SIMONS, B. D., CHARALAMBOUS, M., FERRON, S. R., HERAULT, Y., PAVLOVIC, G., FERGUSON-SMITH, A. C. & WATT, F. M. (2013) Distinct fibroblast lineages determine dermal architecture in skin development and repair. Nature, 504, 277-81.

DUBOIS, C. M., LAPRISE, M. H., BLANCHETTE, F., GENTRY, L. E. & LEDUC, R. (1995) Processing of transforming growth factor beta 1 precursor by human furin convertase. J Biol Chem, 270, 10618-24.

DYER, C. E., SHUTTLEWORTH, C. A. & KIELTY, C. M. (1995) Conformation and function of fibrillin 8-cysteine motifs. Biochem Soc Trans, 23, 506S.

EKHOLM, E., HANKENSON, K. D., UUSITALO, H., HILTUNEN, A., GARDNER, H., HEINO, J. & PENTTINEN, R. (2002) Diminished callus size and cartilage synthesis in alpha 1 beta 1 integrin-deficient mice during bone fracture healing. Am J Pathol, 160, 1779-85.

ELBASHIR, S. M., HARBORTH, J., LENDECKEL, W., YALCIN, A., WEBER, K. & TUSCHL, T. (2001) Duplexes of 21-nucleotide RNAs mediate RNA interference in cultured mammalian cells. Nature, 411, 494-8.

ENGEL, J., FURTHMAYR, H., ODERMATT, E., VON DER MARK, H., AUMAILLEY, M., FLEISCHMAJER, R. & TIMPL, R. (1985) Structure and macromolecular organisation of type VI collagen. Ann N Y Acad Sci, 460, 25-37.

ENGEL, J., ODERMATT, E., ENGEL, A., MADRI, J. A., FURTHMAYR, H., ROHDE, H. & TIMPL, R. (1981) Shapes, domain organisations and flexibility of laminin and fibronectin, two multifunctional proteins of the extracellular matrix. J Mol Biol, 150, 97-120.

ERAT, M. C., SLADEK, B., CAMPBELL, I. D. & VAKONAKIS, I. (2013) Structural analysis of collagen type I interactions with human fibronectin reveals a cooperative binding mode. J Biol Chem, 288, 17441-50.

ESHGHI, S. A. S., DV (2008) ECM presents important biochemical and mechanical cues to stem cells Stem book (Internet). Cambridge, MA, Hardvard.

EVANS, D. J. & NODEN, D. M. (2006) Spatial relations between avian craniofacial neural crest and paraxial mesoderm cells. Dev Dyn, 235, 1310-25.

EVSEENKO, D., ZHU, Y., SCHENKE-LAYLAND, K., KUO, J., LATOUR, B., GE, S., SCHOLES, J., DRAVID, G., LI, X., MACLELLAN, W. R. & CROOKS, G. M. (2010) Mapping the first stages of mesoderm commitment during differentiation of human embryonic stem cells. Proc Natl Acad Sci U S A, 107, 13742-7.

EYRE, D. R., PIETKA, T., WEIS, M. A. & WU, J. J. (2004) Covalent cross-linking of the NC1 domain of collagen type IX to collagen type II in cartilage. J Biol Chem, 279, 2568-74.

FAIVRE, L., COLLOD-BEROUD, G., LOEYS, B. L., CHILD, A., BINQUET, C., GAUTIER, E., CALLEWAERT, B., ARBUSTINI, E., MAYER, K., ARSLAN-KIRCHNER, M., KIOTSEKOGLOU, A., COMEGLIO, P., MARZILIANO, N., DIETZ, H. C., HALLIDAY, D., BEROUD, C., BONITHON-KOPP, C., CLAUSTRES, M., MUTI, C., PLAUCHU, H., ROBINSON, P. N., ADES, L. C., BIGGIN, A., BENETTS, B., BRETT, M., HOLMAN, K. J., DE BACKER, J., COUCKE, P., FRANCKE, U., DE PAEPE, A., JONDEAU, G. & BOILEAU, C. (2007) Effect of mutation type and location on clinical outcome in 1,013 probands with Marfan syndrome or related phenotypes and FBN1 mutations: an international study. Am J Hum Genet, 81, 454-66.

FAIVRE, L., MASUREL-PAULET, A., COLLOD-BEROUD, G., CALLEWAERT, B. L., CHILD, A. H., STHENEUR, C., BINQUET, C., GAUTIER, E., CHEVALLIER, B., HUET, F., LOEYS, B. L., ARBUSTINI, E., MAYER, K., ARSLAN-KIRCHNER, M., KIOTSEKOGLOU, A., COMEGLIO, P., GRASSO, M., HALLIDAY, D. J., BEROUD, C., BONITHON-KOPP, C., CLAUSTRES, M., ROBINSON, P. N., ADES, L., DE BACKER, J., COUCKE, P., FRANCKE,

U., DE PAEPE, A., BOILEAU, C. & JONDEAU, G. (2009) Clinical and molecular study of 320 children with Marfan syndrome and related type I fibrillinopathies in a series of 1009 probands with pathogenic FBN1 mutations. Pediatrics, 123, 391-8.

FASSLER, R., SCHNEGELSBERG, P. N., DAUSMAN, J., SHINYA, T., MURAGAKI, Y., MCCARTHY, M. T., OLSEN, B. R. & JAENISCH, R. (1994) Mice lacking alpha 1 (IX) collagen develop noninflammatory degenerative joint disease. Proc Natl Acad Sci U S A, 91, 5070-4.

FAVREAU, C., HIGUET, D., COURVALIN, J. C. & BUENDIA, B. (2004) Expression of a mutant lamin A that causes Emery-Dreifuss muscular dystrophy inhibits in vitro differentiation of C2C12 myoblasts. Mol Cell Biol, 24, 1481-92.

FERNANDEZ-REAL, J. M., CATALAN, V., MORENO-NAVARRETE, J. M., GOMEZ-AMBROSI, J., ORTEGA, F. J., RODRIGUEZ-HERMOSA, J. I., RICART, W. & FRUHBECK, G. (2010) Study of caveolin-1 gene expression in whole adipose tissue and its subfractions and during differentiation of human adipocytes. Nutr Metab (Lond), 7, 20.

FERRARI, G., CUSELLA-DE ANGELIS, G., COLETTA, M., PAOLUCCI, E., STORNAIUOLO, A., COSSU, G. & MAVILIO, F. (1998) Muscle regeneration by bone marrow-derived myogenic progenitors. Science, 279, 1528-30.

FFRENCH-CONSTANT, C. & HYNES, R. O. (1989) Alternative splicing of fibronectin is temporally and spatially regulated in the chicken embryo. Development, 106, 375-88.

FLAUMENHAFT, R., ABE, M., SATO, Y., MIYAZONO, K., HARPEL, J., HELDIN, C. H. & RIFKIN, D. B. (1993) Role of the latent TGF-beta binding protein in the activation of latent TGF-beta by co-cultures of endothelial and smooth muscle cells. J Cell Biol, 120, 995-1002.

FLETCHER, J. M., FERRIER, P. M., GARDNER, J. O., HARKNESS, L., DHANJAL, S., SERHAL, P., HARPER, J., DELHANTY, J., BROWNSTEIN, D. G., PRASAD, Y. R., LEBKOWSKI, J., MANDALAM, R., WILMUT, I. & DE SOUSA, P. A. (2006) Variations in humanized and defined culture conditions supporting derivation of new human embryonic stem cell lines. Cloning Stem Cells, 8, 319-34.

FOGH, J., FOGH, J. M. & ORFEO, T. (1977) One hundred and twenty-seven cultured human tumor cell lines producing tumors in nude mice. J Natl Cancer Inst, 59, 221-6.

FORREST, A. R., KAWAJI, H., REHLI, M., BAILLIE, J. K., DE HOON, M. J., LASSMANN, T., ITOH, M., SUMMERS, K. M., SUZUKI, H., DAUB, C. O., KAWAI, J., HEUTINK, P., HIDE, W., FREEMAN, T. C., LENHARD, B., BAJIC, V. B., TAYLOR, M. S., MAKEEV, V. J., SANDELIN, A., HUME, D. A., CARNINCI, P. & HAYASHIZAKI, Y. (2014) A promoter-level mammalian expression atlas. Nature, 507, 462-70.

FORTUNATI, D., CHAU, D. Y., WANG, Z., COLLIGHAN, R. J. & GRIFFIN, M. (2014) Cross-linking of collagen I by tissue transglutaminase provides a promising biomaterial for promoting bone healing. Amino Acids, 46, 1751-61.

FRANCKE, U., BERG, M. A., TYNAN, K., BRENN, T., LIU, W., AOYAMA, T., GASNER, C., MILLER, D. C. & FURTHMAYR, H. (1995) A Gly1127Ser mutation in an EGF-like domain of the fibrillin-1 gene is a risk factor for ascending aortic aneurysm and dissection. Am J Hum Genet, 56, 1287-96.

FRANTZ, C., STEWART, K. M. & WEAVER, V. M. (2010) The extracellular matrix at a glance. J Cell Sci, 123, 4195-200.

FREDERIC, M. Y., MONINO, C., MARSCHALL, C., HAMROUN, D., FAIVRE, L., JONDEAU, G., KLEIN, H. G., NEUMANN, L., GAUTIER, E., BINQUET, C., MASLEN, C., GODFREY, M., GUPTA, P., MILEWICZ, D., BOILEAU, C., CLAUSTRES, M., BEROUD, C. & COLLOD-BEROUD, G. (2009) The FBN2 gene: new mutations, locus-specific database (Universal Mutation Database FBN2), and genotype-phenotype correlations. Hum Mutat, 30, 181-90.

FREEMAN, T. C., GOLDOVSKY, L., BROSCH, M., VAN DONGEN, S., MAZIERE, P., GROCOCK, R. J., FREILICH, S., THORNTON, J. & ENRIGHT, A. J. (2007) Construction, visualisation, and

clustering of transcription networks from microarray expression data. PLoS Comput Biol, 3, 2032-42.

GALIC, S., OAKHILL, J. S. & STEINBERG, G. R. (2009) Adipose tissue as an endocrine organ. Mol Cell Endocrinol, 316, 129-39.

GAJ, T., GERSBACH, C. A. & BARBAS, C. F., 3RD (2013) ZFN, TALEN, and CRISPR/Cas-based methods for genome engineering. Trends Biotechnol, 31, 397-405.

GEISER, A. G., HUMMEL, C. W., DRAPER, M. W., HENCK, J. W., COHEN, I. R., RUDMANN, D. G., DONNELLY, K. B., ADRIAN, M. D., SHEPHERD, T. A., WALLACE, O. B., MCCANN, D. J., OLDHAM, S. W., BRYANT, H. U., SATO, M. & DODGE, J. A. (2005) A new selective estrogen receptor modulator with potent uterine antagonist activity, agonist activity in bone, and minimal ovarian stimulation. Endocrinology, 146, 4524-35.

GEORGE, E. L., GEORGES-LABOUESSE, E. N., PATEL-KING, R. S., RAYBURN, H. & HYNES, R. O. (1993) Defects in mesoderm, neural tube and vascular development in mouse embryos lacking fibronectin. Development, 119, 1079-91.

GERBER, E. E., GALLO, E. M., FONTANA, S. C., DAVIS, E. C., WIGLEY, F. M., HUSO, D. L. & DIETZ, H. C. (2013) Integrin-modulating therapy prevents fibrosis and autoimmunity in mouse models of scleroderma. Nature, 503, 126-30.

GILBERT, S. (2000) Developmental Biology, Sunderland, MA, Sinaver Associates

GILSANZ, V., HU, H. H. & KAJIMURA, S. (2012) Relevance of brown adipose tissue in infancy and adolescence. Pediatr Res, 73, 3-9.

GIRALT, M. & VILLARROYA, F. (2013) White, brown, beige/brite: different adipose cells for different functions? Endocrinology, 154, 2992-3000.

GLASS, D. A., 2ND, BIALEK, P., AHN, J. D., STARBUCK, M., PATEL, M. S., CLEVERS, H., TAKETO, M. M., LONG, F., MCMAHON, A. P., LANG, R. A. & KARSENTY, G. (2005) Canonical Wnt signaling in differentiated osteoblasts controls osteoclast differentiation. Dev Cell, 8, 751-64.

GODFREY, M., MENASHE, V., WELEBER, R. G., KOLER, R. D., BIGLEY, R. H., LOVRIEN, E., ZONANA, J. & HOLLISTER, D. W. (1990) Cosegregation of elastin-associated microfibrillar abnormalities with the Marfan phenotype in families. Am J Hum Genet, 46, 652-60.

GOLDBERG, B. & GREEN, H. (1964) An Analysis of Collagen Secretion by Established Mouse Fibroblast Lines. J Cell Biol, 22, 227-58.

GOLDBLATT, J., HYATT, J., EDWARDS, C. & WALPOLE, I. (2011) Further evidence for a marfanoid syndrome with neonatal progeroid features and severe generalized lipodystrophy due to frameshift mutations near the 3' end of the FBN1 gene. Am J Med Genet A, 155A, 717-20.

GOLDRING, M. B., BIRKHEAD, J. R., SUEN, L. F., YAMIN, R., MIZUNO, S., GLOWACKI, J., ARBISER, J. L. & APPERLEY, J. F. (1994) Interleukin-1 beta-modulated gene expression in immortalized human chondrocytes. J Clin Invest, 94, 2307-16.

GOLDRING, M. B., TSUCHIMOCHI, K. & IJIRI, K. (2006) The control of chondrogenesis. J Cell Biochem, 97, 33-44.

GOLDSMITH, E. C., HOFFMAN, A., MORALES, M. O., POTTS, J. D., PRICE, R. L., MCFADDEN, A., RICE, M. & BORG, T. K. (2004) Organisation of fibroblasts in the heart. Dev Dyn, 230, 787-94.

GRAHAM, F. L., SMILEY, J., RUSSELL, W. C. & NAIRN, R. (1977) Characteristics of a human cell line transformed by DNA from human adenovirus type 5. J Gen Virol, 36, 59-74.

GRAHAM, F. L. & VAN DER EB, A. J. (1973) A new technique for the assay of infectivity of human adenovirus 5 DNA. Virology, 52, 456-67.

GRAHAM, F. L., VAN DER EB, A. J. & HEIJNEKER, H. L. (1974) Size and location of the transforming region in human adenovirus type 5 DNA. Nature, 251, 687-91.

GRAUL-NEUMANN, L. M., KIENITZ, T., ROBINSON, P. N., BAASANJAV, S., KAROW, B., GILLESSEN-KAESBACH, G., FAHSOLD, R., SCHMIDT, H., HOFFMANN, K. & PASSARGE, E. (2010) Marfan syndrome with neonatal progeroid syndrome-like lipodystrophy associated with a novel frameshift mutation at the 3' terminus of the FBN1-gene. Am J Med Genet A, 152A, 2749-55.

GREENWOOD, F. C., LANDON, J. & STAMP, T. C. (1966) The plasma sugar, free fatty acid, cortisol, and growth hormone response to insulin. I. In control subjects. J Clin Invest, 45, 429-36.

GREY, F., MEYERS, H., WHITE, E. A., SPECTOR, D. H. & NELSON, J. (2007) A human cytomegalovirus-encoded microRNA regulates expression of multiple viral genes involved in replication. PLoS Pathog, 3, e163.

GRINNELL, F. & FELD, M. K. (1979) Initial adhesion of human fibroblasts in serum-free medium: possible role of secreted fibronectin. Cell, 17, 117-29.

GROENINK, M., DEN HARTOG, A. W., FRANKEN, R., RADONIC, T., DE WAARD, V., TIMMERMANS, J., SCHOLTE, A. J., VAN DEN BERG, M. P., SPIJKERBOER, A. M., MARQUERING, H. A., ZWINDERMAN, A. H. & MULDER, B. J. (2013) Losartan reduces aortic dilatation rate in adults with Marfan syndrome: a randomized controlled trial. Eur Heart J, 34, 3491-500.

GROSS, D. A. & SILVER, D. L. (2014) Cytosolic lipid droplets: from mechanisms of fat storage to disease. Crit Rev Biochem Mol Biol, 49, 304-26.

GUO, D. C., PANNU, H., TRAN-FADULU, V., PAPKE, C. L., YU, R. K., AVIDAN, N., BOURGEOIS, S., ESTRERA, A. L., SAFI, H. J., SPARKS, E., AMOR, D., ADES, L., MCCONNELL, V., WILLOUGHBY, C. E., ABUELO, D., WILLING, M., LEWIS, R. A., KIM, D. H., SCHERER, S., TUNG, P. P., AHN, C., BUJA, L. M., RAMAN, C. S., SHETE, S. S. & MILEWICZ, D. M. (2007) Mutations in smooth muscle alpha-actin (ACTA2) lead to thoracic aortic aneurysms and dissections. Nat Genet, 39, 1488-93.

GUO, G., BAUER, S., HECHT, J., SCHULZ, M. H., BUSCHE, A. & ROBINSON, P. N. (2008) A short ultraconserved sequence drives transcription from an alternate FBN1 promoter. Int J Biochem Cell Biol, 40, 638-50.

GUO, G., RODELSPERGER, C., DIGWEED, M. & ROBINSON, P. N. (2013) Regulation of fibrillin-1 gene expression by Sp1. Gene, 527, 448-55.

GUPTA, P. A., PUTNAM, E. A., CARMICAL, S. G., KAITILA, I., STEINMANN, B., CHILD, A., DANESINO, C., METCALFE, K., BERRY, S. A., CHEN, E., DELORME, C. V., THONG, M. K., ADES, L. C. & MILEWICZ, D. M. (2002) Ten novel FBN2 mutations in congenital contractural arachnodactyly: delineation of the molecular pathogenesis and clinical phenotype. Hum Mutat, 19, 39-48.

GUPTA, P. A., WALLIS, D. D., CHIN, T. O., NORTHRUP, H., TRAN-FADULU, V. T., TOWBIN, J. A. & MILEWICZ, D. M. (2004) FBN2 mutation associated with manifestations of Marfan syndrome and congenital contractural arachnodactyly. J Med Genet, 41, e56.

GUTMAN, A. & KORNBLIHTT, A. R. (1987) Identification of a third region of cell-specific alternative splicing in human fibronectin mRNA. Proc Natl Acad Sci U S A, 84, 7179-82.

HABASHI, J. P., DOYLE, J. J., HOLM, T. M., AZIZ, H., SCHOENHOFF, F., BEDJA, D., CHEN, Y., MODIRI, A. N., JUDGE, D. P. & DIETZ, H. C. (2011) Angiotensin II type 2 receptor signaling attenuates aortic aneurysm in mice through ERK antagonism. Science, 332, 361-5.

HABASHI, J. P., JUDGE, D. P., HOLM, T. M., COHN, R. D., LOEYS, B. L., COOPER, T. K., MYERS, L., KLEIN, E. C., LIU, G., CALVI, C., PODOWSKI, M., NEPTUNE, E. R., HALUSHKA, M. K., BEDJA, D., GABRIELSON, K., RIFKIN, D. B., CARTA, L., RAMIREZ, F., HUSO, D. L. &

DIETZ, H. C. (2006) Losartan, an AT1 antagonist, prevents aortic aneurysm in a mouse model of Marfan syndrome. Science, 312, 117-21.

HAHM, J. R., NOH, H. S., HA, J. H., ROH, G. S. & KIM, D. R. (2014) Alpha-lipoic acid attenuates adipocyte differentiation and lipid accumulation in 3T3-L1 cells via AMPK-dependent autophagy. Life Sci, 100, 125-32.

HALFON, S., ABRAMOV, N., GRINBLAT, B. & GINIS, I. (2010) Markers distinguishing mesenchymal stem cells from fibroblasts are downregulated with passaging. Stem Cells Dev, 20, 53-66.

HALPER, J. & KJAER, M. (2014) Basic components of connective tissues and extracellular matrix: elastin, fibrillin, fibulins, fibrinogen, fibronectin, laminin, tenascins and thrombospondins. Adv Exp Med Biol, 802, 31-47.

HAMALAINEN, E. R., JONES, T. A., SHEER, D., TASKINEN, K., PIHLAJANIEMI, T. & KIVIRIKKO, K. I. (1991) Molecular cloning of human lysyl oxidase and assignment of the gene to chromosome 5q23.3-31.2. Genomics, 11, 508-16.

HAMILL, K. J., KLIGYS, K., HOPKINSON, S. B. & JONES, J. C. (2009) Laminin deposition in the extracellular matrix: a complex picture emerges. J Cell Sci, 122, 4409-17.

HANDFORD, P. A., DOWNING, A. K., REINHARDT, D. P. & SAKAI, L. Y. (2000) Fibrillin: from domain structure to supramolecular assembly. Matrix Biol, 19, 457-70.

HANSSEN, E., FRANC, S. & GARRONE, R. (1998) Fibrillin-rich microfibrils: structural modifications during ageing in normal human zonule. J Submicrosc Cytol Pathol, 30, 365-9.

HARMS, M. & SEALE, P. (2013) Brown and beige fat: development, function and therapeutic potential. Nat Med, 19, 1252-63.

HASSEL, D., DAHME, T., ERDMANN, J., MEDER, B., HUGE, A., STOLL, M., JUST, S., HESS, A., EHLERMANN, P., WEICHENHAN, D., GRIMMLER, M., LIPTAU, H., HETZER, R., REGITZ-ZAGROSEK, V., FISCHER, C., NURNBERG, P., SCHUNKERT, H., KATUS, H. A. & ROTTBAUER, W. (2009) Nexilin mutations destabilize cardiac Z-disks and lead to dilated cardiomyopathy. Nat Med, 15, 1281-8.

HASENFUSS, G. (1998) Animal models of human cardiovascular disease, heart failure and hypertrophy. Cardiovasc Res, 39, 60-76.

HAY, E. D. (2005) The mesenchymal cell, its role in the embryo, and the remarkable signaling mechanisms that create it. Dev Dyn, 233, 706-20.

HAYASHI, M., NINOMIYA, Y., HAYASHI, K., LINSENMAYER, T. F., OLSEN, B. R. & TRELSTAD, R. L. (1988) Secretion of collagen types I and II by epithelial and endothelial cells in the developing chick cornea demonstrated by in situ hybridization and immunohistochemistry. Development, 103, 27-36.

HAYASHIZAKI, Y. & CARNINCI, P. (2006) Genome Network and FANTOM3: assessing the complexity of the transcriptome. PLoS Genet, 2, e63.

HE, C. & KLIONSKY, D. J. (2009) Regulation mechanisms and signaling pathways of autophagy. Annu Rev Genet, 43, 67-93.

HEATLEY, F. & SCOTT, J. E. (1988) A water molecule participates in the secondary structure of hyaluronan. Biochem J, 254, 489-93.

HEISKALA, M., PETERSON, P. A. & YANG, Y. (2001) The roles of claudin superfamily proteins in paracellular transport. Traffic, 2, 93-8.

HERNANDEZ, M. R. (1992) Ultrastructural immunocytochemical analysis of elastin in the human lamina cribrosa. Changes in elastic fibers in primary open-angle glaucoma. Invest Ophthalmol Vis Sci, 33, 2891-903.

HINDSON, V. J., ASHWORTH, J. L., ROCK, M. J., CUNLIFFE, S., SHUTTLEWORTH, C. A. & KIELTY, C. M. (1999) Fibrillin degradation by matrix metalloproteinases: identification of amino- and carboxy-terminal cleavage sites. FEBS Lett, 452, 195-8.

HIRANI, R., HANSSEN, E. & GIBSON, M. A. (2007) LTBP-2 specifically interacts with the amino-terminal region of fibrillin-1 and competes with LTBP-1 for binding to this microfibrillar protein. Matrix Biol, 26, 213-23.

HIRATA, H., SOKABE, M. & LIM, C. T. (2014) Molecular mechanisms underlying the force-dependent regulation of actin-to-ECM linkage at the focal adhesions. Prog Mol Biol Transl Sci, 126, 135-54.

HIROHATA, S., WANG, L. W., MIYAGI, M., YAN, L., SELDIN, M. F., KEENE, D. R., CRABB, J. W. & APTE, S. S. (2002) Punctin, a novel ADAMTS-like molecule, ADAMTSL-1, in extracellular matrix. J Biol Chem, 277, 12182-9.

HO, C. Y., JAALOUK, D. E., VARTIAINEN, M. K. & LAMMERDING, J. (2013) Lamin A/C and emerin regulate MKL1-SRF activity by modulating actin dynamics. Nature, 497, 507-11.

HOLMES, K. C., POPP, D., GEBHARD, W. & KABSCH, W. (1990) Atomic model of the actin filament. Nature, 347, 44-9.

HORIKOSHI, N., CONG, J., KLEY, N. & SHENK, T. (1999) Isolation of differentially expressed cDNAs from p53-dependent apoptotic cells: activation of the human homologue of the Drosophila peroxidasin gene. Biochem Biophys Res Commun, 261, 864-9.

HORN, D. & ROBINSON, P. N. (2011) Progeroid facial features and lipodystrophy associated with a novel splice site mutation in the final intron of the FBN1 gene. Am J Med Genet A, 155A, 721-4.

HOUSTON, B., STEWART, A. J. & FARQUHARSON, C. (2004) PHOSPHO1-A novel phosphatase specifically expressed at sites of mineralisation in bone and cartilage. Bone, 34, 629-37.

HOWERTON, K., SCHLAEPFER, D. D. & ILIC, D. (2008) Establishment of cell lines from mouse embryos with early embryonic lethality. Cell Commun Adhes, 15, 379-83.

HUANG DA, W., SHERMAN, B. T. & LEMPICKI, R. A. (2009a) Bioinformatics enrichment tools: paths toward the comprehensive functional analysis of large gene lists. Nucleic Acids Res, 37, 1-13.

HUANG DA, W., SHERMAN, B. T. & LEMPICKI, R. A. (2009b) Systematic and integrative analysis of large gene lists using DAVID bioinformatics resources. Nat Protoc, 4, 44-57.

HUANG, C., JACKSON, M., SAMUEL, K., TAYLOR, A. H., LOWELL, S. & FORRESTER, L. M. (2013) Haematopoietic differentiation is inhibited when Notch activity is enhanced in FLK1(+) mesoderm progenitors. Stem Cell Res, 11, 1273-87.

HUANG, C., XUE, M., CHEN, H., JIAO, J., HERSCHMAN, H. R., O'KEEFE, R. J. & ZHANG, X. (2014) The spatiotemporal role of COX-2 in osteogenic and chondrogenic differentiation of periosteum-derived mesenchymal progenitors in fracture repair. PLoS One, 9, e100079.

HUANG, L., ZHENG, M., ZHOU, Q. M., ZHANG, M. Y., YU, Y. H., YUN, J. P. & WANG, H. Y. (2012) Identification of a 7-gene signature that predicts relapse and survival for early stage patients with cervical carcinoma. Med Oncol, 29, 2911-8.

HUANG, W., CHUNG, U. I., KRONENBERG, H. M. & DE CROMBRUGGHE, B. (2001) The chondrogenic transcription factor Sox9 is a target of signaling by the parathyroid hormone-related peptide in the growth plate of endochondral bones. Proc Natl Acad Sci U S A, 98, 160-5.

HUANG, Z., REN, P. G., MA, T., SMITH, R. L. & GOODMAN, S. B. (2010) Modulating osteogenesis of mesenchymal stem cells by modifying growth factor availability. Cytokine, 51, 305-10.

HUME, D. A., SUMMERS, K. M., RAZA, S., BAILLIE, J. K. & FREEMAN, T. C. (2010) Functional clustering and lineage markers: insights into cellular differentiation and gene function from large-scale microarray studies of purified primary cell populations. Genomics, 95, 328-38.

HYYTIAINEN, M., PENTTINEN, C. & KESKI-OJA, J. (2004) Latent TGF-beta binding proteins: extracellular matrix association and roles in TGF-beta activation. Crit Rev Clin Lab Sci, 41, 233-64.

IEDA, M., TSUCHIHASHI, T., IVEY, K. N., ROSS, R. S., HONG, T. T., SHAW, R. M. & SRIVASTAVA, D. (2009) Cardiac fibroblasts regulate myocardial proliferation through beta1 integrin signaling. Dev Cell, 16, 233-44.

ISOGAI, Z., ONO, R. N., USHIRO, S., KEENE, D. R., CHEN, Y., MAZZIERI, R., CHARBONNEAU, N. L., REINHARDT, D. P., RIFKIN, D. B. & SAKAI, L. Y. (2003) Latent transforming growth factor beta-binding protein 1 interacts with fibrillin and is a microfibril-associated protein. J Biol Chem, 278, 2750-7.

JACQUINET, A., VERLOES, A., CALLEWAERT, B., COREMANS, C., COUCKE, P., DE PAEPE, A., KORNAK, U., LEBRUN, F., LOMBET, J., PIERARD, G. E., ROBINSON, P. N., SYMOENS, S., VAN MALDERGEM, L. & DEBRAY, F. G. (2014) Neonatal progeroid variant of Marfan syndrome with congenital lipodystrophy results from mutations at the 3' end of FBN1 gene. Eur J Med Genet, 57, 230-4.

JAMES, C. G., APPLETON, C. T., ULICI, V., UNDERHILL, T. M. & BEIER, F. (2005) Microarray analyses of gene expression during chondrocyte differentiation identifies novel regulators of hypertrophy. Mol Biol Cell, 16, 5316-33.

JANSON, D. G., SAINTIGNY, G., VAN ADRICHEM, A., MAHE, C. & EL GHALBZOURI, A. (2012) Different gene expression patterns in human papillary and reticular fibroblasts. J Invest Dermatol, 132, 2565-72.

JANSON, D., SAINTIGNY, G., MAHE, C. & EL GHALBZOURI, A. (2013) Papillary fibroblasts differentiate into reticular fibroblasts after prolonged in vitro culture. Exp Dermatol, 22, 48-53.

JENSEN, S. A., VRHOVSKI, B. & WEISS, A. S. (2000) Domain 26 of tropoelastin plays a dominant role in association by coacervation. J Biol Chem, 275, 28449-54.

JENSEN, S. A., ASPINALL, G. & HANDFORD, P. A. (2014) C-terminal propeptide is required for fibrillin-1 secretion and blocks premature assembly through linkage to domains cbEGF41-43. Proc Natl Acad Sci U S A, 111, 10155-60.

JOE, B., SAAD, Y., DHINDAW, S., LEE, N. H., FRANK, B. C., ACHINIKE, O. H., LUU, T. V., GOPALAKRISHNAN, K., TOLAND, E. J., FARMS, P., YERGA-WOOLWINE, S., MANICKAVASAGAM, E., RAPP, J. P., GARRETT, M. R., COE, D., APTE, S. S., RANKINEN, T., PERUSSE, L., EHRET, G. B., GANESH, S. K., COOPER, R. S., O'CONNOR, A., RICE, T., WEDER, A. B., CHAKRAVARTI, A., RAO, D. C. & BOUCHARD, C. (2009) Positional identification of variants of Adamts16 linked to inherited hypertension. Hum Mol Genet, 18, 2825-38.

JOHNSON, R. L. & TABIN, C. J. (1997) Molecular models for vertebrate limb development. Cell, 90, 979-90.

JONES, C. J., SEAR, C. H. & GRANT, M. E. (1980) An ultrastructural study of fibroblasts derived from bovine ligamentum nuchae and their capacity for elastogenesis in culture. J Pathol, 131, 35-53.

JUDGE, D. P., BIERY, N. J., KEENE, D. R., GEUBTNER, J., MYERS, L., HUSO, D. L., SAKAI, L. Y. & DIETZ, H. C. (2004) Evidence for a critical contribution of haploinsufficiency in the complex pathogenesis of Marfan syndrome. J Clin Invest, 114, 172-81.

JURGENSEN, H. J., MADSEN, D. H., INGVARSEN, S., MELANDER, M. C., GARDSVOLL, H., PATTHY, L., ENGELHOLM, L. H. & BEHRENDT, N. (2011) A novel functional role of collagen glycosylation: interaction with the endocytic collagen receptor uparap/ENDO180. J Biol Chem, 286, 32736-48.

KAGAN, H. M. & SULLIVAN, K. A. (1982) Lysyl oxidase: preparation and role in elastin biosynthesis. Methods Enzymol, 82 Pt A, 637-50.

KAINOV, Y., FAVORSKAYA, I., DELEKTORSKAYA, V., CHEMERIS, G., KOMELKOV, A., ZHURAVSKAYA, A., TRUKHANOVA, L., ZUEVA, E., TAVITIAN, B., DYAKOVA, N., ZBOROVSKAYA, I. & TCHEVKINA, E. (2014) CRABP1 provides high malignancy of transformed mesenchymal cells and contributes to the pathogenesis of mesenchymal and neuroendocrine tumors. Cell Cycle, 13, 1530-9.

KAKEHI, K., KINOSHITA, M. & YASUEDA, S. (2003) Hyaluronic acid: separation and biological implications. J Chromatogr B Analyt Technol Biomed Life Sci, 797, 347-55.

KANAMORI-KATAYAMA, M., ITOH, M., KAWAJI, H., LASSMANN, T., KATAYAMA, S., KOJIMA, M., BERTIN, N., KAIHO, A., NINOMIYA, N., DAUB, C. O., CARNINCI, P., FORREST, A. R. & HAYASHIZAKI, Y. (2011) Unamplified cap analysis of gene expression on a single-molecule sequencer. Genome Res, 21, 1150-9.

KARAMARITI, E., MARGARITI, A., WINKLER, B., WANG, X., HONG, X., BABAN, D., RAGOUSSIS, J., HUANG, Y., HAN, J. D., WONG, M. M., SAG, C. M., SHAH, A. M., HU, Y. & XU, Q. (2013) Smooth muscle cells differentiated from reprogrammed embryonic lung fibroblasts through DKK3 signaling are potent for tissue engineering of vascular grafts. Circ Res, 112, 1433-43.

KANG, H., SUNG, J., JUNG, H. M., WOO, K. M., HONG, S. D. & ROH, S. (2011) Insulin-like growth factor 2 promotes osteogenic cell differentiation in the parthenogenetic murine embryonic stem cells. Tissue Eng Part A, 18, 331-41.

KARDASSIS, D., MURPHY, C., FOTSIS, T., MOUSTAKAS, A. & STOURNARAS, C. (2009) Control of transforming growth factor beta signal transduction by small GTPases. FEBS J, 276, 2947-65.

KASAMATSU, S., HACHIYA, A., FUJIMURA, T., SRIWIRIYANONT, P., HAKETA, K., VISSCHER, M. O., KITZMILLER, W. J., BELLO, A., KITAHARA, T., KOBINGER, G. P. & TAKEMA, Y. (2012) Essential role of microfibrillar-associated protein 4 in human cutaneous homeostasis and in its photoprotection. Sci Rep, 1, 164.

KATO, A., OKAMOTO, O., WU, W., MATSUO, N., KUMAI, J., YAMADA, Y., KATAGIRI, F., NOMIZU, M. & FUJIWARA, S. (2014) Identification of fibronectin binding sites in dermatopontin and their biological function. J Dermatol Sci, 76, 51-9.

KATOH, M. (2002) GIPC gene family (Review). Int J Mol Med, 9, 585-9.

KAWAI, J., SHINAGAWA, A., SHIBATA, K., YOSHINO, M., ITOH, M., ISHII, Y., ARAKAWA, T., HARA, A., FUKUNISHI, Y., KONNO, H., ADACHI, J., FUKUDA, S., AIZAWA, K., IZAWA, M., NISHI, K., KIYOSAWA, H., KONDO, S., YAMANAKA, I., SAITO, T., OKAZAKI, Y., GOJOBORI, T., BONO, H., KASUKAWA, T., SAITO, R., KADOTA, K., MATSUDA, H., ASHBURNER, M., BATALOV, S., CASAVANT, T., FLEISCHMANN, W., GAASTERLAND, T., GISSI, C., KING, B., KOCHIWA, H., KUEHL, P., LEWIS, S., MATSUO, Y., NIKAIDO, I., PESOLE, G., QUACKENBUSH, J., SCHRIML, L. M., STAUBLI, F., SUZUKI, R., TOMITA, M., WAGNER, L., WASHIO, T., SAKAI, K., OKIDO, T., FURUNO, M., AONO, H., BALDARELLI, R., BARSH, G., BLAKE, J., BOFFELLI, D., BOJUNGA, N., CARNINCI, P., DE BONALDO, M. F., BROWNSTEIN, M. J., BULT, C., FLETCHER, C., FUJITA, M., GARIBOLDI, M., GUSTINCICH, S., HILL, D., HOFMANN, M., HUME, D. A., KAMIYA, M., LEE, N. H., LYONS, P., MARCHIONNI, L., MASHIMA, J., MAZZARELLI, J., MOMBAERTS, P., NORDONE, P., RING, B., RINGWALD, M., RODRIGUEZ, I., SAKAMOTO, N., SASAKI, H., SATO, K., SCHONBACH, C., SEYA, T., SHIBATA, Y., STORCH, K. F., SUZUKI, H., TOYO-OKA, K., WANG, K. H., WEITZ, C., WHITTAKER, C., WILMING, L., WYNSHAW-BORIS, A., YOSHIDA, K., HASEGAWA, Y., KAWAJI, H., KOHTSUKI, S. & HAYASHIZAKI, Y. (2001) Functional annotation of a full-length mouse cDNA collection. Nature, 409, 685-90.

KEENE, D. R., MADDOX, B. K., KUO, H. J., SAKAI, L. Y. & GLANVILLE, R. W. (1991) Extraction of extendable beaded structures and their identification as fibrillin-containing extracellular matrix microfibrils. J Histochem Cytochem, 39, 441-9.

KEENE, D. R., JORDAN, C. D., REINHARDT, D. P., RIDGWAY, C. C., ONO, R. N., CORSON, G. M., FAIRHURST, M., SUSSMAN, M. D., MEMOLI, V. A. & SAKAI, L. Y. (1997) Fibrillin-1 in human cartilage: developmental expression and formation of special banded fibers. J Histochem Cytochem, 45, 1069-82.

KEWLEY, M. A., WILLIAMS, G. & STEVEN, F. S. (1978) Studies of elastic tissue formation in the developing bovine ligamentum nuchae. J Pathol, 124, 95-101.

KIANI, C., CHEN, L., WU, Y. J., YEE, A. J. & YANG, B. B. (2002) Structure and function of aggrecan. Cell Res, 12, 19-32.

KIELTY, C. M., BALDOCK, C., LEE, D., ROCK, M. J., ASHWORTH, J. L. & SHUTTLEWORTH, C. A. (2002) Fibrillin: from microfibril assembly to biomechanical function. Philos Trans R Soc Lond B Biol Sci, 357, 207-17.

KIELTY, C. M., BERRY, L., WHITTAKER, S. P., GRANT, M. E. & SHUTTLEWORTH, C. A. (1993) Microfibrillar assemblies of foetal bovine skin. Developmental expression and relative abundance of type VI collagen and fibrillin. Matrix, 13, 103-12.

KIELTY, C. M. & SHUTTLEWORTH, C. A. (1993a) Synthesis and assembly of fibrillin by fibroblasts and smooth muscle cells. J Cell Sci, 106 (Pt 1), 167-73.

KIELTY, C. M. & SHUTTLEWORTH, C. A. (1993b) The role of calcium in the organisation of fibrillin microfibrils. FEBS Lett, 336, 323-6.

KIELTY, C. M., PHILLIPS, J. E., CHILD, A. H., POPE, F. M. & SHUTTLEWORTH, C. A. (1994) Fibrillin secretion and microfibril assembly by Marfan dermal fibroblasts. Matrix Biol, 14, 191-9.

KIELTY, C. M. & SHUTTLEWORTH, C. A. (1994) Abnormal fibrillin assembly by dermal fibroblasts from two patients with Marfan syndrome. J Cell Biol, 124, 997-1004.

KIELTY, C. M. & SHUTTLEWORTH, C. A. (1997) Microfibrillar elements of the dermal matrix. Microsc Res Tech, 38, 413-27.

KIELTY, C. M., SHUTTLEWORTH, C. A. & GRANT, M. E. (1991) Studies on microfibrils of developing bovine elastic tissues. Biochem Soc Trans, 19, 383S.

KIELTY, C. M., WHITTAKER, S. P., GRANT, M. E. & SHUTTLEWORTH, C. A. (1992) Type VI collagen microfibrils: evidence for a structural association with hyaluronan. J Cell Biol, 118, 979-90.

KIKKAWA, Y., SANZEN, N., FUJIWARA, H., SONNENBERG, A. & SEKIGUCHI, K. (2000) Integrin binding specificity of laminin-10/11: laminin-10/11 are recognized by alpha 3 beta 1, alpha 6 beta 1 and alpha 6 beta 4 integrins. J Cell Sci, 113 (Pt 5), 869-76.

KINSEY, R., WILLIAMSON, M. R., CHAUDHRY, S., MELLODY, K. T., MCGOVERN, A., TAKAHASHI, S., SHUTTLEWORTH, C. A. & KIELTY, C. M. (2008) Fibrillin-1 microfibril deposition is dependent on fibronectin assembly. J Cell Sci, 121, 2696-704.

KIRSCHNER, R., HUBMACHER, D., IYENGAR, G., KAUR, J., FAGOTTO-KAUFMANN, C., BROMME, D., BARTELS, R. & REINHARDT, D. P. (2011) Classical and neonatal Marfan syndrome mutations in fibrillin-1 cause differential protease susceptibilities and protein function. J Biol Chem, 286, 32810-23.

KITAHAMA, S., GIBSON, M. A., HATZINIKOLAS, G., HAY, S., KULIWABA, J. L., EVDOKIOU, A., ATKINS, G. J. & FINDLAY, D. M. (2000) Expression of fibrillins and other microfibril-associated proteins in human bone and osteoblast-like cells. Bone, 27, 61-7.

KITAJIMA, S., TAKAGI, A., INOUE, T. & SAGA, Y. (2000) MesP1 and MesP2 are essential for the development of cardiac mesoderm. Development, 127, 3215-26.

KLOTING, N., KOCH, L., WUNDERLICH, T., KERN, M., RUSCHKE, K., KRONE, W., BRUNING, J. C. & BLUHER, M. (2008) Autocrine IGF-1 action in adipocytes controls systemic IGF-1 concentrations and growth. Diabetes, 57, 2074-82.

KNAUFF, E. A., FRANKE, L., VAN ES, M. A., VAN DEN BERG, L. H., VAN DER SCHOUW, Y. T., LAVEN, J. S., LAMBALK, C. B., HOEK, A., GOVERDE, A. J., CHRISTIN-MAITRE, S., HSUEH, A. J., WIJMENGA, C. & FAUSER, B. C. (2009) Genome-wide association study in premature ovarian failure patients suggests ADAMTS19 as a possible candidate gene. Hum Reprod, 24, 2372-8.

KOCABAS, A. M., CROSBY, J., ROSS, P. J., OTU, H. H., BEYHAN, Z., CAN, H., TAM, W. L., ROSA, G. J., HALGREN, R. G., LIM, B., FERNANDEZ, E. & CIBELLI, J. B. (2006) The transcriptome of human oocytes. Proc Natl Acad Sci U S A, 103, 14027-32.

KOCH, M., OLSON, P. F., ALBUS, A., JIN, W., HUNTER, D. D., BRUNKEN, W. J., BURGESON, R. E. & CHAMPLIAUD, M. F. (1999) Characterization and expression of the laminin gamma3 chain: a novel, non-basement membrane-associated, laminin chain. J Cell Biol, 145, 605-18.

KODZIUS, R., KOJIMA, M., NISHIYORI, H., NAKAMURA, M., FUKUDA, S., TAGAMI, M., SASAKI, D., IMAMURA, K., KAI, C., HARBERS, M., HAYASHIZAKI, Y. & CARNINCI, P. (2006) CAGE: cap analysis of gene expression. Nat Methods, 3, 211-22.

KOKUBU, C., HEINZMANN, U., KOKUBU, T., SAKAI, N., KUBOTA, T., KAWAI, M., WAHL, M. B., GALCERAN, J., GROSSCHEDL, R., OZONO, K. & IMAI, K. (2004) Skeletal defects in ringelschwanz mutant mice reveal that Lrp6 is required for proper somitogenesis and osteogenesis. Development, 131, 5469-80.

KOZUKA, J., YOKOTA, H., ARAI, Y., ISHII, Y. & YANAGIDA, T. (2007) Dynamic polymorphism of actin as activation mechanism for cell motility. Biosystems, 88, 273-82.

KRAMER, I., HALLEUX, C., KELLER, H., PEGURRI, M., GOOI, J. H., WEBER, P. B., FENG, J. Q., BONEWALD, L. F. & KNEISSEL, M. (2010) Osteocyte Wnt/beta-catenin signaling is required for normal bone homeostasis. Mol Cell Biol, 30, 3071-85.

KUMTA, N. B., IRANI, S. F., SEKHRI, R. R. & PUNWANI, D. V. (1976) Congenital contractural arachnodactyly. J Postgrad Med, 22, 191-3.

KUROSAWA, N., CHEN, G. Y., KADOMATSU, K., IKEMATSU, S., SAKUMA, S. & MURAMATSU, T. (2001) Glypican-2 binds to midkine: the role of glypican-2 in neuronal cell adhesion and neurite outgrowth. Glycoconj J, 18, 499-507.

LACRO, R. V., DIETZ, H. C., SLEEPER, L. A., YETMAN, A. T., BRADLEY, T. J., COLAN, S. D., PEARSON, G. D., SELAMET TIERNEY, E. S., LEVINE, J. C., ATZ, A. M., BENSON, D. W., BRAVERMAN, A. C., CHEN, S., DE BACKER, J., GELB, B. D., GROSSFELD, P. D., KLEIN, G. L., LAI, W. W., LIOU, A., LOEYS, B. L., MARKHAM, L. W., OLSON, A. K., PARIDON, S. M., PEMBERTON, V. L., PIERPONT, M. E., PYERITZ, R. E., RADOJEWSKI, E., ROMAN, M. J., SHARKEY, A. M., STYLIANOU, M. P., WECHSLER, S. B., YOUNG, L. T. & MAHONY, L. (2014) Atenolol versus losartan in children and young adults with Marfan's syndrome. N Engl J Med, 371, 2061-71.

LATTIN, J. E., SCHRODER, K., SU, A. I., WALKER, J. R., ZHANG, J., WILTSHIRE, T., SAIJO, K., GLASS, C. K., HUME, D. A., KELLIE, S. & SWEET, M. J. (2008) Expression analysis of G Protein-Coupled Receptors in mouse macrophages. Immunome Res, 4, 5.

LAMOUILLE, S., XU, J. & DERYNCK, R. (2014) Molecular mechanisms of epithelial-mesenchymal transition. Nat Rev Mol Cell Biol, 15, 178-96.

LAURENT, T. C., LAURENT, U. B. & FRASER, J. R. (1996) The structure and function of hyaluronan: An overview. Immunol Cell Biol, 74, A1-7.

LAUSCH, E., KEPPLER, R., HILBERT, K., CORMIER-DAIRE, V., NIKKEL, S., NISHIMURA, G., UNGER, S., SPRANGER, J., SUPERTI-FURGA, A. & ZABEL, B. (2009) Mutations in MMP9 and MMP13 determine the mode of inheritance and the clinical spectrum of metaphyseal anadysplasia. Am J Hum Genet, 85, 168-78.

LEE, A., HAKUNO, F., NORTHCOTT, P., PESSIN, J. E. & ROZAKIS ADCOCK, M. (2013) Nexilin, a cardiomyopathy-associated F-actin binding protein, binds and regulates IRS1 signaling in skeletal muscle cells. PLoS One, 8, e55634.

LEE, B., GODFREY, M., VITALE, E., HORI, H., MATTEI, M. G., SARFARAZI, M., TSIPOURAS, P., RAMIREZ, F. & HOLLISTER, D. W. (1991) Linkage of Marfan syndrome and a phenotypically related disorder to two different fibrillin genes. Nature, 352, 330-4.

LEE, N. Y., RAY, B., HOW, T. & BLOBE, G. C. (2008) Endoglin promotes transforming growth factor beta-mediated Smad 1/5/8 signaling and inhibits endothelial cell migration through its association with GIPC. J Biol Chem, 283, 32527-33.

LEE, S. H., PARK, H. S., LEE, J. A., SONG, Y. S., JANG, Y. J., KIM, J. H., LEE, Y. J. & HEO, Y. (2012) Fibronectin gene expression in human adipose tissue and its associations with obesity-related genes and metabolic parameters. Obes Surg, 23, 554-60.

LENHARD, B., SANDELIN, A. & CARNINCI, P. (2012) Metazoan promoters: emerging characteristics and insights into transcriptional regulation. Nat Rev Genet, 13, 233-45.

LEHTONEN, H. J., SIPPONEN, T., TOJKANDER, S., KARIKOSKI, R., JARVINEN, H., LAING, N. G., LAPPALAINEN, P., AALTONEN, L. A. & TUUPANEN, S. (2012) Segregation of a missense variant in enteric smooth muscle actin gamma-2 with autosomal dominant familial visceral myopathy. Gastroenterology, 143, 1482-1491 e3.

LESLIE, E. J., MANSILLA, M. A., BIGGS, L. C., SCHUETTE, K., BULLARD, S., COOPER, M., DUNNWALD, M., LIDRAL, A. C., MARAZITA, M. L., BEATY, T. H. & MURRAY, J. C. (2012) Expression and mutation analyses implicate ARHGAP29 as the etiologic gene for the cleft lip with or without cleft palate locus identified by genome-wide association on chromosome 1p22. Birth Defects Res A Clin Mol Teratol, 94, 934-42.

LI, J. & ZHANG, Y. (2014) Relationship between promoter sequence and its strength in gene expression. Eur Phys J E Soft Matter, 37, 44.

LI, S., VAN DEN DIEPSTRATEN, C., D'SOUZA, S. J., CHAN, B. M. & PICKERING, J. G. (2003) Vascular smooth muscle cells orchestrate the assembly of type I collagen via alpha2beta1 integrin, RhoA, and fibronectin polymerization. Am J Pathol, 163, 1045-56.

LI, W. J., JIANG, Y. J. & TUAN, R. S. (2006) Chondrocyte phenotype in engineered fibrous matrix is regulated by fiber size. Tissue Eng, 12, 1775-85.

LI, X., WANG, J., LI, W., XU, Y., SHAO, D., XIE, Y., XIE, W., KUBOTA, T., NARIMATSU, H. & ZHANG, Y. (2011) Characterization of ppGalNAc-T18, a member of the vertebrate-specific Y subfamily of UDP-N-acetyl-alpha-D-galactosamine:polypeptide N-acetylgalactosaminyltransferases. Glycobiology, 22, 602-15.

LI, Y., FROMME, T., SCHWEIZER, S., SCHOTTL, T. & KLINGENSPOR, M. (2014) Taking control over intracellular fatty acid levels is essential for the analysis of thermogenic function in cultured primary brown and brite/beige adipocytes. EMBO Rep.

LIAO, Y. F., GOTWALS, P. J., KOTELIANSKY, V. E., SHEPPARD, D. & VAN DE WATER, L. (2002) The EIIIA segment of fibronectin is a ligand for integrins alpha 9beta 1 and alpha 4beta 1 providing a novel mechanism for regulating cell adhesion by alternative splicing. J Biol Chem, 277, 14467-74.

LILLICO, S. G., PROUDFOOT, C., CARLSON, D. F., STVERAKOVA, D., NEIL, C., BLAIN, C., KING, T. J., RITCHIE, W. A., TAN, W., MILEHAM, A. J., MCLAREN, D. G., FAHRENKRUG, S. C. & WHITELAW, C. B. (2013) Live pigs produced from genome edited zygotes. Sci Rep, 3, 2847.

LIM, J. M., SHERLING, D., TEO, C. F., HAUSMAN, D. B., LIN, D. & WELLS, L. (2008) Defining the regulated secreted proteome of rodent adipocytes upon the induction of insulin resistance. J Proteome Res, 7, 1251-63.

LIM, J. S. & LEE, D. H. (2013) Changes in bone mineral density and body composition of children with well-controlled homocystinuria caused by CBS deficiency. Osteoporos Int, 24, 2535-8.

LIM, R. & ZAHEER, A. (1996) In vitro enhancement of p38 mitogen-activated protein kinase activity by phosphorylated glia maturation factor. J Biol Chem, 271, 22953-6.

LIMA, B. L., SANTOS, E. J., FERNANDES, G. R., MERKEL, C., MELLO, M. R., GOMES, J. P., SOUKOYAN, M., KERKIS, A., MASSIRONI, S. M., VISINTIN, J. A. & PEREIRA, L. V. (2010) A new mouse model for marfan syndrome presents phenotypic variability associated with the genetic background and overall levels of Fbn1 expression. PLoS One, 5, e14136.

LIN, F. (2012) Adipose tissue-derived mesenchymal stem cells: a fat chance of curing kidney disease? Kidney Int, 82, 731-3.

LIN, G., TIEDEMANN, K., VOLLBRANDT, T., PETERS, H., BATGE, B., BRINCKMANN, J. & REINHARDT, D. P. (2002) Homo- and heterotypic fibrillin-1 and -2 interactions constitute the basis for the assembly of microfibrils. J Biol Chem, 277, 50795-804.

LLOYD, D. J., TREMBATH, R. C. & SHACKLETON, S. (2002) A novel interaction between lamin A and SREBP1: implications for partial lipodystrophy and other laminopathies. Hum Mol Genet, 11, 769-77.

LODISH H, B. A., ZIPURSKY SL, ET AL. (2000) Molecular Cell Biology, New York W.H Freeman.

LOEYS, B. L., CHEN, J., NEPTUNE, E. R., JUDGE, D. P., PODOWSKI, M., HOLM, T., MEYERS, J., LEITCH, C. C., KATSANIS, N., SHARIFI, N., XU, F. L., MYERS, L. A., SPEVAK, P. J., CAMERON, D. E., DE BACKER, J., HELLEMANS, J., CHEN, Y., DAVIS, E. C., WEBB, C. L., KRESS, W., COUCKE, P., RIFKIN, D. B., DE PAEPE, A. M. & DIETZ, H. C. (2005) A syndrome of altered cardiovascular, craniofacial, neurocognitive and skeletal development caused by mutations in TGFBR1 or TGFBR2. Nat Genet, 37, 275-81.

LOEYS, B. L., DIETZ, H. C., BRAVERMAN, A. C., CALLEWAERT, B. L., DE BACKER, J., DEVEREUX, R. B., HILHORST-HOFSTEE, Y., JONDEAU, G., FAIVRE, L., MILEWICZ, D. M., PYERITZ, R. E., SPONSELLER, P. D., WORDSWORTH, P. & DE PAEPE, A. M. (2010) The revised Ghent nosology for the Marfan syndrome. J Med Genet, 47, 476-85.

LOEYS, B. L., SCHWARZE, U., HOLM, T., CALLEWAERT, B. L., THOMAS, G. H., PANNU, H., DE BACKER, J. F., OSWALD, G. L., SYMOENS, S., MANOUVRIER, S., ROBERTS, A. E., FARAVELLI, F., GRECO, M. A., PYERITZ, R. E., MILEWICZ, D. M., COUCKE, P. J., CAMERON, D. E., BRAVERMAN, A. C., BYERS, P. H., DE PAEPE, A. M. & DIETZ, H. C. (2006) Aneurysm syndromes caused by mutations in the TGF-beta receptor. N Engl J Med, 355, 788-98.

LONNQVIST, L., KARTTUNEN, L., RANTAMAKI, T., KIELTY, C., RAGHUNATH, M. & PELTONEN, L. (1996) A point mutation creating an extra N-glycosylation site in fibrillin-1 results in neonatal Marfan syndrome. Genomics, 36, 468-75.

LOOTS, G. G. & OVCHARENKO, I. (2004) rVISTA 2.0: evolutionary analysis of transcription factor binding sites. Nucleic Acids Res, 32, W217-21.

LUNNEY, J. K. (2007) Advances in swine biomedical model genomics. Int J Biol Sci, 3, 179-84.

LUTHER, P. K. (2009) The vertebrate muscle Z-disc: sarcomere anchor for structure and signalling. J Muscle Res Cell Motil, 30, 171-85.

MA, S., LIEBERMAN, S., TURINO, G. M. & LIN, Y. Y. (2003) The detection and quantitation of free desmosine and isodesmosine in human urine and their peptide-bound forms in sputum. Proc Natl Acad Sci U S A, 100, 12941-3.

MABBOTT, N. A., KENNETH BAILLIE, J., KOBAYASHI, A., DONALDSON, D. S., OHMORI, H., YOON, S. O., FREEDMAN, A. S., FREEMAN, T. C. & SUMMERS, K. M. (2011) Expression of mesenchyme-specific gene signatures by follicular dendritic cells: insights from the meta-analysis of microarray data from multiple mouse cell populations. Immunology, 133, 482-98.

MACEK, M., HURYCH, J., CHVAPIL, M. & KADLECOVA, V. (1966) Study of fibroblasts in Marfan's syndrome. Humangenetik, 3, 87-97.

MACKIE, E. J., AHMED, Y. A., TATARCZUCH, L., CHEN, K. S. & MIRAMS, M. (2008) Endochondral ossification: how cartilage is converted into bone in the developing skeleton. Int J Biochem Cell Biol, 40, 46-62.

MACLEAN, G., DOLLE, P. & PETKOVICH, M. (2009) Genetic disruption of CYP26B1 severely affects development of neural crest derived head structures, but does not compromise hindbrain patterning. Dev Dyn, 238, 732-45.

MACRAE, V. E., DAVEY, M. G., MCTEIR, L., NARISAWA, S., YADAV, M. C., MILLAN, J. L. & FARQUHARSON, C. (2010) Inhibition of PHOSPHO1 activity results in impaired skeletal mineralisation during limb development of the chick. Bone, 46, 1146-55.

MAEDA, N., NISHIYORI, H., NAKAMURA, M., KAWAZU, C., MURATA, M., SANO, H., HAYASHIDA, K., FUKUDA, S., TAGAMI, M., HASEGAWA, A., MURAKAMI, K., SCHRODER, K., IRVINE, K., HUME, D., HAYASHIZAKI, Y., CARNINCI, P. & SUZUKI, H. (2008) Development of a DNA barcode tagging method for monitoring dynamic changes in gene expression by using an ultra high-throughput sequencer. Biotechniques, 45, 95-7.

MAHER, J. F. (1970) Criteria for diagnosis of pyelonephritis. Mod Treat, 7, 253-7.

MANNIK, J., MEYERS, A. & DALHAIMER, P. (2014) Isolation of cellular lipid droplets: two purification techniques starting from yeast cells and human placentas. J Vis Exp.

MAO, Y. & SCHWARZBAUER, J. E. (2005) Fibronectin fibrillogenesis, a cell-mediated matrix assembly process. Matrix Biol, 24, 389-99.

MARIENCHECK, M. C., DAVIS, E. C., ZHANG, H., RAMIREZ, F., ROSENBLOOM, J., GIBSON, M. A., PARKS, W. C. & MECHAM, R. P. (1995) Fibrillin-1 and fibrillin-2 show temporal and tissue-specific regulation of expression in developing elastic tissues. Connect Tissue Res, 31, 87-97.

MARIMAN, E. C. & WANG, P. (2010) Adipocyte extracellular matrix composition, dynamics and role in obesity. Cell Mol Life Sci, 67, 1277-92.

MARIOTTI, E., MIRABELLI, P., ABATE, G., SCHIATTARELLA, M., MARTINELLI, P., FORTUNATO, G., DI NOTO, R. & DEL VECCHIO, L. (2008) Comparative characteristics of mesenchymal stem cells from human bone marrow and placenta: CD10, CD49d, and CD56 make a difference. Stem Cells Dev, 17, 1039-41.

MARTIN, A. & CANO, A. (2010) Tumorigenesis: Twist1 links EMT to self-renewal. Nat Cell Biol, 12, 924-5.

MASSAM-WU, T., CHIU, M., CHOUDHURY, R., CHAUDHRY, S. S., BALDWIN, A. K., MCGOVERN, A., BALDOCK, C., SHUTTLEWORTH, C. A. & KIELTY, C. M. (2010) Assembly of fibrillin microfibrils governs extracellular deposition of latent TGF beta. J Cell Sci, 123, 3006-18.

MASSE, K., BHAMRA, S., EASON, R., DALE, N. & JONES, E. A. (2007) Purine-mediated signalling triggers eye development. Nature, 449, 1058-62.

MATT, P. & ECKSTEIN, F. (2012) Novel pharmacological strategies to prevent aortic complications in Marfan syndrome. J Geriatr Cardiol, 8, 254-7.

MATT, P., SCHOENHOFF, F., HABASHI, J., HOLM, T., VAN ERP, C., LOCH, D., CARLSON, O. D., GRISWOLD, B. F., FU, Q., DE BACKER, J., LOEYS, B., HUSO, D. L., MCDONNELL, N. B., VAN EYK, J. E. & DIETZ, H. C. (2009) Circulating transforming growth factor-beta in Marfan syndrome. Circulation, 120, 526-32.

MATTHEW, J. D., KHROMOV, A. S., MCDUFFIE, M. J., SOMLYO, A. V., SOMLYO, A. P., TANIGUCHI, S. & TAKAHASHI, K. (2000) Contractile properties and proteins of smooth muscles of a calponin knockout mouse. J Physiol, 529 Pt 3, 811-24.

MATTHIAS, A., OHLSON, K. B., FREDRIKSSON, J. M., JACOBSSON, A., NEDERGAARD, J. & CANNON, B. (2000) Thermogenic responses in brown fat cells are fully UCP1-dependent. UCP2 or UCP3 do not substitute for UCP1 in adrenergically or fatty scid-induced thermogenesis. J Biol Chem, 275, 25073-81.

MAYNE, R., VAN DER REST, M., NINOMIYA, Y. & OLSEN, B. R. (1985) The structure of type IX collagen. Ann N Y Acad Sci, 460, 38-46.

MCBEAN, G. J. (2011) The transsulfuration pathway: a source of cysteine for glutathione in astrocytes. Amino Acids, 42, 199-205.

MCCORMICK, D., VAN DER REST, M., GOODSHIP, J., LOZANO, G., NINOMIYA, Y. & OLSEN, B. R. (1987) Structure of the glycosaminoglycan domain in the type IX collagen-proteoglycan. Proc Natl Acad Sci U S A, 84, 4044-8.

MCGIVNEY, B. A., MCGETTIGAN, P. A., BROWNE, J. A., EVANS, A. C., FONSECA, R. G., LOFTUS, B. J., LOHAN, A., MACHUGH, D. E., MURPHY, B. A., KATZ, L. M. & HILL, E. W. (2010) Characterization of the equine skeletal muscle transcriptome identifies novel functional responses to exercise training. BMC Genomics, 11, 398.

MCINERNEY-LEO, A. M., MARSHALL, M. S., GARDINER, B., COUCKE, P. J., VAN LAER, L., LOEYS, B. L., SUMMERS, K. M., SYMOENS, S., WEST, J. A., WEST, M. J., PAUL WORDSWORTH, B., ZANKL, A., LEO, P. J., BROWN, M. A. & DUNCAN, E. L. (2014) Whole exome sequencing is an efficient, sensitive and specific method of mutation detection in osteogenesis imperfecta and Marfan syndrome. Bonekey Rep, 2, 456.

MEEUSEN EN, S. K., HIRST SJ, BISCHOF RJ (2009) Sheep as a model species fo rthe study and treatment of human asthma and other respiratory diseases. Drug Discovery Today: Disease Models 6, 101-106.

MELO, F. & BRANDAN, E. (1993) Decorin is specifically solubilized by heparin from the extracellular matrix of rat skeletal muscles. FEBS Lett, 319, 249-52.

MERCADO, M. L., AMENTA, A. R., HAGIWARA, H., RAFII, M. S., LECHNER, B. E., OWENS, R. T., MCQUILLAN, D. J., FROEHNER, S. C. & FALLON, J. R. (2006) Biglycan regulates the expression and sarcolemmal localization of dystrobrevin, syntrophin, and nNOS. FASEB J, 20, 1724-6.

MEYER, L. R., ZWEIG, A. S., HINRICHS, A. S., KAROLCHIK, D., KUHN, R. M., WONG, M., SLOAN, C. A., ROSENBLOOM, K. R., ROE, G., RHEAD, B., RANEY, B. J., POHL, A., MALLADI, V. S., LI, C. H., LEE, B. T., LEARNED, K., KIRKUP, V., HSU, F., HEITNER, S., HARTE, R. A., HAEUSSLER, M., GURUVADOO, L., GOLDMAN, M., GIARDINE, B. M., FUJITA, P. A., DRESZER, T. R., DIEKHANS, M., CLINE, M. S., CLAWSON, H., BARBER, G. P., HAUSSLER, D. & KENT, W. J. (2012) The UCSC Genome Browser database: extensions and updates 2013. Nucleic Acids Res, 41, D64-9.

MICHIE, P. T., BUDD, T. W., TODD, J., ROCK, D., WICHMANN, H., BOX, J. & JABLENSKY, A. V. (2000) Duration and frequency mismatch negativity in schizophrenia. Clin Neurophysiol, 111, 1054-65.

MICHIGAMI, T. (2014) Current understanding on the molecular basis of chondrogenesis. Clin Pediatr Endocrinol, 23, 1-8.

MIETTINEN, P. J., EBNER, R., LOPEZ, A. R. & DERYNCK, R. (1994) TGF-beta induced transdifferentiation of mammary epithelial cells to mesenchymal cells: involvement of type I receptors. J Cell Biol, 127, 2021-36.

MILEWICZ, D. M., GROSSFIELD, J., CAO, S. N., KIELTY, C., COVITZ, W. & JEWETT, T. (1995) A mutation in FBN1 disrupts profibrillin processing and results in isolated skeletal features of the Marfan syndrome. J Clin Invest, 95, 2373-8.

MILLER, S. G., DE VOS, P., GUERRE-MILLO, M., WONG, K., HERMANN, T., STAELS, B., BRIGGS, M. R. & AUWERX, J. (1996) The adipocyte specific transcription factor C/EBPalpha modulates human ob gene expression. Proc Natl Acad Sci U S A, 93, 5507-11.

MILLER, G., NEILAN, M., CHIA, R., GHERYANI, N., HOLT, N., CHARBIT, A., WELLS, S., TUCCI, V., LALANNE, Z., DENNY, P., FISHER, E. M., CHEESEMAN, M., ASKEW, G. N. & DEAR, T. N. (2010) ENU mutagenesis reveals a novel phenotype of reduced limb strength in mice lacking fibrillin 2. PLoS One, 5, e9137.

MINER, J. H., CUNNINGHAM, J. & SANES, J. R. (1998) Roles for laminin in embryogenesis: exencephaly, syndactyly, and placentopathy in mice lacking the laminin alpha5 chain. J Cell Biol, 143, 1713-23.

MINER, J. H., LEWIS, R. M. & SANES, J. R. (1995) Molecular cloning of a novel laminin chain, alpha 5, and widespread expression in adult mouse tissues. J Biol Chem, 270, 28523-6.

MING, J. E., KAUPAS, M. E., ROESSLER, E., BRUNNER, H. G., GOLABI, M., TEKIN, M., STRATTON, R. F., SUJANSKY, E., BALE, S. J. & MUENKE, M. (2002) Mutations in PATCHED-1, the receptor for SONIC HEDGEHOG, are associated with holoprosencephaly. Hum Genet, 110, 297-301.

MINGUILLON, C., DEL BUONO, J. & LOGAN, M. P. (2005) Tbx5 and Tbx4 are not sufficient to determine limb-specific morphologies but have common roles in initiating limb outgrowth. Dev Cell, 8, 75-84.

MITCHISON, T. J. & CRAMER, L. P. (1996) Actin-based cell motility and cell locomotion. Cell, 84, 371-9.

MIZUGUCHI, T., COLLOD-BEROUD, G., AKIYAMA, T., ABIFADEL, M., HARADA, N., MORISAKI, T., ALLARD, D., VARRET, M., CLAUSTRES, M., MORISAKI, H., IHARA, M., KINOSHITA, A., YOSHIURA, K., JUNIEN, C., KAJII, T., JONDEAU, G., OHTA, T., KISHINO, T., FURUKAWA, Y., NAKAMURA, Y., NIIKAWA, N., BOILEAU, C. & MATSUMOTO, N. (2004) Heterozygous TGFBR2 mutations in Marfan syndrome. Nat Genet, 36, 855-60.

MIZUNO, M., TAKEBE, T., KOBAYASHI, S., KIMURA, S., MASUTANI, M., LEE, S., JO, Y. H., LEE, J. I. & TANIGUCHI, H. (2014) Elastic cartilage reconstruction by transplantation of cultured hyaline cartilage-derived chondrocytes. Transplant Proc, 46, 1217-21.

MOGILNER, A. & RUBINSTEIN, B. (2010) Actin disassembly 'clock' and membrane tension determine cell shape and turning: a mathematical model. J Phys Condens Matter, 22, 194118.

MONTGOMERY, R. A., GERAGHTY, M. T., BULL, E., GELB, B. D., JOHNSON, M., MCINTOSH, I., FRANCOMANO, C. A. & DIETZ, H. C. (1998) Multiple molecular mechanisms underlying subdiagnostic variants of Marfan syndrome. Am J Hum Genet, 63, 1703-11.

MORIMOTO, M., TAKAHASHI, Y., ENDO, M. & SAGA, Y. (2005) The Mesp2 transcription factor establishes segmental borders by suppressing Notch activity. Nature, 435, 354-9.

MOSTAFAVI-POUR, Z., ASKARI, J. A., WHITTARD, J. D. & HUMPHRIES, M. J. (2001) Identification of a novel heparin-binding site in the alternatively spliced IIICS region of fibronectin: roles of integrins and proteoglycans in cell adhesion to fibronectin splice variants. Matrix Biol, 20, 63-73.

MUDD, S. H. (2011) Hypermethioninemias of genetic and non-genetic origin: A review. Am J Med Genet C Semin Med Genet, 157C, 3-32.

MUKHERJEE, T. M. & WILLIAMS, A. W. (1967) A comparative study of the ultrastructure of microvilli in the epithelium of small and large intestine of mice. J Cell Biol, 34, 447-61.

MUNGER, J. S., HUANG, X., KAWAKATSU, H., GRIFFITHS, M. J., DALTON, S. L., WU, J., PITTET, J. F., KAMINSKI, N., GARAT, C., MATTHAY, M. A., RIFKIN, D. B. & SHEPPARD, D. (1999) The integrin alpha v beta 6 binds and activates latent TGF beta 1: a mechanism for regulating pulmonary inflammation and fibrosis. Cell, 96, 319-28.

MUNROE, R. J., BERGSTROM, R. A., ZHENG, Q. Y., LIBBY, B., SMITH, R., JOHN, S. W., SCHIMENTI, K. J., BROWNING, V. L. & SCHIMENTI, J. C. (2000) Mouse mutants from chemically mutagenized embryonic stem cells. Nat Genet, 24, 318-21.

MURAKAMI, S., KAN, M., MCKEEHAN, W. L. & DE CROMBRUGGHE, B. (2000) Up-regulation of the chondrogenic Sox9 gene by fibroblast growth factors is mediated by the mitogen-activated protein kinase pathway. Proc Natl Acad Sci U S A, 97, 1113-8.

MUTSAERS, A. J. & WALKLEY, C. R. (2014) Cells of origin in osteosarcoma: mesenchymal stem cells or osteoblast committed cells? Bone, 62, 56-63.

NAKAJIMA, Y., MIYAZONO, K., KATO, M., TAKASE, M., YAMAGISHI, T. & NAKAMURA, H. (1997) Extracellular fibrillar structure of latent TGF beta binding protein-1: role in TGF beta-dependent endothelial-mesenchymal transformation during endocardial cushion tissue formation in mouse embryonic heart. J Cell Biol, 136, 193-204.

NAKASHIMA, K., ZHOU, X., KUNKEL, G., ZHANG, Z., DENG, J. M., BEHRINGER, R. R. & DE CROMBRUGGHE, B. (2002) The novel zinc finger-containing transcription factor osterix is required for osteoblast differentiation and bone formation. Cell, 108, 17-29.

NARITA, A., ODA, T. & MAEDA, Y. (2011) Structural basis for the slow dynamics of the actin filament pointed end. EMBO J, 30, 1230-7.

NATAATMADJA, M., WEST, J. & WEST, M. (2006) Overexpression of transforming growth factor-beta is associated with increased hyaluronan content and impairment of repair in Marfan syndrome aortic aneurysm. Circulation, 114, I371-7.

NEDERGAARD, J., PETROVIC, N., LINDGREN, E. M., JACOBSSON, A. & CANNON, B. (2005) PPARgamma in the control of brown adipocyte differentiation. Biochim Biophys Acta, 1740, 293-304.

NEPTUNE, E. R., FRISCHMEYER, P. A., ARKING, D. E., MYERS, L., BUNTON, T. E., GAYRAUD, B., RAMIREZ, F., SAKAI, L. Y. & DIETZ, H. C. (2003) Dysregulation of TGF-beta activation contributes to pathogenesis in Marfan syndrome. Nat Genet, 33, 407-11.

NEUHUBER, B., GALLO, G., HOWARD, L., KOSTURA, L., MACKAY, A. & FISCHER, I. (2004) Reevaluation of in vitro differentiation protocols for bone marrow stromal cells: disruption of actin cytoskeleton induces rapid morphological changes and mimics neuronal phenotype. J Neurosci Res, 77, 192-204.

NIEDERREITHER, K., ABU-ABED, S., SCHUHBAUR, B., PETKOVICH, M., CHAMBON, P. & DOLLE, P. (2002) Genetic evidence that oxidative derivatives of retinoic acid are not involved in retinoid signaling during mouse development. Nat Genet, 31, 84-8.

NIJBROEK, G., SOOD, S., MCINTOSH, I., FRANCOMANO, C. A., BULL, E., PEREIRA, L., RAMIREZ, F., PYERITZ, R. E. & DIETZ, H. C. (1995) Fifteen novel FBN1 mutations causing Marfan syndrome detected by heteroduplex analysis of genomic amplicons. Am J Hum Genet, 57, 8-21.

NINOMIYA, H., ELINSON, R. P. & WINKLBAUER, R. (2004) Antero-posterior tissue polarity links mesoderm convergent extension to axial patterning. Nature, 430, 364-7.

NISHIUCHI, R., TAKAGI, J., HAYASHI, M., IDO, H., YAGI, Y., SANZEN, N., TSUJI, T., YAMADA, M. & SEKIGUCHI, K. (2006) Ligand-binding specificities of laminin-binding integrins: a comprehensive survey of laminin-integrin interactions using recombinant alpha3beta1, alpha6beta1, alpha7beta1 and alpha6beta4 integrins. Matrix Biol, 25, 189-97.

NISTALA, H., LEE-ARTEAGA, S., CARTA, L., COOK, J. R., SMALDONE, S., SICILIANO, G., RIFKIN, A. N., DIETZ, H. C., RIFKIN, D. B. & RAMIREZ, F. (2010a) Differential effects of alendronate and losartan therapy on osteopenia and aortic aneurysm in mice with severe Marfan syndrome. Hum Mol Genet, 19, 4790-8.

NISTALA, H., LEE-ARTEAGA, S., SMALDONE, S., SICILIANO, G., CARTA, L., ONO, R. N., SENGLE, G., ARTEAGA-SOLIS, E., LEVASSEUR, R., DUCY, P., SAKAI, L. Y., KARSENTY, G. & RAMIREZ, F. (2010b) Fibrillin-1 and -2 differentially modulate endogenous TGF-beta and BMP bioavailability during bone formation. J Cell Biol, 190, 1107-21.

NIWA, H., MIYAZAKI, J. & SMITH, A. G. (2000) Quantitative expression of Oct-3/4 defines differentiation, dedifferentiation or self-renewal of ES cells. Nat Genet, 24, 372-6.

NOBLESSE, E., CENIZO, V., BOUEZ, C., BOREL, A., GLEYZAL, C., PEYROL, S., JACOB, M. P., SOMMER, P. & DAMOUR, O. (2004) Lysyl oxidase-like and lysyl oxidase are present in the dermis and epidermis of a skin equivalent and in human skin and are associated to elastic fibers. J Invest Dermatol, 122, 621-30.

NODA, S., ITO, M., WATANABE, S., TAKAHASHI, K. & MARUYAMA, K. (1992) Conformational changes of actin induced by calponin. Biochem Biophys Res Commun, 185, 481-7.

NOTREDAME, C., HIGGINS, D. G. & HERINGA, J. (2000) T-Coffee: A novel method for fast and accurate multiple sequence alignment. J Mol Biol, 302, 205-17.

NIJBROEK, G., SOOD, S., MCINTOSH, I., FRANCOMANO, C. A., BULL, E., PEREIRA, L., RAMIREZ, F., PYERITZ, R. E. & DIETZ, H. C. (1995) Fifteen novel FBN1 mutations causing Marfan syndrome detected by heteroduplex analysis of genomic amplicons. Am J Hum Genet, 57, 8-21.

OKAMATSU-OGURA, Y., FUKANO, K., TSUBOTA, A., UOZUMI, A., TERAO, A., KIMURA, K. & SAITO, M. (2014) Thermogenic ability of uncoupling protein 1 in beige adipocytes in mice. PLoS One, 8, e84229.

OKAMOTO, O. & FUJIWARA, S. (2006) Dermatopontin, a novel player in the biology of the extracellular matrix. Connect Tissue Res, 47, 177-89.

OKAMURA, H. & MATSUMOTO, Y. (1984) A case of Ehlers-Danlos syndrome associated with cleft lip and palate. J Laryngol Otol, 98, 311-5.

OKAZAKI, Y., FURUNO, M., KASUKAWA, T., ADACHI, J., BONO, H., KONDO, S., NIKAIDO, I., OSATO, N., SAITO, R., SUZUKI, H., YAMANAKA, I., KIYOSAWA, H., YAGI, K., TOMARU, Y., HASEGAWA, Y., NOGAMI, A., SCHONBACH, C., GOJOBORI, T., BALDARELLI, R., HILL, D. P., BULT, C., HUME, D. A., QUACKENBUSH, J., SCHRIML, L. M., KANAPIN, A., MATSUDA, H., BATALOV, S., BEISEL, K. W., BLAKE, J. A., BRADT, D., BRUSIC, V., CHOTHIA, C., CORBANI, L. E., COUSINS, S., DALLA, E., DRAGANI, T. A., FLETCHER, C. F., FORREST, A., FRAZER, K. S., GAASTERLAND, T., GARIBOLDI, M., GISSI, C., GODZIK, A., GOUGH, J., GRIMMOND, S., GUSTINCICH, S., HIROKAWA, N., JACKSON, I. J., JARVIS, E. D., KANAI, A., KAWAJI, H., KAWASAWA, Y., KEDZIERSKI, R. M., KING, B. L., KONAGAYA, A., KUROCHKIN, I. V., LEE, Y., LENHARD, B., LYONS, P. A., MAGLOTT, D. R., MALTAIS, L., MARCHIONNI, L., MCKENZIE, L., MIKI, H., NAGASHIMA, T., NUMATA, K., OKIDO, T., PAVAN, W. J., PERTEA, G., PESOLE, G., PETROVSKY, N., PILLAI, R., PONTIUS, J. U., QI, D., RAMACHANDRAN, S., RAVASI, T., REED, J. C., REED, D. J., REID, J., RING, B. Z., RINGWALD, M., SANDELIN, A., SCHNEIDER, C., SEMPLE, C. A., SETOU, M., SHIMADA, K., SULTANA, R., TAKENAKA, Y., TAYLOR, M. S., TEASDALE, R. D., TOMITA, M., VERARDO, R., WAGNER, L., WAHLESTEDT, C., WANG, Y., WATANABE, Y., WELLS, C., WILMING, L. G., WYNSHAW-BORIS, A., YANAGISAWA, M., et al. (2002) Analysis of the mouse transcriptome based on functional annotation of 60,770 full-length cDNAs. Nature, 420, 563-73.

OHTSUKA, T., NAKANISHI, H., IKEDA, W., SATOH, A., MOMOSE, Y., NISHIOKA, H. & TAKAI, Y. (1998) Nexilin: a novel actin filament-binding protein localised at cell-matrix adherens junction. J Cell Biol, 143, 1227-38.

OLIVIERI, J., SMALDONE, S. & RAMIREZ, F. (2010) Fibrillin assemblies: extracellular determinants of tissue formation and fibrosis. Fibrogenesis Tissue Repair, 3, 24.

OLSKI, T. M., NOEGEL, A. A. & KORENBAUM, E. (2001) Parvin, a 42 kDa focal adhesion protein, related to the alpha-actinin superfamily. J Cell Sci, 114, 525-38.

ONIMARU, K., SHOGUCHI, E., KURATANI, S. & TANAKA, M. (2011) Development and evolution of the lateral plate mesoderm: comparative analysis of amphioxus and lamprey with implications for the acquisition of paired fins. Dev Biol, 359, 124-36.

ORPHANIDES, G., LAGRANGE, T. & REINBERG, D. (1996) The general transcription factors of RNA polymerase II. Genes Dev, 10, 2657-83.

OSE, L. & MCKUSICK, V. A. (1977) Prophylactiv use of propranolol in the Marfan syndrome to prevent aortic dissection. Birth Defects Orig Artic Ser, 13, 163-9.

OTA, T., SUZUKI, Y., NISHIKAWA, T., OTSUKI, T., SUGIYAMA, T., IRIE, R., WAKAMATSU, A., HAYASHI, K., SATO, H., NAGAI, K., KIMURA, K., MAKITA, H., SEKINE, M., OBAYASHI, M., NISHI, T., SHIBAHARA, T., TANAKA, T., ISHII, S., YAMAMOTO, J., SAITO, K., KAWAI, Y., ISONO, Y., NAKAMURA, Y., NAGAHARI, K., MURAKAMI, K., YASUDA, T., IWAYANAGI, T., WAGATSUMA, M., SHIRATORI, A., SUDO, H., HOSOIRI, T., KAKU, Y., KODAIRA, H., KONDO, H., SUGAWARA, M., TAKAHASHI, M., KANDA, K., YOKOI, T., FURUYA, T., KIKKAWA, E., OMURA, Y., ABE, K., KAMIHARA, K., KATSUTA, N., SATO, K., TANIKAWA, M., YAMAZAKI, M., NINOMIYA, K., ISHIBASHI, T., YAMASHITA, H., MURAKAWA, K., FUJIMORI, K., TANAI, H., KIMATA, M., WATANABE, M., HIRAOKA, S., CHIBA, Y., ISHIDA, S., ONO, Y., TAKIGUCHI, S., WATANABE, S., YOSIDA, M., HOTUTA, T., KUSANO, J., KANEHORI, K., TAKAHASHI-FUJII, A., HARA, H., TANASE, T. O., NOMURA, Y., TOGIYA, S., KOMAI, F., HARA, R., TAKEUCHI, K., ARITA, M., IMOSE, N., MUSASHINO, K., YUUKI, H., OSHIMA, A., SASAKI, N., AOTSUKA, S., YOSHIKAWA, Y., MATSUNAWA, H., ICHIHARA, T., SHIOHATA, N., SANO, S., MORIYA, S., MOMIYAMA, H., SATOH, N., TAKAMI, S., TERASHIMA, Y., SUZUKI, O., NAKAGAWA, S., SENOH, A., MIZOGUCHI, H., GOTO, Y., SHIMIZU, F., WAKEBE, H., HISHIGAKI, H., WATANABE, T., SUGIYAMA, A., et al. (2004) Complete sequencing and characterization of 21,243 full-length human cDNAs. Nat Genet, 36, 40-5.

OVCHARENKO, I., LOOTS, G. G., GIARDINE, B. M., HOU, M., MA, J., HARDISON, R. C., STUBBS, L. & MILLER, W. (2005) Mulan: multiple-sequence local alignment and visualization for studying function and evolution. Genome Res, 15, 184-94.

OVCHARENKO, I., NOBREGA, M. A., LOOTS, G. G. & STUBBS, L. (2004) ECR Browser: a tool for visualizing and accessing data from comparisons of multiple vertebrate genomes. Nucleic Acids Res, 32, W280-6.

PADALKAR, M. V., SPENCER, R. G. & PLESHKO, N. (2013) Near infrared spectroscopic evaluation of water in hyaline cartilage. Ann Biomed Eng, 41, 2426-36.

PALUKURU, U. P., MCGOVERIN, C. M. & PLESHKO, N. (2014) Assessment of hyaline cartilage matrix composition using near infrared spectroscopy. Matrix Biol.

PANKOV, R. & YAMADA, K. M. (2002) Fibronectin at a glance. J Cell Sci, 115, 3861-3.

PANNU, H., FADULU, V. T., CHANG, J., LAFONT, A., HASHAM, S. N., SPARKS, E., GIAMPIETRO, P. F., ZALESKI, C., ESTRERA, A. L., SAFI, H. J., SHETE, S., WILLING, M. C., RAMAN, C. S. & MILEWICZ, D. M. (2005) Mutations in transforming growth factor-beta receptor type II cause familial thoracic aortic aneurysms and dissections. Circulation, 112, 513-20.

PARK, E. S., PUTNAM, E. A., CHITAYAT, D., CHILD, A. & MILEWICZ, D. M. (1998) Clustering of FBN2 mutations in patients with congenital contractural arachnodactyly indicates an important role of the domains encoded by exons 24 through 34 during human development. Am J Med Genet, 78, 350-5.

PARK, J. & SCHWARZBAUER, J. E. (2013) Mammary epithelial cell interactions with fibronectin stimulate epithelial-mesenchymal transition. Oncogene, 33, 1649-57.

PASARICA, M., GOWRONSKA-KOZAK, B., BURK, D., REMEDIOS, I., HYMEL, D., GIMBLE, J., RAVUSSIN, E., BRAY, G. A. & SMITH, S. R. (2009) Adipose tissue collagen VI in obesity. J Clin Endocrinol Metab, 94, 5155-62.

PATWARI, P., EMILSSON, V., SCHADT, E. E., CHUTKOW, W. A., LEE, S., MARSILI, A., ZHANG, Y., DOBRIN, R., COHEN, D. E., LARSEN, P. R., ZAVACKI, A. M., FONG, L. G., YOUNG, S. G. & LEE, R. T. (2011) The arrestin domain-containing 3 protein regulates body mass and energy expenditure. Cell Metab, 14, 671-83.

PAUTKE, C., SCHIEKER, M., TISCHER, T., KOLK, A., NETH, P., MUTSCHLER, W. & MILZ, S. (2004) Characterization of osteosarcoma cell lines MG-63, Saos-2 and U-2 OS in comparison to human osteoblasts. Anticancer Res, 24, 3743-8.

PEES, C., LACCONE, F., HAGL, M., DEBRAUWER, V., MOSER, E. & MICHEL-BEHNKE, I. (2013) Usefulness of losartan on the size of the ascending aorta in an unselected cohort of children, adolescents, and young adults with Marfan syndrome. Am J Cardiol, 112, 1477-83.

PEGLION, F., LLENSE, F. & ETIENNE-MANNEVILLE, S. (2014) Adherens junction treadmilling during collective migration. Nat Cell Biol, 16, 639-51.

PEIRCE, V., CAROBBIO, S. & VIDAL-PUIG, A. (2014) The different shades of fat. Nature, 510, 76-83.

PEREIRA, L., ANDRIKOPOULOS, K., TIAN, J., LEE, S. Y., KEENE, D. R., ONO, R., REINHARDT, D. P., SAKAI, L. Y., BIERY, N. J., BUNTON, T., DIETZ, H. C. & RAMIREZ, F. (1997) Targetting of the gene encoding fibrillin-1 recapitulates the vascular aspect of Marfan syndrome. Nat Genet, 17, 218-22.

PEREIRA, L., LEE, S. Y., GAYRAUD, B., ANDRIKOPOULOS, K., SHAPIRO, S. D., BUNTON, T., BIERY, N. J., DIETZ, H. C., SAKAI, L. Y. & RAMIREZ, F. (1999) Pathogenetic sequence for aneurysm revealed in mice underexpressing fibrillin-1. Proc Natl Acad Sci U S A, 96, 3819-23.

PERRY, D. J. (1999) Hyperhomocysteinaemia. Baillieres Best Pract Res Clin Haematol, 12, 451-77.

PETERFI, Z., TOTH, Z. E., KOVACS, H. A., LAZAR, E., SUM, A., DONKO, A., SIROKMANY, G., SHAH, A. M. & GEISZT, M. (2013) Peroxidasin-like protein: a novel peroxidase homologue in the human heart. Cardiovasc Res, 101, 393-9.

PIERLEONI, C., VERDENELLI, F., CASTELLUCCI, M. & CINTI, S. (1998) Fibronectins and basal lamina molecules expression in human subcutaneous white adipose tissue. Eur J Histochem, 42, 183-8.

PIHA-GOSSACK, A., SOSSIN, W. & REINHARDT, D. P. (2012) The evolution of extracellular fibrillins and their functional domains. PLoS One, 7, e33560.

PITTENGER, M. F., MACKAY, A. M., BECK, S. C., JAISWAL, R. K., DOUGLAS, R., MOSCA, J. D., MOORMAN, M. A., SIMONETTI, D. W., CRAIG, S. & MARSHAK, D. R. (1999) Multilineage potential of adult human mesenchymal stem cells. Science, 284, 143-7.

PLUM, L. A. & CLAGETT-DAME, M. (1995) 9-cis-retinoic acid selectively activates the cellular retinoic acid binding protein-II gene in human neuroblastoma cells. Arch Biochem Biophys, 319, 457-63.

POPAT, M. T., DYAR, O. J. & BLOGG, C. E. (1991) Comparison of the effects of oral nizatidine and ranitidine on gastric volume and pH in patients undergoing gynaecological laparoscopy. Anaesthesia, 46, 816-9.

PRIMAKOFF, P. & MYLES, D. G. (2000) The ADAM gene family: surface proteins with adhesion and protease activity. Trends Genet, 16, 83-7.

PROCKOP, D. J. (1997) Marrow stromal cells as stem cells for nonhematopoietic tissues. Science, 276, 71-4.

PRODOEHL, M. J., HATZIRODOS, N., IRVING-RODGERS, H. F., ZHAO, Z. Z., PAINTER, J. N., HICKEY, T. E., GIBSON, M. A., RAINEY, W. E., CARR, B. R., MASON, H. D., NORMAN, R. J., MONTGOMERY, G. W. & RODGERS, R. J. (2009) Genetic and gene expression analyses of

the polycystic ovary syndrome candidate gene fibrillin-3 and other fibrillin family members in human ovaries. Mol Hum Reprod, 15, 829-41.

PROVENZANO, P. P. & KEELY, P. J. (2011) Mechanical signaling through the cytoskeleton regulates cell proliferation by coordinated focal adhesion and Rho GTPase signaling. J Cell Sci, 124, 1195-205.

PUTNAM, E. A., ZHANG, H., RAMIREZ, F. & MILEWICZ, D. M. (1995) Fibrillin-2 (FBN2) mutations result in the Marfan-like disorder, congenital contractural arachnodactyly. Nat Genet, 11, 456-8.

QI, B., NEWCOMER, R. G. & SANG, Q. X. (2009) ADAM19/adamalysin 19 structure, function, and role as a putative target in tumors and inflammatory diseases. Curr Pharm Des, 15, 2336-48.

QIN, Z. (2011) The use of THP-1 cells as a model for mimicking the function and regulation of monocytes and macrophages in the vasculature. Atherosclerosis, 221, 2-11.

QUONDAMATTEO, F., REINHARDT, D. P., CHARBONNEAU, N. L., POPHAL, G., SAKAI, L. Y. & HERKEN, R. (2002) Fibrillin-1 and fibrillin-2 in human embryonic and early fetal development. Matrix Biol, 21, 637-46.

RAHMAN, M. M., GHOSH, M., SUBRAMANI, J., FONG, G. H., CARLSON, M. E. & SHAPIRO, L. H. (2013) CD13 regulates anchorage and differentiation of the skeletal muscle satellite stem cell population in ischemic injury. Stem Cells, 32, 1564-77.

RAIS, Y., ZVIRAN, A., GEULA, S., GAFNI, O., CHOMSKY, E., VIUKOV, S., MANSOUR, A. A., CASPI, I., KRUPALNIK, V., ZERBIB, M., MAZA, I., MOR, N., BARAN, D., WEINBERGER, L., JAITIN, D. A., LARA-ASTIASO, D., BLECHER-GONEN, R., SHIPONY, Z., MUKAMEL, Z., HAGAI, T., GILAD, S., AMANN-ZALCENSTEIN, D., TANAY, A., AMIT, I., NOVERSHTERN, N. & HANNA, J. H. (2013) Deterministic direct reprogramming of somatic cells to pluripotency. Nature, 502, 65-70.

RAMACHANDRAN, G. N. & KARTHA, G. (1954) Structure of collagen. Nature, 174, 269-70.

RAMACHANDRAN, G. N. & KARTHA, G. (1955) Structure of collagen. Nature, 176, 593-5.

RAMIREZ, F. & SAKAI, L. Y. (2009) Biogenesis and function of fibrillin assemblies. Cell Tissue Res, 339, 71-82.

RAMIREZ, F., SAKAI, L. Y., DIETZ, H. C. & RIFKIN, D. B. (2004) Fibrillin microfibrils: multipurpose extracellular networks in organismal physiology. Physiol Genomics, 19, 151-4.

RAUSCHER, S., BAUD, S., MIAO, M., KEELEY, F. W. & POMES, R. (2006) Proline and glycine control protein self-organisation into elastomeric or amyloid fibrils. Structure, 14, 1667-76.

RAVASI, T., SUZUKI, H., CANNISTRACI, C. V., KATAYAMA, S., BAJIC, V. B., TAN, K., AKALIN, A., SCHMEIER, S., KANAMORI-KATAYAMA, M., BERTIN, N., CARNINCI, P., DAUB, C. O., FORREST, A. R., GOUGH, J., GRIMMOND, S., HAN, J. H., HASHIMOTO, T., HIDE, W., HOFMANN, O., KAMBUROV, A., KAUR, M., KAWAJI, H., KUBOSAKI, A., LASSMANN, T., VAN NIMWEGEN, E., MACPHERSON, C. R., OGAWA, C., RADOVANOVIC, A., SCHWARTZ, A., TEASDALE, R. D., TEGNER, J., LENHARD, B., TEICHMANN, S. A., ARAKAWA, T., NINOMIYA, N., MURAKAMI, K., TAGAMI, M., FUKUDA, S., IMAMURA, K., KAI, C., ISHIHARA, R., KITAZUME, Y., KAWAI, J., HUME, D. A., IDEKER, T. & HAYASHIZAKI, Y. (2010) An atlas of combinatorial transcriptional regulation in mouse and man. Cell, 140, 744-52.

RAZANI, B. & LISANTI, M. P. (2001) Caveolin-deficient mice: insights into caveolar function human disease. J Clin Invest, 108, 1553-61.

RAZANI, B., ZHANG, X. L., BITZER, M., VON GERSDORFF, G., BOTTINGER, E. P. & LISANTI, M. P. (2001) Caveolin-1 regulates transforming growth factor (TGF)-beta/SMAD signaling through an interaction with the TGF-beta type I receptor. J Biol Chem, 276, 6727-38.

REBER-MULLER, S., SPISSINGER, T., SCHUCHERT, P., SPRING, J. & SCHMID, V. (1995) An extracellular matrix protein of jellyfish homologous to mammalian fibrillins forms different fibrils depending on the life stage of the animal. Dev Biol, 169, 662-72.

REGNIER, C. H., MASSON, R., KEDINGER, V., TEXTORIS, J., STOLL, I., CHENARD, M. P., DIERICH, A., TOMASETTO, C. & RIO, M. C. (2002) Impaired neural tube closure, axial skeleton malformations, and tracheal ring disruption in TRAF4-deficient mice. Proc Natl Acad Sci U S A, 99, 5585-90.

REINHARDT, D. P., KEENE, D. R., CORSON, G. M., POSCHL, E., BACHINGER, H. P., GAMBEE, J. E. & SAKAI, L. Y. (1996) Fibrillin-1: organisation in microfibrils and structural properties. J Mol Biol, 258, 104-16.

REINHARDT, D. P., MECHLING, D. E., BOSWELL, B. A., KEENE, D. R., SAKAI, L. Y. & BACHINGER, H. P. (1997) Calcium determines the shape of fibrillin. J Biol Chem, 272, 7368-73.

RESENDE, T. P., ANDRADE, R. P. & PALMEIRIM, I. (2014) Timing embryo segmentation: dynamics and regulatory mechanisms of the vertebrate segmentation clock. Biomed Res Int, 2014, 718683.

RHINN, M., SCHUHBAUR, B., NIEDERREITHER, K. & DOLLE, P. (2011) Involvement of retinol dehydrogenase 10 in embryonic patterning and rescue of its loss of function by maternal retinaldehyde treatment. Proc Natl Acad Sci U S A, 108, 16687-92.

RICH, A. & CRICK, F. H. (1955) The structure of collagen. Nature, 176, 915-6.

RICHANY, S. F., BAST, T. H. & ANGEVINE, D. M. (1959) Localization of alkaline phosphatase in the histogenesis of cartilage and bone. J Bone Joint Surg Am, 41-A, 939-47.

RIMM, D. L., KOSLOV, E. R., KEBRIAEI, P., CIANCI, C. D. & MORROW, J. S. (1995) Alpha 1(E)-catenin is an actin-binding and -bundling protein mediating the attachment of F-actin to the membrane adhesion complex. Proc Natl Acad Sci U S A, 92, 8813-7.

RITTY, T. M., BROEKELMANN, T. J., WERNECK, C. C. & MECHAM, R. P. (2003) Fibrillin-1 and -2 contain heparin-binding sites important for matrix deposition and that support cell attachment. Biochem J, 375, 425-32.

ROBERTSON, I., JENSEN, S. & HANDFORD, P. (2010) TB domain proteins: evolutionary insights into the multifaceted roles of fibrillins and LTBPs. Biochem J, 433, 263-76.

ROBINSON, M. D., MCCARTHY, D. J. & SMYTH, G. K. (2009) edgeR: a Bioconductor package for differential expression analysis of digital gene expression data. Bioinformatics, 26, 139-40.

ROCK, M. J., CAIN, S. A., FREEMAN, L. J., MORGAN, A., MELLODY, K., MARSON, A., SHUTTLEWORTH, C. A., WEISS, A. S. & KIELTY, C. M. (2004) Molecular basis of elastic fiber formation. Critical interactions and a tropoelastin-fibrillin-1 cross-link. J Biol Chem, 279, 23748-58.

ROCKEY, D. C., WEYMOUTH, N. & SHI, Z. (2013) Smooth muscle alpha actin (Acta2) and myofibroblast function during hepatic wound healing. PLoS One, 8, e77166.

ROPERS, F., DERIVERY, E., HU, H., GARSHASBI, M., KARBASIYAN, M., HEROLD, M., NURNBERG, G., ULLMANN, R., GAUTREAU, A., SPERLING, K., VARON, R. & RAJAB, A. (2011) Identification of a novel candidate gene for non-syndromic autosomal recessive intellectual disability: the WASH complex member SWIP. Hum Mol Genet, 20, 2585-90.

ROSEN, E. D. & MACDOUGALD, O. A. (2006) Adipocyte differentiation from the inside out. Nat Rev Mol Cell Biol, 7, 885-96.

ROSS, R. & BORNSTEIN, P. (1969) The elastic fiber. I. The separation and partial characterization of its macromolecular components. J Cell Biol, 40, 366-81.

ROSS, R. & GREENLEE, T. K., JR. (1966) Electron microscopy: attachment sites between connective tissue cells. Science, 153, 997-9.

ROSSI, P., KARSENTY, G., ROBERTS, A. B., ROCHE, N. S., SPORN, M. B. & DE CROMBRUGGHE, B. (1988) A nuclear factor 1 binding site mediates the transcriptional activation of a type I collagen promoter by transforming growth factor-beta. Cell, 52, 405-14.

ROSTAS, K., KONDOROSI, E., HORVATH, B., SIMONCSITS, A. & KONDOROSI, A. (1986) Conservation of extended promoter regions of nodulation genes in Rhizobium. Proc Natl Acad Sci U S A, 83, 1757-61.

RUOSLAHTI, E. (1996) RGD and other recognition sequences for integrins. Annu Rev Cell Dev Biol, 12, 697-715.

RUSS, A. P., WATTLER, S., COLLEDGE, W. H., APARICIO, S. A., CARLTON, M. B., PEARCE, J. J., BARTON, S. C., SURANI, M. A., RYAN, K., NEHLS, M. C., WILSON, V. & EVANS, M. J. (2000) Eomesodermin is required for mouse trophoblast development and mesoderm formation. Nature, 404, 95-9.

SABATIER, L., CHEN, D., FAGOTTO-KAUFMANN, C., HUBMACHER, D., MCKEE, M. D., ANNIS, D. S., MOSHER, D. F. & REINHARDT, D. P. (2009) Fibrillin assembly requires fibronectin. Mol Biol Cell, 20, 846-58.

SABATIER, L., MIOSGE, N., HUBMACHER, D., LIN, G., DAVIS, E. C. & REINHARDT, D. P. (2010) Fibrillin-3 expression in human development. Matrix Biol, 30, 43-52.

SABATIER, L., DJOKIC, J., HUBMACHER, D., DZAFIK, D., NELEA, V. & REINHARDT, D. P. (2014) Heparin/heparan sulfate controls fibrillin-1, -2 and -3 self-interactions in microfibril assembly. FEBS Lett, 588, 2890-7.

SADIQ, M. A. & VANDERVEEN, D. (2013) Genetics of ectopia lentis. Semin Ophthalmol, 28, 313-20.

SAGA, Y., HATA, N., KOBAYASHI, S., MAGNUSON, T., SELDIN, M. F. & TAKETO, M. M. (1996) MesP1: a novel basic helix-loop-helix protein expressed in the nascent mesodermal cells during mouse gastrulation. Development, 122, 2769-78.

SAGA, Y., HATA, N., KOSEKI, H. & TAKETO, M. M. (1997) Mesp2: a novel mouse gene expressed in the presegmented mesoderm and essential for segmentation initiation. Genes Dev, 11, 1827-39.

SAHARINEN, J., TAIPALE, J. & KESKI-OJA, J. (1996) Association of the small latent transforming growth factor-beta with an eight cysteine repeat of its binding protein LTBP-1. EMBO J, 15, 245-53.

SAKAI, L. Y., KEENE, D. R. & ENGVALL, E. (1986) Fibrillin, a new 350-kD glycoprotein, is a component of extracellular microfibrils. J Cell Biol, 103, 2499-509.

SAMUEL, C. S., SAKAI, L. Y. & AMENTO, E. P. (2003) Relaxin regulates fibrillin 2, but not fibrillin 1, mRNA and protein expression by human dermal fibroblasts and murine fetal skin. Arch Biochem Biophys, 411, 47-55.

SANDOR, G. G., ALGHAMDI, M. H., RAFFIN, L. A., POTTS, M. T., WILLIAMS, L. D., POTTS, J. E., KIESS, M. & VAN BREEMEN, C. (2014) A randomized, double blind pilot study to assess the effects of losartan vs. atenolol on the biophysical properties of the aorta in patients with Marfan and Loeys-Dietz syndromes. Int J Cardiol, 179, 470-5.

SANTINI, F., MARZULLO, P., ROTONDI, M., CECCARINI, G., PAGANO, L., IPPOLITO, S., CHIOVATO, L. & BIONDI, B. (2014) MECHANISMS IN ENDOCRINOLOGY: The crosstalk between thyroid gland and adipose tissue: signal integration in health and disease. Eur J Endocrinol, 171, R137-R152.

SARAS, J., FRANZEN, P., ASPENSTROM, P., HELLMAN, U., GONEZ, L. J. & HELDIN, C. H. (1997) A novel GTPase-activating protein for Rho interacts with a PDZ domain of the protein-tyrosine phosphatase PTPL1. J Biol Chem, 272, 24333-8.

SARRAZIN, S., LAMANNA, W. C. & ESKO, J. D. (2011) Heparan sulfate proteoglycans. Cold Spring Harb Perspect Biol, 3.

SATO, T., SAITO, T., KYOGOKU, Y. & FURUYAMA, T. (1979) [Immune complex and nephritis]. Nihon Rinsho, 37, 2797-804.

SATO, S., TANAKA, M., MIURA, H., IKEO, K., GOJOBORI, T., TAKEUCHI, T. & YAMAMOTO, H. (2001) Functional conservation of the promoter regions of vertebrate tyrosinase genes. J Investig Dermatol Symp Proc, 6, 10-8.

SCHAFER, G., NARASIMHA, M., VOGELSANG, E. & LEPTIN, M. (2014) Cadherin switching during the formation and differentiation of the Drosophila mesoderm - implications for epithelial-to-mesenchymal transitions. J Cell Sci, 127, 1511-22.

SCHERER, P. E., OKAMOTO, T., CHUN, M., NISHIMOTO, I., LODISH, H. F. & LISANTI, M. P. (1996) Identification, sequence, and expression of caveolin-2 defines a caveolin gene family. Proc Natl Acad Sci U S A, 93, 131-5.

SCHLUMBERGER, W., THIE, M., RAUTERBERG, J. & ROBENEK, H. (1991) Collagen synthesis in cultured aortic smooth muscle cells. Modulation by collagen lattice culture, transforming growth factor-beta 1, and epidermal growth factor. Arterioscler Thromb, 11, 1660-6.

SCHUG, J., SCHULLER, W. P., KAPPEN, C., SALBAUM, J. M., BUCAN, M. & STOECKERT, C. J., JR. (2005) Promoter features related to tissue specificity as measured by Shannon entropy. Genome Biol, 6, R33.

SCHULZ, H., KOLDE, R., ADLER, P., AKSOY, I., ANASTASSIADIS, K., BADER, M., BILLON, N., BOEUF, H., BOURILLOT, P. Y., BUCHHOLZ, F., DANI, C., DOSS, M. X., FORRESTER, L., GITTON, M., HENRIQUE, D., HESCHELER, J., HIMMELBAUER, H., HUBNER, N., KARANTZALI, E., KRETSOVALI, A., LUBITZ, S., PRADIER, L., RAI, M., REIMAND, J., ROLLETSCHEK, A., SACHINIDIS, A., SAVATIER, P., STEWART, F., STORM, M. P., TROUILLAS, M., VILO, J., WELHAM, M. J., WINKLER, J., WOBUS, A. M. & HATZOPOULOS, A. K. (2009) The FunGenES database: a genomics resource for mouse embryonic stem cell differentiation. PLoS One, 4, e6804.

SEDWICK, W. D., KUTLER, M., FRAZER, T., BROWN, O. E. & LASZLO, J. (1979) New dose-time relationships of folate antagonists to sustain inhibition of human lymphoblasts and leukemic cells in vitro. Cancer Res, 39, 3612-8.

SENGLE, G., TSUTSUI, K., KEENE, D. R., TUFA, S. F., CARLSON, E. J., CHARBONNEAU, N. L., ONO, R. N., SASAKI, T., WIRTZ, M. K., SAMPLES, J. R., FESSLER, L. I., FESSLER, J. H., SEKIGUCHI, K., HAYFLICK, S. J. & SAKAI, L. Y. (2010) Microenvironmental regulation by fibrillin-1. PLoS Genet, 8, e1002425.

SENGLE, G., CHARBONNEAU, N. L., ONO, R. N., SASAKI, T., ALVAREZ, J., KEENE, D. R., BACHINGER, H. P. & SAKAI, L. Y. (2008) Targeting of bone morphogenetic protein growth factor complexes to fibrillin. J Biol Chem, 283, 13874-88.

SENGLE, G., ONO, R. N., SASAKI, T. & SAKAI, L. Y. (2010) Prodomains of transforming growth factor beta (TGFbeta) superfamily members specify different functions: extracellular matrix interactions and growth factor bioavailability. J Biol Chem, 286, 5087-99.

SEVERIN, J., LIZIO, M., HARSHBARGER, J., KAWAJI, H., DAUB, C. O., HAYASHIZAKI, Y., BERTIN, N. & FORREST, A. R. (2014) Interactive visualization and analysis of large-scale sequencing datasets using ZENBU. Nat Biotechnol, 32, 217-9.

SEVILLA, C. A., DALECKI, D. & HOCKING, D. C. (2010) Extracellular matrix fibronectin stimulates the self-assembly of microtissues on native collagen gels. Tissue Eng Part A, 16, 3805-19.

SEVILLA, C. A., DALECKI, D. & HOCKING, D. C. (2013) Regional fibronectin and collagen fibril co-assembly directs cell proliferation and microtissue morphology. PLoS One, 8, e77316.

SHABALINA, I. G., PETROVIC, N., DE JONG, J. M., KALINOVICH, A. V., CANNON, B. & NEDERGAARD, J. (2013) UCP1 in brite/beige adipose tissue mitochondria is functionally thermogenic. Cell Rep, 5, 1196-203.

SHAW, G., MORSE, S., ARARAT, M. & GRAHAM, F. L. (2002) Preferential transformation of human neuronal cells by human adenoviruses and the origin of HEK 293 cells. FASEB J, 16, 869-71.

SHI, M., ZHU, J., WANG, R., CHEN, X., MI, L., WALZ, T. & SPRINGER, T. A. (2011) Latent TGF-beta structure and activation. Nature, 474, 343-9.

SHIOKAWA, S., YOSHIMURA, Y., SAWA, H., NAGAMATSU, S., HANASHI, H., SAKAI, K., ANDO, M. & NAKAMURA, Y. (1999) Functional role of arg-gly-asp (RGD)-binding sites on beta1 integrin in embryo implantation using mouse blastocysts and human decidua. Biol Reprod, 60, 1468-74.

SHIRAKI, T., KONDO, S., KATAYAMA, S., WAKI, K., KASUKAWA, T., KAWAJI, H., KODZIUS, R., WATAHIKI, A., NAKAMURA, M., ARAKAWA, T., FUKUDA, S., SASAKI, D., PODHAJSKA, A., HARBERS, M., KAWAI, J., CARNINCI, P. & HAYASHIZAKI, Y. (2003) Cap analysis gene expression for high-throughput analysis of transcriptional starting point and identification of promoter usage. Proc Natl Acad Sci U S A, 100, 15776-81.

SHORES, J., BERGER, K. R., MURPHY, E. A. & PYERITZ, R. E. (1994) Progression of aortic dilatation and the benefit of long-term beta-adrenergic blockade in Marfan's syndrome. N Engl J Med, 330, 1335-41.

SHOULDERS, M. D. & RAINES, R. T. (2009) Collagen structure and stability. Annu Rev Biochem, 78, 929-58.

SILLAR, B. & PLINT, C. W. (1989) The price of a false-negative result of mammography and an overenthusiastic lay press. Med J Aust, 151, 418.

SINGH, J. & PADGETT, R. A. (2009) Rates of in situ transcription and splicing in large human genes. Nat Struct Mol Biol, 16, 1128-33.

SINGH, K. K., SHUKLA, P. C., ROMMEL, K., SCHMIDTKE, J. & ARSLAN-KIRCHNER, M. (2006) Sequence variations in the 5' upstream regions of the FBN1 gene associated with Marfan syndrome. Eur J Hum Genet, 14, 876-9.

SINGH, K. K., SHUKLA, P. C. & SCHMIDTKE, J. (2008) Conservation of 5'-upstream region of the FBN1 gene in primates. Eur J Hum Genet, 16, 869-72.

SINGH, P., CARRAHER, C. & SCHWARZBAUER, J. E. (2010) Assembly of fibronectin extracellular matrix. Annu Rev Cell Dev Biol, 26, 397-419.

SMALL, M. B., GLUZMAN, Y. & OZER, H. L. (1982) Enhanced transformation of human fibroblasts by origin-defective simian virus 40. Nature, 296, 671-2.

SPLETTSTOESSER, T., HOLMES, K. C., NOE, F. & SMITH, J. C. (2011) Structural modeling and molecular dynamics simulation of the actin filament. Proteins, 79, 2033-43.

SREEDHARAN, S., STEPHANSSON, O., SCHIOTH, H. B. & FREDRIKSSON, R. (2010) Long evolutionary conservation and considerable tissue specificity of several atypical solute carrier transporters. Gene, 478, 11-8.

STARKE, J., WEHRLE-HALLER, B. & FRIEDL, P. (2014) Plasticity of the actin cytoskeleton in response to extracellular matrix nanostructure and dimensionality. Biochem Soc Trans, 42, 1356-66.

STEIN, G. S., LIAN, J. B., VAN WIJNEN, A. J., STEIN, J. L., MONTECINO, M., JAVED, A., ZAIDI, S. K., YOUNG, D. W., CHOI, J. Y. & POCKWINSE, S. M. (2004) Runx2 control of organisation, assembly and activity of the regulatory machinery for skeletal gene expression. Oncogene, 23, 4315-29.

STEPHENS, D. J. (2012) Cell biology: Collagen secretion explained. Nature, 482, 474-5.

STIPP, C. S., LITWACK, E. D. & LANDER, A. D. (1994) Cerebroglycan: an integral membrane heparan sulfate proteoglycan that is unique to the developing nervous system and expressed specifically during neuronal differentiation. J Cell Biol, 124, 149-60.

STRAUSBERG, R. L., FEINGOLD, E. A., GROUSE, L. H., DERGE, J. G., KLAUSNER, R. D., COLLINS, F. S., WAGNER, L., SHENMEN, C. M., SCHULER, G. D., ALTSCHUL, S. F., ZEEBERG, B., BUETOW, K. H., SCHAEFER, C. F., BHAT, N. K., HOPKINS, R. F., JORDAN, H., MOORE, T., MAX, S. I., WANG, J., HSIEH, F., DIATCHENKO, L., MARUSINA, K., FARMER, A. A., RUBIN, G. M., HONG, L., STAPLETON, M., SOARES, M. B., BONALDO, M. F., CASAVANT, T. L., SCHEETZ, T. E., BROWNSTEIN, M. J., USDIN, T. B., TOSHIYUKI, S., CARNINCI, P., PRANGE, C., RAHA, S. S., LOQUELLANO, N. A., PETERS, G. J., ABRAMSON, R. D., MULLAHY, S. J., BOSAK, S. A., MCEWAN, P. J., MCKERNAN, K. J., MALEK, J. A., GUNARATNE, P. H., RICHARDS, S., WORLEY, K. C., HALE, S., GARCIA, A. M., GAY, L. J., HULYK, S. W., VILLALON, D. K., MUZNY, D. M., SODERGREN, E. J., LU, X., GIBBS, R. A., FAHEY, J., HELTON, E., KETTEMAN, M., MADAN, A., RODRIGUES, S., SANCHEZ, A., WHITING, M., YOUNG, A. C., SHEVCHENKO, Y., BOUFFARD, G. G., BLAKESLEY, R. W., TOUCHMAN, J. W., GREEN, E. D., DICKSON, M. C., RODRIGUEZ, A. C., GRIMWOOD, J., SCHMUTZ, J., MYERS, R. M., BUTTERFIELD, Y. S., KRZYWINSKI, M. I., SKALSKA, U., SMAILUS, D. E., SCHNERCH, A., SCHEIN, J. E., JONES, S. J. & MARRA, M. A. (2002) Generation and initial analysis of more than 15,000 full-length human and mouse cDNA sequences. Proc Natl Acad Sci U S A, 99, 16899-903.

STRACHEN T., R., AP. (2004) Human Molecular Genetics New York, NY, Garland Science

STRUTZ, F., OKADA, H., LO, C. W., DANOFF, T., CARONE, R. L., TOMASZEWSKI, J. E. & NEILSON, E. G. (1995) Identification and characterization of a fibroblast marker: FSP1. J Cell Biol, 130, 393-405.

SU, A. I., WILTSHIRE, T., BATALOV, S., LAPP, H., CHING, K. A., BLOCK, D., ZHANG, J., SODEN, R., HAYAKAWA, M., KREIMAN, G., COOKE, M. P., WALKER, J. R. & HOGENESCH, J. B. (2004) A gene atlas of the mouse and human protein-encoding transcriptomes. Proc Natl Acad Sci U S A, 101, 6062-7.

SUEYOSHI, T., YAMAMOTO, K. & AKIYAMA, H. (2012) Conditional deletion of Tgfbr2 in hypertrophic chondrocytes delays terminal chondrocyte differentiation. Matrix Biol, 31, 352-9.

SUMMERS, K. M., NATAATMADJA, M., XU, D., WEST, M. J., MCGILL, J. J., WHIGHT, C., COLLEY, A. & ADES, L. C. (2005) Histopathology and fibrillin-1 distribution in severe early onset Marfan syndrome. Am J Med Genet A, 139, 2-8.

SUMMERS, K. M., BOKIL, N. J., BAISDEN, J. M., WEST, M. J., SWEET, M. J., RAGGATT, L. J. & HUME, D. A. (2009) Experimental and bioinformatic characterisation of the promoter region of the Marfan syndrome gene, FBN1. Genomics, 94, 233-40.

SUMMERS, K. M., RAZA, S., VAN NIMWEGEN, E., FREEMAN, T. C. & HUME, D. A. (2010) Co-expression of FBN1 with mesenchyme-specific genes in mouse cell lines: implications for phenotypic variability in Marfan syndrome. Eur J Hum Genet, 18, 1209-15.

SUMMERS, K. M., WEST, J. A., HATTAM, A., STARK, D., MCGILL, J. J. & WEST, M. J. (2012) Recent developments in the diagnosis of Marfan syndrome and related disorders. Med J Aust, 197, 494-7.

SUNSHINE, J. H. (1999) Employment among recent residency program graduates. JAMA, 281, 611.

SUZUKI, H., FORREST, A. R., VAN NIMWEGEN, E., DAUB, C. O., BALWIERZ, P. J., IRVINE, K. M., LASSMANN, T., RAVASI, T., HASEGAWA, Y., DE HOON, M. J., KATAYAMA, S., SCHRODER, K., CARNINCI, P., TOMARU, Y., KANAMORI-KATAYAMA, M., KUBOSAKI, A., AKALIN, A., ANDO, Y., ARNER, E., ASADA, M., ASAHARA, H., BAILEY, T., BAJIC, V. B., BAUER, D., BECKHOUSE, A. G., BERTIN, N., BJORKEGREN, J., BROMBACHER, F., BULGER, E., CHALK, A. M., CHIBA, J., CLOONAN, N., DAWE, A., DOSTIE, J., ENGSTROM, P. G., ESSACK, M., FAULKNER, G. J., FINK, J. L., FREDMAN, D., FUJIMORI, K., FURUNO, M., GOJOBORI, T., GOUGH, J., GRIMMOND, S. M., GUSTAFSSON, M., HASHIMOTO, M., HASHIMOTO, T., HATAKEYAMA, M., HEINZEL, S., HIDE, W., HOFMANN, O., HORNQUIST, M., HUMINIECKI, L., IKEO, K., IMAMOTO, N., INOUE, S.,

INOUE, Y., ISHIHARA, R., IWAYANAGI, T., JACOBSEN, A., KAUR, M., KAWAJI, H., KERR, M. C., KIMURA, R., KIMURA, S., KIMURA, Y., KITANO, H., KOGA, H., KOJIMA, T., KONDO, S., KONNO, T., KROGH, A., KRUGER, A., KUMAR, A., LENHARD, B., LENNARTSSON, A., LINDOW, M., LIZIO, M., MACPHERSON, C., MAEDA, N., MAHER, C. A., MAQUNGO, M., MAR, J., MATIGIAN, N. A., MATSUDA, H., MATTICK, J. S., MEIER, S., MIYAMOTO, S., MIYAMOTO-SATO, E., NAKABAYASHI, K., NAKACHI, Y., NAKANO, M., NYGAARD, S., OKAYAMA, T., OKAZAKI, Y., OKUDA-YABUKAMI, H., ORLANDO, V., OTOMO, J., PACHKOV, M., PETROVSKY, N., et al. (2009) The transcriptional network that controls growth arrest and differentiation in a human myeloid leukemia cell line. Nat Genet, 41, 553-62.

SZUCSIK, J. C. & LESSARD, J. L. (1995) Cloning and sequence analysis of the mouse smooth muscle gamma-enteric actin gene. Genomics, 28, 154-62.

TAKAHASHI, K., TAKAHASHI, J., OKANO, S., KURAMI, M., UEDA, N. & HAZUE, M. (1987) Evaluation of in vivo stability of Ga-67 labeled human fibrinogen; analysis of plasma radioactivity using rats. Kaku Igaku, 24, 1771-4.

TAKAHASHI, S., LEISS, M., MOSER, M., OHASHI, T., KITAO, T., HECKMANN, D., PFEIFER, A., KESSLER, H., TAKAGI, J., ERICKSON, H. P. & FASSLER, R. (2007) The RGD motif in fibronectin is essential for development but dispensable for fibril assembly. J Cell Biol, 178, 167-78.

TAKAHASHI, Y., KOIZUMI, K., TAKAGI, A., KITAJIMA, S., INOUE, T., KOSEKI, H. & SAGA, Y. (2000) Mesp2 initiates somite segmentation through the Notch signalling pathway. Nat Genet, 25, 390-6.

TAKENOUCHI, T., HIDA, M., SAKAMOTO, Y., TORII, C., KOSAKI, R., TAKAHASHI, T. & KOSAKI, K. (2013) Severe congenital lipodystrophy and a progeroid appearance: Mutation in the penultimate exon of FBN1 causing a recognizable phenotype. Am J Med Genet A, 161A, 3057-62.\

TAKEUCHI, J. K., KOSHIBA-TAKEUCHI, K., MATSUMOTO, K., VOGEL-HOPKER, A., NAITOH-MATSUO, M., OGURA, K., TAKAHASHI, N., YASUDA, K. & OGURA, T. (1999) Tbx5 and Tbx4 genes determine the wing/leg identity of limb buds. Nature, 398, 810-4.

TAN, P. W., SONG, C. & LALONDE, D. (2009) Ehlers-Danlos syndrome associated with cleft lip and palate. Can J Plast Surg, 17, e24-6.

TANAKA, S., UCHIYAMA, M., SUZUKI, T. & SHOJI, Y. (1975) [Oscilloscopic analysis of stimulus waves in the diagnosis of complications after pacemaker implantation and detection of battery dissipation]. Kyobu Geka, 28, 287-90.

TANG, J., TAYLOR, D. W. & TAYLOR, K. A. (2001) The three-dimensional structure of alpha-actinin obtained by cryoelectron microscopy suggests a model for Ca(2+)-dependent actin binding. J Mol Biol, 310, 845-58.

TANI, T. T. & MERCURIO, A. M. (2001) PDZ interaction sites in integrin alpha subunits. T14853, TIP/GIPC binds to a type I recognition sequence in alpha 6A/alpha 5 and a novel sequence in alpha 6B. J Biol Chem, 276, 36535-42.

TANNY, J. C., ERDJUMENT-BROMAGE, H., TEMPST, P. & ALLIS, C. D. (2007) Ubiquitylation of histone H2B controls RNA polymerase II transcription elongation independently of histone H3 methylation. Genes Dev, 21, 835-47.

TAO, G., LEVAY, A. K., PEACOCK, J. D., HUK, D. J., BOTH, S. N., PURCELL, N. H., PINTO, J. R., GALANTOWICZ, M. L., KOCH, M., LUCCHESI, P. A., BIRK, D. E. & LINCOLN, J. (2012) Collagen XIV is important for growth and structural integrity of the myocardium. J Mol Cell Cardiol, 53, 626-38.

TAY, Y., ZHANG, J., THOMSON, A. M., LIM, B. & RIGOUTSOS, I. (2008) MicroRNAs to Nanog, Oct4 and Sox2 coding regions modulate embryonic stem cell differentiation. Nature, 455, 1124-8.

THEOCHARIDIS, A., VAN DONGEN, S., ENRIGHT, A. J. & FREEMAN, T. C. (2009) Network visualization and analysis of gene expression data using BioLayout Express(3D). Nat Protoc, 4, 1535-50.

THOMAS, D. M., JOHNSON, S. A., SIMS, N. A., TRIVETT, M. K., SLAVIN, J. L., RUBIN, B. P., WARING, P., MCARTHUR, G. A., WALKLEY, C. R., HOLLOWAY, A. J., DIYAGAMA, D., GRIM, J. E., CLURMAN, B. E., BOWTELL, D. D., LEE, J. S., GUTIERREZ, G. M., PISCOPO, D. M., CARTY, S. A. & HINDS, P. W. (2004) Terminal osteoblast differentiation, mediated by runx2 and p27KIP1, is disrupted in osteosarcoma. J Cell Biol, 167, 925-34.

THOMSON, J. A., ITSKOVITZ-ELDOR, J., SHAPIRO, S. S., WAKNITZ, M. A., SWIERGIEL, J. J., MARSHALL, V. S. & JONES, J. M. (1998) Embryonic stem cell lines derived from human blastocysts. Science, 282, 1145-7.

THOMPSON, R. J., JACKSON, M. F., OLAH, M. E., RUNGTA, R. L., HINES, D. J., BEAZELY, M. A., MACDONALD, J. F. & MACVICAR, B. A. (2008) Activation of pannexin-1 hemichannels augments aberrant bursting in the hippocampus. Science, 322, 1555-9.

THORSON, W., DIAZ-HORTA, O., FOSTER, J., 2ND, SPILIOPOULOS, M., QUINTERO, R., FAROOQ, A., BLANTON, S. & TEKIN, M. (2013) De novo ACTG2 mutations cause congenital distended bladder, microcolon, and intestinal hypoperistalsis. Hum Genet, 133, 737-42.

TIEDEMANN, K., BATGE, B., MULLER, P. K. & REINHARDT, D. P. (2001) Interactions of fibrillin-1 with heparin/heparan sulfate, implications for microfibrillar assembly. J Biol Chem, 276, 36035-42.

TO, W. S. & MIDWOOD, K. S. (2011) Plasma and cellular fibronectin: distinct and independent functions during tissue repair. Fibrogenesis Tissue Repair, 4, 21.

TONTONOZ, P., HU, E. & SPIEGELMAN, B. M. (1994) Stimulation of adipogenesis in fibroblasts by PPAR gamma 2, a lipid-activated transcription factor. Cell, 79, 1147-56.

TOOLE, B. P. (2000) Hyaluronan is not just a goo! J Clin Invest, 106, 335-6.

TSUCHIYA, S., YAMABE, M., YAMAGUCHI, Y., KOBAYASHI, Y., KONNO, T. & TADA, K. (1980) Establishment and characterization of a human acute monocytic leukemia cell line (THP-1). Int J Cancer, 26, 171-6.

TSUTSUMI, S., SHIMAZU, A., MIYAZAKI, K., PAN, H., KOIKE, C., YOSHIDA, E., TAKAGISHI, K. & KATO, Y. (2001) Retention of multilineage differentiation potential of mesenchymal cells during proliferation in response to FGF. Biochem Biophys Res Commun, 288, 413-9.

TRINDADE, P. T. (2013) Losartan treatment in adult patients with Marfan syndrome: can we finally COMPARE? Eur Heart J, 34, 3469-71.

TURTOI, A., BLOMME, A., BELLAHCENE, A., GILLES, C., HENNEQUIERE, V., PEIXOTO, P., BIANCHI, E., NOEL, A., DE PAUW, E., LIFRANGE, E., DELVENNE, P. & CASTRONOVO, V. (2013) Myoferlin is a key regulator of EGFR activity in breast cancer. Cancer Res, 73, 5438-48.

UMEZAWA, A., TACHIBANA, K., HARIGAYA, K., KUSAKARI, S., KATO, S., WATANABE, Y. & TAKANO, T. (1991) Colony-stimulating factor 1 expression is down-regulated during the adipocyte differentiation of H-1/A marrow stromal cells and induced by cachectin/tumor necrosis factor. Mol Cell Biol, 11, 920-7.

URBANEK, M., SAM, S., LEGRO, R. S. & DUNAIF, A. (2007) Identification of a polycystic ovary syndrome susceptibility variant in fibrillin-3 and association with a metabolic phenotype. J Clin Endocrinol Metab, 92, 4191-8.

VAIDYANATHAN, B. (2008) Role of beta-blockers in Marfan's syndrome and bicuspid aortic valve: A time for re-appraisal. Ann Pediatr Cardiol, 1, 149-52.

VALENTINO, T., PALMIERI, D., VITIELLO, M., SIMEONE, A., PALMA, G., ARRA, C., CHIEFFI, P., CHIARIOTTI, L., FUSCO, A. & FEDELE, M. (2012) Embryonic defects and growth alteration in mice with homozygous disruption of the Patz1 gene. J Cell Physiol, 228, 646-53.

VAN BERLO, J. H., VONCKEN, J. W., KUBBEN, N., BROERS, J. L., DUISTERS, R., VAN LEEUWEN, R. E., CRIJNS, H. J., RAMAEKERS, F. C., HUTCHISON, C. J. & PINTO, Y. M. (2005) A-type lamins are essential for TGF-beta1 induced PP2A to dephosphorylate transcription factors. Hum Mol Genet, 14, 2839-49.

VAN DEN BOGAERDT, A. J., VAN DER VEEN, V. C., VAN ZUIJLEN, P. P., REIJNEN, L., VERKERK, M., BANK, R. A., MIDDELKOOP, E. & ULRICH, M. M. (2009) Collagen cross-linking by adipose-derived mesenchymal stromal cells and scar-derived mesenchymal cells: Are mesenchymal stromal cells involved in scar formation? Wound Repair Regen, 17, 548-58.

VAN VARK, L. C., BERTRAND, M., AKKERHUIS, K. M., BRUGTS, J. J., FOX, K., MOURAD, J. J. & BOERSMA, E. (2012) Angiotensin-converting enzyme inhibitors reduce mortality in hypertension: a meta-analysis of randomized clinical trials of renin-angiotensin-aldosterone system inhibitors involving 158,998 patients. Eur Heart J, 33, 2088-97.

VANDEKERCKHOVE, J. & WEBER, K. (1979) The complete amino acid sequence of actins from bovine aorta, bovine heart, bovine fast skeletal muscle, and rabbit slow skeletal muscle. A protein-chemical analysis of muscle actin differentiation. Differentiation, 14, 123-33.

VAZQUEZ-VELA, M. E., TORRES, N. & TOVAR, A. R. (2008) White adipose tissue as endocrine organ and its role in obesity. Arch Med Res, 39, 715-28.

VEGA, J. A., ESTEBAN, I., NAVES, F. J., DEL VALLE, M. E. & MALINOVSKY, L. (1995) Immunohistochemical localization of laminin and type IV collagen in human cutaneous sensory nerve formations. Anat Embryol (Berl), 191, 33-9.

VEIGA-CASTELLI, L. C., SILVA, J. C., MEOLA, J., FERRIANI, R. A., YOSHIMOTO, M., SANTOS, S. A., SQUIRE, J. A. & MARTELLI, L. (2010) Genomic alterations detected by comparative genomic hybridization in ovarian endometriomas. Braz J Med Biol Res, 43, 799-805.

VELLING, T., RISTELI, J., WENNERBERG, K., MOSHER, D. F. & JOHANSSON, S. (2002) Polymerization of type I and III collagens is dependent on fibronectin and enhanced by integrins alpha 11beta 1 and alpha 2beta 1. J Biol Chem, 277, 37377-81.

VERBOUT, A. J. (1985) The development of the vertebral column. Adv Anat Embryol Cell Biol, 90, 1-122.

VON GISE, A. & PU, W. T. (2012) Endocardial and epicardial epithelial to mesenchymal transitions in heart development and disease. Circ Res, 110, 1628-45.

WAGGETT, A. D., KIELTY, C. M. & SHUTTLEWORTH, C. A. (1993) Microfibrillar elements in the synovial joint: presence of type VI collagen and fibrillin-containing microfibrils. Ann Rheum Dis, 52, 449-53.

WALLIS, D. D., TAN, F. K., KIELTY, C. M., KIMBALL, M. D., ARNETT, F. C. & MILEWICZ, D. M. (2001) Abnormalities in fibrillin 1-containing microfibrils in dermal fibroblast cultures from patients with systemic sclerosis (scleroderma). Arthritis Rheum, 44, 1855-64.

WALLIS, D. D., PUTNAM, E. A., CRETOIU, J. S., CARMICAL, S. G., CAO, S. N., THOMAS, G. & MILEWICZ, D. M. (2003) Profibrillin-1 maturation by human dermal fibroblasts: proteolytic processing and molecular chaperones. J Cell Biochem, 90, 641-52.

WANG, H., LI, Z., WANG, J., SUN, K., CUI, Q., SONG, L., ZOU, Y., WANG, X., LIU, X., HUI, R. & FAN, Y. (2010) Mutations in NEXN, a Z-disc gene, are associated with hypertrophic cardiomyopathy. Am J Hum Genet, 87, 687-93.

WANG, P., KEIJER, J., BUNSCHOTEN, A., BOUWMAN, F., RENES, J. & MARIMAN, E. (2006) Insulin modulates the secretion of proteins from mature 3T3-L1 adipocytes: a role for transcriptional regulation of processing. Diabetologia, 49, 2453-62.

WANG, W. J., HAN, P., ZHENG, J., HU, F. Y., ZHU, Y., XIE, J. S., GUO, J., ZHANG, Z., DONG, J., ZHENG, G. Y., CAO, H., LIU, T. S., FU, Q., SUN, L., YANG, B. B. & TIAN, X. L. (2012) Exon 47 skipping of fibrillin-1 leads preferentially to cardiovascular defects in patients with thoracic aortic aneurysms and dissections. J Mol Med (Berl), 91, 37-47.

WANG, W., ZHANG, W., HAN, Y., CHEN, J., WANG, Y., ZHANG, Z. & HUI, R. (2005) NELIN, a new F-actin associated protein, stimulates HeLa cell migration and adhesion. Biochem Biophys Res Commun, 330, 1127-31.

WANG, Y. & BEYDOUN, M. A. (2007) The obesity epidemic in the United States--gender, age, socioeconomic, racial/ethnic, and geographic characteristics: a systematic review and meta-regression analysis. Epidemiol Rev, 29, 6-28.

WANG, Y., WAN, C., DENG, L., LIU, X., CAO, X., GILBERT, S. R., BOUXSEIN, M. L., FAUGERE, M. C., GULDBERG, R. E., GERSTENFELD, L. C., HAASE, V. H., JOHNSON, R. S., SCHIPANI, E. & CLEMENS, T. L. (2007) The hypoxia-inducible factor alpha pathway couples angiogenesis to osteogenesis during skeletal development. J Clin Invest, 117, 1616-26.

WEI, C., LIU, J., YU, Z., ZHANG, B., GAO, G. & JIAO, R. (2013) TALEN or Cas9 - rapid, efficient and specific choices for genome modifications. J Genet Genomics, 40, 281-9.

WEI, J. H., CAO, J. Z., ZHANG, D., LIAO, B., ZHONG, W. M., LU, J., ZHAO, H. W., ZHANG, J. X., TONG, Z. T., FAN, S., LIANG, C. Z., LIAO, Y. B., PANG, J., WU, R. H., FANG, Y., CHEN, Z. H., LI, B., XIE, D., CHEN, W. & LUO, J. H. (2014) EIF5A2 predicts outcome in localised invasive bladder cancer and promotes bladder cancer cell aggressiveness in vitro and in vivo. Br J Cancer, 110, 1767-77.

WELCH, M. P., ODLAND, G. F. & CLARK, R. A. (1990) Temporal relationships of F-actin bundle formation, collagen and fibronectin matrix assembly, and fibronectin receptor expression to wound contraction. J Cell Biol, 110, 133-45.

WESS, T. J., PURSLOW, P. P. & KIELTY, C. M. (1997) Fibrillin-rich microfibrils: an X-ray diffraction study of the fundamental axial periodicity. FEBS Lett, 413, 424-8.

WESS, T. J., PURSLOW, P. P. & KIELTY, C. M. (1998) X-Ray diffraction studies of fibrillin-rich microfibrils: effects of tissue extension on axial and lateral packing. J Struct Biol, 122, 123-7.

WEST, C. C., MURRAY, I. R., GONZALEZ, Z. N., HINDLE, P., HAY, D. C., STEWART, K. J. & PEAULT, B. (2014) Ethical, legal and practical issues of establishing an adipose stem cell bank for research. J Plast Reconstr Aesthet Surg, 67, 745-51.3

WILSON, D., PETHICA, R., ZHOU, Y., TALBOT, C., VOGEL, C., MADERA, M., CHOTHIA, C. & GOUGH, J. (2009) SUPERFAMILY--sophisticated comparative genomics, data mining, visualization and phylogeny. Nucleic Acids Res, 37, D380-6.

WIMMER, E. A., JACKLE, H., PFEIFLE, C. & COHEN, S. M. (1993) A Drosophila homologue of human Sp1 is a head-specific segmentation gene. Nature, 366, 690-4.

WINDER, S. J. & WALSH, M. P. (1990) Structural and functional characterization of calponin fragments. Biochem Int, 22, 335-41.

WIPFF, P. J. & HINZ, B. (2008) Integrins and the activation of latent transforming growth factor beta1 - an intimate relationship. Eur J Cell Biol, 87, 601-15.

WU, J., BOSTROM, P., SPARKS, L. M., YE, L., CHOI, J. H., GIANG, A. H., KHANDEKAR, M., VIRTANEN, K. A., NUUTILA, P., SCHAART, G., HUANG, K., TU, H., VAN MARKEN LICHTENBELT, W. D., HOEKS, J., ENERBACK, S., SCHRAUWEN, P. & SPIEGELMAN, B. M. (2012) Beige adipocytes are a distinct type of thermogenic fat cell in mouse and human. Cell, 150, 366-76.

XIE, H. Q., CHOI, R. C., LEUNG, K. W., SIOW, N. L., KONG, L. W., LAU, F. T., PENG, H. B. & TSIM, K. W. (2007) Regulation of a transcript encoding the proline-rich membrane anchor of globular

muscle acetylcholinesterase. The suppressive roles of myogenesis and innervating nerves. J Biol Chem, 282, 11765-75.

XU, K., SACHARIDOU, A., FU, S., CHONG, D. C., SKAUG, B., CHEN, Z. J., DAVIS, G. E. & CLEAVER, O. (2011) Blood vessel tubulogenesis requires Rasip1 regulation of GTPase signaling. Dev Cell, 20, 526-39.

XU, J., BAE, E., ZHANG, Q., ANNIS, D. S., ERICKSON, H. P. & MOSHER, D. F. (2009) Display of cell surface sites for fibronectin assembly is modulated by cell adherence to (1)F3 and C-terminal modules of fibronectin. PLoS One, 4, e4113.

XUE, B., RIM, J. S., HOGAN, J. C., COULTER, A. A., KOZA, R. A. & KOZAK, L. P. (2007) Genetic variability affects the development of brown adipocytes in white fat but not in interscapular brown fat. J Lipid Res, 48, 41-51.

YACOUB, M. & RADFORD, M. (2014) COMPARE and Pediatric Heart Network Investigator trials: Losartan finally validated in humans with Marfan, but much work remains! Glob Cardiol Sci Pract, 2014, 371-8.

YADAV, H., QUIJANO, C., KAMARAJU, A. K., GAVRILOVA, O., MALEK, R., CHEN, W., ZERFAS, P., ZHIGANG, D., WRIGHT, E. C., STUELTEN, C., SUN, P., LONNING, S., SKARULIS, M., SUMNER, A. E., FINKEL, T. & RANE, S. G. (2011) Protection from obesity and diabetes by blockade of TGF-beta/Smad3 signaling. Cell Metab, 14, 67-79.

YAMAUCHI, M. & SRICHOLPECH, M. (2012) Lysine post-translational modifications of collagen. Essays Biochem, 52, 113-33.

YAN, X., LIN, J., MARKUS, A., ROLFS, A. & LUO, J. (2011) Regional expression of ADAM19 during chicken embryonic development. Dev Growth Differ, 53, 333-46.

YANAGISAWA, Y., ITO, E., YUASA, Y. & MARUYAMA, K. (2002) The human DNA methyltransferases DNMT3A and DNMT3B have two types of promoters with different CpG contents. Biochim Biophys Acta, 1577, 457-65.

YANG, X., MATSUDA, K., BIALEK, P., JACQUOT, S., MASUOKA, H. C., SCHINKE, T., LI, L., BRANCORSINI, S., SASSONE-CORSI, P., TOWNES, T. M., HANAUER, A. & KARSENTY, G. (2004) ATF4 is a substrate of RSK2 and an essential regulator of osteoblast biology; implication for Coffin-Lowry Syndrome. Cell, 117, 387-98.

YANG, Z., MU, Z., DABOVIC, B., JURUKOVSKI, V., YU, D., SUNG, J., XIONG, X. & MUNGER, J. S. (2007) Absence of integrin-mediated TGFbeta1 activation in vivo recapitulates the phenotype of TGFbeta1-null mice. J Cell Biol, 176, 787-93.

YETMAN, A. T., BORNEMEIER, R. A. & MCCRINDLE, B. W. (2005) Usefulness of enalapril versus propranolol or atenolol for prevention of aortic dilation in patients with the Marfan syndrome. Am J Cardiol, 95, 1125-7.

YLATUPA, S., HAGLUND, C., MERTANIEMI, P., VAHTERA, E. & PARTANEN, P. (1995) Cellular fibronectin in serum and plasma: a potential new tumour marker? Br J Cancer, 71, 578-82.

YONEZAWA, I., KATO, K., YAGITA, H., YAMAUCHI, Y. & OKUMURA, K. (1996) VLA-5-mediated interaction with fibronectin induces cytokine production by human chondrocytes. Biochem Biophys Res Commun, 219, 261-5.

YOSHIDA, C. A., YAMAMOTO, H., FUJITA, T., FURUICHI, T., ITO, K., INOUE, K., YAMANA, K., ZANMA, A., TAKADA, K., ITO, Y. & KOMORI, T. (2004) Runx2 and Runx3 are essential for chondrocyte maturation, and Runx2 regulates limb growth through induction of Indian hedgehog. Genes Dev, 18, 952-63.

YOSHIDA, T., VIVATBUTSIRI, P., MORRISS-KAY, G., SAGA, Y. & ISEKI, S. (2008) Cell lineage in mammalian craniofacial mesenchyme. Mech Dev, 125, 797-808.

YOSHINAGA, K., OBATA, H., JURUKOVSKI, V., MAZZIERI, R., CHEN, Y., ZILBERBERG, L., HUSO, D., MELAMED, J., PRIJATELJ, P., TODOROVIC, V., DABOVIC, B. & RIFKIN, D. B.

(2008) Perturbation of transforming growth factor (TGF)-beta1 association with latent TGF-beta binding protein yields inflammation and tumors. Proc Natl Acad Sci U S A, 105, 18758-63.

YURCHENCO, P. D., AMENTA, P. S. & PATTON, B. L. (2004) Basement membrane assembly, stability and activities observed through a developmental lens. Matrix Biol, 22, 521-38.

ZAHEER, A. & LIM, R. (1996) In vitro inhibition of MAP kinase (ERK1/ERK2) activity by phosphorylated glia maturation factor (GMF). Biochemistry, 35, 6283-8.

ZAMBRANO, N. Z., MONTES, G. S., SHIGIHARA, K. M., SANCHEZ, E. M. & JUNQUEIRA, L. C. (1982) Collagen arrangement in cartilages. Acta Anat (Basel), 113, 26-38.

ZARDI, L., CECCONI, C., BARBIERI, O., CARNEMOLLA, B., PICCA, M. & SANTI, L. (1979) Concentration of fibronectin in plasma of tumor-bearing mice and synthesis by Ehrlich ascites tumor cells. Cancer Res, 39, 3774-9.

ZAVADIL, J. & BOTTINGER, E. P. (2005) TGF-beta and epithelial-to-mesenchymal transitions. Oncogene, 24, 5764-74.

ZEMMYO, M., MEHARRA, E. J., KUHN, K., CREIGHTON-ACHERMANN, L. & LOTZ, M. (2003) Accelerated, aging-dependent development of osteoarthritis in alpha1 integrin-deficient mice. Arthritis Rheum, 48, 2873-80.

ZHANG, H., APFELROTH, S. D., HU, W., DAVIS, E. C., SANGUINETI, C., BONADIO, J., MECHAM, R. P. & RAMIREZ, F. (1994) Structure and expression of fibrillin-2, a novel microfibrillar component preferentially located in elastic matrices. J Cell Biol, 124, 855-63.

ZHANG, H., HU, W. & RAMIREZ, F. (1995) Developmental expression of fibrillin genes suggests heterogeneity of extracellular microfibrils. J Cell Biol, 129, 1165-76.

ZHANG, Y. E. (2009) Non-Smad pathways in TGF-beta signaling. Cell Res, 19, 128-39.

ZHANG, Z. D., PACCANARO, A., FU, Y., WEISSMAN, S., WENG, Z., CHANG, J., SNYDER, M. & GERSTEIN, M. B. (2007) Statistical analysis of the genomic distribution and correlation of regulatory elements in the ENCODE regions. Genome Res, 17, 787-97.

ZILBERBERG, L., TODOROVIC, V., DABOVIC, B., HORIGUCHI, M., COUROUSSE, T., SAKAI, L. Y. & RIFKIN, D. B. (2012) Specificity of latent TGF-beta binding protein (LTBP) incorporation into matrix: role of fibrillins and fibronectin. J Cell Physiol, 227, 3828-36.

ZUBIRIA, M. G., VIDAL-BRAVO, J., SPINEDI, E. & GIOVAMBATTISTA, A. (2014) Relationship between impaired adipogenesis of retroperitoneal adipose tissue and hypertrophic obesity: role of endogenous glucocorticoid excess. J Cell Mol Med, 18, 1549-1561.